UNIVERSITAT POLITÈCNICA DE VALÈNCIA

Programa de Doctorado en Ingeniería y Producción Industrial

Limpieza de membranas de ultrafiltración aplicadas en la industria alimentaria por medio de técnicas no convencionales y caracterización del ensuciamiento de las membranas

TESIS DOCTORAL

Autora: María José Corbatón Báguena

Directoras: Dra. Silvia Álvarez Blanco

Dra. María Cinta Vincent Vela

Valencia, Septiembre de 2015

AGRADECIMIENTOS

Tras meses de duro trabajo y años de experimentación, esta Tesis ve la luz. No hubiera sido posible realizarla sin la ayuda de muchas personas a las que he encontrado en el camino y que, de una u otra manera, muchas veces sin tan siquiera esperarlo, me han dado una valiosa opinión con la que solucionar los contratiempos que se iban presentando. Incapaz de nombrar en estas páginas una a una a todas esas personas, me disculpo con ellas y destaco a continuación, mi sincero agradecimiento a todos los que me han "guiado" hasta ver la luz.

A mis directoras de Tesis, las Dras. Silvia Álvarez Blanco y María Cinta Vincent Vela, por todo el tiempo, el esfuerzo y la paciencia dedicados durante estos cuatro años y sobre todo, por los buenos consejos que han hecho posible la presentación de esta Tesis.

A todos los profesores del Dpto. de Ingeniería Química y Nuclear, por el cariño con el que me han tratado todos estos años desde que empecé la titulación de Ingeniería Química. Gracias especialmente a los Drs. Valentín Pérez Herranz y Emma Ortega Navarro, por la ayuda prestada en los ensayos con campos eléctricos.

A todo el personal del Institute on Membrane Technology (Istituto per la Tecnologia delle Membrane-Consiglio Nazionale delle Ricerche, ITM-CNR) dirigido por la Dra. Lidietta Giorno, por el apoyo, no sólo en el laboratorio sino también personal, prestado durante la estancia

realizada allí, y en especial, a los Drs. Annarosa Gugliuzza, Alfredo Cassano, Rosalinda Mazzei y Carmela Conidi. Grazie mille!

Al Ministerio de Economía y Competitividad, por financiar económicamente esta investigación mediante el proyecto CTM2010-20186 y las becas BES-2011-044112 y EEBB-I-14-09011.

A la familia García Ivars, por haberme acogido como una más de la familia desde el primer día, por los buenos momentos que hemos pasado juntos y por los que seguro vendrán.

A toda mi familia, en especial a mis padres y mis hermanas, por compartir mis alegrías con cada nuevo logro y mantenerme en el camino correcto y con los pies en la tierra. Y a mis yayos, por enseñarme a explicar qué es un proceso de membranas para “no ingenieros”. Muchísimas gracias a todos vosotros por estar siempre a mi lado apoyándome.

“And last but not least”, al Dr. Jorge García Ivars, por darme siempre una opinión sincera del trabajo y aguantar al pie del cañón los buenos, y no tan buenos, momentos de redacción de este trabajo. Sabes que esta Tesis es tan tuya como mía porque, de otro modo, no hubiera sido posible.

¡Muchas gracias a todos!

ÍNDICE

ÍNDICE DE TABLAS

ÍNDICE DE FIGURAS

RESÚMENES

Título: "Limpieza de membranas de ultrafiltración aplicadas en la industria alimentaria por medio de técnicas no convencionales y caracterización del ensuciamiento de las membranas".

Resumen

En la presente Tesis Doctoral se investigó la aplicación de dos técnicas no convencionales (disoluciones salinas y campos eléctricos) para limpiar membranas de ultrafiltración que previamente habían sido ensuciadas con disoluciones modelo de lactosuero. Además, se estudió el ensuciamiento de las membranas causado por las diferentes disoluciones ensayadas, caracterizando el mismo mediante el ajuste de distintos modelos matemáticos semi-empíricos a los resultados experimentales de variación de la densidad de flujo de permeado con el tiempo.

Los ensayos se realizaron a escala de laboratorio con cuatro membranas de ultrafiltración de diferente material (cerámicas y orgánicas) y umbral de corte molecular (5, 15, 30 y 50 kDa) y con tres disoluciones modelo de lactosuero consistentes en disoluciones acuosas de seroalbúmina bovina (BSA), BSA con $CaCl_2$ y concentrado de proteínas de lactosuero (WPC). Cada ensayo fue dividido en cuatro etapas: ensuciamiento con la disolución modelo, primer aclarado, limpieza y segundo aclarado. Las condiciones

experimentales durante la primera etapa fueron las mismas en todos los casos, para poder evaluar la influencia de las condiciones experimentales durante la etapa de limpieza (tipo de disolución salina, concentración de sal, temperatura de la disolución, velocidad tangencial y potencial de campo eléctrico aplicado) en la eficacia del proceso de limpieza. Los modelos matemáticos considerados fueron los modelos de Hermia adaptados a flujo tangencial, un modelo combinado basado en las ecuaciones de Hermia de bloqueo completo de poros y formación de torta y un modelo de resistencias en serie.

Los resultados obtenidos durante la etapa de ensuciamiento demostraron que los modelos matemáticos utilizados son capaces de predecir con una elevada exactitud el descenso de la densidad de flujo de permeado con el tiempo, determinándose el valor de los parámetros característicos de dichos modelos y los mecanismos de ensuciamiento responsables principalmente de dicho descenso. En cuanto a los ensayos de limpieza de las membranas utilizadas, los resultados indicaron que tanto las disoluciones salinas como los campos eléctricos son técnicas efectivas para recuperar las propiedades permselectivas de las membranas, utilizando un intervalo de concentración de sal óptimo.

Títol: "Neteja de membranes d'ultrafiltració aplicades en la indústria alimentaria per mitjà de tècniques no convencionals i caracterització de l'embrutament de les membranes".

Resum

En la present Tesi Doctoral es va investigar l'aplicació de dues tècniques no convencionals (dissolucions salines i camps elèctrics) per a netejar membranes d'ultrafiltració que prèviament havien sigut embrutades amb dissolucions model de sèrum de llet. A més, es va estudiar l'embrutament de les membranes causat per les diferents dissolucions assajades, caracteritzant el mateix mitjançant l'ajust de distints models matemàtics semi-empírics als resultats experimentals de variació de la densitat de flux de permeat amb el temps.

Els experiments es realitzaren a escala de laboratori amb quatre membranes d'ultrafiltració de diferent material (ceràmiques i orgàniques) i umbral de tall molecular (5, 15, 30 i 50 kDa) i amb tres dissolucions model de sèrum de llet consistents en dissolucions aquoses de seroalbúmina bovina (BSA), BSA amb $CaCl_2$ i concentrat de proteïnes de sèrum de llet (WPC). Cada experiment fou dividit en quatre etapes: embrutament amb la dissolució model, primer aclarat, neteja i segon aclarat. Les condicions experimentals durant la primera etapa van ser les mateixes en tots els casos, per a poder evaluar la influència de les condicions experimentals durant l'etapa de neteja (classe de dissolució salina, concentració de sal, temperatura de la dissolució, velocitat tangencial i potencial de camp elèctric aplicat) en l'eficàcia del procés de neteja. Els models

matemàtics utilitzats varen ser els models d'Hermia adaptats a flux tangencial, un model combinat basat en las equacions d'Hermia de bloqueig complet de porus i formació de torta i un model de resistències en serie.

Els resultats obtinguts durant l'etapa d'embrutament demostraren que els models matemàtics utilitzats són capaços de predir amb una elevada exactitud el descens de densitat de flux de permeat amb el temps, determinant-se el valor dels paràmetres característics dels citats models i els mecanismes d'embrutament responsables principalment del citat descens. En quant als experiments de neteja de les membranes utilitzades, els resultats indicaren que tant les dissolucions salines com els camps elèctrics són tècniques efectives per a recuperar les propietats permselectives de les membranes, utilitzant un interval de concentració de sal òptim.

Title: "Cleaning of ultrafiltration membranes used in the food industry by means of non conventional techniques and characterization of membrane fouling".

Abstract

In this PhD Thesis, the application of two non conventional techniques (saline solutions and electric fields) to clean ultrafiltration membranes that were previously fouled with whey model solutions was investigated. In addition, the membrane fouling caused by the different model solutions was studied as well. This fouling was characterised by fitting different semi-empirical mathematical models to the experimental data of permeate flux evolution with time.

Experiments were performed at a laboratory scale with four ultrafiltration membranes of different material (ceramic and organic) and molecular weight cut-off (5, 15, 30 and 50 kDa) and three different whey model solutions consisting of aqueous solutions of bovine serum albumin (BSA), BSA with $CaCl_2$ and whey protein concentrate (WPC). Each experiment was divided in four steps: fouling with the model solution, first rinsing, cleaning and second rinsing. Experimental conditions during the first stage were the same in all the cases, so that it could be determined the influence of the experimental conditions during the cleaning step (type of saline solution, salt concentration, cleaning solution temperature, crossflow velocity and potential of the electric field) on the cleaning efficiency. The mathematical models considered were the Hermia's models adapted to crossflow filtration, a combined model based on Hermia's

equations of complete pore blocking and cake formation and a resistance-in-series model.

The results obtained during the fouling step demonstrated that the mathematical models used were able to predict with high accuracy the permeate flux decline with time. The value of the model characteristic parameters and the fouling mechanisms mainly responsible for that decline were determined. Regarding the cleaning experiments for the membranes used, the results indicated that both, saline solutions and electric fields, were effective techniques to recover the membrane permselective properties when an optimal salt concentration range was considered.

CAPÍTULO I

Introducción

1.1. MOTIVACIÓN

En las últimas décadas, los procesos de separación con membranas han sido implementados en diversas industrias, entre ellas la industria alimentaria y, más concretamente, la industria láctea, debido a sus numerosas ventajas frente a los métodos convencionales de concentración, purificación y fraccionamiento. Entre estas ventajas, cabe destacar su simplicidad, elevada selectividad, condiciones de operación suaves, facilidad de escalado y reducido consumo energético. Entre los procesos de separación por membranas más utilizados en la industria láctea, destaca la ultrafiltración (UF), utilizada para aplicaciones como concentración de la leche o concentración de proteínas de lactosuero.

No obstante, estos procesos presentan un principal inconveniente: el descenso de la densidad de flujo de permeado con el tiempo como consecuencia del ensuciamiento de las membranas. Este ensuciamiento conlleva la disminución de la producción global y de la vida útil de las membranas, así como un aumento de los costes de operación y del consumo de energía.

Para intentar recuperar las propiedades permselectivas de las membranas y garantizar el funcionamiento óptimo de la instalación, se llevan a cabo procesos de limpieza y desinfección periódicamente en los que se eliminan los depósitos de ensuciamiento. Sin embargo, dichas etapas de limpieza implican una interrupción de la producción, un aumento de los costes de operación y de energía eléctrica y un impacto negativo sobre la vida útil de las membranas. Por todo ello,

la investigación se ha centrado en los últimos años en minimizar el proceso de ensuciamiento, optimizar las etapas de limpieza e implementar nuevas metodologías para eliminar la suciedad de las membranas de manera más efectiva y menos dañina para las membranas y el medioambiente.

La mayoría de los trabajos bibliográficos centrados en la limpieza de membranas, utilizan métodos convencionales en los que intervienen sustancias químicas de diferente naturaleza (ácidos, bases, agentes tensioactivos, quelantes). Estos métodos pueden ocasionar, a largo plazo, daños en las membranas y/o cambios en su estructura a la vez que suponen un sobrecoste en el proceso de producción global y generan elevados volúmenes de aguas residuales. Es por ello que, recientemente, los investigadores han centrado sus esfuerzos en proponer nuevas técnicas de limpieza alternativas a las convencionales, como las disoluciones salinas o los campos eléctricos. Con ellas, se espera alargar la vida útil de las membranas de UF y aumentar la productividad global del proceso.

En la presente Tesis Doctoral se proponen, ensayan y optimizan técnicas innovadoras de limpieza de membranas de UF utilizadas en la industria alimentaria, y más concretamente, en el tratamiento de lactosuero. Además, se llevará a cabo el estudio y caracterización del ensuciamiento causado en las membranas utilizando disoluciones modelo propias de dichas industrias.

1.2. OBJETIVOS

El principal objetivo de esta Tesis Doctoral consiste en proponer, ensayar y optimizar técnicas efectivas de limpieza de membranas de ultrafiltración utilizadas en la industria alimentaria, concretamente, en la industria láctea para el tratamiento del lactosuero. Dichas técnicas de limpieza serán metodologías innovadoras alternativas a las convencionales: disoluciones salinas y campos eléctricos.

Para alcanzar dicho objetivo principal, se han planteado los siguientes objetivos específicos:

- Estudiar el ensuciamiento depositado y/o adsorbido sobre membranas de ultrafiltración utilizadas en la industria láctea.
- Relacionar dicho ensuciamiento con el tipo de alimentación y las características de las membranas.
- Analizar el ajuste de distintos modelos matemáticos a los datos experimentales obtenidos durante la etapa de ensuciamiento.
- Investigar el efecto de las condiciones de operación durante la etapa de limpieza sobre la eficacia de ese mismo proceso, para cada una de las técnicas ensayadas.
- Relacionar el tipo de membrana y su ensuciamiento con el método de limpieza más eficaz para su tratamiento desde el punto de vista de recuperación de las propiedades permselectivas de la membrana.

1.3. CONTRIBUCIÓN DE LA TESIS DOCTORAL

Entre las principales contribuciones de esta Tesis Doctoral, pueden destacarse las siguientes:

- Realización de una revisión bibliográfica acerca de los principales mecanismos de ensuciamiento, modelos de ensuciamiento y métodos de limpieza, convencionales y alternativos, de membranas aplicadas a procesos de UF.
- Análisis y comparación del ajuste de distintos modelos matemáticos aplicados al ensuciamiento causado por disoluciones modelo de lactosuero.
- Determinación de los mecanismos de ensuciamiento responsables del mismo en función de las características de las membranas y disoluciones utilizadas.
- Propuesta de las condiciones de operación más efectivas para limpiar cada una de las membranas utilizadas, en función de la disolución alimento ensayada durante la etapa de ensuciamiento y de la técnica de limpieza aplicada.
- Comparación de las distintas técnicas de limpieza de membranas.

Por otra parte, los resultados recogidos en esta Tesis han sido presentados en distintos congresos y conferencias de ámbito tanto nacional como internacional:

- Network of Young Membrains 2011 (NYM13)
- International Congress on Membranes and Membrane Processes (ICOM 2011)

- 2012 Conference and Exhibition Desalination for the Environment. Clean Water and Energy
- International Congress of Chemical Engineering (ANQUEICCE 2012)
- Network of Young Membrains 2012 (NYM14)
- Euromembrane 2012
- Workshop Membrane Processes for Industrial Control with Water and Products Recovery
- 29th EMS Summer School 2013. Membranes for liquid separations from an industrial & academic point of view.
- 6th Membrane Conference of Visegrad Countries (PERMEA 2013)
- 2014 Conference and Exhibition Desalination for the Environment. Clean Water and Energy
- IX Congreso Iberoamericano en Ciencia y Tecnología de Membranas (CITEM 2014)
- XXXI EMS Summer School 2014 on Innovative Membrane Systems
- EuroMed 2015. Desalination for Clean Water and Energy.

Además, y puesto que esta Tesis Doctoral se presenta como un compendio de publicaciones, la Tabla 1 recoge la lista de artículos en revistas científicas a los que este trabajo ha dado lugar.

Tabla 1. Lista de publicaciones

Título	Revista	Factor de impacto
Cleaning of ultrafiltration membranes fouled with BSA by means of saline solutions *Doi:10.1016/j.seppur.2014.01.035*	Separation and Purification Technology	3.091
Salt cleaning of ultrafiltration membranes fouled by whey model solutions *Doi:10.1016/j.seppur.2014.05.029*	Separation and Purification Technology	3.091
Fouling mechanisms of ultrafiltration membranes fouled with whey model solutions *Doi:10.1016/j.desal.2015.01.019*	Desalination	3.756
Destabilization and removal of immobilized enzymes adsorbed onto polyethersulfone ultrafiltration membranes by salt solutions *Doi: 10.1016/j.memsci.2015.03.061*	Journal of Membrane Science	5.056
Utilization of NaCl solutions to clean ultrafiltration membranes fouled by whey protein concentrates *Doi: 10.1016/j.seppur.2015.06.039*	Separation and Purification Technology	3.091
Application of electric fields to clean ultrafiltration membranes fouled with whey model solutions *En revisión en la revista indicada*	Separation and Purification Technology	3.091

1.4. ESTRUCTURA DE LA TESIS DOCTORAL

Tras un primer capítulo ("Capítulo I. Introducción") en el que se presentan los principales objetivos, la motivación, las contribuciones y la estructura de esta Tesis Doctoral, se expone una revisión bibliográfica ("Capítulo II. Antecedentes") acerca de los mecanismos de ensuciamiento predominantes en las membranas de UF utilizadas en la industria alimentaria y, más concretamente, en la industria láctea, así como de los métodos de limpieza convencionales y alternativos utilizados para este tipo de membranas.

A continuación, en el "Capítulo III. Metodología experimental" se describirán brevemente las plantas piloto utilizadas, las membranas y los productos químicos necesarios para llevar a cabo los ensayos y los diferentes protocolos de ensuciamiento, limpieza y análisis químicos realizados.

En cuanto a los resultados, éstos han sido divididos en seis capítulos. En primer lugar, se exponen los resultados correspondientes a los ensayos de ensuciamiento con las distintas disoluciones modelo de lactosuero ("Capítulo IV. Modelización del ensuciamiento de las membranas"). Seguidamente, en los Capítulos V, VI, VII y VIII se recogen los resultados correspondientes a la técnica de limpieza de membranas mediante disoluciones salinas utilizando diferentes disoluciones durante la etapa de ensuciamiento: tres disoluciones modelo de lactosuero (seroalbúmina bovina, BSA, BSA con $CaCl_2$ y concentrados de proteínas del lactosuero, WPC) y una disolución propia de la industria de zumos y bebidas, que es una

disolución enzimática de pectinasas. El Capítulo V contiene a su vez un subapartado en el que se compara la eficacia del proceso de limpieza de membranas ensuciadas con seroalbúmina bovina (BSA) obtenida mediante métodos hidráulicos con la determinada mediante métodos químicos. Finalmente, el "Capítulo IX. Limpieza de membranas mediante campos eléctricos" incluye los resultados correspondientes a la técnica de limpieza mediante generación de campos eléctricos, así como una comparación entre las dos técnicas de limpieza ensayadas.

Esta Tesis finaliza con un capítulo en el que se recogen las conclusiones más destacadas a lo largo de todo el trabajo ("Capítulo X. Conclusiones finales").

La Fig. 1 representa de manera esquemática la estructura de la Tesis Doctoral detallada anteriormente.

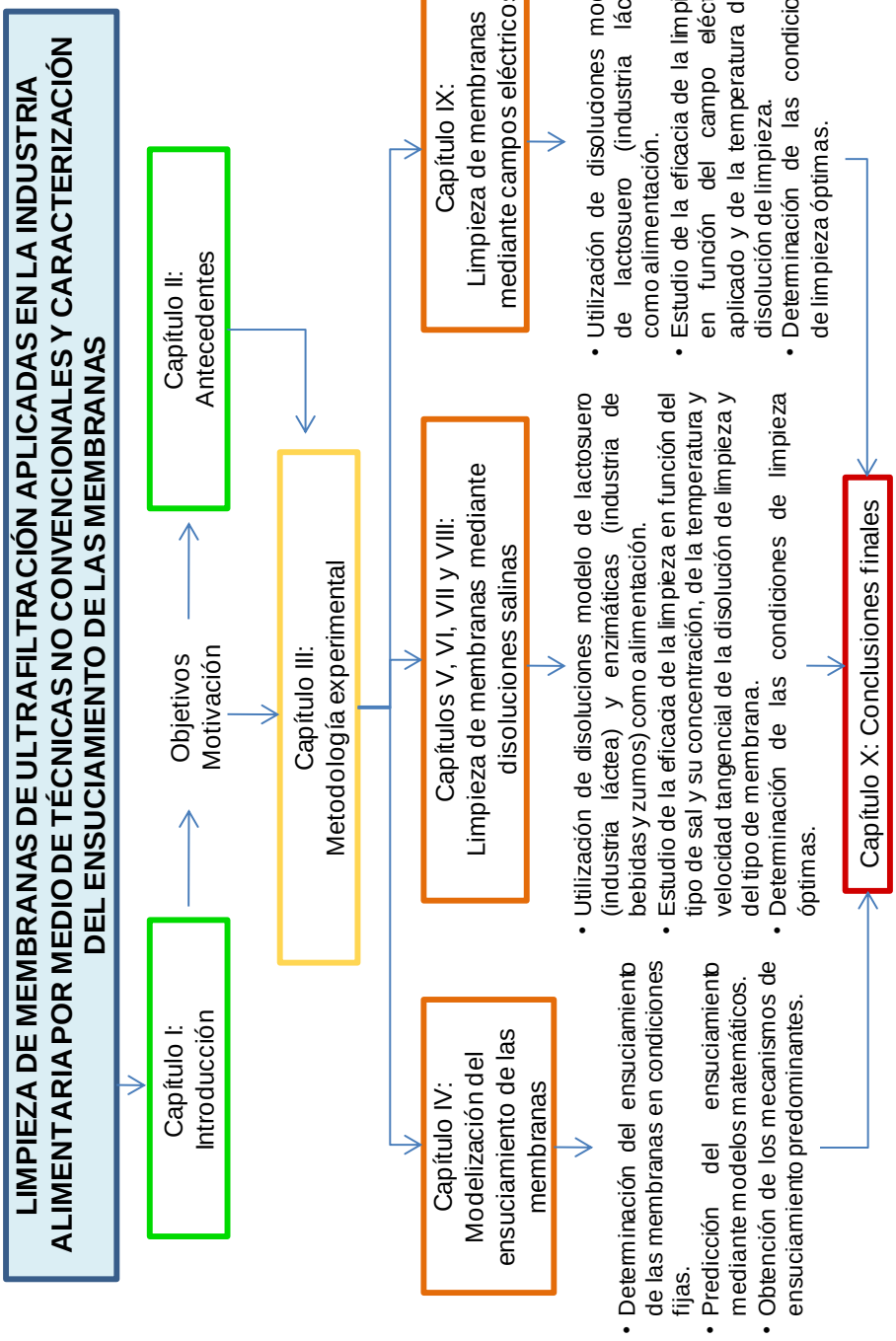

Fig. 1. *Esquema de la estructura de la Tesis Doctoral*

CAPÍTULO II

Antecedentes

2.1. INDUSTRIA ALIMENTARIA

La industria alimentaria es uno de los sectores industriales más importantes y dinámicos a nivel europeo. Incluye un numeroso grupo de industrias, entre las que destacan las industrias láctea, de bebidas y zumos, cárnica, de frutas y verduras, de cereales, etc. Según datos de la Organización de las Naciones Unidas para la Alimentación y la Agricultura (Food and Agriculture Organization of the United Nations, FAO), la industria alimentaria está constituida por cerca de 310000 empresas y representa el 14.5 % de la facturación total del sector industrial (aproximadamente, 917 billones de euros). La Fig. 2 muestra la evolución del índice de producción alimentaria (expresado en dólares, $) en Europa desde el año 2003 hasta el año 2013 (último dato disponible) (www.fao.org).

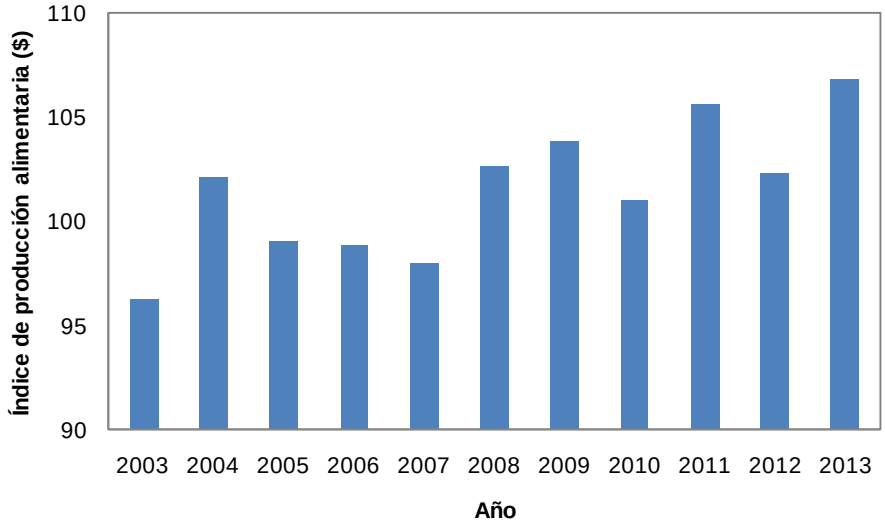

Fig. 2. *Evolución de la producción alimentaria en Europa*

Puesto que la presente Tesis Doctoral se centra en el estudio del tratamiento de lactosuero, un subproducto de la industria láctea, se describen, a continuación, las principales características de la leche, sus productos derivados y sus principales usos.

2.1.1. Industria láctea

La leche y los productos lácteos son parte fundamental de la dieta humana desde tiempos inmemorables. Según datos de la FAO, durante el año 2013 se produjeron más de 746 millones de toneladas de leche a nivel mundial. La mayor parte de dicha producción proviene de la ganadería bovina (83%), seguida de búfalos (13%), cabras (2%), ovejas (1%) y camellos (0.3%). Aproximadamente, el 0.7% restante proviene de otros mamíferos, como los equinos (burras y yeguas) y los yaks (www.fao.org).

El principal constituyente de la leche es agua, seguido de grasa, proteínas y lactosa. El resto está formado por minerales y trazas de vitaminas y compuestos nitrogenados no proteicos (NNP) (ver Fig. 3). A continuación se describen brevemente algunos de estos componentes (Gordon, 1997):

- **Grasa**: aproximadamente el 99% de la grasa presente en la leche de origen bovino se encuentra en forma de triglicéridos, formados por tres moléculas de ácidos grasos (generalmente de cadena corta, es decir, ente 4 y 10 átomos de carbono) unidos mediante una molécula de glicerol. Estos ácidos grasos son responsables, principalmente, de las propiedades organolépticas de los productos lácteos derivados, como por

ejemplo, los quesos.

- **Lactosa**: es el azúcar característico de la leche obtenida de mamíferos. Entre las propiedades más importantes de este disacárido de glucosa y galactosa destacan su carácter reductor, su limitada solubilidad en agua (cerca de 21 g por cada 100 g de agua), su transformación en ácido láctico mediante bacterias y su hidrólisis en glucosa y galactosa mediante enzimas.
- **Proteínas**: las proteínas de la leche se dividen en dos grandes tipos: caseína y proteínas del lactosuero. La principal diferencia entre ambas reside en el pH al que precipitan: mientras que la caseína es insoluble a un pH alrededor de 4.6, las proteínas de lactosuero permanecen en la disolución en esas condiciones. Durante la producción de queso, la caseína (en una proporción con respecto al resto de proteínas del lactosuero de, aproximadamente, un 80 %) precipita, mientras que las demás proteínas permanecen en el lactosuero.
- **Minerales**: las principales sales presentes en la leche están constituidas por Ca, Mg, K, Na, Cl, PO_4, bicarbonato, citrato y, en menor medida, Cu, Zn y Fe. Además de encontrarse en forma de sales disueltas, las sales de K y Na se pueden presentar en forma coloidal unidas a los grupos fosfato y carboxilo negativamente cargados de la caseína. Este equilibrio entre las sales disueltas y las sales en forma coloidal, conocido como equilibrio salino, puede verse alterado por cambios de pH, temperatura y/o concentración,

como ocurre, por ejemplo, en el tratamiento a altas temperaturas durante el procesado de la leche.

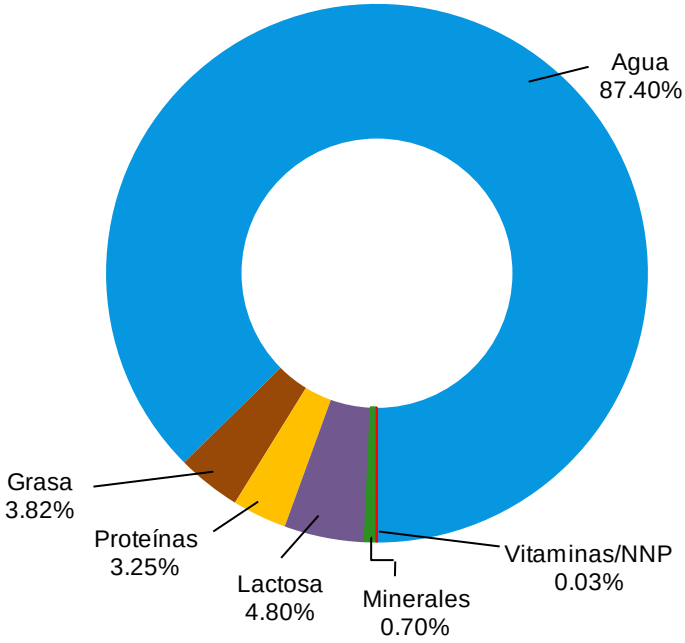

Fig. 3. *Composición típica de la leche de vaca*

En la actualidad, la leche se somete a distintos procesos para dar lugar a una gran variedad de productos lácteos derivados. Uno de los más importantes, es el queso. La Fig. 4 recoge las principales etapas del proceso de elaboración de queso a partir de los componentes de la leche (Chandan y Kilara, 2011). Durante la producción de queso se genera uno de los subproductos más importantes de la industria láctea: el lactosuero. Éste puede definirse como el producto líquido generado tras la separación de la cuajada durante la elaboración del queso y de la caseína. Por cada kg de queso producido, se estima que se generan 9 kg de lactosuero líquido. Éste representa

aproximadamente, el 85 % del volumen de la leche y contiene cerca del 55 % de sus nutrientes, con una demanda biológica de oxígeno (DBO) de 35000 mg O_2/L y un valor de demanda química de oxígeno (DQO) mayor de 60000 mg O_2/L (Acevedo Correa, 2010). Debido al negativo impacto ambiental que puede producir su descarga y a sus potenciales aplicaciones, el lactosuero se ha convertido en un subproducto de alto valor añadido. La Fig. 5 recoge algunos de los principales usos del lactosuero y de los productos que de él se derivan (Madrid Vicente, 1981).

El aspecto general del lactosuero es un líquido de color amarillo verdoso con un alto contenido en azúcares, proteínas, sales minerales, vitaminas y trazas de materia grasa.

En función del proceso de obtención de la cuajada, es decir, del tipo de coagulación que dará lugar al queso, pueden diferenciarse dos tipos de lactosuero: dulce y ácido. La composición típica de cada uno de ellos se muestra en la Tabla 2 (Goulas y Grandison, 2008).

- **Lactosuero dulce**: se obtiene utilizando enzimas de tipo cuajo para precipitar la caseína, como por ejemplo, en el queso Cheddar. Es el más abundante a nivel industrial.
- **Lactosuero ácido**: se produce durante la producción de quesos de coagulación ácida (o por acidificación), como en el caso del queso Cottage. Debido a la fermentación del ácido láctico, éste tipo de lactosuero contiene una mayor cantidad de sales minerales, como fósforo y calcio.

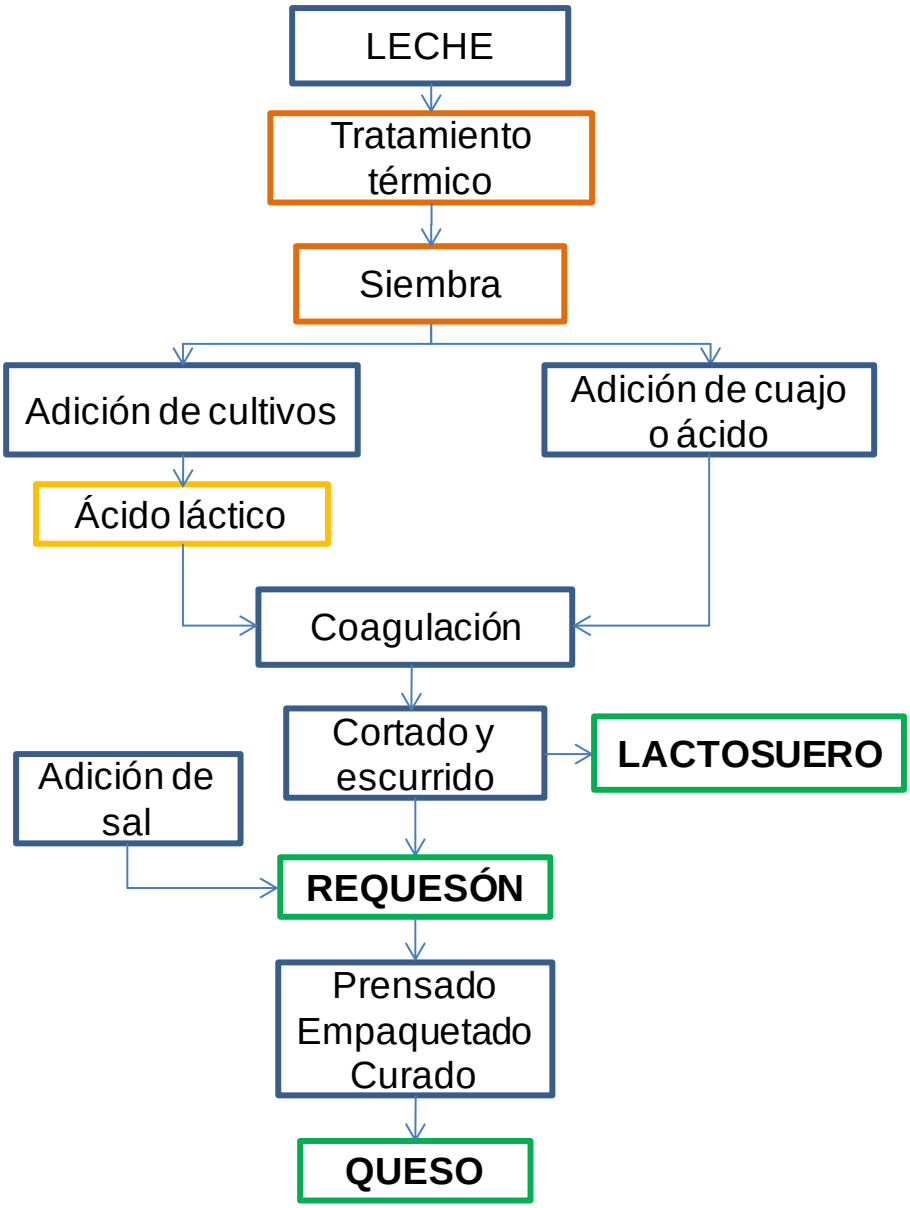

Fig. 4. *Etapas de la elaboración del queso*

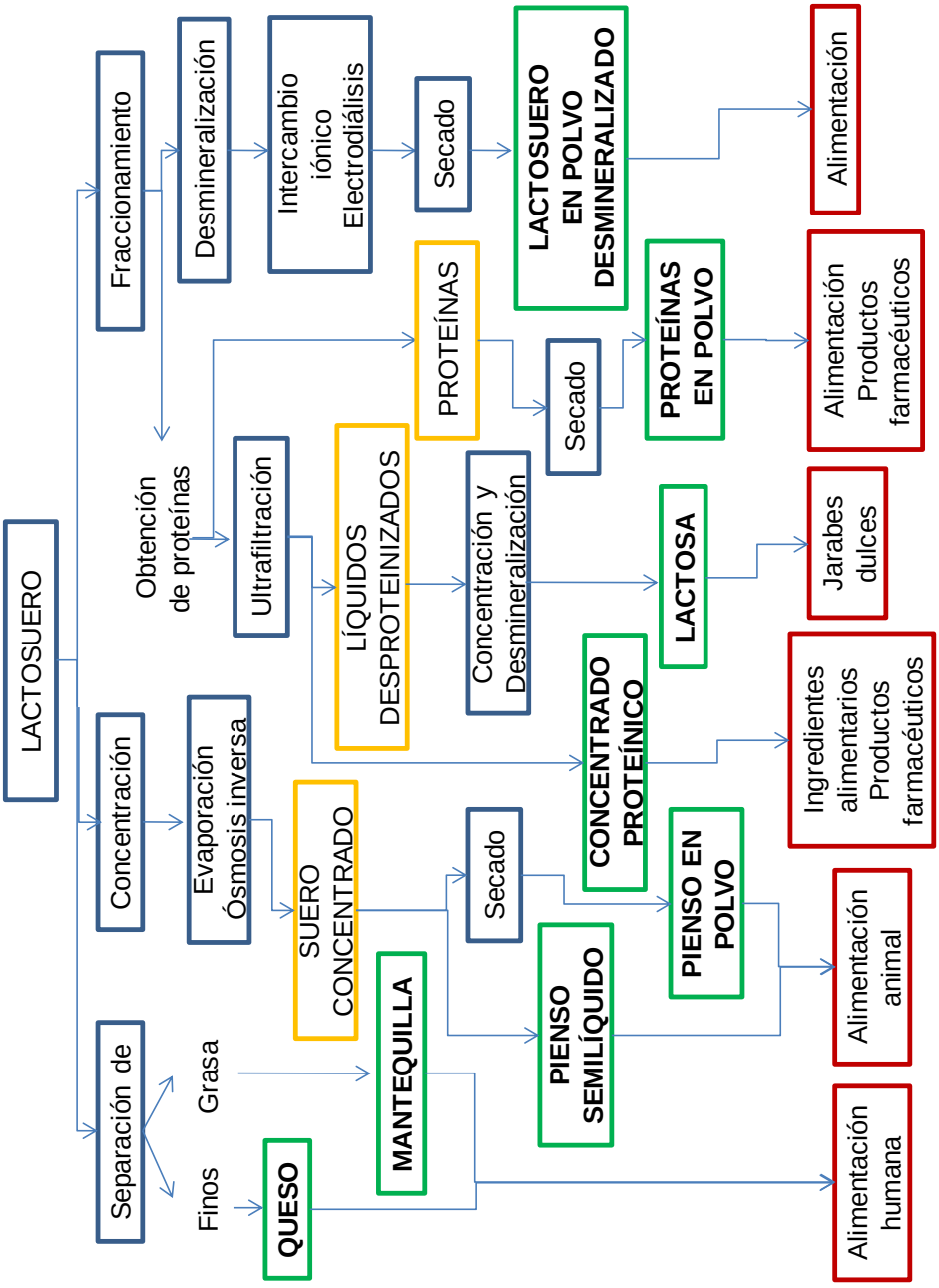

Fig. 5. *Usos del lactosuero*

Tabla 2. Composición típica del lactosuero dulce y ácido

Componente	Lactosuero dulce	Lactosuero ácido
Acidez (pH)	5.6 - 6.1	4.7
Humedad (%)	93.2 - 93.6	93.2
Sólidos totales (%)	6.4 - 6.8	6.8
Contenido en sólidos (%)		
Lactosa	4.9 - 5.1	4.3 - 4.4
Proteínas	0.8 - 0.9	0.8
Materia grasa	0.3	0.1
Ácido láctico	0.2	0.5 - 0.6
Cenizas	0.6 - 0.7	0.8
Contenido en minerales (%)		
Ca	0.06	0.10
P	0.04	0.05
Fe	0.001	0.001
K	0.13	0.14
Na	0.05	0.05
Cl	0.10	0.10
Mg	0.01	0.02
Contenido en vitaminas (mg/100 g)		
Vitamina A	< 10	< 10
Tiamina	0.04	0.04
Riboflavina	0.16	0.14
Niacina	0.08	0.08
Ácido pantoténico	0.40	0.40
Vitamina B_6	0.03	0.04
Ácido nicotínico	0.20	—

Una de las principales aplicaciones del lactosuero es la recuperación de su fracción proteínica por su alto valor biológico, nutricional y funcional, debido a su alto contenido en aminoácidos esenciales y a sus propiedades gelificantes y espumantes (Wit, 1998). Las proteínas mayoritarias en el lactosuero son: β-lactoglobulina (β-Lg), α-lactalbúmina (α-La), seroalbúmina bovina (BSA) e inmunoglobulinas (Ig). Las propiedades más destacadas de cada una

de ellas se muestran en la Tabla 3 (Cayot y Lorient, 1997; Edwards y Jameson, 2014).

- **β-lactoglobulina**: pertenece a la familia de las lipocalinas, debido a la habilidad para unirse a moléculas hidrofóbicas pequeñas. Existen diversas variantes de la β-Lg bovina, siendo las más conocidas β-LgA y β-LgB. Dichas variantes se diferencian en dos aminoácidos. La estructura cuaternaria de la proteína varía entre los monómeros, dímeros y oligómeros en función del pH, la temperatura y la fuerza iónica; aunque la forma prevalente es la dímera. Esta diferente asociación se debe al equilibrio entre las interacciones hidrofóbicas, electrostáticas y por puentes de hidrógeno.
- **α-lactalbúmina**: se encuentra en la leche de todos los mamíferos. En el caso de la α-La bovina, la forma holo de dicha proteína se combina con los iones Ca^{2+}, siendo esta forma la más abundante en la leche. Además, es uno de los componentes reguladores del complejo lactosa sintasa, encargado de transferir galactosa a glucosa.
- **Seroalbúmina bovina**: es un constituyente tanto del suero sanguíneo como de la leche de todos los mamíferos. Actúa como transportador de moléculas hidrofóbicas. Además, la BSA del suero sanguíneo juega un papel importante en el control de las propiedades de reducción-oxidación de compuestos (redox). Aunque no se ha especificado este mismo comportamiento en el caso de la BSA de la leche, se considera que podría afectar a las propiedades organolépticas de la misma.

- **Inmunoglobulinas**: componen una diversa familia de proteínas, entre las cuales la Ig G es la subfamilia predominante en la leche bovina. Su principal función es conferir inmunidad al neonato mientras su sistema inmunológico se está desarrollando, mediante el enlace con los sitios específicos de la superficie de las bacterias. De esta manera, dichas bacterias quedan inactivadas.

Tabla 3. Propiedades de las proteínas del lactosuero

Característica	β-Lg	α-La	BSA	Ig
Cantidad en lactosuero (%)	50	19	5	13
Peso molecular (kg/mol)	18	14	69.00	150-1000
Nº aminoácidos	162	123	583	>500
Enlaces disulfuro	2	4	17	4
Grupos tiol	1	0	1	–
Punto isoeléctrico (pI)	5.2	4.5-4.8	4.7-4.9	5.5-8.3
Hidrofobicidad (kJ/residuo)	508	468	468	458

Las proteínas del lactosuero mantienen sus conformaciones nativas en un rango relativamente limitado de temperaturas. Por encima de dichas temperaturas, como por ejemplo, a las alcanzadas durante el proceso de esterilización de la leche, estas proteínas se desnaturalizan y forman agregados (Anema, 2014). Por este motivo, junto con el coste económico que suponen los procesos convencionales como la evaporación, los procesos de separación por membranas son ampliamente utilizados en la industria láctea para concentrar, fraccionar y purificar las proteínas del lactosuero (Kumar *et al.*, 2013). Dos de los principales productos obtenidos mediante estos procesos son los concentrados de proteínas (Whey Protein Concentrates, WPC), utilizados como ingredientes alimentarios, y los aislados de proteínas (Whey Protein Isolates, WPI), empleados en la

preparación de productos de alto valor añadido, como proteínas puras. La diferencia entre ambos productos radica en su contenido proteico: la concentración de proteínas varía entre el 35 y el 80 % en los WPC, mientras que en el caso de los WPI el contenido en proteínas es mayor del 85 % en base seca (Lucena *et al.*, 2006).

2.2. PROCESOS DE SEPARACIÓN POR MEMBRANAS

Una membrana es una barrera semipermeable y selectiva al paso de distintas sustancias. De esta manera, la corriente de entrada al proceso de separación por membranas (corriente alimento) se divide en dos corrientes: aquella que contiene las sustancias que han atravesado la membrana (permeado) y la corriente que contiene los compuestos que han quedado retenidos sobre la membrana (rechazo). Para que esta separación tenga lugar, las membranas se ven sometidas a la acción de una fuerza impulsora: presión, presión parcial, potencial eléctrico o concentración (Mulder, 2000; Baker, 2004).

Entre ellos, los procesos de membranas basados en un gradiente de presión son los más utilizados a nivel industrial, por ejemplo, en las industrias alimentaria, textil, tratamiento de agua para consumo humano, desalación de agua del mar y salobre, etc. (Van der Bruggen *et al.*, 2003). En concreto en la industria alimentaria, este tipo de procesos representan el 20-30 % de los 250 millones de euros de facturación de membranas utilizadas a nivel industrial, donde las mayores aplicaciones se encuentran en la industria láctea (procesos de concentración y purificación de proteínas del lactosuero, desmineralización de lactosuero, estandarización y concentración de la leche), seguida de la industria de bebidas (estabilización de la cerveza y el vino para prevenir la descomposición microbiana, eliminación de coloides y levaduras,

purificación y concentración de zumos) y de los productos derivados del huevo (Daufin *et al.*, 2001; Hinková *et al.*, 2005).

La implantación de los procesos de separación por membranas en las últimas décadas se ha incrementado debido, principalmente, a dos importantes ventajas de este tipo de procesos (Daufin *et al.*, 2001):

- Desde el punto de vista medioambiental, los procesos de membranas se consideran "procesos limpios", puesto que no utilizan otros compuestos auxiliares (como por ejemplo, disolventes). Además, permiten la recuperación de fracciones de alto valor añadido durante el tratamiento de efluentes y aguas residuales.
- Desde el punto de vista económico, comparados con los procesos tradicionales de concentración (procesos térmicos) y separación (decantación, centrifugación, etc.), los procesos de membranas destacan por su facilidad de implementación y automatización, flexibilidad (sistemas modulares) y carácter compacto (m^2 de membrana por m^3 de alimentación).

Los procesos de separación de membranas basados en un gradiente de presión pueden clasificarse en cuatro tipos, dependiendo del tamaño de poro de las membranas, el intervalo de presión transmembranal aplicada y las sustancias rechazadas, de acuerdo con la Tabla 4 y la Fig. 6: microfiltración (MF), ultrafiltración (UF), nanofiltración (NF) y ósmosis inversa (OI) (Van der Bruggen *et al.*, 2003).

Tabla 4. Clasificación de los procesos de membrana según el gradiente de presión aplicado

Proceso	Presión (bar)	Tamaño de poro (nm)	Permeabilidad ($L \cdot h^{-1} \cdot m^{-2} \cdot bar^{-1}$)	Mecanismo de separación
MF	0.1-2	100-10000	>1000	Tamizado ("sieving")
UF	0.1-5	2-100	10-1000	Tamizado
NF	3-20	0.5-2	1.5-30	Tamizado e interacción electrostática
OI	5-120	<0.5	0.05-1.5	Disolución-difusión

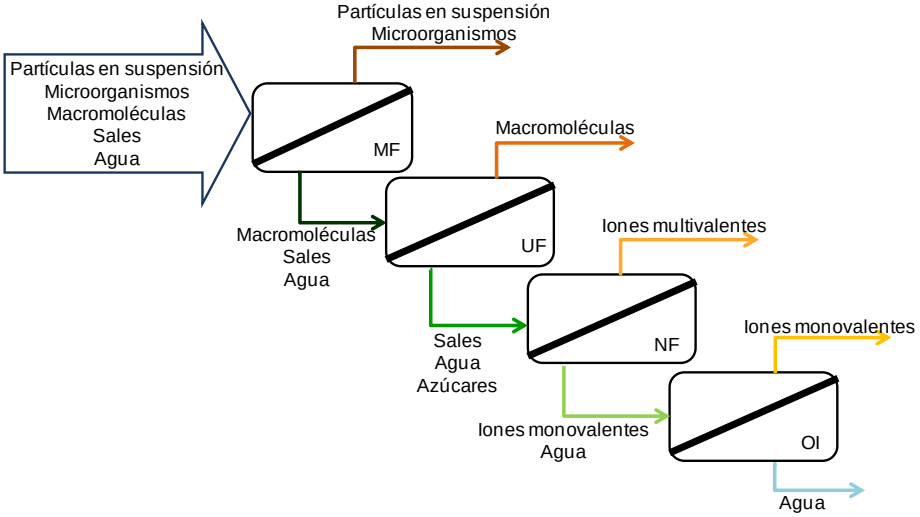

Fig. 6. *Selectividad de los procesos de membranas basados en gradiente de presión*

Dado que la presente Tesis Doctoral se centra en el campo de las membranas de UF, a continuación se describirán los distintos tipos de membranas de UF.

2.2.1. Ultrafiltración

La UF es el proceso de membranas más ampliamente utilizado. Originalmente, se desarrolló para tratar aguas residuales, eliminando las partículas de mayor tamaño que contenían (Shon *et al.*, 2004). En la actualidad, son numerosos los ámbitos industriales en los que las membranas de UF se aplican: tratamiento de aguas residuales procedentes del procesado de aceitunas (El-Abassi *et al.*, 2014), producción de agua potable (Gao *et al.*, 2011), clarificación de zumos de frutas (Ruby Figueroa *et al.*, 2011), concentración de proteínas del lactosuero (Arunkumar y Etzel, 2015), concentración de tinta procedente de aguas residuales de procesos de impresión (Lipnizki, 2008), etc.

Básicamente, las membranas de UF consisten en una capa fina que permite el paso selectivo de sustancias a través de la membrana (capa activa) unida a un soporte más grueso y de mayor porosidad que la capa activa que favorece la permeabilidad de dichas sustancias. Las membranas con este tipo de configuración reciben el nombre de membranas asimétricas o anisotrópicas (Baker, 2004). En función del material del que está constituida la membrana, éstas pueden clasificarse en dos tipos:

- **Orgánicas**: están formadas por polímeros, entre los que destacan polisulfona, poliétersulfona, poliacrilonitrilo, poliimida, poliéterimida, acetato de celulosa, etc. La elección de este polímero dependerá de las características finales deseadas en la membrana, como hidrofilicidad/hidrofobicidad y resistencia química y térmica (Mulder, 2000).

- **Inorgánicas**: están compuestas principalmente por óxidos de aluminio, titanio o silicio. A diferencia de las membranas orgánicas, las membranas inorgánicas son químicamente inertes y presentan una alta resistencia térmica, mecánica y química. Esta elevada estabilidad favorece la utilización de estas membranas en aplicaciones alimentarias, biotecnológicas y farmacéuticas, donde los procesos de limpieza y esterilización (mediante vapor o agentes agresivos, como los compuestos clorados) se realizan repetidamente (Baker, 2004).

Atendiendo a la configuración de las membranas en un módulo, éstas pueden clasificarse en distintos tipos (Mulder, 2000):

- **Planas**: en este tipo de módulos, las membranas se colocan en una configuración tipo "sándwich", en la cual se coloca un espaciador entre las membranas para permitir el paso de la corriente alimento. La densidad de empaquetamiento, es decir, el ratio área de membrana por volumen de módulo, es de aproximadamente 100-400 $m^2 \cdot m^{-3}$.
- **Arrollamiento en espiral**: a partir de la configuración de las membranas dentro de un módulo plano, la configuración de arrollamiento en espiral consiste básicamente en enrollar alrededor de un tubo colector de permeado, las membranas planas y los correspondientes espaciadores. De esta manera, el espaciador actúa además como un promotor de turbulencias. La densidad de empaquetamiento en este tipo de membranas es de 300-1000 $m^2 \cdot m^{-3}$, por lo que, debido a

su carácter compacto, son uno de los tipos de módulos más utilizados a nivel industrial.

- **Tubulares**: generalmente, las membranas tubulares presentan un diámetro de al menos, 10 mm. Pueden colocarse dentro de un módulo de membranas en número variable, desde 1 hasta 18, aproximadamente. Existen diferentes configuraciones de membranas tubulares, en función del número de canales en el interior del tubo. En este caso, la corriente alimento circula por el interior de las membranas tubulares. El principal inconveniente de este tipo de configuración es su baja densidad de empaquetamiento, menor de 300 $m^2 \cdot m^{-3}$. Sin embargo, dada su baja tendencia al ensuciamiento y a su facilidad de limpieza, sobretodo en el caso de las membranas tubulares cerámicas, son la configuración más utilizada en la industria láctea.
- **Capilares y de fibra hueca**: la configuración de estas membranas es similar a las membranas tubulares. Sin embargo, las principales diferencias radican en el menor tamaño de las membranas capilares y de fibra hueca y en que no necesitan ubicarse dentro de un módulo que actúe de soporte. En este tipo de membranas, la alimentación puede circular en dos sentidos diferentes: desde el interior del capilar ("lumen side") hacia el exterior o bien desde el exterior del capilar ("shell side") hacia el interior. La densidad de empaquetamiento se encuentra, en el caso de las membranas capilares, alrededor de 600-1200 $m^2 \cdot m^{-3}$; mientras que las membranas de fibra hueca presentan la

densidad de empaquetamiento más elevada (hasta 30000 $m^2 \cdot m^{-3}$).

A pesar de las numerosas ventajas que ofrece la implantación de los procesos de separación por membranas en la industria, y en particular de las membranas de UF en la industria alimentaria, estas membranas presentan un principal inconveniente: la disminución de la densidad de flujo de permeado durante el tiempo de operación debido al ensuciamiento sufrido por las membranas. Este efecto conlleva una reducción de la producción global del proceso, así como un aumento de los costes de mantenimiento y limpieza (Zydney *et al.*, 2003). En el siguiente apartado se detallarán los tipos de ensuciamiento que pueden producirse, sus causas y las posibles técnicas para reducirlo y predecirlo.

2.3. ENSUCIAMIENTO DE MEMBRANAS Y MODELOS MATEMÁTICOS

Como se ha comentado anteriormente en este Capítulo, las membranas de UF son muy utilizadas en la industria alimentaria en general, y en la industria láctea en particular, en distintas aplicaciones como la concentración de la leche y la purificación, concentración y fraccionamiento de proteínas del lactosuero (Nigam *et al.*, 2008; Kazemimoghadam y Mohammadi, 2007). Durante estos procesos, las membranas se ensucian debido, principalmente, a las proteínas presentes en la leche y en el lactosuero, las cuales son retenidas por la membrana.

El fenómeno de ensuciamiento viene determinado por las interacciones entre las moléculas de suciedad y entre dichas moléculas y la superficie de la membrana. La magnitud de estas interacciones depende de las condiciones de operación del proceso de UF, como la velocidad tangencial, la presión transmembranal, la composición de la corriente alimento o la temperatura (Wang *et al.*, 2012). Por un lado, existe una repulsión electrostática entre las distintas moléculas de ensuciamiento, dado que para un determinado valor de pH, todas poseen la misma carga superficial. En el caso de las proteínas más abundantes presentes en el lactosuero (α-La, β-Lg y BSA), dicha carga es negativa a pH neutro. La repulsión electrostática será menor cuanto más cercano sea el pH de la disolución al punto isoeléctrico (pI) de las sustancias en disolución,

valor de pH en el que la carga superficial de dichas sustancias es cero (Huisman *et al.*, 2000). Además, en el caso en el que las membranas presenten la misma carga superficial que la de las moléculas de suciedad, la repulsión electrostática también tendrá lugar en la superficie de la membrana y dichas moléculas, disminuyendo la adsorción de las mismas sobre la membrana. Por otra parte, cuando la estructura química de los grupos funcionales es similar entre la membrana y las moléculas de suciedad, puede producirse una interacción hidrofóbica/hidrofílica, en función de la naturaleza de dichos grupos (Liu *et al.*, 2000). Por consiguiente, el mayor o menor ensuciamiento producido en las membranas será resultado de un balance de fuerzas entre la repulsión electrostática y las interacciones hidrofóbicas/hidrofílicas.

Además del fenómeno de ensuciamiento propiamente dicho, durante el proceso de UF tiene lugar una acumulación de las moléculas de soluto que constituyen la corriente alimento en las proximidades de la superficie de la membrana (capa límite). Este hecho se conoce con el nombre de polarización por concentración y está principalmente causado por las limitaciones inherentes al proceso de transferencia de materia, es decir, la causa radica en fenómenos hidrodinámicos y difusivos. El aumento de concentración de soluto en las inmediaciones de la membrana como consecuencia de la polarización por concentración puede dar lugar a la formación de una capa gel sobre la superficie de la membrana (Zhao *et al.*, 2000). La Fig. 7 muestra una representación esquemática del proceso de polarización por concentración y de la formación de capa gel (Baker, 2004).

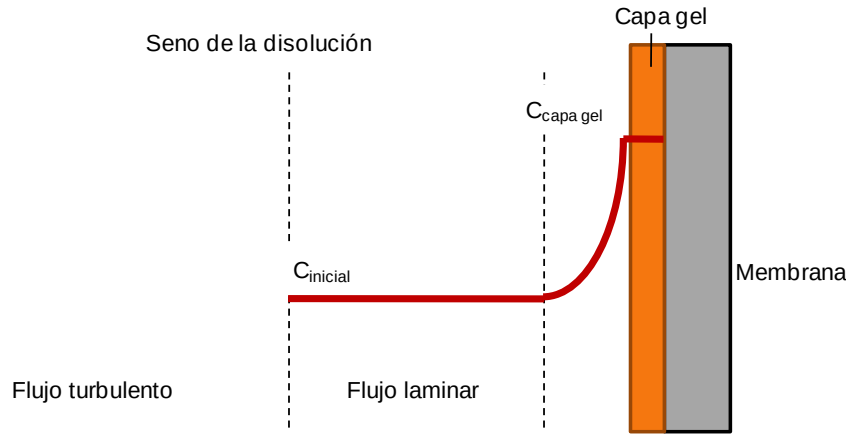

Fig. 7. *Esquema de los fenómenos de polarización por concentración y formación de capa gel*

2.3.1. Tipos de ensuciamiento

Existen distintas clasificaciones del ensuciamiento producido en las membranas de UF. Una de estas clasificaciones se basa en la naturaleza de las sustancias que causan dicho ensuciamiento, distinguiéndose cuatro tipos (Liu *et al.*, 2001):

- **Inorgánico**: también conocido como "scaling", se debe a la acumulación de sales minerales o hidróxidos metálicos precipitados sobre la superficie de la membrana, aunque también pueden quedar atrapados en la estructura porosa de la membrana. Dicha precipitación se produce al exceder la concentración de saturación de estas especies. Aunque este tipo de ensuciamiento es característico de las membranas de OI y NF, en el caso de las membranas de UF puede llegar a producirse por la unión de los iones susceptibles de precipitar

con otros agentes de ensuciamiento, lo que provoca la precipitación y acumulación de los primeros (Shirazi *et al.*, 2010).

- **Orgánico**: se produce durante el tratamiento de corrientes con un alto contenido en materia orgánica, como por ejemplo, en el tratamiento de disoluciones propias de la industria láctea. En este caso, las proteínas presentes en dichas disoluciones pueden acumularse sobre la superficie de la membrana e incluso, penetrar en su estructura porosa. Otras corrientes que pueden causar ensuciamiento severo de tipo orgánico sobre las membranas son las que contienen ácido húmico (Hong y Elimelech, 1997).
- **Coloidal**: las partículas causantes de este tipo de ensuciamiento pueden ser de origen orgánico, inorgánico o mixto. Su acumulación sobre la superficie de la membrana provoca un ensuciamiento que puede ser fácilmente eliminado mediante procesos de limpieza hidráulicos, como por ejemplo, “backflushing”. Sin embargo, en el caso de que el tamaño de los coloides sea menor que el tamaño de poro de la membrana, éstos pueden penetrar en la estructura porosa de la misma. En este último caso, serían necesarios protocolos de limpieza más agresivos para eliminar el ensuciamiento coloidal (Kwon *et al.*, 2006).
- **Microbiano**: como su nombre indica, consiste en el ensuciamiento producido por la acumulación de bacterias y otros microorganismos en la superficie de la membrana. Estos microorganismos generan diversas sustancias extracelulares que los protegen en cierta medida de los

compuestos químicos utilizados durante las etapas de limpieza. Este tipo de ensuciamiento es especialmente importante en la industria láctea, donde, para evitarlo, los protocolos de limpieza incluyen etapas de desinfección utilizando, por ejemplo, compuestos clorados (D'Souza y Mawson, 2005).

Otra posible clasificación del ensuciamiento de las membranas atiende a la facilidad con la que el mismo puede ser eliminado. En otras palabras, está relacionado con el lugar en la que las partículas se acumulan y los métodos para eliminarlos (Fig. 8). Así, el ensuciamiento puede clasificarse en (Baker, 2004):

- **Reversible**: se debe generalmente a la deposición superficial de moléculas de suciedad sobre la superficie de la membrana. Este tipo de ensuciamiento puede ser controlado mediante el uso de altas velocidades tangenciales o promotores de turbulencia y utilizando membranas con carga contraria a la carga superficial de las moléculas de suciedad, de manera que se minimicen las fuerzas de adhesión molécula-membrana. Los métodos de limpieza físicos, como la aireación o el contralavado ("backwashing") son suficientes para eliminar el ensuciamiento reversible.
- **Irreversible**: aunque también puede incluir el ensuciamiento provocado por las moléculas más fuertemente adsorbidas sobre la superficie de la membrana, el ensuciamiento irreversible está principalmente causado por partículas de menor tamaño que los poros de la membrana y que penetran en el interior de la estructura porosa de la misma. Para

eliminar este tipo de ensuciamiento son necesarios métodos de limpieza químicos, puesto que los métodos físicos no son suficientes (Bai *et al.*, 2013).

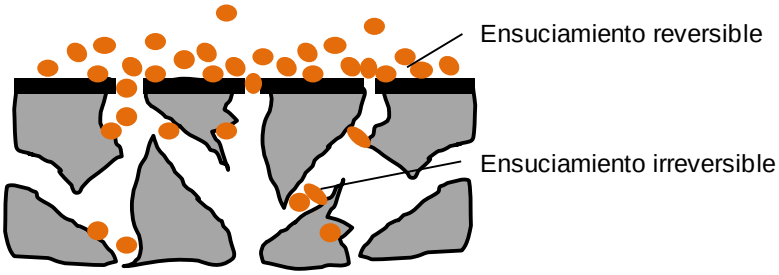

Fig. 8. *Representación del ensuciamiento reversible e irreversible*

2.3.2. Mecanismos de ensuciamiento y modelos matemáticos

El ensuciamiento de las membranas explicado anteriormente tiene lugar según distintos mecanismos. Estos pueden clasificarse de la siguiente manera (ver Fig. 9) (Ruby Figueroa *et al.*, 2011; Vincent Vela *et al.*, 2009; Salahi *et al.*, 2010):

- Si las moléculas de suciedad son más pequeñas que los poros de la membrana, éstas pueden penetrar en la estructura interna de la membrana. En consecuencia, el radio efectivo de poro se reduce gradualmente (**ensuciamiento por adsorción o bloqueo estándar de los poros**).
- Cuando las moléculas de suciedad tienen un tamaño similar al de los poros de la membrana, éstas pueden taponar parcial o completamente la entrada de los poros de manera

superficial (**bloqueo intermedio o completo de los poros, respectivamente**).

- En el caso en el que las moléculas de suciedad tienen un tamaño mucho mayor que el de los poros de la membrana, éstas se depositan sobre la superficie de la misma, llegando a formar en algunos casos una torta (**mecanismo de formación de torta**).

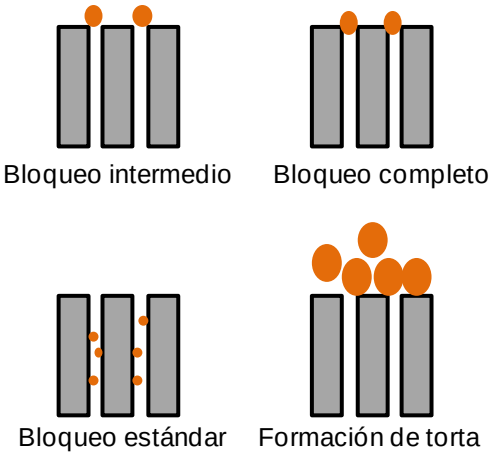

Fig. 9. *Esquema de los distintos mecanismos de ensuciamiento*

Debido a las consecuencias negativas que conllevan los fenómenos de ensuciamiento, determinar las condiciones de operación óptimas para minimizarlo, así como poder predecir el descenso de la densidad de flujo de permeado con el tiempo son aspectos clave en los procesos de UF. Para llevar a cabo esta predicción, diversos autores han desarrollado y/o adaptado modelos matemáticos basados en las condiciones experimentales del proceso y en parámetros teóricos (Hermia, 1982; Vincent Vela *et al.*, 2009; Ho y Zydney, 2003; Peng y Tremblay, 2008; Yee *et al.*, 2009).

Entre los distintos modelos matemáticos, los modelos empíricos son capaces de predecir los datos experimentales con una alta precisión. Sin embargo, la ecuación general de estos modelos no considera parámetros teóricos. Esto implica que la descripción teórica de los fenómenos de ensuciamiento y sus mecanismos no está reflejada en la ecuación general de estos modelos, por lo que la relación entre la disminución de la densidad de flujo de permeado y los mecanismos de ensuciamiento propios del proceso de UF no puede ser completamente explicada. Un ejemplo de este tipo de modelos son las ecuaciones obtenidas mediante análisis de regresión (Baranyi *et al.*, 1996). Por el contrario, los modelos completamente teóricos contribuyen a la explicación de los fenómenos de ensuciamiento y sus mecanismos durante el proceso de UF. Sin embargo, la precisión del ajuste de estos modelos es menor al no considerar todas las condiciones experimentales del propio proceso.

Por estas razones, los modelos semi-empíricos son los más ampliamente utilizados, porque a partir de formas simplificadas de las leyes científicas e incluyendo un cierto número de parámetros con significado físico, son capaces de predecir con elevada precisión los datos experimentales obtenidos y describir, simultáneamente, los mecanismos de ensuciamiento que tienen lugar (Vincent Vela, 2009; Mah *et al.*, 2012).

Entre los distintos modelos matemáticos disponibles en la bibliografía, los modelos semi-empíricos de Hermia (Hermia, 1982) desarrollados para filtración convencional (“dead-end”) y la adaptación de los mismo a filtración tangencial (“crossflow”) son los

más ampliamente utilizados por distintos autores para ajustar los datos experimentales obtenidos en diversos procesos de UF y explicar los mecanismos de ensuciamiento producidos por diferentes alimentaciones (Mohammadi y Esmaeelifar, 2005; Vincent Vela, 2009; Salahi *et al.*, 2010; Kaya *et al.*, 2010). Los modelos de Hermia consideran cuatro mecanismos de ensuciamiento principales, que coinciden con los mecanismos explicados anteriormente: bloqueo completo, intermedio y estándar de poros y formación de torta. Las hipótesis en las que se basa cada uno de estos mecanismos se detallan en el Capítulo IV (Corbatón-Báguena *et al.*, 2015).

A pesar de la precisión de su ajuste, los modelos de Hermia proporcionan una ecuación matemática para cada mecanismo de ensuciamiento diferente, sin considerar las posibles interacciones entre distintos mecanismos. Sin embargo, de acuerdo con diversos autores (Ho y Zydney, 2000; Nigam *et al.*, 2008), la evolución de la densidad de flujo de permeado con el tiempo puede dividirse en varias etapas: durante los primeros minutos tiene lugar un descenso rápido de la densidad de flujo de permeado causado por el fenómeno de polarización por concentración (etapa 1); a continuación, la densidad de flujo disminuye gradualmente debido al taponamiento y/o bloqueo de los poros y a la aparición de una torta encima de la superficie de la membrana (etapa 2); en la última etapa, la torta formada aumenta su espesor, alcanzando finalmente el estado estacionario (etapa 3) (ver Fig. 10).

Por este motivo, algunos autores combinaron ecuaciones características de diferentes mecanismos de ensuciamiento en una

única ecuación general del modelo matemático. Por ejemplo, De la Casa *et al.* (De la Casa *et al.*, 2008) combinó las ecuaciones correspondientes a los mecanismos de bloqueo completo de poros y formación de torta propuestos por Hermia para filtración convencional en un único modelo. En base a esta combinación, en la presente Tesis Doctoral se han utilizado las ecuaciones correspondientes a los mecanismos de bloqueo de poros y formación de torta adaptados a flujo tangencial para proponer la ecuación general del modelo combinado.

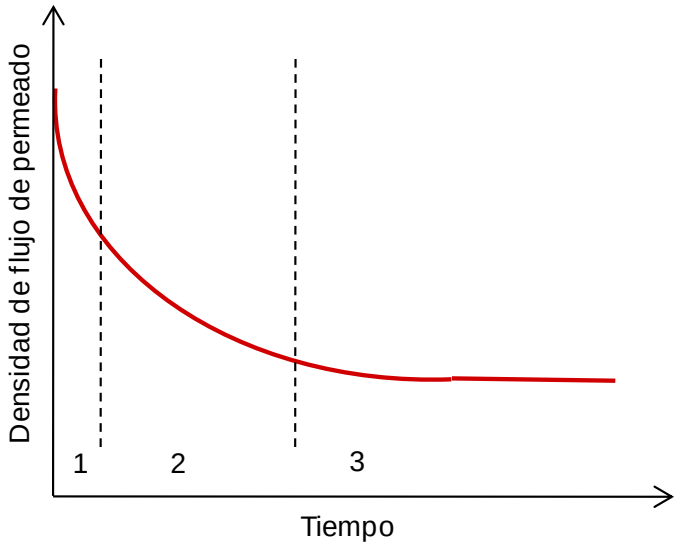

Fig. 10. *Evolución de la densidad de flujo de permeado con el tiempo*

Por otra parte, los modelos de resistencias en serie son los modelos empíricos más utilizados (Choi *et al.,* 2000; Carrère *et al.*, 2001). Este tipo de modelos se basa en la ley de Darcy, según la cual la densidad de flujo de permeado es inversamente proporcional a la resistencia total al paso de fluido a través de la membrana. A medida que la membrana se va ensuciando durante el proceso de UF, la

resistencia total puede expresarse como la suma de la resistencia intrínseca de la membrana y de las diferentes resistencias asociadas a cada uno de los mecanismos o fenómenos de ensuciamiento que están teniendo lugar (adsorción, torta, irreversible, reversible, etc.).

La explicación detallada de cada uno de los modelos utilizados, así como las ecuaciones generales de cada uno de ellos, se encuentra en el Capítulo IV de esta Tesis.

2.4. TÉCNICAS DE LIMPIEZA DE MEMBRANAS

Debido al ensuciamiento en las membranas, cada cierto tiempo éstas deben acondicionarse para eliminar las moléculas de suciedad de la superficie de la membrana y del interior de su estructura porosa y recuperar las propiedades permselectivas de la misma (Blanpain-Avet, 2009). En la industria alimentaria, los procesos de limpieza de membranas de UF son una etapa fundamental del proceso global de producción. En muchos casos, los protocolos de limpieza necesitan llevarse a cabo todos los días, constituyendo más del 80 % de los costes totales de producción (Almécija *et al.*, 2009b). Por esta razón, seleccionar los mejores protocolos de limpieza y las condiciones de operación más adecuadas para optimizar el proceso de limpieza es de gran importancia (Kazemimoghadam y Mohammadi, 2007). Sin embargo, la elección de un protocolo de limpieza u otro viene determinada por la localización del ensuciamiento (superficial, interno en la estructura porosa, etc.), la composición de la alimentación, el tipo de moléculas de suciedad depositadas sobre la superficie de la membrana o en el interior de su estructura porosa (Cabero *et al.*, 1999).

2.4.1. Tipos de métodos de limpieza

Una clasificación básica de los métodos de limpieza de membranas consiste en la división de dichos métodos en físicos y químicos. Los métodos físicos están basados en la aplicación de esfuerzos mecánicos para eliminar las partículas adsorbidas sobre la superficie

de la membrana (ensuciamiento reversible) (Zhao *et al.*, 2000). La principal ventaja de estos métodos radica en que no utilizan reactivos químicos, por lo que el impacto medioambiental de las aguas residuales generadas en el proceso de limpieza es menor. Además, son métodos más rápidos que los protocolos químicos, conllevando una degradación menor de las membranas, aunque la eficacia de limpieza alcanzada con este tipo de métodos es menor (Judd *et al.*, 2008). Algunos de los métodos físicos más importantes se describen a continuación (Zhao *et al.*, 2000):

- **Backflushing**: es uno de los métodos físicos más utilizados en la industria. Consiste en aplicar presión en el lado del permeado, de manera que éste vuelva a atravesar la membrana. La efectividad de este método depende no sólo de la naturaleza del ensuciamiento, sino también de la frecuencia e intensidad con la que se invierte el flujo de permeado.
- **Aireación**: como su nombre indica, este método se basa en la introducción de aire de manera periódica, en el mismo sentido de flujo que la corriente alimento. El aire permite el debilitamiento de la capa de suciedad depositada sobre la membrana. Este método se utiliza principalmente en biorreactores de membrana (MBR) y en membranas de fibra hueca (Wang *et al.*, 2014).
- **Promotores de turbulencias**: este método consiste en la mejora de las condiciones hidrodinámicas en las proximidades de la superficie de la membrana. De esta manera, se incrementa el fenómeno de transferencia de

materia a la vez que se reduce el fenómeno de polarización por concentración. Este método físico es especialmente importante en membranas de arrollamiento en espiral (Krstić *et al.*, 2002).

- **Ultrasonidos**: este método de limpieza se fundamenta en el fenómeno de cavitación, según el cual las burbujas de aire formadas colapsan e implosionan. La efectividad de este método depende de la potencia y frecuencia de los ultrasonidos (Muthukumaran *et al.*, 2004). Cuando los ultrasonidos se aplican a un medio líquido (generalmente, la corriente alimento), se producen ciclos de compresión y expansión del medio. Durante el ciclo de compresión, las micro burbujas colapsan, emitiendo energía, lo que permite la limpieza de la membrana (Li *et al.*, 2002). Otra manera de aplicar la técnica de ultrasonidos consiste en instalar una celda o módulo con la membrana en su interior dentro del baño de ultrasonidos (Cai *et al.*, 2010).
- **Campos eléctricos**: aunque se detallará más adelante en este mismo Capítulo, la limpieza mediante campos eléctricos es una técnica novedosa comenzada a aplicar en los últimos años. Se basa en la diferente carga que presentan las proteínas y la membrana en un determinado intervalo de pH. Al aplicar un campo eléctrico, las partículas con carga opuesta (moléculas de suciedad) son atraídas hacia uno de los electrodos, generalmente colocado en el seno de la disolución alimento, pudiendo eliminarse de la superficie de la membrana (Tarazaga *et al.*, 2006).

Por otra parte, los métodos químicos de limpieza de membranas son los más utilizados a nivel industrial por su mayor eficacia respecto a los métodos de limpieza físicos (Kazemimoghadam y Mohammadi, 2007). Los métodos químicos se basan en la acción específica de un determinado reactivo químico sobre las partículas de suciedad adsorbidas tanto en la superficie de la membrana como en su estructura interna. Por tanto, este tipo de métodos resulta especialmente eficaz para eliminar el ensuciamiento irreversible ocasionado en las membranas. La mayoría de estos métodos incluyen agentes químicos como ácidos, álcalis, surfactantes, desinfectantes o combinaciones de ellos, causando reacciones de hidrólisis, peptización, saponificación y solubilización, entre otras (Chen *et al.*, 2003). A continuación se detallan cada uno de estos agentes químicos:

- **Álcalis**: son el grupo de agentes químicos de limpieza más ampliamente utilizados, destacando los hidróxidos, silicatos, carbonatos, bicarbonatos, orto y metasilicatos de sodio. Son especialmente efectivos en la eliminación de materia orgánica, debido a las reacciones de hidrólisis y solubilización que se producen al aumentar la carga orgánica del compuesto a eliminar por efecto del incremento del pH de la disolución (Ang *et al.*, 2006).
- **Ácidos**: utilizados principalmente cuando el ensuciamiento de las membranas se debe a especies de naturaleza inorgánica, entre los ácidos más utilizados destacan los ácidos nítrico, fosfórico y cítrico (Blanpain-Avet *et al.*, 2009; Woo *et al.*, 2015).

- **Surfactantes o tensioactivos**: son compuestos con grupos hidrofóbicos e hidrofílicos utilizados para mejorar la mojabilidad de especies poco solubles en agua y así, poder eliminar estas especies de la membrana. Al ser menos agresivos que los álcalis y los ácidos, se suelen aplicar en membranas que presentan limitaciones de pH. Su mecanismo de actuación se basa en la difusión desde el seno de la disolución de limpieza hasta la capa de ensuciamiento y la posterior solubilización de las moléculas de suciedad adheridas a la membrana mediante la formación de micelas alrededor de dichas moléculas (Naim *et al.*, 2012; Suárez *et al.*, 2012).
- **Agentes complejantes**: estos agentes químicos rompen la estructura de la capa de ensuciamiento mediante su enlace con los cationes divalentes (como el catión Ca^{+2}) presentes en dicha capa, que actúan como agentes de entrecruzamiento de las moléculas orgánicas. Uno de los agentes complejantes más utilizado es el ácido etilendiaminotetraacético (EDTA) (Hong y Elimelech, 1997; Ang *et al.*, 2011).
- **Enzimas**: estos agentes biológicos son de especial importancia en el caso de membranas con baja resistencia térmica, química o de pH, debido a la capacidad de las enzimas para llevar a cabo la limpieza de las membranas en unas condiciones de operación más suaves (Argüello *et al.*, 2003). Entre sus principales ventajas destacan el menor consumo energético (por la operación a temperaturas suaves) e impacto ambiental (puesto que son compuestos

biodegradables). Sin embargo, presentan como principal inconveniente el hecho de que sólo actúan sobre cierto tipos de ensuciamiento.

- **Desinfectantes**: en el caso en que pueda ocurrir el crecimiento de microorganismos en la membrana, se utilizan agentes desinfectantes, entre los que destaca el hipoclorito de sodio (Paugam *et al.*, 2010). Sin embargo, este tipo de agentes no puede utilizarse en membranas sensibles a altas concentraciones de cloro o pH.

En el caso de la industria alimentaria, en particular en la industria láctea, diversos autores (Almécija *et al.*, 2009a; Almécija *et al.*, 2009b) proponen el mismo protocolo de limpieza química de membranas: en primer lugar, se realiza una limpieza con álcalis, seguida de un aclarado para eliminar los restos de agente de limpieza. A continuación, se lleva a cabo una etapa de limpieza ácida, seguida de su correspondiente aclarado. Finalmente, si las características permselectivas de la membrana no coinciden con las que presentaba la membrana originalmente, se recomienda realizar una tercera etapa de limpieza utilizando surfactantes o desinfectantes, como hipoclorito sódico o sodio dodecil sulfato.

La efectividad de este protocolo de limpieza química depende, en gran medida, de las condiciones de operación aplicadas durante el mismo (Blanpain-Avet *et al.*, 2009). Algunos de los factores más influyentes sobre el proceso de limpieza química se destacan a continuación:

- **Temperatura**: en general, en los procesos de transferencia de materia, el coeficiente de difusión aumenta a medida que la temperatura aumenta y, así, la velocidad con la que las moléculas de suciedad migran desde la superficie de la membrana hacia la disolución de limpieza aumenta. Además, las altas temperaturas pueden debilitar la estructura de la capa de ensuciamiento depositada sobre la membrana, facilitando su hinchamiento y su eliminación. Por otra parte, la temperatura aumenta la velocidad con la que las reacciones químicas tienen lugar, por lo que la interacción entre las moléculas de suciedad y las de agente de limpieza es mayor a medida que se incrementa la temperatura de la disolución de limpieza (Lee y Elimelech, 2007).
- **Velocidad tangencial**: cuando la velocidad tangencial aumenta, el esfuerzo cortante generado también aumenta, lo que provoca la erosión de la capa de suciedad y su eliminación de la superficie de la membrana. Además, el aumento de velocidad tangencial también favorece la generación de turbulencia cerca de la superficie de la membrana, lo que favorece la migración de las moléculas de suciedad desde la superficie de la membrana hasta el seno de la disolución de limpieza (Smith *et al.*, 2006; Mores y Davis, 2002).
- **Presión transmembranal**: al tratarse de la fuerza impulsora del proceso de UF, la presión transmembranal es la causa de que las moléculas de suciedad se muevan hacia la superficie de la membrana. Por tanto, durante la etapa de limpieza, cuanto menor sea la presión transmembranal aplicada menor

será la fuerza con la que las moléculas tanto de suciedad como de agente de limpieza se desplazan hacia la membrana. De esta manera, se evita la compactación de la capa de ensuciamiento ya formada sobre la membrana, así como la acumulación de moléculas de agente de limpieza en la misma (Zhao *et al.*, 2000).

- **Concentración del agente de limpieza**: además del coste económico que supone la utilización en exceso de reactivos químicos durante la limpieza de las membranas, otros autores han demostrado que existe una concentración óptima de agente de limpieza a la que llevar a cabo dicho proceso. Hasta ese valor óptimo, un aumento de concentración favorece la limpieza, pero por encima de dicha concentración, los mecanismos de ensuciamiento y limpieza por parte de las moléculas de estos agentes químicos podrían ser competitivos (Cabero Cabero, 1997; Argüello *et al.*, 2002).
- **pH y fuerza iónica del medio**: cuando se ultrafiltran disoluciones que presentan especies cargadas (como es el caso de las proteínas durante la UF del lactosuero), las interacciones soluto-soluto y soluto-membrana pueden variar significativamente en función del valor de pH y de la fuerza iónica de la disolución. Generalmente, a valores de pH cercanos al pI de la proteína, la repulsión electrostática entre ellas es muy pequeña, por lo que podrían precipitar sobre la superficie de la membrana. Además, la carga superficial de las membranas también puede verse afectada por el valor de pH, pudiendo generarse una repulsión electrostática entre las

moléculas de suciedad y la membrana. Este hecho facilitaría la limpieza de las membranas (Matzinos y Álvarez, 2002).

A pesar de la mayor o menor efectividad de los métodos químicos de limpieza, los agentes convencionales anteriormente citados pueden ser agresivos con las membranas y dañarlas más o menos rápidamente, reduciendo su vida útil y su selectividad, así como aumentando los costes de producción (grandes consumos de agua y energía y larga duración del ciclo de limpieza) (Blanpain-Avet, 2009). Además, estos agentes de limpieza convencionales presentan un impacto medioambiental negativo cuando son descargados como aguas residuales después del proceso de limpieza. Para solventar estos problemas, algunos autores han propuesto limpiezas basadas en técnicas alternativas, como los ultrasonidos, los campos eléctricos y las disoluciones salinas han aumentado en los últimos años (Muthukumaran *et al.*, 2004; Tarazaga *et al.*, 2006; Lee y Elimelech, 2007). A continuación se describen dos de dichas técnicas alternativas (disoluciones salinas y campos eléctricos), que corresponden con las técnicas consideradas en la presente Tesis Doctoral.

2.4.2. Limpieza mediante disoluciones salinas

La utilización de disoluciones salinas como técnica de limpieza es un proceso todavía en investigación, puesto que se desconocen exactamente los mecanismos que permiten la eliminación de la materia orgánica adsorbida en la membrana.

El principal trabajo en el que se han empleado disoluciones salinas para la limpieza de membranas ha sido realizado por Lee y Elimelech (2007). Estos autores investigaron la limpieza de membranas de OI que habían sido previamente ensuciadas con disoluciones de materia orgánica natural, alginatos y pectinas. Como agentes de limpieza, se utilizaron distintos tipos de sales (NaCl, $NaNO_3$, KCl, CaCl, NH_4Cl y Na_2SO_4) y muestras de agua de mar. Los resultados de los ensayos de limpieza demostraron que, entre las sales inertes utilizadas, las disoluciones de NaCl a bajas concentraciones (25 mM) fueron las más efectivas para limpiar las membranas de OI. Los ensayos de limpieza realizados con muestras de agua de mar (con una fuerza iónica similar a la de las disoluciones de NaCl 100 mM) demostraron que el agua de mar podía ser efectiva para eliminar los depósitos de ensuciamiento acumulados en las membranas ensayadas. De acuerdo con estos autores, la limpieza mediante disoluciones salinas tiene lugar según dos mecanismos: en primer lugar, se ocasionan cambios en la capa de ensuciamiento unida a la membrana debido a la diferencia de concentración de sal entre el seno de la disolución y la capa de ensuciamiento. Esta diferencia de presión osmótica tiene como consecuencia el hinchamiento de la capa de suciedad y, por consiguiente, el debilitamiento de la interacción capa-membrana debido a la disminución de las fuerzas de adhesión entre las moléculas de suciedad que forman la capa. A continuación, se produce una reacción de intercambio iónico entre los iones de la sal y los iones presentes en la capa de suciedad (por ejemplo, el catión Ca^{+2} que une las cadenas de proteínas). Al realizarse este intercambio iónico, la capa de ensuciamiento se rompe y puede eliminarse de la superficie de la membrana,

transportando dichas moléculas hacia el seno de la disolución (ver Fig. 11).

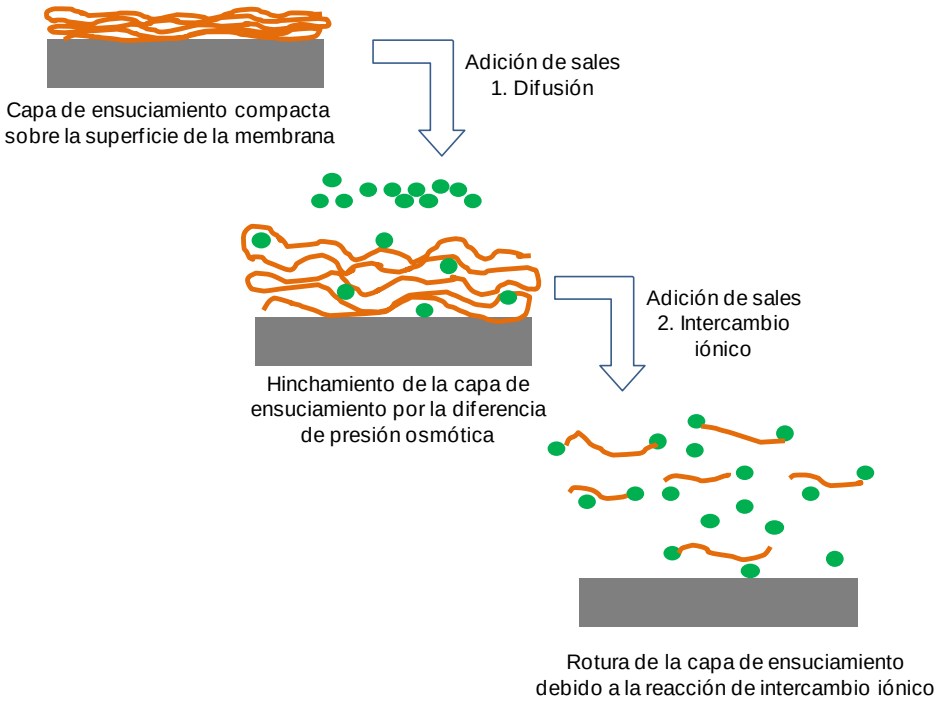

Fig. 11. *Esquema del mecanismo de limpieza mediante disoluciones salinas propuesto por Lee y Elimelech (2007)*

Por otra parte, algunos autores (Hofmeister, 1888; Curtis y Lue, 2006; Tsumoto *et al.*, 2007; Zhang, 2012) han investigado el efecto de distintos cationes y aniones sobre la interacción proteína-proteína. De acuerdo con la capacidad de dichos iones para precipitar las proteínas (efecto "salting-out") o bien aumentar su solubilidad (efecto "salting-in"), Hofmeister (Hofmeister, 1888) ordenó diferentes sales en una serie (Fig. 12). En base a esta serie, otros autores (Tsumoto *et al.*, 2007) han demostrado que algunas de ellas, como NaCl, producen un incremento en la solubilidad de las proteínas, mientras

que otras, como Na_2SO_4, la disminuyen. Por su parte, Nucci y Vanderkooi (Nucci y Vanderkooi, 2008) estudiaron la habilidad de cationes mono y divalentes para precipitar proteínas. Entre ellos, el calcio fue uno de los que presentó un mayor efecto "salting-out", lo cual confirma estudios previos en los que el calcio actuaba como enlace entre las cadenas de proteínas (Ang y Elimelech, 2007).

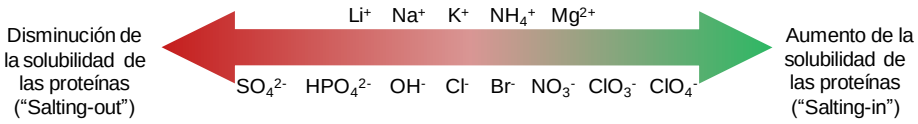

Fig. 12. *Clasificación de distintos iones en función de su carácter "salting-in" y "salting-out" propuesto por Hofmeister (1888)*

Finalmente, Zhang (Zhang, 2012) investigó las interacciones proteína-proteína en diferentes disoluciones salinas a distintos valores de pH (mayores y menores del punto isoeléctrico de las proteínas), describiendo el mecanismo responsable de los cambios en dichas interacciones mediante la diferente capacidad de hidratación de los cationes y aniones estudiados. De acuerdo con la ley de afinidad al agua, algunos aniones monovalentes como el ión Cl^- están débilmente hidratados dado que su tamaño es mucho mayor que el de los cationes monovalentes, por lo que interaccionan preferiblemente con los grupos de las cadenas proteínicas débilmente cargados. Éste es el caso de los residuos positivamente cargados de las cadenas de proteínas y los grupos funcionales no polares. El efecto de dicha interacción es el aumento de la solubilidad de las proteínas, debido al incremento de las fuerzas electrostáticas de repulsión entre las mismas a pH superiores a su punto isoeléctrico (pI).

Finalmente, Matzinos y Álvarez (Matzinos y Álvarez, 2002) investigaron el efecto de la fuerza iónica de la disolución de limpieza sobre la eficacia de este proceso, demostrando que un aumento de la fuerza iónica del medio durante la etapa de aclarado incrementaba la cantidad de calcio eliminado, debido al aumento de su solubilidad a bajos valores de fuerza iónica y a la eliminación del calcio unido a las proteínas. Concretamente, este estudio se realizó con disoluciones de lactosuero en las que los iones calcio y fosfato forman sales insolubles que pueden precipitar sobre la superficie de la membrana. Gracias a la adición de NaCl a la disolución de aclarado, la cantidad de calcio eliminado aumentó considerablemente, lo que demuestra la efectividad de las disoluciones salinas eliminando parte del ensuciamiento inorgánico.

2.4.3. Limpieza mediante campos eléctricos

La investigación de la aplicación de campos eléctricos como técnica física de limpieza ha aumentado en los últimos años en distintos procesos de separación por membranas, especialmente MF y UF. Este método se fundamenta en la generación de un campo eléctrico entre dos electrodos (ánodo y cátodo) situados a ambos lados de la membrana o bien siendo la membrana uno de los electrodos (Huotari *et al.*, 1999). El mecanismo de limpieza se basa en la aparición de una fuerza electrostática de repulsión adicional que provoca el desplazamiento de partículas desde uno de los electrodos al otro (Qin *et al.*, 2011). Para que dicho desplazamiento se lleve a cabo, resulta especialmente importante conocer la carga superficial de las

partículas que se pretenden transferir y la carga de la membrana, para el valor de pH de la disolución de limpieza.

La mayoría de estudios que han aplicado campos eléctricos a procesos de UF se centran en el aumento de la densidad de flujo de permeado durante la etapa de ensuciamiento, al disminuir la polarización por concentración y la formación de torta (Tarazaga *et al.*, 2006; Song *et al.*, 2010; Agana *et al.*, 2012; Holder *et al.*, 2013). En estos casos, los campos eléctricos se aplican para mejorar el comportamiento de membranas poliméricas e inorgánicas utilizadas para tratar disoluciones de diferentes partículas cargadas (BSA, hidrolizados de caseína, aguas residuales de post-electrodeposición de pinturas). Al aplicar un determinado potencial entre ambos electrodos, las partículas cargadas se transfieren desde la superficie de la membrana hacia el electrodo que se encuentra en el seno de la disolución o en el rechazo (según si la membrana es tubular o plana). En el caso de las disoluciones proteínicas, este electrodo suele estar cargado positivamente (ánodo) para que las proteínas, que generalmente presentan carga negativa al pH típico de las disoluciones tratadas, se desplacen hacia él. Así pues, la disolución alimento quedará concentrada en las sustancias deseadas, pudiendo impedirse el paso de estas sustancias que, de acuerdo con su tamaño de poro y sin la aplicación de campos eléctricos, no serían retenidas por la membrana.

Algunos autores (Holder *et al.*, 2013) han aplicado campos eléctricos durante la etapa de limpieza en membranas de UF de poliétersulfona ensuciadas con disoluciones de hidrolizados de caseína. De acuerdo

con estos autores, tras el proceso de ensuciamiento en ausencia de campos eléctricos las membranas se limpiaron parcialmente, puesto que determinados péptidos permanecieron depositados sobre su superficie.

En la presente Tesis Doctoral, los campos eléctricos se aplicarán durante la etapa de limpieza en membranas que habían sido previamente ensuciadas con disoluciones de proteínas, por lo que el objetivo de la aplicación de este método de limpieza consistirá en eliminar la capa de ensuciamiento adherida sobre la superficie de la membrana.

2.4.4. Evaluación de la eficacia del proceso de limpieza

Al finalizar el proceso de limpieza, resulta imprescindible evaluar la eficacia de dicho proceso para conocer si las propiedades permselectivas de la membrana han sido recuperadas y, por tanto, coinciden con las que presentaba inicialmente. Una clasificación básica de los criterios de evaluación de la eficacia del proceso de limpieza los divide en hidráulicos, químicos y microbiológicos, aunque generalmente los dos últimos suelen englobarse en un único tipo (Blanpain-Avet *et al.*, 2009).

Los criterios hidráulicos se basan en la comparación de la densidad de flujo de permeado con agua pura de la membrana original y de la membrana tras el proceso de limpieza. Esta comparación se realiza en las mismas condiciones experimentales de presión

transmembranal, velocidad tangencial, temperatura, etc. En el Capítulo III se detalla la ecuación utilizada para evaluar la eficacia del proceso de limpieza. Aunque los métodos hidráulicos son ampliamente utilizados por su rapidez, estas medidas de densidad de flujo pueden no representar inequívocamente la situación real en la membrana, como por ejemplo en los siguientes casos:

- La morfología y/o las propiedades de la superficie de la membrana se han visto alteradas por el efecto del reactivo químico.
- Existen depósitos de suciedad entre los poros o dentro del soporte que no afectan a la densidad de flujo de permeado.
- En caso de que exista materia orgánica tras el protocolo de limpieza, puede desarrollarse un crecimiento microbiano en la membrana.

Por su parte, los criterios químicos consisten en la determinación de las especies químicas que conforman la morfología de la membrana tras el proceso de limpieza. Entre las diferentes técnicas utilizadas para evaluar la estructura y composición de la membrana, las más destacadas son la espectroscopía de infrarrojos con transformada de Fourier y sistema de reflectancia total atenuada ("Attenuated Total Reflectance-Fourier Transformate Infrared Spectroscopy", ATR-FTIR,), la microscopía electrónica de barrido ("Scanning Electron Microscopy", SEM), la microscopía de energía dispersiva de rayos X ("Energy Dispersive X-ray", EDX) y la microscopía de fuerza atómica ("Atomic Force Microscopy", AFM). El empleo de estas técnicas permite conocer de manera precisa la composición química de la estructura de la membrana, la composición y la distribución de

especies químicas procedentes del ensuciamiento sobre la superficie de la membrana, la porosidad y rugosidad de la membrana y las fuerzas de adhesión entre las moléculas de suciedad (Delaunay *et al.*, 2008; Kim *et al.*, 2008). Sin embargo, el principal inconveniente de los métodos químicos de evaluación de la eficacia del proceso de limpieza es su carácter destructivo, es decir, es necesario romper la membrana para poder determinar sus características, por lo que resulta imposible reutilizarla de nuevo en el proceso.

En la presente Tesis Doctoral, la eficacia del proceso de limpieza se ha evaluado mayoritariamente mediante criterios hidráulicos que se describen con detalle en el Capítulo III de esta Tesis. Sin embargo, en algunas condiciones que resultaron óptimas para las disoluciones tratadas (ensayos con BSA y disoluciones enzimáticas utilizando membranas poliméricas), se comprobó también la eficacia del proceso de limpieza utilizando criterios químicos.

2.5. BIBLIOGRAFÍA

ACEVEDO CORREA D. (2010). “Gelificación fría de las proteínas del lactosuero” en *ReCiTeIA*, vol. 10, p. 1-19.

AGANA B.A., REEVE D. y ORBELL J.D. (2012). “The influence of an applied electric field during ceramic ultrafiltration of post-electrodeposition rinse wastewater” en *Water Research*, vol. 46, p. 3574-3584.

ALMÉCIJA M.C. *et al.* (2009a). “Analysis of cleaning protocols in ceramic membranes by liquid-liquid displacement porosimetry” en *Desalination*, vol. 245, p. 541-545.

ALMÉCIJA M.C. *et al.* (2009b). “Influence of the cleaning temperature on the permeability of ceramic membranes” en *Desalination*, vol. 245, p. 708-713.

ANEMA S.G. (2014). “The whey proteins in milk: thermal denaturation, physical interactions and effects on the functional properties of milk” en Taylor S.L. *Milk Proteins: From Expression to Food (Second Edition)*. Londres: Elsevier.

ANG W.S., LEE S. y ELIMELECH M. (2006). “Chemical and physical aspects of cleaning of organic-fouled reverse osmosis membranes” en *Journal of Membrane Science*, vol. 272, p. 198-210.

ANG W.S. y ELIMELECH M. (2007). “Protein (BSA) fouling of reverse osmosis membranes: Implications for wastewater reclamation” en *Journal of Membrane Science*, vol. 296, p. 83-92.

ANG W.S. *et al.* (2011). “Chemical cleaning of RO membranes fouled by wastewater effluent: Achieving higher efficiency with dual-step cleaning” en *Journal of Membrane Science*, vol. 382, p. 100-106.

ARGÜELLO M.A. *et al.* (2002). "Enzymatic cleaning of inorganic ultrafiltration membranes fouled by whey proteins" en *Journal of Agricultural and Food Chemistry*, vol. 50, p. 1951-1958.

ARGÜELLO M.A. *et al.* (2003). "Enzymatic cleaning of inorganic ultrafiltration membranes used for whey protein fractionation" en *Journal of Membrane Science*, vol. 216, p. 121-134.

ARUNKUMAR A. y ETZEL M.R. (2015). "Negatively charged tangential flow ultrafiltration membranes for whey protein concentration" en *Journal of Membrane Science*, vol. 475, p. 340-348.

BAI L. *et al.* (2013) "Membrane fouling during ultrafiltration (UF) of surface water: Effects of sludge discharge interval (SDI)" en *Desalination*, vol. 319, p. 18-24.

BAKER R.W. (2004). *Membrane Technology and Applications (Second edition)*, Reino Unido: John Wiley & Sons, Ltd.

BARANYI J. *et al.* (1996). "Effects of parameterization on the performance of empirical models used in predictive microbiology" en *Food Microbiology*, vol. 13, p. 83-91.

BLANPAIN-AVET P., MIGDAL J.F. y BÉNÉZECH T. (2009). "Chemical cleaning of a tubular ceramic microfiltration membrane fouled with a whey protein concentrate suspension – characterization of hydraulic and chemical cleanliness" en *Journal of Membrane Science*, vol. 337, p. 153-174.

CABERO CABERO M.L. (1997). *Limpieza química de membranas inorgánicas: Aplicación al tratamiento de lactosuero.* Tesis Doctoral. Oviedo: Universidad de Oviedo, <http://hdl.handle.net/10651/13566>.

CABERO M.L. *et al.* (1999). "Rinsing of ultrafiltration ceramic membranes fouled with whey proteins: effects on cleaning procedures" en *Journal of Membrane Science*, vol. 154, p. 239-250.

CAI M., ZHAO S. y LIANG H. (2010). "Mechanisms for the enhancement of ultrafiltration and membrane cleaning by different ultrasonic frequencies" en *Desalination*, vol. 263, p. 133-138.

CARRÈRE H., BLASZKOW F. y ROUX DE BALMANN H. (2001). "Modelling the clarification of lactic acid fermentation broths by cross-flow microfiltration" en *Journal of Membrane Science*, vol. 186, p. 219-230.

CAYOT P. y LORIENT D. (1997). "Chapter 8. Structure-Function Relationships of Whey Proteins" en Damodaran S. y Paraf A. *Food Proteins and their applications.* Nueva York: Marcel Dekker Inc.

CHANDAN R.C. y KILARA A. (2011). *Dairy Ingredients for Food Processing.* Iowa: Wiley-Blackwell.

CHEN J.P., KIM S.L. y TING Y.P. (2003). "Optimization of membrane physical and chemical cleaning by a statistically designed approach" en *Journal of Membrane Science*, vol. 219, p. 27-45.

CHOI S.-W. *et al.* (2000). "Modeling of the permeate flux during microfiltration of BSA-adsorbed microspheres in a stirred cell" en *Journal of Colloid and Interface Science*, vol. 228, p. 270-278.

CORBATÓN BÁGUENA M.J., ÁLVAREZ BLANCO S. y VINCENT VELA M.C. (2011). *Limpieza de membranas de ultrafiltración aplicadas en la industria alimentaria por medio de disoluciones salinas y caracterización del ensuciamiento de las membranas.* Trabajo Final de Máster. Valencia: Universitat Politècnica de València, <https://riunet.upv.es/handle/10251/15691> [Consulta: 1 de junio de 2015].

CORBATÓN-BÁGUENA M.J., ÁLVAREZ-BLANCO S. y VINCENT-VELA M.C. (2015). "Fouling mechanisms of ultrafiltration membranes fouled with whey model solutions" en *Desalination*, vol. 360, p. 87-96.

CURTIS R.A. y LUE L. (2006). "A molecular approach to bioseparations: protein-protein and protein-salt interactions" en *Chemical Engineering Science*, vol. 61, p. 907-923.

DAUFIN G. *et al.* (2001). "Recent and emerging applications of membrane processes in the food and dairy industry" en *Food and Bioproducts Processing*, vol. 79, p. 89-102.

DE LA CASA E.J. *et al.* (2008). "A combined fouling model to describe the influence of electrostatic environment on the cross-flow microfiltration of BSA" en *Journal of Membrane Science*, vol. 318, p. 247-254.

DELAUNAY D. *et al.* (2008). "Mapping of protein fouling by FTIR-ATR as experimental tool to study membrane fouling and fluid velocity profile in various geometries and validation by CFD simulation" en *Chemical Engineering and Processing*, vol. 47, p. 1106-1117.

D'SOUZA N.M. y MAWSON A.J. (2005). "Membrane cleaning in the dairy industry: a review" en *Critical Reviews in Food Science and Nutrition*, vol. 45, p. 125-134.

EDWARDS P.B. y JAMESON G.B. (2014). "Chapter 7: Structure and stability of whey proteins" en Taylor S.L. *Milk Proteins: From Expression to Food (Second Edition)*, Londres: Elsevier.

EL-ABASSI A. *et al.* (2014). "Application of ultrafiltration for olive processing wastewaters treatment" en *Journal of Cleaner Production*, vol. 65, p. 432-438.

GAO W. *et al.* (2011). “Membrane fouling control in ultrafiltration technology for drinking water production” en *Desalination*, vol. 272, p. 1-8.

GORDON J. (1997). “Dairy products” en Ranken M.D., Kill R.C., Baker C.G.J. *Food Industries Manual*. Londres: Blackie Academic & Professional.

GOULAS A. y GRANDISON A.S. (2008). “Applications of Membrane Separations” en Britz T.J. y Robinson R.K. *Advanced Dairy Science and Technology*. Reino Unido: Blackwell Publishing.

HERMIA J. (1982). “Constant pressure blocking filtration laws-application to power-law non-Newtonian fluids” en *Trans IChemE*, vol. 60, p. 183-187.

HINKOVÁ A. *et al.* (2005). “Application of cross-flow ultrafiltration on inorganic membranes in purification of food materials” en *Czech Journal of Food Science*, vol. 23, p. 103-110.

HO C.-C. y ZYDNEY L. (2000). “A combined pore blockage and cake filtration model for protein fouling during microfiltration” en *Journal of Colloid and Interface Science*, vol. 232, p. 389-399.

HOFMEISTER F. (1888). “Zur lehre von der wirkung der salze” en *Archiv for Experimentelle Pathologie und Pharmakologie*, vol. 24, p. 247.

HOLDER A., WEIK J. y HINRICHS J. (2013). “A study of fouling during long-term fractionation of functional peptides by means of cross-flow ultrafiltration and cross-flow electro membrane filtration” en *Journal of Membrane Science*, vol. 446, p. 440-448.

HONG S. y ELIMELECH M. (1997). “Chemical and physical aspects of natural organic matter (NOM) fouling of nanofiltration membranes” en *Journal of Membrane Science*, vol. 132, p. 159-181.

HUISMAN I.H., PRÁDANOS P. y HERNÁNDEZ A. (2000). “The effect of protein-protein and protein-membrane interactions on membrane fouling in ultrafiltration” en *Journal of Membrane Science*, vol. 179, p. 79-90.

HUOTARI H.M. TRÄGÅRDH G. y HUISMAN I.H. (1999). “Crossflow membrane filtration enhanced by an external DC electric field: A review” en *Trans IChemE*, vol. 77, p. 461-468.

JUDD S., KIM B. y AMY G. (2008). “Membrane Bio-reactors” en HenzeM., Van Loosdrecht M., Ekama G. y Brdjanovic D. *Biological Wastewater Treatment: Principles, Modelling and Design*. Londres: IWA Publishing.

KAYA Y. *et al.* (2010). “The effect of transmembrane pressure and pH on treatment of paper machine process waters by using a two-step nanofiltration process” en *Desalination*, vol. 250, p. 150-157.

KAZEMIMOGHADAM M. y MOHAMMADI T. (2007). “Chemical cleaning of ultrafiltration membranes in the milk industry” en *Desalination*, vol. 204, p. 213-218.

KIM J., CAI Z. y BENJAMIN M.M. (2008). “Effects of adsorbents on membrane fouling by natural organic matter” en *Journal of Membrane Science*, vol. 310, p. 356-364.

KRSTIĆ D.M. *et al.* (2002). “The effect of turbulence promoter on cross-flow microfiltration of skim milk” en *Journal of Membrane Science*, vol. 208, p. 303-314.

KUMAR P. *et al.* (2013). “Perspective of Membrane Technology in Dairy Industry: A Review” en *Asian-Australasian Journal of Animal Science*, vol. 26, p. 1347-1358.

KWON B. *et al.* (2006). “Organic nanocolloid fouling in UF membranes” en *Journal of Membrane Science*, vol. 279, p. 209-219.

LEE S. y ELIMELECH M. (2007). “Salt cleaning of organic-fouled reverse osmosis membranes” en *Water Research*, vol. 41, p. 1134-1142.

LI J., SANDERSON R.D. y JACOBS E.P. (2002). “Ultrasonic cleaning of nylon microfiltration membranes fouled by Kraft paper mil effluent” en *Journal of Membrane Science*, vol. 205, p. 247-257.

LIPNIZKI F. (2008). “Opportunities and challenges of using ultrafiltration for the concentration of diluted coating materials” en *Desalination*, vol. 224, p. 98-104.

LIU C. *et al.* (2001). “Membrane chemical cleaning: from art to science” en *AWWA Membrane Technology Conference*. San Antonio, TX.

LUCENA M.E. *et al.* (2006). “Beta-lactoglobulin removal from whey protein concentrates. Production of milk derivatives as a base for infant formulas” en *Separation and Purification Technology,* vol. 52, p. 310-316.

MADRID VICENTE A. (1981). *Modernas técnicas de aprovechamiento del lactosuero*. España: Almansa.

MAH S.-K. *et al.* (2012). “Ultrafiltration of pal oil-oleic acid-glycerin solutions: fouling mechanism identification, fouling mechanism analysis and membrane characterizations” en *Separation and Purification Technology*, vol. 98, p. 419-431.

MATZINOS P. y ÁLVAREZ R. (2002). “Effect of ionic strength on rinsing and alkaline cleaning of ultrafiltration inorganic membranes fouled with whey proteins” en *Journal of Membrane Science*, vol. 208, p. 23-20.

MOHAMMADI T. y ESMAEELIFAR A. (2005). "Wastewater treatment of a vegetable oil factory by a hybrid ultrafiltration-activated carbon process" en *Journal of Membrane Science*, vol. 254, p. 129-137.

MORES W.D. y DAVIS R.H. (2002). "Yeast foulant removal by backpulses in crossflow microfiltration" en *Journal of Membrane Science*, vol. 208, p. 389-404.

MULDER, M. (2000). *Basic Principles of Membrane Technology.* Holanda: Kluwer Academic Publishers.

MUTHUKUMARAN S. *et al.* (2004). "The use of ultrasonic cleaning for ultrafiltration membranes in the dairy industry" en *Separation and Purification Technology*, vol. 39, p. 99-107.

NAIM R., LEVITSKY I. y GITIS V. (2012). "Surfactant cleaning of UF membranes fouled by proteins" en *Separation and Purification Technology*, vol. 94, p. 39-43.

NIGAM M.O., BANSAL B. y CHEN X.D. (2008). "Fouling and cleaning of whey protein concentrate fouled ultrafiltration membranes" en *Desalination*, vol. 218, p. 313-322.

NUCCI N.V. y VANDERKOOI J.M. (2008). "Effects of salts of the Hofmeister series on the hydrogen bond network of water" en *Journal of Molecular Liquids*, vol. 143, p. 160-170.

OGUNBIYI O.O., MILES N.J. y HILAL N. (2008). "The effects of performance and cleaning cycles of new tubular ceramic microfiltration membrane fouled with a model yeast suspension" en *Desalination*, vol. 220, p. 273-289.

ORGANIZACIÓN DE LAS NACIONES UNIDAS PARA LA ALIMENTACIÓN Y LA AGRICULTURA. <http://www.fao.org/home/en/> [Consulta: 1 de junio de 2015]

PAUGAM L. DELAUNAY D. y RABILLER-BAUDRY M. (2010). "Cleaning efficiency and impact on production fluxes of oxidising disinfectants on a PES ultrafiltration membrane fouled with proteins" en *Food and Bioproducts Processing*, vol. 88, p. 425-429.

PENG H. y TREMBLAY A.Y. (2008). "Membrane regeneration and filtration modeling in treating oily wastewaters" en *Journal of Membrane Science*, vol. 324, p. 59-66.

QIN F.G.F., MAWSON J. y ZENG X.A. (2011). "Experimental study of fouling and cleaning of sintered stainless steel membrane in electro-microfiltration of calcium salt particles" en *Membranes*, vol. 1, p. 119-131.

RUBY FIGUEROA R.A., CASSANO A. y DRIOLI E. (2011). "Ultrafiltration of orange press liquor: Optimization for permeate flux and fouling index by response surface methodology" en *Separation and Purification Technology*, vol. 80, p. 1-10.

SALAHI A., ABBASI M. y MOHAMMADI T. (2010). "Permeate flux decline during UF of oily wastewater: experimental and modelling" en *Desalination*, vol. 251, p. 153-160.

SHIRAZI S., LIN C.-J. y CHEN D. (2010). "Inorganic fouling of pressure–driven membrane processes. A critical review" en *Desalination*, vol. 250, p. 236-248.

SHON H.K. *et al.* (2004). "Effect of pretreatment on the fouling of membranes: application in biologically treated sewage effluent" en *Journal of Membrane Science*, vol. 234, p. 111-120.

SMITH P.J. *et al.* (2006). "Productivity enhancement in a cross-flow ultrafiltration membrane system through automated de-clogging operations" en *Journal of Membrane Science*, vol. 280, p. 82-88.

SONG W. *et al.* (2010). “Rapid concentration of protein solution by a crossflow electro-ultrafiltration process” en *Separation and Purification Technology*, vol. 73, p. 310-318.

SUÁREZ L. *et al.* (2012). “Membrane technology for the recovery of detergent compounds: A review” en *Journal of Industrial and Engineering Chemistry,* vol. 18, p. 1859-1873.

TARAZAGA C.C., CAMPDERRÓS M.E. y PÉREZ PADILLA A. (2006). “Physical cleaning by means of electric field in the ultrafiltration of a biological solution” en *Journal of Membrane Science*, vol. 278, p. 219-224.

TSUMOTO K. *et al.* (2007). “Effects of salts on protein-surface interactions: Applications for column chromatography” en *Journal of Pharmaceutical Science*, vol. 96, p. 1677-1690.

VAN DER BRUGGEN B. *et al.* (2003). “A review of pressure-driven membrane processes in wastewater treatment and drinking water production” en *Environmental Progress*, vol. 22, p. 46-56.

VINCENT VELA M.C. *et al.* (2009). “Analysis of membrane pore blocking models adapted to crossflow ultrafiltration in the ultrafiltration of PEG” en *Chemical Engineering Journal*, vol. 149, p. 232-241.

WANG C. *et al.* (2012). “Membrane fouling mechanisms in ultrafiltration of succinic acid fermentation broth” en *Bioresource Technology*, vol. 116, p. 366-371.

WANG Z. *et al.* (2014). “Membrane cleaning in membrane bioreactors: A review" en *Journal of Membrane Science*, vol. 468, p. 276-307.

WIT J.N. (1998). “Nutritional and functional characteristics of whey proteins in food products” en *Journal of Dairy Science*, vol. 81, p. 597-608.

WOO Y.C. *et al.* (2015). “Characteristics of membrane fouling by consecutive chemical cleaning in pressurized ultrafiltration as pre-treatment of seawater desalination” en *Desalination*, vol. 269, p. 51-61.

YEE K.W.K., WILEY D.E. y BAO J. (2009). “A unified model of the time dependence flux decline for the ultrafiltration of whey” en *Journal of Membrane Science*, vol. 332, p. 69-80.

ZHANG J. (2012). “Protein-protein interactions in salt solutions” en Cai W. y Hong H. *Protein-protein interactions – Computational and experimental tools*. Intech.

ZHAO Y.-J. *et al.* (2000). “Fouling and cleaning of membrane-a literatura review” en *Journal of Environmental Sciences*, vol. 12, p. 241-251.

ZYDNEY A.L., HO C.-C. y YUAN W. (2003). “Fouling phenomena during microfiltration:effects of pore blockage, cake filtration and membrane morphology” en Bhattacharyya D. y Butterfield A. *New insights into membrane science and technology: polymeric and biofunctional membranes (Membrane Science and Technology Series).* Amsterdam: Elsevier.

CAPÍTULO III

Metodología experimental

3.1. EQUIPOS Y MATERIALES UTILIZADOS

3.1.1. Planta piloto

Tanto los ensayos de ensuciamiento como los ensayos de limpieza se llevaron a cabo en una planta de UF convencional (VF-S11, Orelis, Francia). Dicha planta constaba de: un tanque de alimentación encamisado de acero inoxidable 316L con un volumen total de 10 L, una bomba volumétrica equipada con variador de velocidad para seleccionar el caudal deseado, dos manómetros situados a la entrada y a la salida del módulo de membranas para medir la caída de presión en el mismo, una válvula reguladora de presión para fijar la presión transmembranal durante la realización de los ensayos y un rotámetro para determinar el valor de caudal de rechazo. Además, la planta estaba equipada con sistemas de medida en línea de temperatura, conductividad y pH, una resistencia eléctrica y un sistema de refrigeración por agua de red para mantener constante la temperatura de los ensayos y una balanza (precisión ±0.001 g) para determinar gravimétricamente el flujo de permeado obtenido durante todas las etapas del proceso. El esquema de la planta de UF se representa en la Fig. 13.

En el caso de los ensayos de limpieza mediante campos eléctricos, se dispuso además de una fuente de alimentación de corriente continua con regulador de potencial e intensidad de corriente (Konstanter SSP, Gossen, Alemania), conectada a la membrana

(cátodo) y a un electrodo de titanio con recubrimiento de iridio que actuó de ánodo (MAGNETO Special Anodes B.V., Holanda). Los ensayos presentados en esta Tesis se realizaron en modo potenciostático, de manera que el potencial aplicado se seleccionó al comienzo de cada ensayo de limpieza. Un esquema detallado de las conexiones entre la fuente de alimentación y los electrodos utilizados durante la limpieza mediante campos eléctricos se muestra en la Fig. 14.

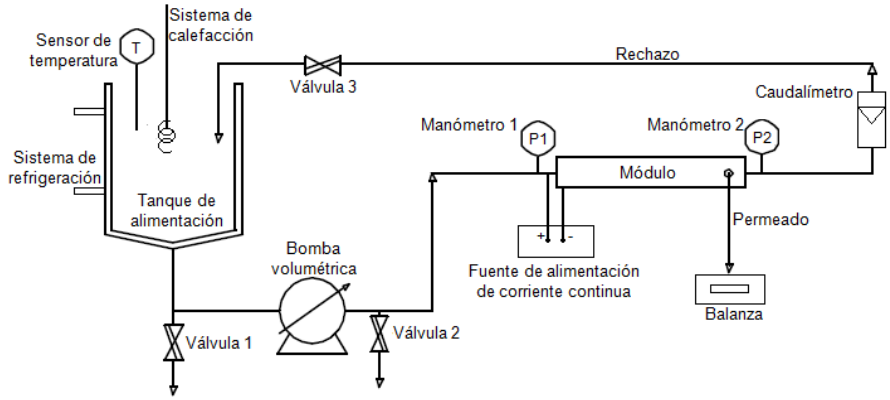

Fig. 13. *Esquema de la planta de UF utilizada*

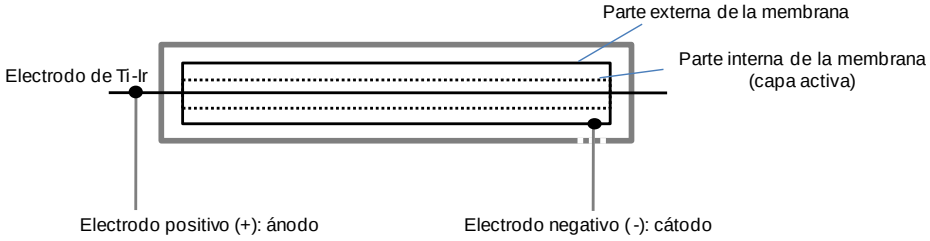

Fig. 14. *Esquema de la conexión de los electrodos*

Dado que durante los ensayos de ensuciamiento y limpieza se utilizaron membranas con distintas configuraciones (plana y tubular),

la planta de UF se equipó con distintos módulos para poder albergar dichas membranas. Así pues, los ensayos con membranas cerámicas tubulares se realizaron en un módulo tubular de acero inoxidable (Carbosep, Orelis, Francia) diseñado para albergar membranas de 20 cm de longitud; mientras que un módulo plano de metacrilato (Rayflow, Orelis, Francia) diseñado para membranas con un área efectiva de 100 cm^2 se utilizó para llevar a cabo los ensayos con membranas poliméricas planas. En el caso de los ensayos de limpieza mediante campos eléctricos con membranas cerámicas, el módulo metálico se sustituyó por un módulo de PlexiglásGS® (Metaval Abella S.L., España) de las mismas dimensiones. Las fotografías de los tres módulos utilizados (Rayflow, tubular de PlexiglásGS® y tubular de acero inoxidable) se observan en la Fig. 15.

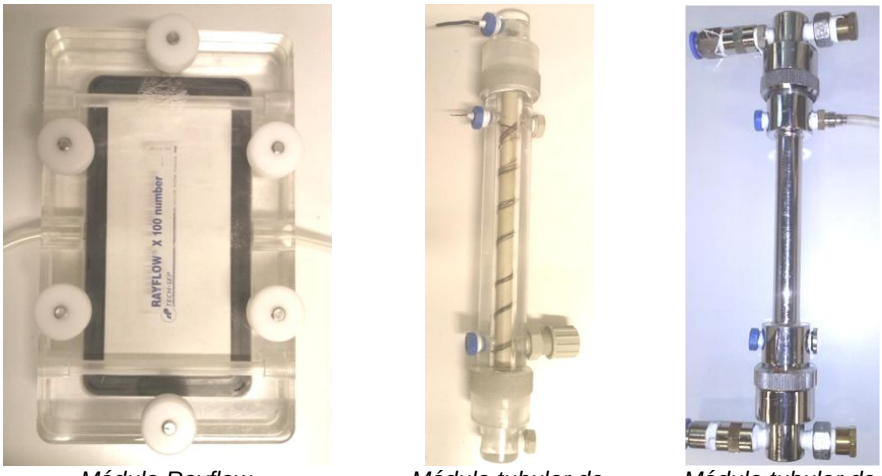

Módulo Rayflow | *Módulo tubular de PlexiglásGS®* | *Módulo tubular de acero inoxidable*

Fig. 15. *Fotografías de los módulos utilizados*

3.1.2. Membranas de ultrafiltración

Con el fin de estudiar la influencia del tipo de membrana sobre el ensuciamiento de las mismas y la eficacia del proceso de limpieza, se utilizaron cuatro membranas de UF de diferentes materiales, umbral de corte molecular ("Molecular Weight Cut-Off", MWCO) y configuración. Las características principales de las dos membranas orgánicas utilizadas (de poliétersulfona, PES, y poliétersulfona permanentemente hidrofílica, PESH) se recogen en la Tabla 5, mientras que las características de las dos membranas cerámicas utilizadas se incluyen en la Tabla 6, de acuerdo con el fabricante.

Estas membranas fueron seleccionadas para la realización de los ensayos por diferentes motivos. En primer lugar, todas ellas presentan un MWCO en el rango típico de las membranas utilizadas para la producción de concentrados de proteínas de lactosuero. Además, todas ellas presentan una gran resistencia térmica y soportan un rango de pH elevado, lo que permite llevar a cabo el estudio de la eficacia del proceso de limpieza incluso con agentes convencionales (como hidróxido e hipoclorito sódico). Finalmente, la distinta composición de la capa activa de las membranas (PES, PESH y ZrO_2-TiO_2) permite determinar la influencia del tipo de material sobre el comportamiento de las membranas durante las etapas de ensuciamiento y limpieza.

Tabla 5. Características principales de las membranas poliméricas utilizadas

Referencia	UP005	UH030
Casa comercial	Microdyn Nadir (Alemania)	
Configuración	Plana	
Área efectiva (cm^2)	100.00	
Temperatura máxima de operación (ºC)	95	
Rango de pH	0-14	
Capa activa	PES[a]	PESH[b]
MWCO (kDa)	5	30
Permeabilidad al agua ($L \cdot m^{-2} \cdot h^{-1} \cdot bar^{-1}$)	42.61	106.17

[a] Poliétersulfona (PES)
[b] Poliétersulfona permanentemente hidrofílica (PESH)

Tabla 6. Características principales de las membranas cerámicas utilizadas

Referencia	INSIDE-CéRAM™	
Casa comercial	TAMI Industries (Francia)	
Configuración	Tubular	
Área efectiva (cm^2)	35.51	
Capa activa	ZrO_2-TiO_2	
Temperatura máxima de operación (ºC)	1000	
Rango de pH	0-14	
MWCO (kDa)	15	50
Permeabilidad al agua ($L \cdot m^{-2} \cdot h^{-1} \cdot bar^{-1}$)	60.37	209.66

3.1.3. Reactivos y productos químicos

Para preparar las disoluciones modelo de lactosuero, se utilizaron, en primer lugar, disoluciones de un solo soluto (proteínas). A continuación, se realizaron ensayos con disoluciones modelo de proteínas y sales y, finalmente, se utilizaron disoluciones reales de lactosuero. Las disoluciones modelo que contenían únicamente proteínas consistieron en disoluciones acuosas de BSA (A3733, Sigma Aldrich, Alemania) con una concentración de 10 $g \cdot L^{-1}$. De

acuerdo con el proveedor, este compuesto se suministra en forma de polvo con un 98 % de pureza, una masa molecular de 66 kDa y un punto isoeléctrico de 4.9. Según diversos autores (Suttiprasit *et al.*, 1992; Wang y Tang, 2011; Afonso *et al.*, 2009), su configuración es elíptica de dimensiones 11.6×2.7×2.7 nm. La proteína BSA es una de las proteínas mayoritarias en el lactosuero y ha sido ampliamente utilizada en disoluciones modelo para la realización de estudios sobre la UF de proteínas (Afonso *et al.*, 2009).

Para simular las disoluciones modelo de proteínas y sales, a la disolución de BSA se añadió cloruro de calcio con una pureza del 95 % a una concentración de 1.65 $g \cdot L^{-1}$ (Panreac, España). Se seleccionó como sal representativa del lactosuero $CaCl_2$, debido a que ambos iones presentan una alta concentración tanto en el lactosuero dulce como en el ácido. Además, numerosos autores han demostrado que la presencia de Ca^{+2} favorece el ensuciamiento de las membranas causado por proteínas (Nucci y Vanderkooi, 2008). Finalmente, las disoluciones reales de lactosuero se prepararon a partir de WPC (Renylat, Industrias Lácteas Asturianas S.A., España) con diferentes concentraciones (22.2, 33.3, 44.4 y 150 $g \cdot L^{-1}$). De acuerdo con el fabricante, el WPC contiene una concentración total de proteínas del 45 %p/p. La concentración de todos estos reactivos se seleccionó en base a la concentración típica de las sustancias utilizadas (proteínas y sales) propias del lactosuero dulce y de los concentrados de proteínas del lactosuero elaborados por UF. La composición del WPC utilizado, de acuerdo con los ensayos de caracterización llevados a cabo en el Departamento de Ingeniería Química y Nuclear, se muestra en la Tabla 7. Las técnicas analíticas

utilizadas para determinar cada uno de los componentes se describen en detalle en la sección “Técnicas analíticas utilizadas”.

Tabla 7. Composición del WPC utilizado

Componente	Concentración en base seca (%p/p)
Materia seca	93.66 ± 0.95
Proteínas	40.74 ± 0.79
Lactosa	38.27 ± 0.49
Grasa	8.14 ± 0.20
Cenizas	7.85 ± 0.07
Ca	0.79 ± 0.06
Na	1.21 ± 0.09
K	1.42 ± 0.02
Cl	4.07 ± 0.24
PO_4-P	0.37 ± 0.03

Por otra parte, para simular una disolución típica de la industria de bebidas y zumos, se utilizaron disoluciones enzimáticas de pectinasas (Pectinex Smash XXL, Novozymes, Dinamarca) a diferentes concentraciones (2, 7.5 y 15 $g \cdot L^{-1}$) con un pH entorno a 4.3. De acuerdo con el proveedor, dichas disoluciones enzimáticas estaban compuestas principalmente por pectinliasas de *Aspergillius niger*. Dichas disoluciones simulan a las empeladas en los procesos de clarificación de zumos.

Con el fin de estudiar la influencia del tipo de sal sobre la eficacia del proceso de limpieza, se utilizaron diferentes disoluciones salinas de NaCl, $NaNO_3$, Na_2SO_4, KCl y NH_4Cl (Panreac, España). Estas disoluciones se prepararon sin ajuste de pH, variando éste entre 6.8-7. Las propiedades físicas de las sales utilizadas así como sus pictogramas correspondientes se muestran en la Tabla 8 (www.panreac.es).

Tabla 8. Propiedades físicas y pictogramas de las sales utilizadas

Propiedades físicas	NaCl	$NaNO_3$	Na_2SO_4	KCl	NH_4Cl
Punto de ebullición (ºC)	1413	380	–	1420	520
Punto de fusión (ºC)	804	309	884	778	-
Densidad relativa al agua	2.17	2.26	2.68	1.98	1.53
Solubilidad en agua ($g \cdot L^{-1}$ a 20 ºC)	360	880	162	340	370
Pictograma	–		–	–	

Finalmente, cuando tras el proceso de limpieza las propiedades permselectivas de las membranas no pudieron recuperarse completamente, se llevaron a cabo protocolos de limpieza convencionales. En el caso de las membranas poliméricas, se utilizaron disoluciones de hidróxido sódico suministrado en forma de lentejas del 98 % de pureza (Panreac, España) a pH 11 y una temperatura de 45 ºC. En el caso de las membranas cerámicas, el agente de limpieza convencional consistió en disoluciones de hipoclorito sódico (Panreac, España) con una concentración de 250 ppm a pH 11 (ajustado mediante la adición de NaOH) a temperaturas entre 50 - 60ºC.

Por otra parte, para cuantificar la concentración de proteínas en las disoluciones alimento así como en las corrientes permeado y rechazo, se utilizaron los reactivos correspondientes al método del ácido bicinconínico (Bicinchoninic acid, BCA) y al método de Bradford (referencias BCA1 y B9643 para el método BCA y B6916 para el método Bradford, Sigma Aldrich, Alemania).

Para preparar el reactivo utilizado en la determinación de la concentración de lactosa en el WPC, fueron necesarios ácido 3,5-dinitrosalicílico (Dinitrosalicylic acid, DNS, Sigma Aldrich, Alemania) y tartrato de sodio y potasio 4-hidrato (Panreac, España). La recta de calibrado se realizó con lactosa 1-hidrato en polvo (Panreac, España).

La determinación de la concentración de dos aniones presentes en el WPC utilizado se llevó a cabo mediante el uso de kits Spectroquant de cloruros y fosfatos (referencia 114730 y 114729, respectivamente, Merck Millipore, España).

Tanto el agua osmotizada como el agua destilada necesarias para preparar las disoluciones de ensuciamiento, limpieza y caracterización se produjeron en el laboratorio del Departamento de Ingeniería Química y Nuclear, mediante un equipo de ósmosis inversa (Osmofilter S.L., España) y una resina de intercambio iónico Station 8000 L 5.2 (Veolia Water Systems, Francia).

3.2. METODOLOGÍA

3.2.1. Caracterización de las membranas

Para determinar la permeabilidad hidráulica de las membranas de UF utilizadas y la resistencia intrínseca de las mismas (R_m), se caracterizaron dichas membranas con agua desionizada en unas condiciones fijas de temperatura (25 ºC) y velocidad tangencial (3 $m \cdot s^{-1}$) y a distintos valores de presión transmembranal (1, 2 y 3 bar). Para el cálculo de la resistencia hidráulica se utilizó la Ley de Darcy (Ec.1), que relaciona la densidad de flujo de permeado con la presión transmembranal, la viscosidad de la disolución alimento y resistencia hidráulica total al paso de fluido. Esta caracterización se llevó a cabo tanto con las membranas nuevas como con las membranas limpias tras el protocolo de limpieza.

$$J = \frac{\Delta P}{\mu \cdot R_t} \qquad \text{Ec. 1}$$

Donde J es la densidad de flujo de permeado, ΔP es la presión transmembranal, μ es la viscosidad de la disolución alimento y R_t es la resistencia hidráulica total.

En el caso del ensayo de caracterización de las membranas nuevas, la disolución alimento fue agua desionizada y, por tanto, la resistencia hidráulica corresponde a la resistencia intrínseca de la membrana (R_m).

3.2.2. Ensayos de ensuciamiento, aclarado y limpieza

Para cada una de las disoluciones modelo de proteínas y enzimáticas, se llevó a cabo un procedimiento experimental basado en cuatro etapas: ensuciamiento, primer aclarado, limpieza y segundo aclarado. La Fig. 16 representa un esquema de dicho protocolo experimental. Es importante destacar que durante todas las etapas del protocolo de ensuciamiento y limpieza se monitorizaron los valores de densidad de flujo de permeado y resistencia hidráulica, calculada esta última a partir de la Ley de Darcy (Ec. 1).

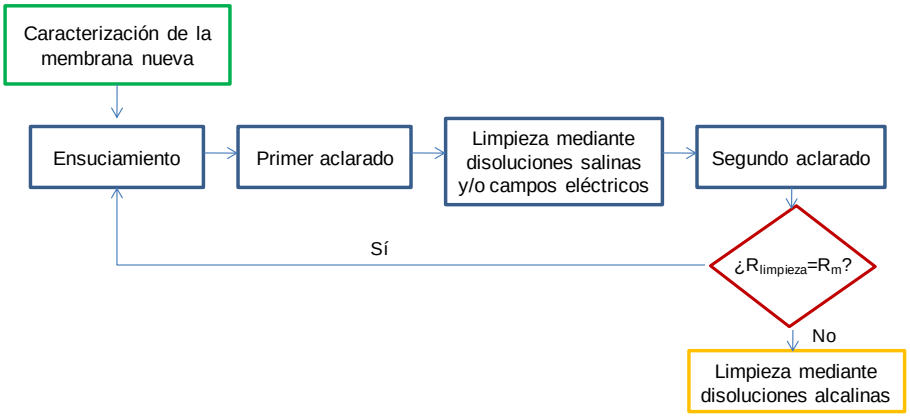

Fig. 16. *Esquema del protocolo de ensuciamiento y limpieza*

El ensuciamiento de las membranas utilizando disoluciones modelo de lactosuero con diferente concentración de proteínas (10, 22.2, 33.3, 44.4 y 150 $g \cdot L^{-1}$) y disoluciones enzimáticas de pectinasas con distinta concentración (2, 7.5 y 15 $g \cdot L^{-1}$) se llevó a cabo en unas condiciones fijas de velocidad tangencial y presión transmembranal (2 $m \cdot s^{-1}$ y 2 bar, respectivamente). Estas condiciones se seleccionaron de acuerdo con las condiciones de operación

empleadas por otros autores en trabajos previos sobre UF de lactosuero (Matzinos y Álvarez, 2002).

Durante esta etapa realizada con las disoluciones modelo de lactosuero, se tomaron muestras de la corriente permeado para determinar la concentración de proteínas presentes en la misma y, a partir de estos resultados, calcular el valor de coeficiente de rechazo de las membranas utilizadas, de acuerdo con la Ec. 2.

$$Rechazo(\%) = \left(1 - \frac{C_p}{C_b}\right) \cdot 100 \qquad \text{Ec. 2}$$

Donde Rechazo es el coeficiente de rechazo, C_p es la concentración de proteínas en la corriente permeado y C_b es la concentración de proteínas en el seno de la disolución alimento.

Tras esta etapa, se realizó un aclarado con agua osmotizada a una presión transmembranal menor que la utilizada en la etapa anterior (1 bar) y a diferentes velocidades tangenciales (entre 1.2 y 4.2 $m \cdot s^{-1}$) para estudiar la influencia de este último parámetro sobre la eficacia del proceso de aclarado. Algunos autores han demostrado que la utilización de presiones transmembranales bajas durante el aclarado y limpieza de las membranas favorecen la descompresión de la capa de ensuciamiento formada durante la etapa de ensuciamiento y por tanto, facilitan su eliminación desde la superficie de la membrana hacia el seno de la disolución (Blanpain-Avet *et al.*, 2009).

Después del aclarado, las membranas se limpiaron utilizando diferentes tipos de sales y condiciones de operación: concentración de sal (0 – 100 mM), temperatura de la disolución de limpieza (25 – 80 ºC) y velocidad tangencial (1.2 – 4.2 $m \cdot s^{-1}$). De esta manera, se investigó la influencia de todos estos parámetros sobre el proceso de limpieza y su eficacia. Finalmente, se procedió a un segundo aclarado de las membranas con el objetivo de eliminar los restos de agentes de limpieza de la superficie de la membrana.

Tal y como se ha comentado anteriormente en este Capítulo, en el caso en el cual la resistencia de las membranas después del último aclarado no coincidiera con la resistencia hidráulica original de las mismas, éstas se sometieron a un proceso de limpieza convencional con álcalis: NaOH a pH 11 y 45 ºC en el caso de las membranas poliméricas y NaOCl a pH 11 (ajustado con NaOH) a 50 – 60 ºC en el caso de las membranas cerámicas. Dichos protocolos son los recomendados por los fabricantes de cada tipo de membranas.

3.2.3. Determinación de la eficacia hidráulica del proceso de limpieza

De acuerdo con los métodos hidráulicos de evaluación de la eficacia del proceso de limpieza, la eficacia del mismo se determinó mediante la comparación de la resistencia intrínseca de la membrana con la obtenida tras el segundo aclarado (R_{2a}), de acuerdo con la Ec. 3. Otros autores (Matzinos y Álvarez, 2002; Daufin *et al.*, 2001; Muthukumaran *et al.*, 2007) habían propuesto ecuaciones similares para calcular la eficacia del proceso de aclarado y limpieza.

$$EHL(\%) = \frac{R_f - R_{2a}}{R_f - R_m} 100 \qquad \text{Ec. 3}$$

Donde EHL es la eficacia hidráulica de limpieza y R_f es la resistencia hidráulica tras la etapa de ensuciamiento.

Así pues, tras finalizar el protocolo de limpieza se determinó el valor de EHL en cada una de las condiciones de operación ensayadas. En algunos de estos casos, como por ejemplo en las condiciones óptimas de limpieza para disoluciones de BSA y disoluciones enzimáticas, se compararon los valores de EHL obtenidos con los resultados de eficacia de limpieza determinados mediante métodos químicos (AFM, SEM y ATR-FTIR). De esta forma, se confirma la validez del método hidráulico empleado para evaluar la eficacia del proceso de limpieza. Esta comparación y sus resultados se detallan en el Capítulo V de esta Tesis Doctoral.

3.2.4. Determinación de la eficacia química del proceso de limpieza

La evaluación de la eficacia del proceso de limpieza mediante métodos químicos se basa en la determinación de la cantidad de especies responsables del ensuciamiento que permanecen sobre la superficie de la membrana después del proceso de limpieza. Para llevar a cabo dicha evaluación, se utilizan diversas técnicas de espectroscopía, algunas de las cuales permiten, además, analizar y comparar las características morfológicas de la membrana nueva, de la capa de ensuciamiento y de la membrana limpia.

En el caso de las membranas ensuciadas con disoluciones de BSA, las imágenes y resultados obtenidos mediante las técnicas SEM, EDX y AFM se realizaron en el Servicio de Microscopía Electrónica de la Universitat Politècnica de València, mientras que la determinación mediante ATR-FTIR se llevó a cabo en el Centro de Biomateriales y Energía Tisular de la misma universidad. Por otra parte, en el caso de las membranas ensuciadas con disoluciones enzimáticas, las medidas de AFM y ATR-FTIR se realizaron en el Institute on Membrane Technology (Istituto per la Tecnologia delle Membrane-Consiglio Nazionale delle Ricerche, ITM-CNR) de la Università della Calabria durante la estancia de investigación. En todos los casos, se determinó la composición de las membranas nuevas, tras la etapa de ensuciamiento y tras el segundo aclarado una vez finalizado el protocolo de limpieza.

3.2.4.1. SEM y EDX

Estas técnicas se realizaron en un microscopio JSM6300 (Jeol Ltd., Japón) con detector de rayos X (Oxford Instruments, Reino Unido). El funcionamiento del microscopio SEM se basa en el barrido de un haz de electrones sobre un área de tamaño deseado (en función del número de aumentos seleccionado). A continuación, el detector de rayos X recoge dichos rayos procedentes de cada uno de los puntos de la superficie sobre los que ha pasado previamente el haz de electrones. Teniendo en cuenta que la energía de cada rayo X viene determinada por el tipo de elemento químico, se puede determinar cualitativa y cuantitativamente la concentración de dichos elementos en el área analizada.

Dado que las muestras precisan ser conductoras para llevar a cabo la determinación en el microscopio SEM, éstas se recubrieron con una capa fina de carbono tras ser secadas en aire para permitir su análisis (García-Ivars *et al.,* 2014).

3.2.4.2. AFM

Las medidas mediante el microscopio AFM se realizaron en las dos Universidades (Universitat Politècnica de València y Università della Calabria) mediante el método "tapping" en aire con un microscopio MultiMode (Digital Instruments, VEECO Metrology Group, EE.UU.) equipado con el software NanoScope para determinar los parámetros característicos de la topografía de la muestra, como por ejemplo, la rugosidad de la superficie. En este caso, una punta afilada situada en el extremo de una palanca flexible recorre la superficie de un área de tamaño seleccionado aplicando de manera constante una pequeña fuerza de interacción. Dicha punta toca de manera intermitente la superficie de la muestra, eliminado las fuerzas laterales y de presión que podrían dañarla y reducir la resolución de la imagen. El barrido que realiza la punta lo realiza un escáner piezo-eléctrico y la interacción entre la punta de la palanca y la muestra se recoge en un detector fotodiodo. A partir de la diferencia de voltaje que detectan los diferentes segmentos del fotodiodo se pueden evaluar los cambios de inclinación o amplitud de oscilación de la punta, quedando representada la topografía de la muestra analizada (De Oliveira, 2012). De las membranas utilizadas, se analizaron muestras de dimensiones 5×5 μm.

Respecto a la rugosidad de la superficie de las muestras determinada mediante el microscopio AFM, existen dos medidas distintas de rugosidad ampliamente utilizadas en la caracterización de la superficie de las membranas (Fig. 17):

- **Rugosidad promedio** (Average roughness, R_a): proporciona el valor de desviación en altura, es decir, el valor promedio de de la altura de cada punto respecto al plano central, para el cual los volúmenes determinados en la imagen por encima y debajo de dicho plano coinciden. Su principal inconveniente es que diferentes perfiles o topografías pueden presentar el mismo valor de R_a. La ecuación general para determinarla es la Ec. 4 (Raposo *et al.*, 2007).

$$R_a = \frac{1}{L}\int_0^L |Z(x)|dx \qquad \text{Ec. 4}$$

  Donde L es la longitud a evaluar y Z(x) es la función que describe el perfil de alturas en cada posición x.

- **Rugosidad cuadrática media** (Root Mean Square roughness, R_{RMS} o R_q): es una medida estadística de la rugosidad de la muestra que representa la desviación estándar entre la altura de cada punto considerado de la superficie con respecto a la media aritmética. La sensibilidad de esta medida es mayor a los picos y los valles de la muestra debido a que considera el cuadrado de la amplitud en su ecuación (De Oliveira, 2012). Este tipo de rugosidad se calcula mediante la Ec. 5 (Chung *et al.*, 2002).

$$R_q = \sqrt{\frac{\sum (Z_i - Z_{avg})^2}{N}} \qquad \text{Ec. 5}$$

Donde Z_i es el valor de altura medido en cada punto, Z_{avg} es el promedio de valores de altura medidos en toda el área seleccionada y N es el número de puntos considerados en el área analizada.

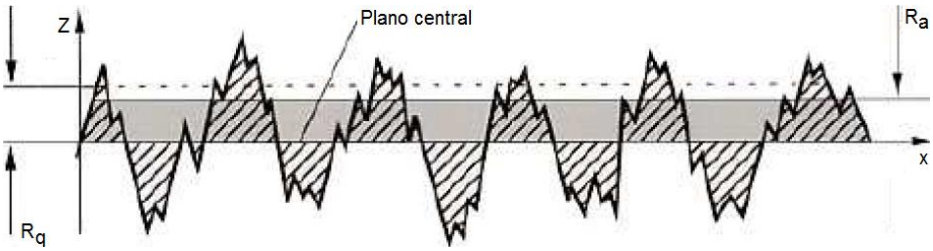

Fig. 17. *Representación de las medidas de rugosidad R_a y R_q*

3.2.4.3. ATR-FTIR

El equipo de ATR-FTIR utilizado en la Universitat Politècnica de València para analizar las membranas en las que se habían utilizado disoluciones de BSA consistió en un espectrómetro Thermo Nicolet® Nexus (Thermo Fisher Scientific, EE.UU.), mientras que el equipo utilizado en el ITM-CNR fue un espectrómetro Spectrum One (Perkin-Elmer, EE.UU.).

La técnica FTIR se basa en la medida de absorción en la región del infrarrojo medio (a longitudes de onda entre 400 y 4000 cm^{-1}) de la muestra problema, que puede encontrarse en cualquiera de los tres

estados característicos (sólido, líquido y gas). Puesto que la combinación y uniones entre los átomos que constituyen un material son características del mismo, los picos de absorción correspondientes a las frecuencias de vibración entre los enlaces de los átomos de la muestra a analizar permiten determinar el espectro de infrarrojo de la misma. Dado que dichas bandas de absorbancia tienen lugar a longitudes de onda concretas de la región del infrarrojo, es posible identificar cualitativamente los grupos funcionales presentes en la muestra problema, así como cuantificar la cantidad de material presente en la misma mediante la evaluación de la altura de los picos de absorbancia. En la técnica ATR-FTIR, el haz de radiación infrarroja emitido se refleja internamente en la interfaz entre la muestra y un medio auxiliar, que debe presentar un índice de refracción muy elevado (Linderberg *et al.*, 2012). En el caso de los equipos utilizados, el medio auxiliar consiste en un cristal de ZnSe.

3.2.5. Técnicas analíticas utilizadas

3.2.5.1. Determinación de la concentración de proteínas en las corrientes permeado y rechazo

Existen diversos métodos disponibles para determinar la concentración de proteínas en una muestra o disolución. Estos métodos se basan en la detección de aminoácidos característicos de las proteínas mediante medida de absorbancia o bien, mediante interacciones entre estos aminoácidos u otros enlaces peptídicos y determinados elementos, como cobre o pigmentos. La elección de

uno u otro método viene determinada por la cantidad de proteína en la muestra a medir, el límite de detección o linealidad del método, su facilidad de uso e, incluso, el tiempo requerido desde la preparación de la muestra hasta la obtención del resultado final (Dean Goldring, 2012).

Uno de estos métodos es el llamado método de medida directa, que consiste en la determinación espectrofotométrica de la absorbancia de la muestra a una longitud de onda de 280 nm. En este valor, los residuos de aminoácidos compuestos por anillos aromáticos en la estructura primaria de las proteínas absorben luz. Estos aminoácidos son, por orden de contribución al fenómeno, triptófano (con una longitud de onda máxima de 279.8 nm), tirosina (274.6 nm) y fenilalanina (279 nm). El método de medida directa se basa en la Ley de Lambert-Beer, según la cual la absorbancia de un compuesto es proporcional a su concentración. La principal ventaja de este método radica en el amplio rango de masa de proteínas que puede ser detectada, desde 20 hasta 3000 µg (Dean Goldring, 2012). Este método fue utilizado para determinar la concentración de proteína presente en la corriente permeado durante la etapa de ensuciamiento llevada a cabo con disoluciones de BSA y BSA con $CaCl_2$, dado que no existían otras especies excepto la propia proteína que interfiriera en la medida realizada. Las rectas de calibrado obtenidas mediante un espectrofotómetro UV-visible HP 8453 (Hewlett Packard, EE.UU.) a una longitud de onda de 278 nm (correspondiente a la absorción máxima de las disoluciones estudiadas) que relacionan la absorbancia de la muestra con la concentración de proteínas

presente en la misma presentaron un coeficiente de regresión R^2 mayor de 0.99.

Otro método ampliamente empleado en la cuantificación de proteínas es el basado en la reacción de las mismas con el ácido bicinconínico (Morton y Evans, 1992; Smith *et al.*, 1985; Krieg *et al.*, 2005; Thanhaeuser *et al.*, 2015). Este método colorimétrico se basa en la formación del complejo Cu^{+2}-proteína (ver Fig. 18) en condiciones alcalinas mediante el uso de un reactivo de trabajo, mezcla de una disolución de ácido bicinconínico, carbonato sódico, tartrato sódico y bicarbonato sódico en NaOH 0.1 N con una disolución de sulfato de cobre (II) pentahidrato al 4 %p/v, en una proporción 50:1. A continuación, tiene lugar la reducción de Cu^{+2} a Cu^{+1}, siendo proporcional esta reducción a la cantidad de proteína presente en la muestra. De acuerdo con el protocolo del ensayo BCA estándar, se mezclan 0.1 mL de muestra con 2 mL del reactivo de trabajo. Esta mezcla se incuba a 37 ºC durante 30 min y, posteriormente, se enfría a temperatura ambiente. Una vez hecho esto, la absorbancia de la mezcla se mide en un espectrofotómetro a 562 nm y se comparan los resultados obtenidos con la recta de calibrado previamente realizada a diferentes concentraciones conocidas de proteína. El rango de linealidad de este método varía entre 200 y 1000 $\mu g \cdot mL^{-1}$ y ente sus ventajas destacan su facilidad de uso, la alta estabilidad del color del complejo formado o la mayor sensibilidad respecto a otros métodos colorimétricos como el método de Lowry, también basado en la formación del complejo Cu^{+2}-proteína (www.sigmaaldrich.com). Este método fue utilizado para determinar la concentración de proteína presente en la disolución enzimática utilizada. La recta de calibrado

obtenida a 562 nm presentó una precisión mayor de 0.99 en términos de R^2.

Finalmente, otro de los métodos colorimétricos utilizados en la presente Tesis Doctoral es el método Bradford (Bradford, 1976; Ku *et al.*, 2013; Qian *et al.*, 2014). Dicho método se basa en la formación de un complejo entre el reactivo Coomassie Brilliant Blue G-250 (ver Fig. 18) y las proteínas presentes en la muestra problema, virando el color del reactivo de marrón rojizo a azul. El complejo formado es el responsable de un aumento de la absorbancia de la muestra a longitudes de onda entre 465 y 595 nm, lo que permite su detección espectrofotométrica. El rango válido de medida varía entre 0.1 y 1.4 $mg \cdot mL^{-1}$ de proteína en la muestra problema. Según el protocolo de medida estándar, 0.1 mL de la muestra se mezclan con 3 mL de reactivo Bradford. Una vez incubada la mezcla a temperatura ambiente entre 5 y 45 min, se miden la misma en un espectrofotómetro a una longitud de onda de 595 nm. Al igual que en el método BCA, la concentración de proteína en la muestra se determina mediante la comparación de la absorbancia medida con la obtenida en la recta de calibrado realizada previamente. La principal ventaja de este método radica en que no es necesario preparar diluciones del reactivo de trabajo y que es compatible con agentes reductores (generalmente utilizados para estabilizar proteínas en disolución), a diferencia del método BCA (www.sigmaaldrich.com). El método Bradford fue empleado en la cuantificación de proteínas en la corriente permeado obtenida en la etapa de ensuciamiento con disoluciones de WPC. Las rectas de calibrado obtenidas presentaron un valor de R^2 mayor de 0.99.

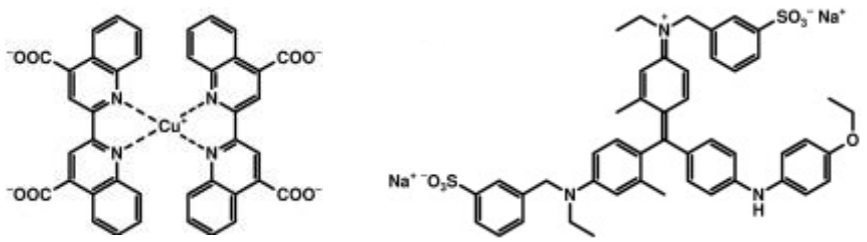

(a) (b)

***Fig. 18**. Estructura de los reactivos utilizados en la cuantificación de proteínas: (a) complejo Cu^{+}-proteína y (b) Coomassie Brilliant Blue G-250 (Thanhaeuser et al., 2015)*

3.2.4.2. Determinación de la composición del WPC empleado

La determinación de la concentración de cada componente que constituye el WPC utilizado para simular las disoluciones de lactosuero se llevó a cabo de la siguiente manera:

- **Proteínas totales**: la concentración total de proteínas en el WPC utilizado se midió mediante el método Bradford explicado anteriormente. Para ello, el WPC en polvo suministrado se disolvió en agua desionizada hasta alcanzar una concentración de 10 $g \cdot L^{-1}$. El resultado demostró que la concentración real de proteínas en base seca fue ligeramente inferior a la indicada por el fabricante (40.74 %p/p frente al 45 % teóricamente esperado).
- **Lactosa**: la cantidad de lactosa se estimó mediante la reacción con ácido 3,5-dinitrosalicílico. Esta reacción ha sido utilizada por otros autores para estimar la cantidad de azúcares reductores en una muestra (Saqib y Whitney, 2011).

Para la preparación del reactivo de trabajo se mezclan 10 g de DNS y 300 g de tartrato de sodio y potasio en 800 mL de NaOH 0.5 N, ajustando el volumen total a 1 L con agua ultrapura. A continuación, se añadieron 4 mL del reactivo de trabajo a 1 mL de la muestra problema. Esta mezcla se mantuvo en un baño de agua a más de 95 ºC durante 5 min, para ser seguidamente transferida a un baño con hielo y, posteriormente, colocada en un baño a una temperatura de 25 ºC. La absorbancia de la muestra se midió a 540 nm utilizando el espectrofotómetro UV-visible anteriormente citado.

- **Cenizas**: El contenido en cenizas se calculó incinerando 1 g del WPC suministrado en polvo en una mufla a 540 ºC durante 1 h (Método Oficial de Análisis 930.30) (AOAC Official Method 930.30, 1930).
- **Cationes**: La concentración de distintos cationes se determinó mediante cromatografía iónica con un cromatógrafo 790 Personal IC equipado con una columna catiónica Metrosep C 2 150 (ambos de Metrohm, Suiza) (Lim *et al.,* 2008).
- **Aniones**: La concentración de aniones se obtuvo mediante kits de medida de cloruro y fosfatos (Mak *et al.*, 2003). En ambos casos, a 1 mL de la muestra preparada se adicionan 0.5 mL del reactivo de trabajo Cl-1K (en el caso de la determinación de cloruros) y 5 gotas del reactivo P-2K junto a 1 dosis del reactivo P-3K (en el caso de la determinación de fosfatos). Una vez transcurridos 5 min, tiempo necesario para que la reacción entre la muestra problema y los reactivos de

trabajo del kit de fosfatos se produjera, se midieron ambas mezclas en un fotómetro Spectroquant® NOVA 60 (Merck Millipore, España). El fotómetro proporciona directamente el valor de concentración de cada uno de los aniones.

- **Grasa**: La concentración de grasa se midió con un equipo MilkoScan FT120 (Gerber Instruments, Suiza). Este tipo de equipos resulta especialmente apropiado para el análisis de productos lácteos complejos mediante la medición de la concentración de distintos componentes, entre ellos la grasa, utilizando la técnica FTIR (Chessa *et al.*, 2014).

3.2.6. Análisis computacional

La caracterización de los mecanismos de ensuciamiento de las membranas se llevó a cabo mediante el ajuste de distintos modelos matemáticos de UF a los datos experimentales obtenidos durante la etapa de ensuciamiento. Este ajuste se realizó mediante el algoritmo "Genfit" del software MathCad®. Dicho algoritmo minimiza la diferencia entre los datos experimentales y los resultados predichos por el modelo mediante una versión optimizada del método Levenberg-Marquadt. La precisión del ajuste de los distintos modelos matemáticos se evaluó en función del coeficiente de regresión R^2 y la desviación estándar.

Por otra parte, el software Statgraphics® Centurion XVI fue utilizado para determinar las ecuaciones que relacionan la eficacia del proceso de limpieza con las variables del proceso, como la temperatura, la concentración de NaCl y la velocidad tangencial,

mediante análisis de regresión múltiple.

Finalmente, los algoritmos “pattern search” del software Matlab® y “Solver” del software Microsoft Excel® permitieron obtener las condiciones de operación óptimas durante la etapa de limpieza en base a las ecuaciones obtenidas mediante el análisis de regresión múltiple.

3.3. BIBLIOGRAFÍA

AFONSO A., MIRANDA J.M. y CAMPOS J.B.L.M. (2009). "Numerical study of BSA ultrafiltration in the limiting flux regime – effect of variable physical properties" en *Desalination*, vol. 249, p. 1139-1150.

AOAC Official Method 930.30 (1930). "Ash of Dried Milk". First Action 1930.

BLANPAIN-AVET P., MIGDAL J.F. y BÉNÉZECH T. (2009). "Chemical cleaning of a tubular ceramic microfiltration membrane fouled with a whey protein concentrate suspension – characterization of hydraulic and chemical cleanliness" en Journal of Membrane Science, vol. 337, p. 153-174.

BRADFORD M.M. (1976). "A rapid and sensitive method for the quantitation of microgram quantities of protein utilizing the principle of protein-dye binding" en *Analytical Biochemistry*, vol. 72, p. 248-254.

CHESSA S. *et al.* (2014). "Selection for milk coagulation properties predicted by Fourier transform infrared spectroscopy in the Italian Holstein-Friesian breed" en *Journal of Dairy Science,* vol. 97, p. 4512-4521.

CHUNG T.-S. *et al.* (2002). "Visualization of the effect of die shear rate on the outer surface morphology of ultrafiltration membranes by AFM" en *Journal of Membrane Science*, vol. 196, p. 251-266.

DAUFIN G. *et al.* (2001). "Recent and emerging applications of membrane processes in the food and dairy industry" en *Food Bioproducts Processing*, vol. 79, p. 89-102.

DEAN GOLDRING J.P. (2012). "Protein quantification methods to determine protein concentration prior to electrophoresis" en Kurien

B.T. y Scofield R.H. *Protein electrophoresis. Methods and protocols*. Nueva York: Springer.

DE OLIVEIRA R.R.L. (2012). "Measurement of the nanoscale roughness by atomic forcé microscopy: Basic principles and applications" en Bellito V. *Atomic Force Microscopy – Imaging, Measuring and Manipulating Surfaces at the Atomic Scale*. InTech. (publicación online).

GARCÍA-IVARS J. *et al.* (2014). "Development of fouling-resistant polyethersulfone ultrafiltration membranes via surface UV photografting with polyethylene glicol/aluminum oxide nanoparticles" en *Separation and Purification Technology*, vol. 135, p. 88-99.

KRIEG R.C. *et al.* (2005). "Protein quantification and its tolerance for different interfering reagents using the BCA-method with regard to 2D SDS PAGE" en *Journal of Biochemical and Biophysical Methods*, vol. 65, p. 13-19.

KU H.-K. *et al.* (2013). "Interpretation of protein quantitation using the Bradford assay: Comparison with two calculation models" en *Analytical Biochemistry*, vol. 434, p. 178-180.

LIM J. *et al.* (2008). "Biochemical indication of microbial mass changes using ATP and DNA measurement in biological treatment of thiocyanate" en *Applied Microbiology and Biotechnology*, vol. 80, p. 525-230.

LINDERBERG C. *et al.* (2012). "ATR-FTIR Spectroscopy" en Chianese A. y Kramer H.J.M. *Industrial Crystallization Process Monitoring*. Alemania: Wiley-VCH.

MAK W.C. *et al.* (2003). "Biosensor for rapid phosphate monitoring in a sequencing batch reactor (SBR) system" en *Biosensors and bioelectronics*, vol. 19, p. 233-237.

MATZINOS P. y ÁLVAREZ R. (2002). "Effect of ionic strength on rinsing and alkaline cleaning of ultrafiltration inorganic membranes fouled with whey proteins" en *Journal of Membrane Science*, vol. 208, p. 23-20.

MERCK MILLIPORE. <http://www.merckmillipore.com/> [Consulta: 1 de junio de 2015].

MORTON R.E. y EVANS T.A. (1992). "Modification of the bicinchoninic acid protein assay to eliminate lipid interference in determining lipoprotein protein content" en *Analytic Biochemistry*, vol. 204, p. 332-334.

MUTHUKUMARAN S. *et al.* (2007). "The application of ultrasound to dairy ultrafiltration: the influence of operating conditions" en *Journal of Food Engineering*, vol. 81, p. 364-373.

NUCCI N.V. y VANDERKOOI J.M. (2008). "Effects of salts of the Hofmeister series on the hydrogen bond network of water" en *Journal of Molecular Liquids*, vol. 143, p. 160-170.

PANREAC QUÍMICA S.L.U. <http://www.panreac.es/es/> [Consulta: 1 de junio de 2015].

QIAN X. *et al.* (2014). "Analysis of the interferences in quantitation of a site-specifically PEGylated exedin-4 analog by the Bradford method" en *Analytical Biochemistry*, vol. 465, p. 50-52.

RAPOSO M., FERREIRA Q. y RIBEIRO P.A. (2007). "A guide for atomic force microscopy analysis of soft condensed matter" en Mendez-Vilas A. Díaz J. *Modern research and educational topics in microscopy*. España: Formatex.

SAQIB A.A.N. y WHITNEY P.J. (2011). "Differential behaviour of the dinitrosalicylic acid (DNS) reagent towards mono- and di-saccharide sugars" en *Biomass and Bioenergy*, vol. 35, p. 4748-4750.

SIGMA ALDRICH Co. LLC. <http://www.sigmaaldrich.com/spain.html> [Consulta: 1 de junio de 2015].

SMITH P.K. *et al.* (1985). "Measurement of protein using bicinchoninic acid" en *Analytical Biochemistry*, vol. 150, p. 76-85.

SUTTIPRASIT P., KRISDHASIMA V. y MCGUIRE J. (1992). "The surface activity of α-lactabumin, β-lactoglobulin and bovine serum albumin" en *Journal of Colloid and Interface Science*, vol. 154, p. 316-326.

THANHAEUSER S.M., WIESER H. y KOEHLER P. (2015). "Spectrophotometric and fluorimetric quantitation of quality-related protein fractions of wheat flour" en *Journal of Cereal Science*, vol. 62, p. 58-65.

WANG Y.-N. y TANG C.Y. (2011). "Protein fouling of nanofiltration, reverse osmosis and ultrafiltration membranes – the role of hydrodynamic conditions, solution chemistry and membrane properties" en *Journal of Membrane Science*, vol. 376, p. 275-282.

CAPÍTULO IV

Modelización del ensuciamiento de las membranas

4.1. MECANISMOS DE ENSUCIAMIENTO DE MEMBRANAS DE ULTRAFILTRACIÓN ENSUCIADAS CON DISOLUCIONES MODELO DE LACTOSUERO

El presente Capítulo consiste en una adaptación al formato de la Tesis Doctoral del artículo titulado "Fouling mechanisms of ultrafiltration membranes fouled with whey model solutions", publicado en la revista Desalination. En él, tres modelos matemáticos de UF se ajustaron a los datos experimentales obtenidos durante la etapa de ensuciamiento con membranas de 5, 30 y 15 kDa, con el fin de determinar los mecanismos de ensuciamiento responsables del ensuciamiento de dichas membranas. Los datos bibliográficos del artículo se destacan a continuación:

***Autores**: M.-J. Corbatón-Báguena, S. Álvarez-Blanco, M.-C. Vincent-Vela*

***Título**: Fouling mechanisms of ultrafiltration membranes fouled with whey model solutions*

***Editorial**: Elsevier*

***Revista**: Desalination año: 2015 vol. 360 p. 87-96*

***Doi**: http://dx.doi.org/10.1016/j.desal.2015.01.019*

Fouling mechanisms of ultrafiltration membranes fouled with whey model solutions

María-José Corbatón-Báguena*, Silvia Álvarez-Blanco, María-Cinta Vincent-Vela

Department of Chemical and Nuclear Engineering, Universitat Politècnica de València, C/Camino de Vera s/n 46022 Valencia, Spain

*Corresponding author: macorba@posgrado.upv.es
Tel: +34963877000 (Ext.: 76383)
Fax: +34963877639 (Ext.: 77639)

Abstract

In this work, three ultrafiltration (UF) membranes with different molecular weight cut-offs (MWCOs) and made of different materials were fouled with several whey model solutions that consisted of bovine serum albumin (BSA) (1 % w/w), BSA (1 % w/w) and $CaCl_2$ (0.06 % w/w in calcium) and whey protein concentrate (WPC) with a total protein content of 45 % w/w at three different concentrations (22.2, 33.3 and 44.4 $g \cdot L^{-1}$). The influence of MWCO and membrane material on the fouling mechanism dominating the UF process was investigated. Experiments were performed using two flat-sheet organic membranes and a ceramic monotubular membrane whose MWCOs were 5, 30 and 15 kDa, respectively. Hermia's models

adapted to crossflow UF, a combined model based on complete blocking and cake formation equations and a resistance-in-series model were fitted to permeate flux decline curves. The results demonstrated that permeate flux decline was accurately predicted by all the models studied. However, the models that fitted the best to permeate flux decline experimental data were the combined model and the resistance-in-series model. Therefore, complete blocking and cake formation were the predominant mechanisms for all the membranes and feed solutions tested.

Keywords: Ultrafiltration; whey model solutions; mathematical models; fouling mechanisms.

4.1.1. Introduction

Ultrafiltration (UF) membranes have been widely used in dairy industries for several applications such as preconcentration of milk, milk dehydration, fractionation of whey, purification of whey proteins, enrichment of micellar casein for the manufacture of milk, etc. (Nigam *et al.*, 2008; Kazemimoghadam and Mohammadi, 2007).

However, one of the major problems in the UF processes applied in dairy industry is membrane fouling. Among the different substances that are present in milk and whey, proteins are the main responsible for membrane fouling (Argüello *et al.*, 2003). The most important consequence of fouling is the gradual permeate flux decline during filtration time. This effect depends on different parameters, such as operating conditions of the UF process (crossflow velocity,

transmembrane pressure, feed concentration and temperature), interactions between foulants and the membrane surface or membrane characteristics (hydrophilicity, pore size and porosity) (Nigam *et al.*, 2008; Wang *et al.*, 2012).

According to the literature, membrane fouling mechanisms can be divided in several types. When the solute molecules are smaller than or similar to the membrane pore size, these molecules can penetrate inside the membrane pores, reducing their effective radius gradually (adsorptive fouling) or causing the entire pore to be completely blocked (pore blocking mechanism) (Salahi *et al.*, 2010; Ruby Figueroa *et al.*, 2011). If solute molecules are much higher than membrane pores, they are deposited on membrane surface. In some cases, the deposited fouling layer may form a cake layer (Tien and Ramarao, 2006; Kim and DiGiano, 2009).

Because of the technical and economical importance of permeate flux decline, determining the optimum operating conditions to minimize fouling and obtaining a model to predict permeate flux decline with time are key steps in UF processes. Previous studies found in the literature have developed permeate flux decline models for UF processes (Ho and Zydney, 2000; Bhattacharya *et al.*, 2001; Duclos-Orsello *et al.*, 2006; Peterson *et al.*, 2007; Yee *et al.*, 2009). Among them, empirical models are the most often used due to their high prediction accuracy because they describe experimental results by fitting a mathematical equation to the data obtained without considering any theoretical parameter (examples of these models are those provided by regression analysis) (Baranyi *et al.*, 1996).

However, as the theoretical description of fouling phenomena and mechanisms is not reflected on the mathematical equation proposed by this type of models, the relationship between permeate flux decline and the fouling mechanism involved in the UF process cannot be explained with empirical models. On the other hand, theoretical models are able to explain the fouling phenomena during membrane filtration, although they are less accurate. For those reasons, semi-empirical models, which use simplified forms of scientific laws and include a certain number of parameters with physical meaning are more appropriate to provide accurate predictions of the permeate flux decline and also to describe the fouling mechanism at the same time (Salahi *et al.*, 2010; Vincent Vela *et al.*, 2009; Mah *et al.*, 2012).

Although several mathematical models can be found in the literature to explain the fouling mechanisms affecting UF membranes (Ho y Zydney, 2000; Yee *et al.*, 2009; Bhattacharjee y Datta, 2003; Peng y Tremblay, 2008), Hermia's models (Hermia, 1982) applied to dead-end filtration and their adaptations to crossflow UF are widely used to fit the experimental data of different UF processes. Previous studies found in the literature have demonstrated that Hermia's models can accurately predict permeate flux decline at different experimental conditions. Mohammadi and Esmaeelifar (2005) analyzed the fouling mechanisms involved in the UF of wastewaters from a vegetable oil factory working at 3 bar and 0.5 $m \cdot s^{-1}$ with a 30 kDa polysulfone membrane. Their results demonstrated that fouling was due to the cake layer formation mechanism, achieving a value of R^2 of 0.99. Vincent Vela *et al.* (2009) investigated the fouling mechanisms involved in PEG UF using a ceramic membrane of 15 kDa. They

obtained that intermediate blocking model was dominant for a transmembrane pressure of 3 bar and a crossflow velocity of 1 $m \cdot s^{-1}$ and in the case of 4 bar and 2 $m \cdot s^{-1}$, with values of R^2 of 0.980 and 0.979, respectively. Salahi *et al.* (2010) studied the UF of oily wastewaters using a polyacrylonitrile membrane of 20 kDa at different transmembrane pressures (1.5, 3 and 4.5 bar) and crossflow velocities (0.25, 0.75 and 1.25 $m \cdot s^{-1}$). For all the experimental conditions tested, the cake layer formation model followed by the intermediate blocking model were the models that fitted the best, with values of R^2 ranging from 0.9852 to 0.9999 in the case of the cake layer formation model and ranging from 0.8710 to 0.9321 for the intermediate blocking model. Kaya *et al.* (2010) applied conventional Hermia's models to predict the fouling mechanism of two nanofiltration membranes (0.4 and 1 kDa) using a paper machine circulation wastewater as feed solution. The best fitting accuracy (R^2 = 0.985) was obtained for the cake layer filtration mechanism followed by the intermediate blocking mechanism (R^2 = 0.982) at a transmembrane pressure of 8 bar.

De la Casa *et al.* (2008) combined two fouling mechanisms of Hermia's models. They proposed two different combinations: the first one considers that only a fraction of membrane surface pores (α) is completely blocked (complete blocking model equation) while part of the foulant molecules may pass through the membrane and be adsorbed on the pore walls that were previously unblocked (1-α) (standard blocking model equation). The second combination takes into account that a cake layer of foulant molecules (cake layer formation model equation) can be formed on the previously deposited

molecules that have previously completely blocked the pores (complete blocking model equation). The combined models were fitted to the experimental data obtained during the microfiltration of 0.25 $g \cdot L^{-1}$ BSA solutions at a transmembrane pressure of 1 bar and a crossflow velocity of 3.28 $m \cdot s^{-1}$.

On the other hand, the resistance-in-series model is one of the most widely used empirical models due to its high accuracy. Choi *et al.* (2000) applied a resistance-in-series model to batch microfiltration of BSA. They considered that total resistance was the sum of the membrane resistance, the cake layer resistance and the fouling resistance. This last one represented the foulant deposits inside the membrane pores. Flux decline predicted by the model was in a good agreement with the experimental data obtained. Carrère *et al.* (2001) used a resistance-in-series model to predict permeate flux decline of lactic acid fermentation broths crossflow filtration at a transmembrane pressure of 2 bar and a crossflow velocity of 4 $m \cdot s^{-1}$. Their model considered four different resistances (the membrane resistance, the resistance of the adsorbed molecules on the membrane surface, the resistance due to concentration polarization and the cake layer resistance). They obtained a good agreement between predicted and experimental data.

The aim of this work was to investigate the fouling mechanisms that affect different UF membranes (two polymeric membranes of 5 and 30 kDa and a ceramic monotubular membrane of 15 kDa) using several whey model solutions (BSA (1 % w/w), BSA (1 % w/w) and $CaCl_2$ (0.06 % w/w in calcium) and whey protein concentrate (WPC)

with a protein content of 45 % at three different concentrations (22.2, 33.3 and 44.4 $g \cdot L^{-1}$)) as feed solutions during the fouling step. For this purpose, several models were fitted to the experimental data obtained during the UF of whey model solutions: Hermia's models adapted to crossflow UF, a resistance-in-series model and a combined model based on the complete blocking and cake layer formation fouling mechanisms. As a novelty, the last model was developed for this work based on the Hermia's equations adapted to crossflow for the two fouling mechanisms considered. The influence of both membrane MWCO and material on the dominating fouling mechanism was investigated. The values of model parameters were estimated for the models with the highest fitting accuracy. Different equations that relate model parameters with operating conditions such as the membrane roughness and the particle size and the protein concentration of the feed solutions were developed.

4.1.2. Modelling

4.1.2.1. Hermia's models

The models developed by Hermia (Hermia, 1982) are based on classical constant pressure dead-end filtration equations. They consider four main types of membrane fouling: complete blocking, intermediate blocking, standard blocking and cake layer formation. These models can be adapted to consider a crossflow configuration (Vincent Vela, 2009; Field *et al.*, 1995; de Barros *et al.*, 2003). Adapted models to crossflow ultrafiltration incorporate the flux associated with the back-transport mass transfer, which is evaluated

at the steady-state (Jarusutthirak *et al.*, 2007). The general equation for Hermia's models adapted to crossflow ultrafiltration is shown in Eq. 6:

$$-\frac{dJ}{dt} = K(J - J_{ss})J^{2-n} \qquad \text{Eq. 6}$$

where J is the permeate flux, K is a model constant and J_{ss} is the permeate flux when the steady-state is achieved.

According to the value of the parameter n, four different models can be distinguished, based on four different fouling mechanisms: complete blocking (n = 2), intermediate blocking (n = 1), standard blocking (n = 1.5) and cake layer formation (n = 0).

In the complete blocking model, a solute molecule that settles on the membrane surface blocks a pore entrance completely, but it cannot penetrate inside the pores. This model assumes that a monomolecular layer is formed on the membrane surface.

The intermediate blocking model is similar to the complete blocking one because it considers that fouling takes place on the membrane surface and not inside the pores. However, intermediate blocking model allows solute molecules to deposit on previously settled ones.

The standard blocking model takes into account that all the membrane pores have the same length and diameter and the solute molecules are smaller than the membrane pore size. Therefore, these molecules can penetrate inside the pores.

When the solute molecules are larger than the membrane pores, they may accumulate on the membrane surface forming a permeable cake layer. This is the basis of the cake layer formation model.

4.1.2.2. Combined model

A combined model based on the crossflow Hermia's equations for complete blocking and cake layer formation was used to predict the permeate flux decline along the whole filtration curve. According to other authors (Ho and Zydney, 2000; de la Casa *et al.*, 2008; Field *et al.*, 1995), typical variation of permeate flux with time involves two fouling mechanisms: a pore blocking during the first minutes of operation that causes a rapid flux decline and a long term flux decline due to the accumulation of foulant molecules on the membrane surface that results in a cake layer formation.

Therefore, the decline in the permeate flux is the sum of the decline due to the complete blocking model and the decline due to the cake layer formation one. Therefore, two model constants have been taken into account: K_c for the complete blocking model and K_g for the cake layer formation model. The combined model also considers that only a fraction of membrane pores are completely blocked (α). Thus, the general equation of the combined model is Eq. 7:

$$J_{combined\ \ model} = \alpha J_{complete\ \ blocking\ model} + (1-\alpha) J_{cake\ layer\ formation\ \ model} \quad \text{Eq. 7}$$

4.1.2.3. Resistance-in-series model

Resistance-in-series model is based on the Darcy's law that relates the permeate flux with the transmembrane pressure and the total hydraulic resistance (Eq. 8):

$$J = \frac{\Delta P}{\mu \cdot R} \qquad \text{Eq. 8}$$

where ΔP is the transmembrane pressure, μ is the feed solution viscosity and R is the total hydraulic resistance.

The total hydraulic resistance can be expressed as the sum of different resistances that take place during the UF process. In this model, the membrane resistance, the cake layer resistance and the adsorption and concentration polarization resistances were considered (Eq. 9).

$$J = \frac{\Delta P}{\mu \cdot \left(R_m + R_a + R_g\right)} \qquad \text{Eq. 9}$$

where R_m is the new membrane resistance, R_a is the resistance due to adsorption on membrane surface and inside its pores and concentration polarization and R_g is the cake layer resistance. In addition, R_a can be fitted using an exponential equation (Choi *et al.*, 2000; Carrère *et al.*, 2001). Therefore, the general equation for the resistance-in-series model is Eq. 10:

$$J = \frac{\Delta P}{\mu \cdot \left(R_m + R'_a \left(1 - exp(-bt)\right) + R_g\right)} \qquad \text{Eq. 10}$$

where R'_a is the steady-state adsorption and concentration polarization resistance and b is the fouling rate due to adsorption.

4.1.3. Experimental

4.1.3.1. Materials

BSA, BSA and $CaCl_2$ and WPC solutions were used as feed solutions to perform the fouling experiments. All these products were supplied in powder form, and were dissolved in deionized water until the desired concentration was achieved for each feed solution. Mean particle size of the feed solutions was determined using a Zetasizer Nano ZS90 (Malvern Instruments Ltd., United Kingdom). BSA (prepared by heat shock fractionation, lyophilized powder, 98 % purity, A3733) was provided by Sigma-Aldrich (Germany), $CaCl_2$ (95 % purity) was purchased from Panreac (Spain) and WPC with a total protein content of 45 % was supplied by Reny Picot (Spain). The composition of the WPC 45 % is shown in Table 9. The following methods were used to estimate the amount of each component in the WPC: bicinchoninic acid method (BCA, Sigma-Aldrich, Germany) for total protein determination (Smith *et al.*, 1985), 3,5-dinitrosalicylic acid (DNS, Sigma-Aldrich, Germany) reaction to estimate the amount of lactose (Miller, 1959), method of incineration in a muffle furnace at 540 ºC for ash content estimation according to the AOAC method

930.30 (AOAC Official Method 930.30, 1930) and cationic chromatography using a “790 Personal IC” chromatograph equipped with a Metrosep C 2 150 column (both supplied by Metrohm, Switzerland) to determine the amount of individual cations. Fat content was measured by a MilkoScan FT120 (Gerber Instruments, Switzerland).

Table 9. Composition of WPC 45 % powder

Component	Value
Total proteins (%)	38.16 ± 0.51
Lactose (%)	42.33 ± 0.16
Fat (%)	9.00 ± 0.45
Ash (%)	6.15 ± 0.07
Ca (%)	0.87 ± 0.08
Na (%)	1.34 ± 0.13
K (%)	1.57 ± 0.01

BSA and WPC are the most widely used compounds to prepare whey model solutions for UF experiments (Nigam *et al.*, 2008; Wang and Tang, 2011; Afonso *et al.*, 2009). In addition, $CaCl_2$ was previously used to study the effect of salts on protein fouling (Almécija *et al.*, 2009; Ang and Elimelech, 2007; Mo *et al.*, 2008).

4.1.3.2. Membranes

Three UF membranes of different materials and MWCOs were used in the experiments: a monotubular ZrO_2-TiO_2 INSIDE CéRAM^{TM} membrane of 15 kDa (TAMI Industries, France), a flat-sheet polyethersulfone (PES) membrane of 5 kDa (Microdyn Nadir, Germany) and a flat-sheet permanently hydrophilic polyethersulfone

(PESH) membrane of 30 kDa (Microdyn Nadir, Germany). The ceramic membrane was 20 cm long with an internal diameter of 0.6 cm and an external diameter of 1 cm and its effective area was 35.5 cm^2. Both polymeric membranes had an effective area of 100 cm^2.

The membranes selected in this work were widely used for treating wastewaters from different industrial fields, such as dye industries (Kawiecka-Skowron and Majewska-Nowak, 2011), pulping plants (Zhang *et al.*, 2010), surface water (Kabsch-Korbutowicz and Urbanowska, 2010), activated sludge plants (Karagündüz and Dizge, 2013) and dairy model solutions (Corbatón-Báguena *et al.*, 2014a; Corbatón-Báguena *et al.*, 2014b), obtaining in all cases high rejection values.

4.1.3.3. Experimental set-up

A VF-S11 UF plant (Orelis, France) was used to perform the fouling experiments in a total recirculation mode. The main parts of the plant are a 10 L feed tank, a temperature regulating system, a variable speed volumetric pump to control the crossflow velocity, two manometers at both sides of the membrane module to measure the transmembrane pressure and a balance (0.001 g accuracy). This experimental set-up is described in (Corbatón-Báguena *et al.*, 2014a).

4.1.3.4. Experimental procedure

Prior to each fouling experiment, a permeability test with deionized water was performed in order to determine the values of R_m for each

membrane used. These values were obtained from the Darcy's law above mentioned (Eq. 8).

Different feed solutions, which contained BSA (1 % w/w), BSA (1 % w/w) and $CaCl_2$ (0.06 % w/w in calcium) and WPC (22.2, 33.3 and 44.4 $g \cdot L^{-1}$), were considered in the fouling tests. Experimental conditions during the fouling step were a transmembrane pressure of 2 bar, a crossflow velocity of 2 $m \cdot s^{-1}$ and a temperature of 25 ºC. The pH values of the feed solutions prepared were in the range 5.97-6.5. The duration of the fouling tests was 2 h. Those conditions were selected according to previous studies on whey ultrafiltration (Matzinos and Álvarez, 2002) because they are commonly used in whey UF. Those conditions also resulted in severe membrane fouling and thus, clear differences among model predictions can also be achieved. During the experiments, the permeate flux was monitored.

After the fouling step, membranes were rinsed with deionized water during 30 min at a temperature of 25 ºC, a transmembrane pressure of 1 bar and a crossflow velocity of 2.18 $m \cdot s^{-1}$ (for the polymeric membranes) and 4.20 $m \cdot s^{-1}$ (for the ceramic membrane). This difference in the values of crossflow velocity was due to the higher membrane roughness of the ceramic membrane in comparison to the polymeric ones. NaCl solutions at a salt concentration of 5 mM, 50 ºC and the same operating conditions of transmembrane pressure and crossflow velocity as those used in the rinsing step were used to clean the membranes during 60 min. After the cleaning procedure, a last rinsing with deionized water was performed again. Further description of the rinsing/cleaning protocols can be found in (Brião y Tavares, 2012).

Finally, to recover the initial membrane permeability if the cleaning procedure with NaCl was not completely effective, the ceramic membrane was cleaned with NaClO aqueous solutions (10 % w/v, Panreac, Spain) at 45 ºC and a pH of 11 and the polymeric membranes were cleaned with NaOH aqueous solutions (98 % purity, Panreac, Spain) at 45 ºC and a pH of 11.

Mathematical models were fitted to the experimental data using the MathCad® Genfit algorithm. The Genfit algorithm minimizes the overall difference between experimental results and the predicted ones by means of an optimized version of the Levenberg-Marquadt method. Fitting accuracy of each model was evaluated in terms of the regression coefficient (R^2) and the standard deviation (SD).

4.1.3.5. AFM measurements

Membranes roughness was measured by using a Multimode Atomic Force Microscope with a NanoScope V controller (Veeco, Santa Barbara, CA, USA) in a tapping mode of imaging at room conditions and recorded images are shown in Fig. 19. Membrane roughness of samples of 5 μm × 5 μm was measured and the results were presented as the Root Mean Square roughness (R_q). It takes into account the standard deviation of the surface height values in a certain area, according to Eq. 11 (Chung *et al.*, 2002):

$$R_q = \sqrt{\frac{\sum \left(Z_i - Z_{avg}\right)^2}{N_p}} \qquad \text{Eq. 11}$$

where Z_i is the height value currently measured, Z_{avg} is the average of the height values and N_p is the number of points in the selected area.

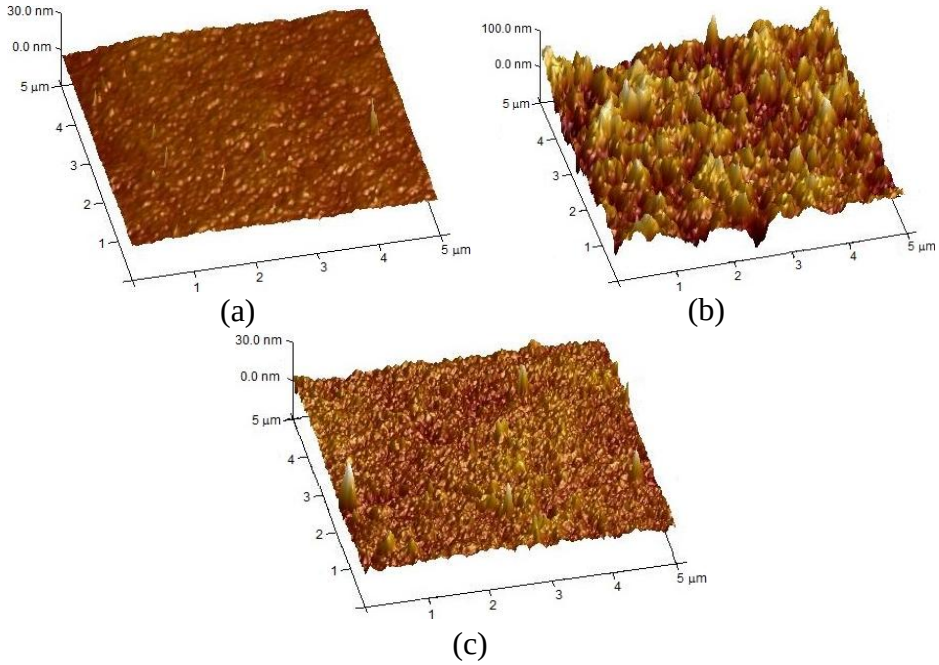

Fig. 19. *AFM images for the membranes of (a) 5 kDa, (b) 15 kDa and (c) 30 kDa*

4.1.4. Results and discussion

The values of the mean particle size of the feed solutions were 3.497±0.078, 4.386±0.705 and 132.000±8.283 nm for the BSA, BSA and $CaCl_2$ and WPC solutions, respectively. The values of the R_m for the membranes used in the experiments were $9.453 \cdot 10^{12}$, $5.001 \cdot 10^{12}$ and $3.794 \cdot 10^{12}$ m^{-1} for the membranes of 5, 15 and 30 kDa, respectively.

Figs. 20 to 24 show the experimental permeate flux decline observed for all the membranes tested during the UF of different feed streams. In Figs. 20-24 permeate flux predictions by means of the three models that showed the highest accuracy (highest R^2 and lowest SD, see Tables 10-14) are represented for each membrane and feed solution considered. Comparing the permeate flux obtained at different WPC concentrations for the same membrane, it can be observed that it decreased as WPC concentration increased for all the membranes tested because the fouling became more severe when WPC concentration increased. In addition, for all the feed solutions tested, the PESH 30 kDa membrane showed the lowest permeate flux decline in comparison with the PES 5 kDa membrane and the ceramic 15 kDa membrane. For example, permeate flux decline was 21.45, 45.60 and 50.97 % for the 30, 5 and 15 kDa membranes, respectively, for the most severe fouling conditions (WPC 45 % at 44.4 $g \cdot L^{-1}$). The reason for that is the hydrophilic nature of the 30 kDa membrane. According to other authors (Rahimpour and Madaeni, 2010; García-Ivars *et al*, 2014), the best antifouling properties (high rejection coefficient, low permeate flux decline and low total filtration resistance) corresponds to the most hydrophilic membranes. Rahimpour and Madaeni (2010) tested several PES membranes during the crossflow filtration of non-skim milk. Their results demonstrated that the hydrophilic PES membranes had a lower permeate flux decline (about 16 %) than the unmodified hydrophobic PES membrane (about 40 %).

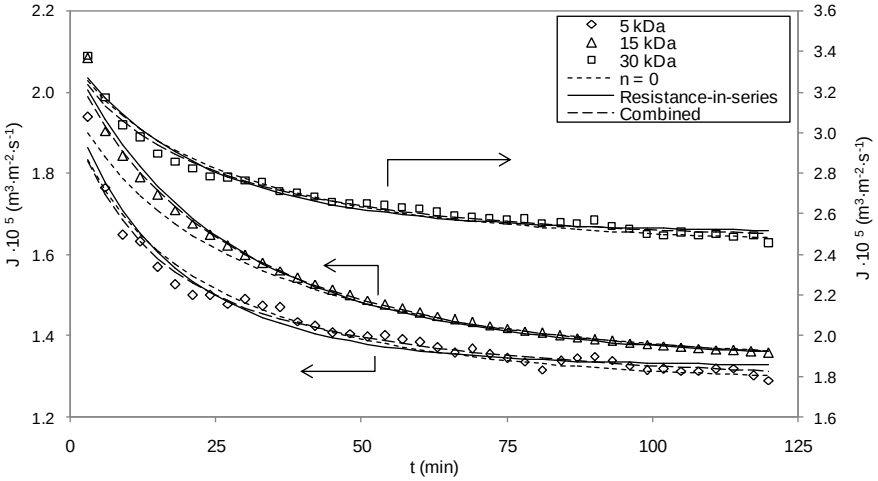

Fig. 20. *Permeate flux predictions for the best fitting models during the ultrafiltration of BSA solutions at 2 bar, 2 m·s^{-1} and 25 ºC (lines: estimated results; symbols: experimental data). The highest fitting accuracy corresponded to the combined model (R^2 of 0.972, 0.993 and 0.976 for the 5, 15 and 30 kDa membranes, respectively)*

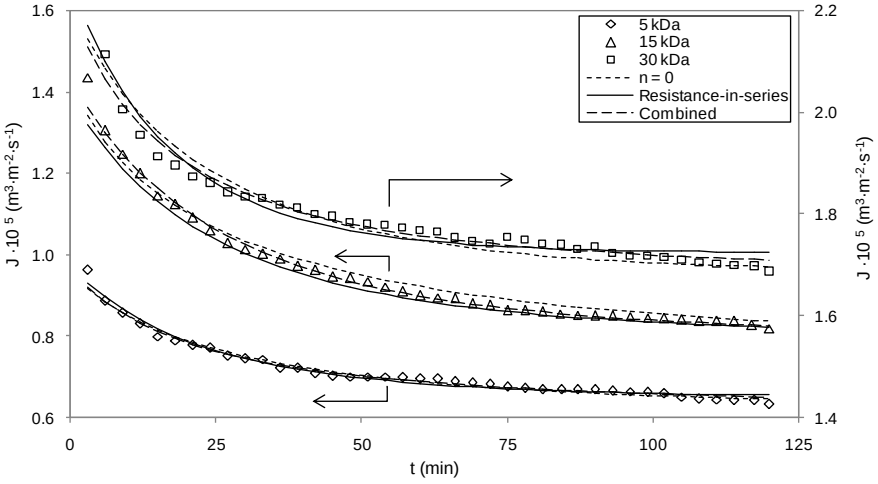

Fig. 21. *Permeate flux predictions for the best fitting models during the ultrafiltration of BSA and $CaCl_2$ solutions at 2 bar, 2 m·s^{-1} and 25 ºC (lines: estimated results; symbols: experimental data). The highest fitting accuracy corresponded to the combined model (R^2 of 0.983 and 0.968 for the 5 and 30 kDa membranes, respectively) and to the resistance-in-series model (R^2 of 0.993 for the 15 kDa membrane)*

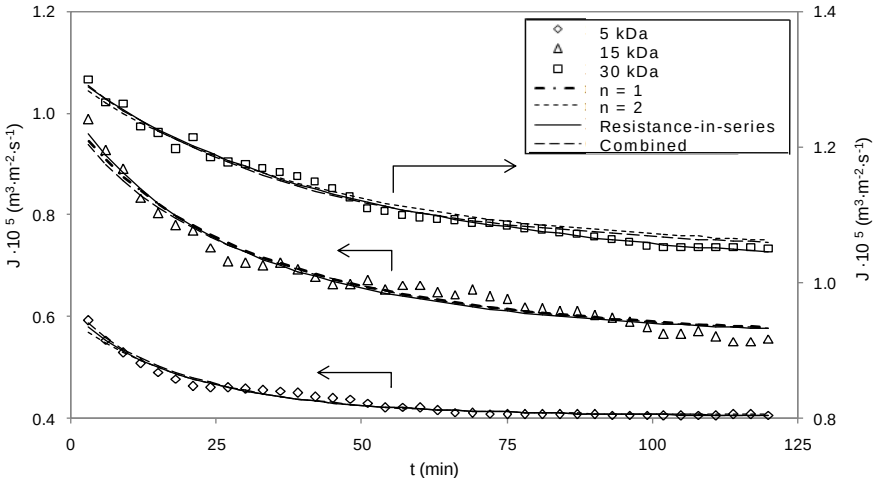

Fig. 22. *Permeate flux predictions for the best fitting models during the ultrafiltration of WPC 45 % (22.2 g·L^{-1}) solutions at 2 bar, 2 m·s^{-1} and 25 ºC (lines: estimated results; symbols: experimental data). The highest fitting accuracy corresponded to the resistance-in-series model (R^2 of 0.982, 0.969 and 0.991 for the 5, 15 and 30 kDa membranes, respectively)*

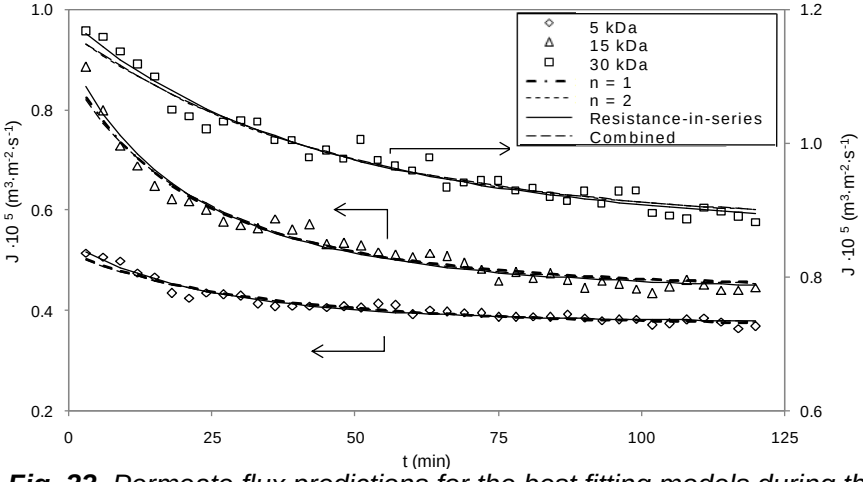

Fig. 23. *Permeate flux predictions for the best fitting models during the ultrafiltration of WPC 45 % (33.3 g·L^{-1}) solutions at 2 bar, 2 m·s^{-1} and 25 ºC (lines: estimated results; symbols: experimental data). The highest fitting accuracy corresponded to the resistance-in-series model (R^2 of 0.952, 0.971 and 0.968 for the 5, 15 and 30 kDa membranes, respectively)*

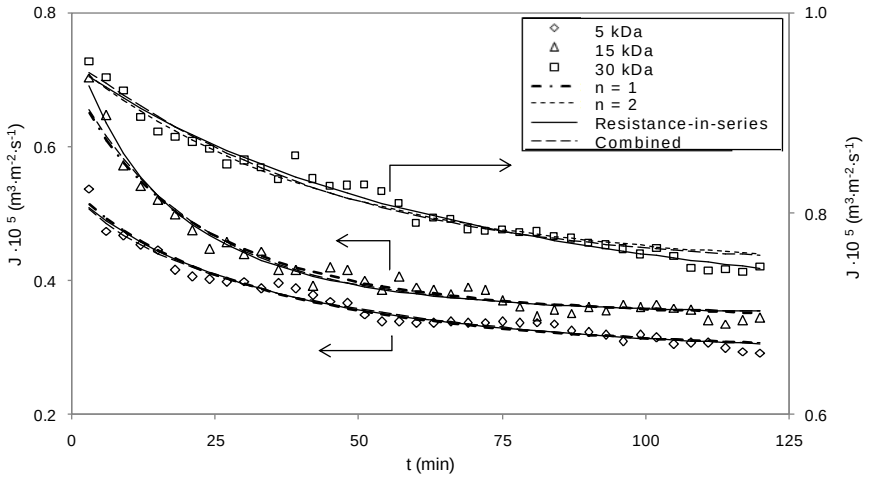

Fig. 24. *Permeate flux predictions for the best fitting models during the ultrafiltration of WPC 45 % (44.4 g·L^{-1}) solutions at 2 bar, 2 m·s^{-1} and 25 ºC (lines: estimated results; symbols: experimental data). The highest fitting accuracy corresponded to the combined model (R^2 of 0.971 for the 5 kDa membrane) and to the resistance-in-series model (R^2 of 0.979 and 0.980 for the 15 and 30 kDa membranes, respectively)*

In addition, membrane fouling is also related to the surface roughness. Evans *et al.* (2008) demonstrated that rougher surfaces favour the entrapment of foulant molecules. This phenomenon can be observed for all the membranes tested comparing permeate flux decline with the Root Mean Square roughness values (R_q) for each membrane tested. The highest flux decline was achieved for the 15 kDa membrane (R_q = 17.900 nm), followed by the 5 kDa membrane (R_q = 0.487 nm and hydrophobic) and the 30 kDa membrane (R_q = 1.657 nm and hydrophilic) (Corbatón-Báguena *et al.*, 2014b). This pattern was in accordance with the results obtained by García-Ivars *et al.* (2014). They demonstrated that PES 30 kDa membranes with high hydrophilicity and low surface roughness had the lowest permeate flux decline during several fouling/rinsing cycles

compared with other modified and unmodified PES membranes with higher surface roughness and hidrophobicity.

Tables 10 to 14 show the fitting accuracy for the Hermia's models adapted to crossflow, the combined model and the resistance-in-series model for all the membranes and feed solutions tested. All the models fitted with almost the same accuracy to the experimental data, with the only exception of the standard blocking model. The fitting accuracy of the standard blocking model (n = 1.5) was very low for all the experimental data considered in this work. Therefore, this model was not considered. This can be explained by the fact that solute molecules were larger than the membrane pores, as in the case of the BSA and BSA and $CaCl_2$ feed solutions (Wang *et al*., 2012). In the case of WPC 45 % feed solutions, at the pH values of the solutions prepared in this work (5.97), the lowest molecular weight proteins tend to form dimers that are larger than the pore size of the membranes (Fox and McSweeney, 2003; Mills and Creamer, 1975). Therefore, they cannot penetrate inside the porous structure.

In Tables 10-14, the models with the best fitting accuracy are highlighted in bold for each membrane and feed solution tested. As it can be observed in Table 10, the combined model was the best for all the membranes when BSA was used as feed solution. When BSA and $CaCl_2$ solutions were ultrafiltered (see Table 11), the combined model had the highest fitting accuracy for the polymeric membranes (5 and 30 kDa). However, the resistance-in-series model had a slightly higher value of R^2 for the 15 kDa ceramic membrane fouled with BSA and $CaCl_2$. In the case of WPC 45 % solutions (Tables 12-

14), the model that fitted the best to the experimental data was the resistance-in-series model for all the membranes, except for the 5 kDa membrane when WPC 45 % at the highest concentration (44.4 $g \cdot L^{-1}$) was tested. In this last case, the best model was the combined one. However, in some cases it is difficult to select the best fitting model between the combined and the resistance-in-series one, such as in the case of the 15 kDa membrane using BSA (Table 10).

According to other authors (Ho and Zydney, 2000; de la Casa *et al*., 2008), the decrease in permeate flux with time can be divided in two stages: first, a rapid flux decline due to a pore blocking phenomena and, after that, a slow decrease until the steady-state is achieved due to the formation of a cake layer. These two stages are those that are considered in the combined model.

Table 10. Models fitting accuracy for the ultrafiltration of BSA solutions at 25 ºC, 2 bar and 2 $m \cdot s^{-1}$: values of R^2 and SD

MWCO (kDa)	Model	R^2	SD
5	Complete blocking (n = 2)	0.922	0.025
	Intermediate blocking (n = 1)	0.948	0.020
	Cake formation (n = 0)	0.962	0.016
	Combined model	**0.972**	**0.013**
	Resistance-in-series model	0.964	0.017
15	Complete blocking (n = 2)	0.981	0.014
	Intermediate blocking (n = 1)	0.904	0.033
	Cake formation (n = 0)	0.991	0.008
	Combined model	**0.993**	**0.007**
	Resistance-in-series model	0.992	0.008
30	Complete blocking (n = 2)	0.936	0.018
	Intermediate blocking (n = 1)	0.957	0.015
	Cake formation (n = 0)	0.970	0.012
	Combined model	**0.976**	**0.010**
	Resistance-in-series model	0.971	0.012

Table 11. Models fitting accuracy for the ultrafiltration of BSA and $CaCl_2$ solutions at 25 ºC, 2 bar and 2 $m \cdot s^{-1}$: values of R^2 and SD

MWCO (kDa)	Model	R^2	SD
5	Complete blocking (n = 2)	0.950	0.022
	Intermediate blocking (n = 1)	0.971	0.016
	Cake formation (n = 0)	0.980	0.013
	Combined model	**0.983**	**0.012**
	Resistance-in-series model	0.980	0.013
15	Complete blocking (n = 2)	0.975	0.024
	Intermediate blocking (n = 1)	0.969	0.026
	Cake formation (n = 0)	0.977	0.022
	Combined model	0.991	0.012
	Resistance-in-series model	**0.993**	**0.012**
30	Complete blocking (n = 2)	0.922	0.017
	Intermediate blocking (n = 1)	0.941	0.015
	Cake formation (n = 0)	0.953	0.013
	Combined model	**0.968**	**0.010**
	Resistance-in-series model	0.965	0.011

Table 12. Models fitting accuracy for the ultrafiltration of WPC 45 % solutions (22.2 $g \cdot L^{-1}$) at 25 ºC, 2 bar and 2 $m \cdot s^{-1}$: values of R^2 and SD

MWCO (kDa)	Model	R^2	SD
5	Complete blocking (n = 2)	0.976	0.014
	Intermediate blocking (n = 1)	0.975	0.014
	Cake formation (n = 0)	0.966	0.017
	Combined model	0.980	0.014
	Resistance-in-series model	**0.982**	**0.013**
15	Complete blocking (n = 2)	0.954	0.032
	Intermediate blocking (n = 1)	0.967	0.028
	Cake formation (n = 0)	0.958	0.031
	Combined model	0.966	0.028
	Resistance-in-series model	**0.969**	**0.028**
30	Complete blocking (n = 2)	0.973	0.010
	Intermediate blocking (n = 1)	0.965	0.012
	Cake formation (n = 0)	0.962	0.012
	Combined model	0.982	0.008
	Resistance-in-series model	**0.991**	**0.006**

Table 13. Models fitting accuracy for the ultrafiltration of WPC 45 % solutions (33.3 $g \cdot L^{-1}$) at 25 ºC, 2 bar and 2 $m \cdot s^{-1}$: values of R^2 and SD

MWCO (kDa)	Model	R^2	SD
5	Complete blocking (n = 2)	0.936	0.022
	Intermediate blocking (n = 1)	0.941	0.021
	Cake formation (n = 0)	0.938	0.021
	Combined model	0.943	0.032
	Resistance-in-series model	**0.952**	**0.020**
15	Complete blocking (n = 2)	0.957	0.036
	Intermediate blocking (n = 1)	0.967	0.032
	Cake formation (n = 0)	0.949	0.039
	Combined model	0.965	0.032
	Resistance-in-series model	**0.971**	**0.031**
30	Complete blocking (n = 2)	0.962	0.015
	Intermediate blocking (n = 1)	0.958	0.016
	Cake formation (n = 0)	0.948	0.017
	Combined model	0.962	0.015
	Resistance-in-series model	**0.968**	**0.014**

Table 14. Models fitting accuracy for the ultrafiltration of WPC 45 % solutions (44.4 $g \cdot L^{-1}$) at 25 ºC, 2 bar and 2 $m \cdot s^{-1}$: values of R^2 and SD

MWCO (kDa)	Model	R^2	SD
5	Complete blocking (n = 2)	0.952	0.032
	Intermediate blocking (n = 1)	0.969	0.027
	Cake formation (n = 0)	0.964	0.029
	Combined model	**0.971**	**0.025**
	Resistance-in-series model	0.969	0.026
15	Complete blocking (n = 2)	0.962	0.036
	Intermediate blocking (n = 1)	0.969	0.031
	Cake formation (n = 0)	0.943	0.040
	Combined model	0.969	0.032
	Resistance-in-series model	**0.979**	**0.030**
30	Complete blocking (n = 2)	0.965	0.013
	Intermediate blocking (n = 1)	0.959	0.014
	Cake formation (n = 0)	0.950	0.016
	Combined model	0.968	0.012
	Resistance-in-series model	**0.980**	**0.009**

The resistance-in-series model takes into account both fouling mechanisms as well as it considers the resistance due to adsorption of solute molecules on the membrane surface and inside its pores and the resistance caused by the cake layer. Therefore, according to both models, both mechanisms (pore blocking and cake layer formation) must be considered to explain membrane fouling when whey model solutions (BSA, BSA and $CaCl_2$ and WPC solutions) are ultrafiltered.

The values of model parameters for the best fitting models are shown in Table 15. When BSA was used as feed solution, the values of the pore blocking parameter, α, indicate that cake layer formation was the predominant fouling mechanism for all the membranes tested. This result is also in agreement with the individual analysis of Hermia's models adapted to crossflow in the case of BSA solutions (see Table 10). The reason can be that solute molecules (67 kDa) are much larger than the pores of the 5, 15 and 30 kDa membranes, thus solute molecules are accumulated on the membrane surface, forming a layer on it. Regarding the values of the cake layer formation model parameter, K_g, and the complete blocking model parameter, K_c, for the 5, 15 and 30 kDa membranes and BSA solutions (Table 15), both parameters decreased when the MWCO increased. It is important to note that one of the hypotheses of the Hermia's complete blocking model is that the pore entrance is completely blocked or sealed when one solute molecule arrives at the membrane surface. Therefore, both models (complete blocking and cake layer formation) consider membrane fouling mechanisms that are external and occur on the membrane surface (Brião and Tavares, 2012).

Table 15. Values of model parameters for the best fitting models

MWCO (kDa)	Feed solution	Resistance-in-series model			Combined model		
		$R'_a \cdot 10^{-13}$ (m^{-1})	$b \cdot 10^4$ (s^{-1})	$R_g \cdot 10^{-13}$ (m^{-1})	K_c (s^{-1})	$K_g \cdot 10^{-6}$ ($s \cdot m^{-2}$)	α (dimensionless)
5	BSA	-	-	-	83.519	2.050	0.349
	BSA + $CaCl_2$	-	-	-	112.731	7.287	0.312
	WPC 45 % (22.2 $g \cdot L^{-1}$)	1.877	6.392	2.792	-	-	-
	WPC 45 % (33.3 $g \cdot L^{-1}$)	1.759	5.306	3.212	-	-	-
	WPC 45 % (44.4 $g \cdot L^{-1}$)	-	-	-	65.898	40.590	0.442
15	BSA	-	-	-	30.042	2.012	0.288
	BSA + $CaCl_2$	1.253	4.250	1.015	-	-	-
	WPC 45 % (22.2 $g \cdot L^{-1}$)	1.789	3.664	1.713	-	-	-
	WPC 45 % (33.3 $g \cdot L^{-1}$)	2.633	4.278	1.945	-	-	-
	WPC 45 % (44.4 $g \cdot L^{-1}$)	3.474	5.394	2.409	-	-	-
30	BSA	-	-	-	7.757	1.212	0.312
	BSA + $CaCl_2$	-	-	-	11.913	3.119	0.287
	WPC 45 % (22.2 $g \cdot L^{-1}$)	0.487	2.951	1.330	-	-	-
	WPC 45 % (33.3 $g \cdot L^{-1}$)	0.696	2.941	1.506	-	-	-
	WPC 45 % (44.4 $g \cdot L^{-1}$)	0.836	2.020	1.978	-	-	-

According to Brião and Tavares (2012), these external membrane fouling mechanisms are related to the difference between the solute molecule size and the membrane pore size. This difference is higher as the MWCO decreases. Thus, a greater amount of particles can be deposited on the membrane surface and a tighter bound cake layer may be formed on the membrane with the lowest MWCO (5 kDa). On the other hand, according to the membrane material, hydrophilic membranes usually have better antifouling properties than those made of hydrophobic materials (Rahimpour and Madaeni, 2010; García-Ivars *et al.*, 2014; Evans *et al.,* 2008). As the 30 kDa membrane was a PESH membrane, the fouling was less severe using the same feed solution and experimental conditions as in the case of the 5 kDa PES membrane. In addition, as it was above mentioned, the lower the membrane roughness is, the less severe the membrane fouling is. For the membranes tested in this work, the roughness of the PESH 30 kDa membrane is very low and similar to that of the hydrophobic PES 5 kDa membrane. However, the surface roughness of the ceramic 15 kDa membrane is much greater. Therefore, the combination of high hydrophilicity and low surface roughness favour the low permeate flux decline observed for the 30 kDa membrane.

When BSA and $CaCl_2$ solutions were used as feed solutions, the best fitting accuracy was obtained with the combined model for the polymeric membranes (5 and 30 kDa). In this case, comparing the values of the parameters when BSA solutions were used and those calculated for BSA and $CaCl_2$ solutions, it can be observed that the values of both parameters considered in this model (K_c and K_g)

increased to a large extent when BSA and $CaCl_2$ were fed simultaneously. Therefore, fouling was more severe when $CaCl_2$ was added to the feed solutions. Calcium salts have been demonstrated to act as bridging agents between proteins, agglomerating them (Almécija *et al.*, 2009; Ang and Elimelech, 2007). Almécija *et al.* (2009) investigated the effect of calcium salts on the UF of whey solutions. They reported that the percentage of membrane blocked pores during UF increased as the concentration of calcium salts increased in the feed solution. Ang and Elimelech (2007) studied the fouling of reverse osmosis membranes using BSA and calcium solutions. They demonstrated that, when calcium concentration increased, permeate flux decline was greater because the electrostatic repulsion among BSA molecules is diminished. De la Casa *et al.* demonstrated that Hermia's models parameters increased as the membrane fouling was more severe during the microfiltration of BSA (de la Casa *et al*., 2008). According to their work, permeate flux reduction and thus, membrane fouling, was greater at values of pH near the isoelectric point of the protein, when protein agglomeration occurs as well. Comparing the values of the Hermia's cake layer formation parameter, they observed that these values increased as membrane fouling was more severe (at pH 7). On the other hand, comparing the values of the model parameters K_c and K_g for the 5 and 30 kDa when BSA and $CaCl_2$ solutions were fed, it can be observed that both parameters decreased as membrane MWCO increased. It indicates a lower permeate flux decline and thus, less severe membrane fouling in the case of the 30 kDa membrane. This pattern is in agreement with that obtained for BSA solutions.

The resistance-in-series model was the model with the highest fitting accuracy when WPC 45 % solutions at a concentration of 22.2 and 33.3 $g \cdot L^{-1}$ were used as feed for all the membranes tested and also for the 15 and 30 kDa membranes using WPC 45 % solutions at 44.4 $g \cdot L^{-1}$. Comparing the values for the model parameters R'_a and R_g, it can be observed that they increased as the MWCO decreased for all the membranes tested. The increase in model parameters with the membrane MWCO is in agreement with the results previously commented for the other feed solutions. In addition, for the 15 and 30 kDa membranes, the values of R'_a and R_g increased when WPC concentration increased from 22.2 to 44.4 $g \cdot L^{-1}$, indicating greater membrane fouling as feed concentration increased. For the 5 kDa membrane, R_g also increased when WPC concentration increased from 22.2 to 33.3 $g \cdot L^{-1}$. However, the value of R'_a was similar for both WPC concentrations. This can be due to the fact that, because of the great difference between the proteins size and the membrane pore size, the possibility of adsorption inside the pores is lower in the case of the membrane with the lowest MWCO (5 kDa) in comparison with the other membranes. Thus, the value of R'_a is similar independently of the WPC concentration.

In order to generalize the values of the model parameters for different membranes, feed solutions and protein concentrations in the feed solution; the model parameters for the two best fitting models (resistance-in-series and combined models) were correlated to three independent variables (membrane surface roughness, mean particle size of the feed solution and protein concentration in the feed solutions) using a multiple regression analysis from Statgraphics®.

The developed equations that relate the values of model parameters (Table 15) to the three independent variables and their combinations at a confidence interval of 95 % (p-values lower than 0.05) are Eqs. 12-17. The accuracy of these equations (Eqs. 12-17) in terms of R^2 was 0.973, 0.926, 0.988, 0.974, 0.984 and 0.971, respectively.

$$R'_a = 1.330 \cdot 10^{13} - 9.212 \cdot 10^{12} \cdot R_q + 4.394 \cdot 10^{10} \cdot r + 4.589 \cdot 10^{11} \cdot {R_q}^2 + \\ + 9.359 \cdot 10^{10} \cdot R_q \cdot C_b$$

Eq. 12

$$b = 8.207 \cdot 10^{-4} - 2.891 \cdot 10^{-4} \cdot R_q + 1.506 \cdot 10^{-5} \cdot {R_q}^2 - 4.405 \cdot 10^{-7} \cdot {C_b}^2$$

Eq. 13

$$R_g = 2.660 \cdot 10^{13} - 1.399 \cdot 10^{13} \cdot R_q + 4.611 \cdot 10^{10} \cdot r + 7.263 \cdot 10^{11} \cdot {R_q}^2 + \\ + 2.020 \cdot 10^{10} \cdot {C_b}^2$$

Eq. 14

$$K_c = 192.336 - 162.484 \cdot R_q + 0.130 \cdot r + 5.210 \cdot {R_q}^2 - 0.302 \cdot {C_b}^2 + \\ + 6.215 \cdot R_q \cdot C_b$$

Eq. 15

$$K_g = -1.998 \cdot 10^9 + 4.528 \cdot 10^7 \cdot R_q + 2.773 \cdot 10^8 \cdot C_b - 2.363 \cdot 10^4 \cdot r^2 - \\ - 7.712 \cdot 10^6 \cdot {C_b}^2 - 4.604 \cdot 10^6 \cdot R_q \cdot C_b + 1.825 \cdot 10^5 \cdot R_q \cdot r$$

Eq. 16

$$a = 7.490 \cdot 10^{-1} - 4.783 \cdot 10^{-2} \cdot C_b - 2.425 \cdot 10^{-3} \cdot {R_q}^2 - 3.608 \cdot 10^{-5} \cdot r^2 - \\ - 4.504 \cdot 10^{-3} \cdot R_q \cdot C_b - 2.089 \cdot 10^{-4} \cdot R_q \cdot r$$

Eq. 17

These equations can be used to predict the best conditions resulting in the lowest possible fouling and thus, in the highest steady-state permeate flux. In the case of the resistance-in-series model, which was one of the most accurate for the experimental data obtained for all the membranes and feed solutions tested, the general model equation (Eq. 10) indicated that the highest steady-state permeate flux was obtained when R'_a and R_g had a value of 0. Therefore, an optimization analysis was performed by means of the Microsoft Excel Solver tool in order to determine the values of the independent variables in Eqs. 7-9 that made R'_a and R_g equal to 0. These values were a membrane surface roughness of 1.605 nm, a particle size of 1.374 nm and a protein concentration in the feed solution of 1.647 $g \cdot L^{-1}$. As it was above mentioned, the lower the protein concentration in the feed solution and its particle size are, the less aggregates are formed and thus, the lower the membrane fouling is. In addition, rougher surfaces allow solute molecules to deposit on them, favouring membrane fouling (García-Ivars *et* al, 2014; Evans *et al*, 2008).

4.1.5. Conclusions

The models studied in this work can predict with high accuracy the experimental permeate flux for all the membranes tested when

different whey model solutions that contained BSA (1 % w/w), BSA (1 % w/w) and $CaCl_2$ (0.06 % w/w in calcium) and WPC with a total protein concentration of 45 % w/w (22.2, 33.3 and 44.4 $g \cdot L^{-1}$) were ultrafiltered at 2 bar and 2 $m \cdot s^{-1}$. By fitting experimental data to all these models, the predominant fouling mechanisms were confirmed for all the membranes and feed solutions tested. Only the Hermia's standard blocking model did not show a very accurate fitting to the experimental data, because solute molecules were much higher than membrane pore size, thus they cannot penetrate inside the membrane porous structure.

According to the accuracy of models fitting, the resistance-in-series model and the combined model achieved the highest R^2 and lowest SD for all the feed solutions and membranes tested. This indicates that both cake layer formation and pore blocking contributed to membrane fouling.

The combination of high hydrophilicity and low surface roughness resulted in a membrane with better antifouling behaviour. Thus, the 30 kDa membrane showed the lowest permeate flux decline and the lowest values of model parameters for all the feed solutions tested.

Acknowledgements

The authors of this work wish to gratefully acknowledge the financial support of the Spanish Ministry of Science and Innovation through the project CTM2010-20186.

Nomenclature

List of symbols

b	Fouling rate due to adsorption (s^{-1})
C_b	Protein concentration in the feed solution ($g \cdot L^{-1}$)
K	Hermia's model constant (units depending on n)
K_c	Complete blocking model constant (s^{-1})
K_g	Cake layer formation model constant ($s \cdot m^{-2}$)
J	Permeate flux ($m^3 \cdot m^{-2} \cdot s^{-1}$)
J_{model}	Permeate flux predicted by each model ($m^3 \cdot m^{-2} \cdot s^{-1}$)
J_{ss}	Steady-state permeate flux ($m^3 \cdot m^{-2} \cdot s^{-1}$)
n	Hermia's model parameter (dimensionless)
N_p	Number of points within the selected area (dimensionless)
ΔP	Transmembrane pressure (bar)
r	Mean particle size (nm)
R	Total hydraulic resistance (m^{-1})
R_a	Resistance due to adsorption on membrane surface and inside its pores and concentration polarization (m^{-1})
R'_a	Steady-state adsorption resistance
R_g	Cake layer resistance (m^{-1})
R_m	New membrane resistance (m^{-1})
R_q	Root Mean Square Roughness (nm)
t	Filtration time (s)
Z_{avg}	Average of the height values of the sample (nm)
Z_i	Value of height currently measured (nm)

Greek letters

α	Fraction of membrane pores completely blocked (dimensionless)
μ	Feed solution viscosity ($kg \cdot m^{-1} \cdot s^{-1}$)

Abbreviations

BSA	Bovine serum albumin
MWCO	Molecular weight cut off
PES	Polyethersulfone
PESH	Permanently hydrophilic polyethersulfone
UF	Ultrafiltration
WPC	Whey protein concentrate

4.2. MECANISMOS DE ENSUCIAMIENTO DE LA MEMBRANA DE 50 kDa

Tal y como se detalla en los Capítulos V y IX de esta Tesis Doctoral, la membrana de 50 kDa fue ensuciada únicamente con disoluciones de BSA. Por este motivo, y dado que los datos referidos a la modelización del ensuciamiento de dicha membrana no se incluyen en la sección 4.1, se describen a continuación los mecanismos principalmente responsables del ensuciamiento de la membrana cerámica de 50 kDa con disoluciones de BSA de 10 $g \cdot L^{-1}$.

La Fig. 25 muestra la evolución de la densidad de flujo de permeado con el tiempo para la membrana de 50 kDa ensuciada con disoluciones de BSA en las mismas condiciones experimentales que el resto de membranas consideradas en la sección 4.1 (2 bar, 2 $m \cdot s^{-1}$ y 25 ºC). Además, en dicha figura también se representan los modelos matemáticos que presentan mejor grado de ajuste (mayores valores de R^2 y menores valores de desviación estándar), de acuerdo con la Tabla 16. Como puede observarse en la Fig. 25, la densidad de flujo de permeado experimentó un descenso considerable (60 %, aproximadamente) durante los 120 min de duración del ensayo de UF. Esta disminución es mayor que la observada para el resto de membranas consideradas (5, 15 y 30 kDa) ensuciadas con BSA en las mismas condiciones experimentales, lo cual indica el ensuciamiento más severo producido en la membrana de mayor MWCO.

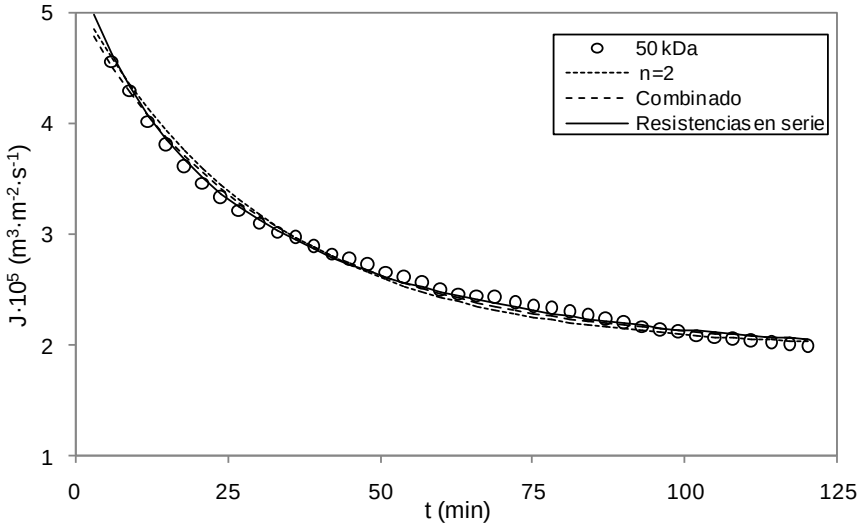

Fig. 25. *Predicción de la variación de la densidad de flujo de permeado con el tiempo para la membrana de 50 kDa ensuciada con disoluciones de BSA (10 g·L^{-1}) a 2 bar, 2 m·s^{-1} y 25 ºC (líneas: resultados predichos; símbolos: datos experimentales)*

La Tabla 16 muestra los valores de precisión del ajuste de los distintos modelos matemáticos a los datos experimentales obtenidos durante la UF de BSA con la membrana de 50 kDa. Como puede observarse, el modelo con el que se obtuvo un mayor valor de R^2 y un menor resultado de desviación estándar fue el modelo de resistencias en serie. De acuerdo con lo explicado en la sección 4.1., el modelo de resistencias en serie tiene en cuenta tanto la resistencia debida a la adsorción de moléculas de soluto sobre la superficie de la membrana y en el interior de sus poros como la resistencia debida a la formación de una capa de ensuciamiento. Por tanto, ambos mecanismos (bloqueo de poros y formación de torta) deben considerarse como principales responsables del ensuciamiento de la membrana de 50 kDa ensuciada con disoluciones de BSA. Además, de acuerdo con los modelos de Hermia adaptados a flujo tangencial,

el modelo que presenta un mayor grado de ajuste es el bloqueo completo de poros, lo que indica que éste es el principal mecanismo de ensuciamiento de la membrana. Este hecho confirma los resultados anteriormente mencionados en cuanto al modelo de resistencias en serie. Finalmente, cabe comentar que el modelo de Hermia de bloqueo estándar no se ajustó correctamente a los datos experimentales, lo que es debido al tamaño similar o ligeramente superior de las moléculas de BSA con respecto al tamaño de poro de la membrana de 50 kDa.

Tabla 16. Precisión del ajuste de los modelos para la UF de disoluciones de BSA (10 $g \cdot L^{-1}$) a 25 ºC, 2 bar y 2 $m \cdot s^{-1}$ para la membrana de 50 kDa: valores de R^2 and desviación estándar

MWCO (kDa)	Modelo	R^2	Desviación estándar
50	Bloqueo completo (n = 2)	0.990	0.025
	Bloqueo intermedio (n = 1)	0.985	0.035
	Formación de torta (n = 0)	0.931	0.065
	Modelo combinado	0.991	0.022
	Modelo de resistencias en serie	**0.997**	**0.016**

La Tabla 17 muestra los valores de los parámetros de los modelos con mejor ajuste (modelos combinado y de resistencias en serie) para la membrana de 50 kDa ensuciada con disoluciones de BSA. De acuerdo con los resultados del modelo de resistencias en serie, se observa que la resistencia debida a la adsorción superficial e interna en la membrana R'_a es mayor que la resistencia debida a la formación de torta R_g. Este hecho se debe al tamaño similar de los poros de la membrana y de las moléculas de BSA, lo cual favorece el taponamiento completo de los poros y la posible entrada de las moléculas de BSA en la estructura porosa de la membrana. En

cuanto al modelo combinado, tal y como detallan Brião y Tavares (2012), tanto el mecanismo de bloqueo completo de poros como la formación de torta son mecanismos de ensuciamiento externos, es decir, tienen lugar sobre la superficie de la membrana debido al sellado externo de los poros y a la acumulación de moléculas de soluto sobre la superficie de la membrana. Por tanto, debido a la menor diferencia entre el tamaño de los poros de la membrana y de las moléculas de BSA, los parámetros relacionados con los mecanismos de ensuciamiento anteriormente mencionados (K_c y K_g) son menores que los obtenidos para el resto de membranas (5, 15 y 30 kDa) ensuciadas con BSA (Tabla 15). Atendiendo al valor del parámetro α, el mecanismo de ensuciamiento predominante es el bloqueo completo de poros, lo que confirma el mayor descenso de densidad de flujo de permeado observado para la membrana de 50 kDa durante la etapa de ensuciamiento con BSA.

Tabla 17. Valores de los parámetros de los modelos con mejor precisión en el ajuste para la membrana de 50 kDa ensuciada con disoluciones de BSA (10 $g \cdot L^{-1}$) a 2 bar y 2 $m \cdot s^{-1}$

MWCO (kDa)	Modelo de resistencias en serie			Modelo combinado		
	$R'_a\ 10^{-13}$ (m^{-1})	$b \cdot 10^{4}$ (s^{-1})	$R_g \cdot 10^{-13}$ (m^{-1})	K_c (s^{-1})	$K_g \cdot 10^{-6}$ ($s \cdot m^{-2}$)	α
50	0.799	2.645	0.219	9.997	0.685	0.845

4.3. BIBLIOGRAFÍA

AFONSO A., MIRANDA J.M. y CAMPOS J.B.L.M. (2009). "Numerical study of BSA ultrafiltration in the limiting flux regime – effect of variable physical properties" en *Desalination*, vol. 249, p. 1139-1150.

ALMÉCIJA M.C. *et al.* (2009). "Influence of the cleaning temperature on the permeability of ceramic membranes" en *Desalination*, vol. 245, p. 708-713.

ANG W.S. y ELIMELECH M. (2007). "Protein (BSA) fouling of reverse osmosis membranes: Implications for wastewater reclamation" en *Journal of Membrane Science*, vol. 296, p. 83-92.

ARGÜELLO M.A. *et al.* (2003). "Enzymatic cleaning of inorganic ultrafiltration membranes used for whey protein fractionation" en *Journal of Membrane Science*, vol. 216, p. 121-134.

AOAC Official Method 930.30. (1930). "Ash of Dried Milk". First action 1930.

BARANYI J. *et al.* (1996). "Effects of parameterization on the performance of empirical models used in "predictive microbiology"" en *Food Microbiology*, vol. 13, p. 83-91.

BHATTACHARJEE C. y DATTA S. (2003). "Analysis of polarized layer resistance during ultrafiltration of PEG-6000: an approach based on filtration theory" en *Separation and Purification Technology*, vol. 33, p. 115-126.

BHATTACHARYA P.K. *et al.* (2001). "Ultrafiltration of sugar cane juice for recovery of sugar: analysis of flux and retention" en *Separation and Purification Technology*, vol. 21, p. 247-259.

BRIÃO V.B. y TAVARES C.R.G. (2012). "Pore blocking mechanism for the recovery of milk solids from dairy wastewater by ultrafiltration" en Brazilian Journal of Chemical Engineering, vol. 29, p. 393-407.

CARRÈRE H., BLASZKOW F. y ROUX DE BALMANN H. (2001). "Modelling the clarification of lactic acid fermentation broths by cross-flow microfiltration" en *Journal of Membrane Science*, vol. 186, p. 219-230.

CHOI S-W. *et al.* (2000). "Modeling of the permeate flux during microfiltration of BSA-adsorbed microspheres in a stirred cell" en *Journal of Colloid and Interface Science*, vol. 228, p. 270-278.

CHUNG T.-S. *et al.* (2002). "Visualization of the effect of die shear rate on the outer surface morphology of ultrafiltration membranes by AFM" en *Journal of Membrane Science*, vol. 196, p. 251-266.

CORBATÓN-BÁGUENA M.J., ÁLVAREZ-BLANCO S. y VINCENT-VELA M.C. (2014a). "Cleaning of ultrafiltration membranes fouled with BSA by means of saline solutions" en *Separation and Purification Technology*, vol. 125, p. 1-10.

CORBATÓN-BÁGUENA M.J., ÁLVAREZ-BLANCO S. y VINCENT-VELA M.C. (2014b). "Salt cleaning of ultrafiltration membranes fouled by whey model solutions" en *Separation and Purification Technology*, vol. 132, p. 226-233.

DE BARROS S.T.D. *et al.* (2003). "Study of fouling mechanism in pineapple juice clarification by ultrafiltration" en *Journal of Membrane Science*, vol. 215, p. 213-224.

DE LA CASA E.J. *et al.* (2008). "A combined fouling model to describe the influence of the electrostatic environment on the cross-flow microfiltration of BSA" en *Journal of Membrane Science*, vol. 318, p. 247-254.

DUCLOS-ORSELLO C., LI W. y HO C-C. (2006). "A three mechanism model to describe fouling of microfiltration membranes" en *Journal of Membrane Science*, vol. 280, p. 856-866.

EVANS P.J. *et al.* (2008). "The influence of hydrophobicity, roughness and charge upon ultrafiltration membranes for black tea liquor clarification" en *Journal of Membrane Science*, vol. 313, p. 250-262.

FIELD R.W. *et al.* (1995). "Critical flux concept for microfiltration fouling" en *Journal of Membrane Science*, vol. 100, p. 259–272.

FOX P.F. y MCSWEENEY P.L.H. (2003). *Advanced Dairy Chemistry: Vol. 1: Proteins, third edition,* Nueva York: Kluwer Academic/Plenum Publishers.

GARCÍA-IVARS J. *et al.* (2014). "Enhancement in hydrophilicity of different polymer phase-inversion ultrafiltration membranes by introducing PEG/Al_2O_3 nanoparticles" en *Separation and Purification Technology*, vol. 128, p. 45-57.

HERMIA J. (1982). "Constant pressure blocking filtration laws – application to power law non-newtonian fluids" en *Trans IChemE*, vol. 60, p. 183-187.

HO C-C. y ZYDNEY L. (2000). "A combined pore blockage and cake filtration model for protein fouling during microfiltration" en *Journal of Colloid and Interface Science*, vol. 232, p. 389-399.

JARUSUTTHIRAK C., MATTARAJ S. y JIRARATANANON R. (2007). "Influence of inorganic scalants and natural organic matter on nanofiltration membrane fouling" en *Journal of Membrane Science*, vol. 287, p. 138-145.

KABSCH-KORBUTOWICZ M. y URBANOWSKA A. (2010). "Water treatment in integrated process using ceramic membranes" *en Polish Journal of Environmental Studies*, vol. 19, p. 731-737.

KARAGÜNDÜZ A. y DIZGE N. (2013). "Investigation of membrane biofouling in cross-flow ultrafiltration of biological suspension" en *Journal of Membrane Science and Technology*, vol. 3, p. 1-5.

KAWIECKA-SKOWRON J. y MAJEWSKA-NOWAK K. (2011). "Effect of dye content in a treated solution on performance of the UF ceramic membrane" en *Environmental Protection Engineering*, vol. 37, p. 5-12.

KAYA Y. *et al.* (2010). "The effect of transmembrane pressure and pH on treatment of paper machine process waters by using a two-step nanofiltration process" en *Desalination*, vol. 250, p. 150-157.

KAZEMIMOGHADAM M. y MOHAMMADI T. (2007). "Chemical cleaning of ultrafiltration membranes in the milk industry" en *Desalination*, vol. 204, p. 213-218.

KIM J. y DIGIANO F.A. (2009). "Fouling models for low-pressure membrane systems" en *Separation and Purification Technology*, vol. 68, p. 293-304.

MAH S-K. *et al.* (2012). "Ultrafiltration of palm oil-oleic acid-glycerin solutions: Fouling mechanism identification, fouling mechanism analysis and membrane characterizations" en *Separation and Purification Technology*, vol. 98, p. 419-431.

MATZINOS P. y ÁLVAREZ R. (2002). "Effect of ionic strength on rinsing and alkaline cleaning of ultrafiltration inorganic membranes fouled with whey proteins" en *Journal of Membrane Science*, vol. 208, p. 23-20.

MILLER G.L. (1959). “Use of dinitrosalicylic acid reagent for determination of reducing sugar” en *Analytical Chemistry*, vol. 31, p. 426-428.

MILLS O.E. y CREAMER L.K.A. (1975). “Conformational change in bovine β-lactoglobulin at low pH” en *Biochimica et Biophysica Acta*, vol. 379 p. 618-626.

MO H., TAY K.G. y NG H.Y. (2008). “Fouling of reverse osmosis membrane by protein (BSA): Effects of pH, calcium, magnesium, ionic strength and temperature” en *Journal of Membrane Science*, vol. 315, p. 28-35.

MOHAMMADI T. y ESMAEELIFAR A. (2005). “Wastewater treatment of a vegetable oil factory by a hybrid ultrafiltration-activated carbon process” en *Journal of Membrane Science*, vol. 254, p. 129-137.

NIGAM M.O., BANSAL B. y CHEN X.D. (2008). “Fouling and cleaning of whey protein concentrate fouled ultrafiltration membranes” en *Desalination*, vol. 218, p. 313-322.

PENG H. y TREMBLAY A.Y. (2008). “Membrane regeneration and filtration modeling in treating oily wastewaters” en *Journal of Membrane Science*, vol. 324, p. 59-66.

PETERSON R., GEETING J. y DANIEL R. (2007). “Estimation of ultrafilter performance based on characterization data” en *Chemical Engineering Technology*, vol. 30, p. 1050-1054.

RAHIMPOUR A. y MADAENI S.S. (2010). “Improvement of performance and surface properties of nano-porous polyethersulfone (PES) membrane using hydrophilic monomers as additives in the casting solution” en *Journal of Membrane Science*, vol. 360, p. 371-379.

RUBY FIGUEROA, R.A., CASSANO A. y DRIOLI E. (2011). "Ultrafiltration of orange press liquor: Optimization for permeate flux and fouling index by response surface methodology" en *Separation and Purification Technology*, vol. 80, p. 1-10.

SALAHI A., ABBASI M. y MOHAMMADI T. (2010). "Permeate flux decline during UF of oily wastewater: experimental and modeling" en *Desalination*, vol. 251, p. 153-160.

SMITH P.K. *et al.* (1985). "Measurement of protein using bicinchoninic acid" en *Analytical Biochemistry*, vol. 150, p. 76-85.

TIEN C. y RAMARAO B.V. (2006). "On analysis of cake formation and growth in cake filtration" en *Journal of the Chinese Institute of Chemical Engineers*, vol. 37, p. 81-94.

VINCENT VELA M.C. *et al.* (2009). "Analysis of membrane pore blocking models adapted to crossflow ultrafiltration in the ultrafiltration of PEG" en *Chemical Engineering Journal*, vol. 149, p. 232-241.

WANG C. *et al.* (2012). "Membrane fouling mechanism in ultrafiltration of succinic acid fermentation broth" en *Bioresource Technolology*, vol. 116, p. 366-371.

WANG Y-N. y TANG C.Y. (2011). "Protein fouling of nanofiltration, reverse osmosis, and ultrafiltration membranes-The role of hydrodynamic conditions, solution chemistry and membrane properties" en *Journal of Membrane Science,* vol. 376, p. 275-282.

YEE K.W.K., WILEY D.E. y BAO J. (2009). "A unified model of the time dependence flux decline for the ultrafiltration of whey" en *Journal of Membrane Science*, vol. 332, p. 69-80.

ZHANG Y. *et al.* (2010). "Using a membrane filtration process to concentrate the effluent from alkaline peroxide mechanical pulping plants" en *Bioresources*, vol. 5, p. 780-795.

CAPÍTULO V

Limpieza mediante disoluciones salinas de membranas ensuciadas con proteínas

5.1. LIMPIEZA DE MEMBRANAS DE ULTRAFILTRACIÓN ENSUCIADAS CON SEROALBÚMINA BOVINA

A continuación se presenta una adaptación al formato de la Tesis Doctoral del artículo titulado "Cleaning of ultrafiltration membranes fouled with BSA by means of saline solutions", publicado en la revista Separation and Purification Technology. En él se investiga la influencia de distintas condiciones de operación durante la etapa de limpieza de las membranas de UF con disoluciones salinas (tipo de sal, concentración de la misma, temperatura y velocidad tangencial de la disolución de limpieza), sobre la eficacia hidráulica del proceso de limpieza (EHL). Este estudio se llevó a cabo con las membranas de 5, 15, 30 y 50 kDa previamente ensuciadas con disoluciones de BSA. Los datos bibliográficos del artículo se destacan a continuación:

***Autores**: M.-J. Corbatón-Báguena, S. Álvarez-Blanco, M.-C. Vincent-Vela*

***Título**: Cleaning of ultrafiltration membranes fouled with BSA by means of saline solutions*

***Editorial**: Elsevier*

***Revista**: Separation and Purification Technology*

año: 2014 vol. 125 p. 1-10

***Doi**: http://dx.doi.org/10.1016/j.seppur.2014.01.035*

Cleaning of ultrafiltration membranes fouled with BSA by means of saline solutions

María-José Corbatón-Báguena, Silvia Álvarez-Blanco*, María-Cinta Vincent-Vela

Department of Chemical and Nuclear Engineering, Universitat Politècnica de València, C/Camino de Vera s/n 46022 Valencia, Spain

*Corresponding author: sialvare@iqn.upv.es
Tel: +34963879630 (Ext.: 79630)
Fax: +34963877639 (Ext.: 77639)

Abstract

In this work, four ultrafiltration (UF) membranes with molecular weight cut-offs (MWCOs) of 5, 15, 30 and 50 kDa, respectively, were fouled with 1 % BSA aqueous solutions and cleaned with different saline solutions. The influence of MWCO, membrane material and operating conditions on the cleaning efficiency was investigated. Saline solutions were able to clean the 5, 15 and 30 kDa membranes, but not the 50 kDa membrane. NaCl, $NaNO_3$, NH_4Cl and KCl were the most effective salts. The cleaning tests demonstrated that the higher the temperature of the saline solution was, the higher the cleaning efficiency was also. In addition, an increase in the crossflow velocity resulted in an increase in the hydraulic cleaning efficiency (HCE).

However, there was an optimum value of salt concentration to clean the membrane effectively. Response Surface Methodology was used to investigate the relationship between salt concentration and temperature in the cleaning process.

Keywords: Ultrafiltration; BSA; saline solutions; cleaning; hydraulic efficiency

5.1.1. Introduction

In the last years, the purification and fractionation of whey proteins has grown in interest due to their nutritional, functional and biological characteristics and their therapeutic and food applications. The major whey proteins are β-lactoglobulin (β-LG), α-lactalbumin (α-LA), bovine serum albumin (BSA) and immunoglobulin (Ig) (Almécija *et al.,* 2009a). Membrane separation technologies are being increasingly used in the food industry to fractionate and purify these proteins as an alternative to the conventional concentration and purification methods (Ogunbiyi *et al.*, 2008). Among all the separation processes, ultrafiltration (UF) is one of the most used in the dairy industry. Its most well-known applications are milk dehydration and whey concentration (Kazemimoghadam and Mohammadi, 2007).

Cleaning of UF membranes in the food industry is a key step of the global process. In most cases, cleaning needs to be carried out up to once a day to remove fouling from the membrane surface and to recover the permeability and selectivity of the membrane (Blanpain-

Avet *et al.,* 2009). Some authors reported that more than 80 % of the total production costs in the dairy industry are attributed to the cleaning of the equipments (Almécija *et al.*, 2009a). For that reason, choosing the best cleaning agents and operating conditions to optimize the cleaning processes is necessary (Kazemimoghadam and Mohammadi, 2007).

Membrane cleaning can be performed by means of physical, chemical and biological cleaning procedures. However, chemical methods are the most often used in the food industry (Kazemimoghadam and Mohammadi, 2007). Some of these chemical agents are acids, alkalis, surfactants, disinfectants or combinations of them. Choosing one or another depends on the feed composition, the type of foulants deposited on the membrane surface and the structure of the membranes (Cabero *et al.*, 1999). However, in order to clean the membranes fouled with milk and whey, most of the studies in the literature recommend the same cleaning protocol: one alkali washing step followed by an acid washing step (Ogunbiyi *et al*, 2008; Kazemimoghadam and Mohammadi, 2007; Almécija *et al.*, 2009b). If the membrane separation characteristics are not the initial ones after this protocol, another washing stage based on disinfectants or surfactants, such as sodium hypochloride or sodium dodecyl sulphate, can be performed (Almécija *et al.*, 2009a).

Nevertheless, these conventional cleaning operations may be aggressive for the membranes and may damage them more or less quickly, reducing the membrane lifetime and selectivity and increasing the productions costs (large energy and water

consumption and long duration of the cleaning cycle) (Blanpain-Avet *et al*, 2009). In addition, conventional cleaning agents have a negative impact on the environment when they are discharged as waste streams after the cleaning process. To overcome these problems, cleaning based on alternative techniques such as ultrasounds, saline solutions or electromagnetic fields are growing in interest in the last years (Muthukumaran *et al.,* 2004; Tarazaga *et al.*, 2006). However, only a few papers are related to the cleaning of membranes by means of saline solutions (Lee and Elimelech, 2007). In this case, previous studies (Lee and Elimelech, 2007) demonstrated that inert salts or even seawater can be effective for removing the natural organic matter deposited on a reverse osmosis membrane. Saline solutions cause changes on the cross-linked fouling layer due to the different concentration in the bulk solution and in the gel layer, breaking the integrity of the gel layer. Then, an ion-exchange reaction between salt ions and foulant molecules occurs, which results in the complete breakup of the gel layer. On the other hand, several authors (Hofmeister, 1888; Curits and Lue, 2006; Zhang, 2012) reported the salting-out and salting-in capability of several anions and cations to decrease or increase protein solubility, respectively. They investigated the protein-protein interactions in different salt solutions at pH values above and below the isoelectric point (pI) of the proteins.

The aim of this work is to evaluate the ability of saline solutions to clean two flat-sheet polymeric UF membranes with molecular weight cut-offs (MWCOs) of 5 and 30 kDa and two monotubular ceramic UF membranes with MWCOs of 15 and 50 kDa fouled by BSA 1 % (w/w).

The influence of MWCO, membrane material and operating conditions of the cleaning process (temperature, crossflow velocity and salt concentration of the cleaning solution) on the efficiency of the cleaning process was investigated. The optimal values of these operating conditions to achieve the highest cleaning efficiency were determined by means of a Response Surface Methodology (RSM) analysis.

5.1.2. Response Surface Methodology

A common method to study the performance of membrane processes is the "one-factor-at-a time" approach, which is based in the variation of one factor while the other factors are kept constant (Ruby Figueroa *et al.*, 2011). In some experimental set-ups, the number of factors to study is large. In the case of membrane technologies these factors usually are transmembrane pressure, crossflow velocity, time, temperature, solute concentration and pH. In this case, a traditional approach may result in a lot of experimental runs that require high energy, chemicals and time consumption. In addition, this approach ignores interaction effects between the considered factors and it is not appropriate to optimize the process (Cojocaru and Zakrzewska-Trznadel, 2007). To overcome these limitations, the RSM analysis can be used.

RSM is a combination of statistical and mathematical techniques widely used in the development, improvement and optimization of processes that contain a variable of interest (response variable)

influenced by several variables, and it is used to evaluate the relative significance of these variables even in the presence of complex interactions. The objective of RSM is the investigation of the response variable over the entire factor space, determining the optimum operating conditions or a region where the response variable satisfies the operating specifications (near to its optimal value) (Ruby Figueroa *et al.*, 2011; Cojocaru and Zakrzewska-Trznadel, 2007; Garg *et al.*, 2008).

5.1.3. Experimental

5.1.3.1. Materials

Fouling experiments were performed using a BSA aqueous solution with a concentration of 1 % (w/w) as a feed solution. BSA was supplied in powder (98% purity, A3733, Sigma-Aldrich) and feed solutions were prepared by dissolving BSA in deionized water until the desired concentration was achieved. BSA has a molecular weight of approximately 66 kDa and its isoelectric point is 4.9, according to the manufacturer. Feed solutions had a pH of about 7, thus BSA has mainly negative net charge on its surface. Its configuration is elliptic (11.6x2.7x2.7 nm) and it is one of the most widely used whey proteins to prepare model solutions for UF experiments (Suttiprasit *et al.*, 1992; Wang and Tang, 2011; Afonso *et al.*, 2009). According to the information provided by the manufacturer, BSA used in the experiments was prepared using a heat shock fractionation method followed by a lyophilization process to obtain BSA in a powder form.

After the fouling step, membranes were rinsed with deionized water to remove the loose protein deposit on the membrane surface. Then, the membranes were cleaned with several saline solutions (NaCl, $NaNO_3$, Na_2SO_4, KCl, and NH_4Cl). The chemicals were supplied by Panreac (Spain). The solutions were prepared dissolving the salts in deionized water with no pH adjustment. Different salt concentrations were used to study the influence of salt type and concentration on HCE.

Finally, the membranes were cleaned to recover their initial permeability conditions if it was necessary. In the case of the polymeric membranes, NaOH (Panreac, Spain) aqueous solutions with a pH of 11 at 45 ºC were used, while NaClO (Panreac, Spain) aqueous solutions with a concentration of 250 ppm (adjusting the pH at 11 with NaOH supplied by Panreac, Spain) were used to clean the ceramic membranes.

5.1.3.2. Membranes

Two monotubular ceramic membranes INSIDE CéRAM^{TM} (TAMI Industries, France) and two flat sheet polymeric membranes (Microdyn-Nadir, Germany) were used in the experiments. The ceramic membranes were 200 mm long with an internal diameter of 6 mm and an external diameter of 10 mm. They consisted of a TiO_2 support layer and a ZrO_2-TiO_2 active layer. The molecular weight cut-offs (MWCOs) of these membranes were 15 and 50 kDa, respectively. Polymeric membranes were polyethersulfone (PES)

membranes with an effective area of 100 cm^2 and two different MWCOs (5 and 30 kDa).

5.1.3.3. Experimental set-up

All fouling and cleaning experiments were performed in a VF-S11 UF plant (Orelis, France). The main parts of the plant are (Fig. 26): a feed tank, a temperature regulating system, a variable speed volumetric pump, two manometers placed at both sides of the membrane module and a scale. The feed tank consists of a 10 L stainless steel tank with a double jacket, which contained the BSA or the cleaning solution. The temperature was kept constant during the experiments by means of the temperature regulating system. Crossflow velocity was controlled with a variable speed volumetric pump. The maximum operating pressure was 4 bar. Pressure drop across the membrane module was measured with two manometers. Finally, a scale (0.001 g accuracy) was used to gravimetrically determine the permeate flux.

Both the retentate and the permeate were recirculated back to the feed tank in order to keep the concentration of the feed solution constant, except in the case of the rinsing step.

5.1.3.4. Experimental procedure

Fouling experiments

Fouling tests were carried out with a 1 % (w/w) BSA aqueous solution at a transmembrane pressure of 2 bar and a crossflow velocity of

2 $m \cdot s^{-1}$. The temperature of the fouling solution was set to 25 ºC. The duration of the fouling tests was 2 h. Those conditions were selected according to previous studies on whey ultrafiltration (Matzinos and Álvarez, 2002). During the experiments, the permeate flux and the hydraulic resistance were monitored to check the fouling process and to ensure that reproducible values of flux and resistance were obtained in all runs. Each fouling experiment was repited a minimum of 10 times and the maximum error among the runs was 10 %.

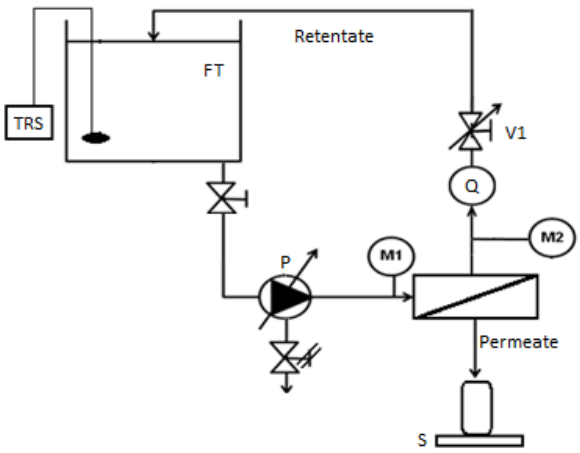

Fig. 26. *Pilot plant used in the experiments (TRS: temperature regulating system; FT: feed tank; P: pump; M1 and M2: manometers; S: scale; V1: regulating pressure valve)*

Permeate concentration of BSA during the fouling tests was measured by an UV-visible spectrophotometer (Hewlett-Packard 8453) at a wavelength of 278 nm. This was the wavelength of maximum absorbance for the BSA solution used as feed. Rejection coefficient was calculated as follows (Eq. 18):

$$Rejection(\%) = \left(1 - \frac{C_p}{C_b}\right) \cdot 100 \qquad \text{Eq. 18}$$

where C_p is the permeate BSA concentration and C_b is the BSA concentration in the feed solution (1 % (w/w)).

At the end of the tests, the hydraulic resistance after the fouling step (R_f) was evaluated by means of Darcy's law (Eq. 19).

$$J = \frac{\Delta P}{\mu \cdot R} \qquad \text{Eq. 19}$$

where J is the permeate flux, ΔP is the transmembrane pressure, μ is the feed solution viscosity and R is the total hydraulic resistance.

Rinsing and cleaning experiments

Cleaning experiments were performed at three different temperatures (25, 37.5 and 50 º C) with different salt concentrations (0, 1.25, 2.5, 5, 7.5, 25 and 100 mM). Transmembrane pressure was 1 bar and crossflow velocity was varied between 1.2 and 4.2 $m \cdot s^{-1}$. The pH of the saline solutions tested varied from 6.8 to 7. Each cleaning experiment was performed twice and the maximum error among the runs was 10 %. After the fouling and cleaning steps, the membranes were rinsed with deionized water at 25 ºC. Rinsing steps were carried out at the same experimental conditions of transmembrane pressure and crossflow velocity as those of the cleaning step. Low transmembrane pressures favour foulants removal and relax the

compressible fouling layer formed in the fouling step (Blanpain-Avet *et al.*, 2009).

Finally, if the initial permeability of the membranes was not recovered after the cleaning process, the ceramic membranes were cleaned with a NaClO aqueous solution at pH 11 and the polymeric membranes were cleaned with NaOH aqueous solutions at pH 11, as it was indicated in section 5.1.3.1 and it was recommended by the manufacturer.

5.1.3.5. Evaluation of membrane cleanliness

The efficiency of the cleaning protocol was determined following the method developed by Daufin *et al.* (2001) and Matzinos and Álvarez (2002). These authors determined the hydraulic resistance of the membrane after each step (fouling, first rinsing, cleaning and second rinsing) when it was cleaned with sodium hydroxide solutions. They proposed the term “hydraulic rinsing efficiency” (HRE) to evaluate the efficiency of the first rinsing to restore the membrane permeability. The HRE is calculated as follows:

$$HRE = \frac{R_f - R_{r1}}{R_f - R_m} \cdot 100 \qquad \text{Eq. 20}$$

where R_f is the hydraulic resistance after the fouling step, R_{r1} is the hydraulic resistance after the first rinsing step and R_m is the hydraulic resistance of the new membrane.

These authors (Daufin *et al.,* 2001; Matzinos and Álvarez, 2002; Muthukumaran *et al.*, 2007), used a similar equation (Eq. 21) to evaluate the efficiency of the entire cleaning process (after the second rinsing) to restore the initial membrane permeability:

$$HCE = \frac{R_f - R_{r2}}{R_f - R_m} 100 \qquad \text{Eq. 21}$$

where HCE is the hydraulic cleaning efficiency and R_{r2} is the hydraulic resistance after the second rinsing.

5.1.3.6. AFM measurements

The roughness of the membranes studied was measured by atomic force microscopy (AFM) using a Multimode atomic force microscope (Veeco, Santa Barbara, CA, USA) equipped with a NanoScope V controller. Measurements were performed at ambient conditions using the tapping mode of imaging. Roughness values were obtained from 5 μm x 5 μm samples and considering the average value of five areas of 1 μm x 1 μm. Among the different parameters to evaluate the membrane roughness, the Root Mean Square roughness (R_q) was selected. This is one of the most often used parameters to study membrane roughness. It represents the standard deviation of the height values (Z) of the surface within a specific area, according to the Eq. 22 (Chung *et al.*, 2002):

$$R_q = \sqrt{\frac{\sum \left(Z_i - Z_{avg}\right)^2}{N_p}} \qquad \text{Eq. 22}$$

where Z_i is the Z value currently measured, Z_{avg} is the average of the Z values and N_p is the number of points within the given area.

5.1.3.7. RSM analysis

After the cleaning processes, a RSM analysis was carried out to evaluate which values of the operating conditions resulted in the highest HCE. The RSM analysis was performed with the Statgraphics® software using a factorial design. The experimental data used for the statistical analysis is shown in Table 18. A relationship between the response variable (HCE) and the design variables (temperature, T_c, NaCl concentration, C, and crossflow velocity, v) was obtained. A Multiple Linear Regression analysis was applied to search for a model equation for HCE as a function of the operating conditions studied. Firstly, all the independent variables and their interactions were taken into account. Then, the coefficients of the regression model with p-values higher than 0.05 were neglected because they were not significant and a new regression analysis was performed.

5.1.3.8. Optimization method

After the RSM analysis, an optimization algorithm based on a pattern search was used to evaluate the values of temperature, NaCl concentration and crossflow velocity that maximize the HCE for each membrane. The optimization method was performed using the "patternsearch" function of Matlab® software.

Table 18. Experimental data for the statistical analysis

MWCO (kDa)	T_c (ºC)	C (mM)	v ($m \cdot s^{-1}$)	HCE (%)
5	25	0	2.18	41.10
	25	2.5	2.18	59.20
	25	5	2.18	60.17
	37.5	0	2.18	57.49
	37.5	2.5	2.18	80.21
	37.5	5	2.18	89.59
	50	0	2.18	75.49
	50	2.5	2.18	94.36
	50	5	2.18	99.58
	50	5	1.69	67.00
	50	5	1.20	45.74
15	25	0	4.20	45.77
	25	2.5	4.20	56.49
	25	5	4.20	49.03
	37.5	0	4.20	59.99
	37.5	2.5	4.20	80.68
	37.5	5	4.20	91.49
	50	0	4.20	58.99
	50	2.5	4.20	100.00
	50	5	4.20	100.00
	50	2.5	3.19	90.07
	50	2.5	2.18	58.93
30	25	0	2.18	35.94
	25	2.5	2.18	58.31
	25	5	2.18	53.32
	37.5	0	2.18	54.24
	37.5	2.5	2.18	77.71
	37.5	5	2.18	87.55
	50	0	2.18	72.67
	50	2.5	2.18	91.23
	50	5	2.18	100.00
	50	5	1.69	85.11
	50	5	1.20	69.27

"Patternsearch" finds the minimum of an objective function by means of a pattern search. As the aim of this work is to achieve the maximum of the model equations HCE_5, HCE_{15} and HCE_{30}, the objective functions selected for the "patternsearch" algorithm were the negative form of these equations ($-HCE_5$, $-HCE_{15}$ and $-HCE_{30}$). In addition, the maximum value of temperature was limited to 50 ºC and the maximum value of crossflow velocity was limited to 2.18 $m \cdot s^{-1}$ for the 5 and 30 kDa membranes and 4.2 $m \cdot s^{-1}$ for the 15 kDa membrane, as these were the higher values tested for these design variables.

5.1.4. Results and discussion

The values of R_m for the membranes used in the experiments were: $9.453 \cdot 10^{12}$, $5.001 \cdot 10^{12}$, $3.794 \cdot 10^{12}$ and $1.921 \cdot 10^{12}$ m^{-1}, for the membranes of 5, 15, 30 and 50 kDa, respectively. These values were taken as a reference to calculate HCE.

5.1.4.1. Fouling experiments

Fig. 27 shows the evolution of permeate flux with time for all the membranes tested at a transmembrane pressure of 2 bar, a crossflow velocity of 2 $m \cdot s^{-1}$ and a temperature of 25 ºC. The experimental data that corresponds to the membrane of 50 kDa show a sharp flux decline in the first minutes of operation. This is not observed for the membranes of 5, 15 and 30 kDa, which show a much lower flux decline rate. This can be attributed to the fact that the 50 kDa

membrane shows a MWCO much closer to the molecular weight of BSA molecules (66 kDa) than the rest of the membranes.

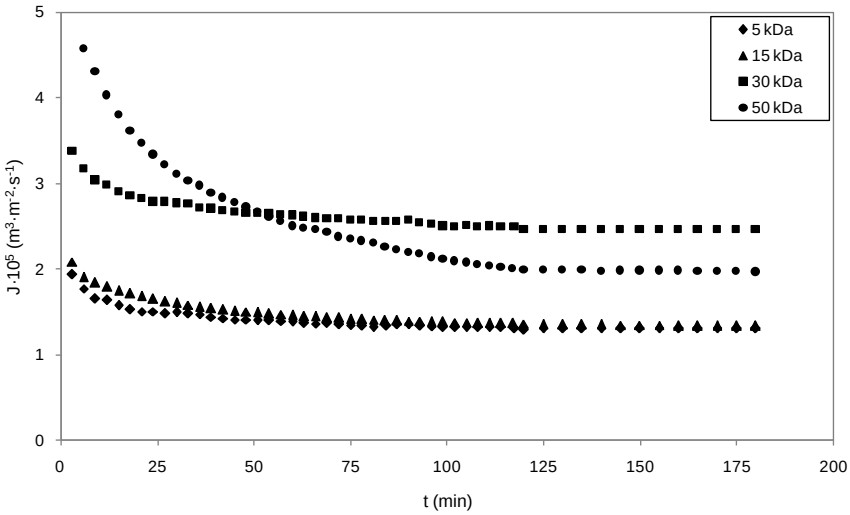

Fig. 27. *Evolution of permeate flux with time during fouling experiments at 2 bar, 2 m·s^{-1} and 25 ºC*

These results are in accordance with previous works. For example, Qu *et al.* (2014) fouled three PES membranes of 10, 30 and 100 kDa with extracellular organic matter (EOM). The molecular weight distribution was divided into two fractions, a high molecular weight fraction (greater than 100 kDa) and a low molecular weight fraction (lower than 100 kDa). They observed that the membranes of 10 and 30 kDa showed the most severe fouling in terms of high relative flux reduction and the worse fouling reversibility. This was due to the fact that the MWCOs of these membranes and the molecular weight of low molecular weight EOM were more similar than in the case of the 100 kDa membrane. Therefore, low molecular weight EOM can penetrate inside the pores of the 10 and 30 kDa membranes and cause pore constriction. As a consequence, these membranes

showed more severe fouling. These authors demonstrated that fouling is more severe when the difference between the membrane MWCO and the molecular weight of solute molecules is lower.

Fig. 28 shows the evolution of the rejection coefficient with time during the fouling step for all the membranes tested. As it can be observed, the rejection coefficient achieved steady-state values after about 100 min of operation for all the membranes tested. Although all the membranes had a rejection coefficient higher than 99 % at the end of the step, the 50 kDa membrane showed the lowest rejection coefficient. This can be explained taking into account the difference between the size of BSA molecules and the membrane pore size. That difference is larger for the low MWCO membranes (5 and 15 kDa) and thus, the values of rejection are higher than in the case of the 30 and 50 kDa membranes. This is in agreement with other authors (Schäfer *et al.*, 2000; Adikane *et al.*, 2004).

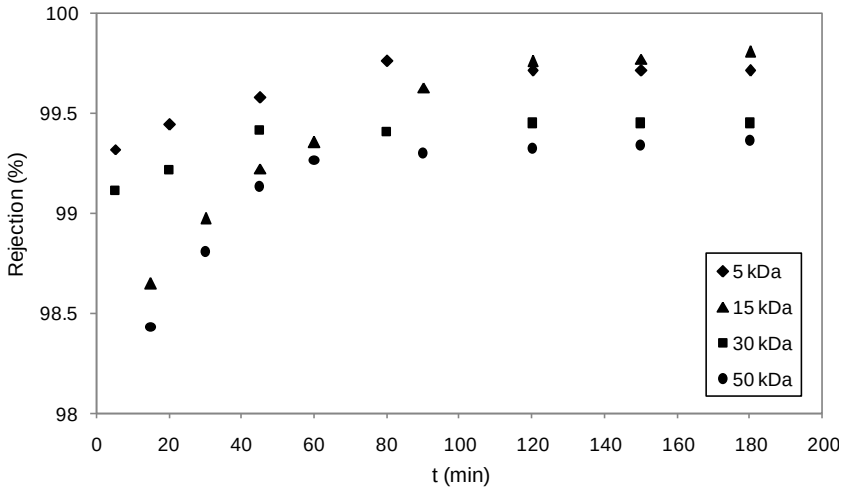

Fig. 28. *Evolution of rejection with time during the fouling step for each membrane*

The evolution of the hydraulic resistance during the four steps (fouling, first rinsing, cleaning and second rinsing) can be observed in Fig. 29. The operating conditions for all the membranes in the cleaning and rinsing steps were the same.

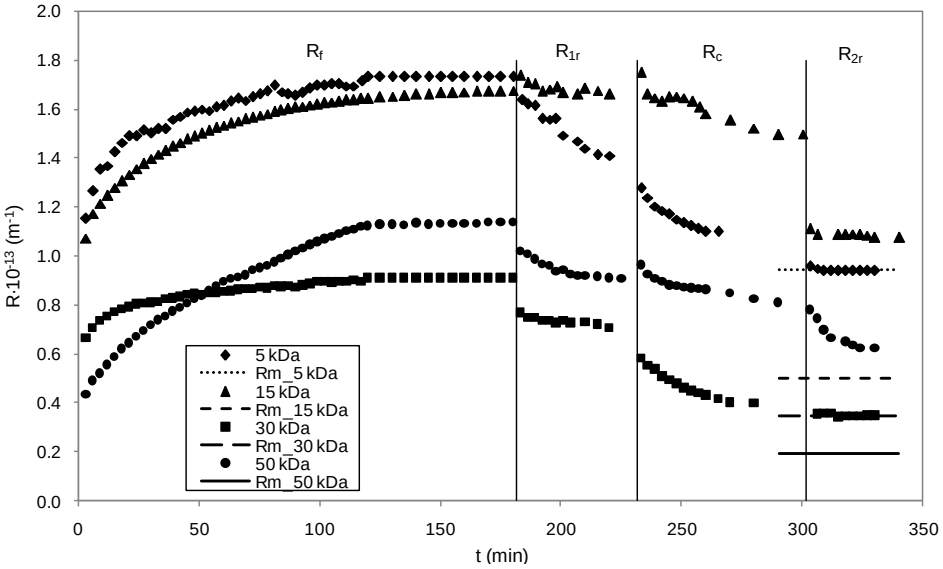

Fig. 29. *Evolution of total hydraulic resistance with time for each membrane (25 ºC, 2 bar and 2 m·s^{-1} in the fouling step; 25 ºC and 1 bar in the rinsing steps and 50 ºC and 1 bar in the cleaning step. Crossflow velocity was 2.18 m·s^{-1} for all the membranes)*

As it can be observed, the original hydraulic membrane resistance was restored for the polymeric membranes (5 and 30 kDa) after the second rinsing step. However, the ceramic membranes were partially cleaned at the experimental conditions tested. The reason for this difference is the higher roughness of ceramic membranes in comparison with polymeric ones (Llanos *et al.*, 2010). The roughness of all the membranes tested was measured by means of AFM and the

values of R_q obtained were 0.487, 17.900, 1.657 and 27.133 nm for the membranes of 5, 15, 30 and 50 kDa, respectively. In order to increase the cleaning efficiency, higher crossflow velocities were considered to clean the ceramic membranes.

5.1.4.2. Cleaning experiments

Effect of the salt type

The 15 kDa membrane was used to investigate the effect of the salt type on the HCE. Fig. 30 shows the values of the HCE obtained when different saline solutions were used to clean this membrane at 25 ºC. The values of the HCE were also compared with the values of the HRE. As it can be observed, the highest values of HCE were obtained for chloride salts and $NaNO_3$. For these saline solutions the HCE was very similar, varying from 45.9 to 55.3 %. These values were considerably higher than the HRE (22.8 %). Therefore, these salts were able to remove part of the fouling layer at the operating conditions considered.

Among all the salts tested, Na_2SO_4 showed the lowest value of HCE (23.4 %) at the experimental conditions tested. This value is very similar to the value of HRE (22.8 %). Therefore, at 25 ºC and 100 mM no improvement on the cleaning efficiency was observed when a Na_2SO_4 solution was used to clean the membrane fouled with a BSA aqueous solution of 1 % (w/w).

Lee and Elimelech (2007) observed that saline solutions were able to clean reverse osmosis membranes fouled with organic matter. They indicated that saline solutions were able to decrease dramatically the foulant-foulant adhesion forces. Lee and Elimelech (2007) performed the cleaning of reverse osmosis membranes fouled with alginates with the same saline solutions as the ones used in this paper to clean the UF membrane fouled with proteins. The differences between the hydraulic cleaning efficiencies obtained by Lee and Elimelech (2007) at 25 ºC and the results shown in Fig. 29 can be due to the different membranes and feed solutions considered. Moreover, these authors used very low feed concentrations. They fouled reverse osmosis membranes with a feed solution of 0.02 $g \cdot L^{-1}$, while, in this paper, a concentration of 10 $g \cdot L^{-1}$ was used to foul UF membranes.

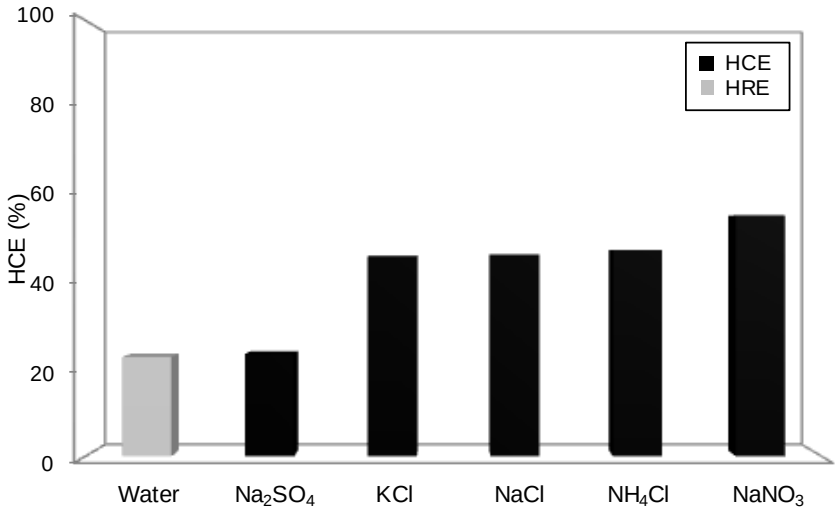

Fig. 30. *Influence of the type of saline solution on the values of HCE (black bars) and comparison with the value of HRE (grey bar) (membrane MWCO: 15 kDa; temperature: 25 ºC; concentration: 100 mM; crossflow velocity: 4.2 $m \cdot s^{-1}$)*

Several authors studied the effect of salts on protein-protein interactions. Tsumoto *et al.* (2007) observed that, at the same concentration, several salts cause a decrease in protein solubility (salting-out effects) while others increase protein-solubility (salting-in effects). The effect of the type of salt was tested at a concentration of 100 mM. This effect was related by several authors to the surface tension of the salt solution (the higher the surface tension, the higher the salting-out effect) and to the type of interactions between the salt and the proteins. Tsumoto *et al.* (2007) studied the preferential interactions of several salts with BSA. They demonstrated that Na_2SO_4 was a strong salting-out salt due to unfavorable interactions with BSA. Thus Na_2SO_4 enhances protein-protein and protein-surface interactions and decreases protein solubility.

Hofmeister (Hofmeister, 1888; Curtis and Lue, 2006) investigated the effect of salts on protein precipitation at high salt concentrations. A ranking of the effectiveness of various cations and anions to precipitate proteins was named as Hofmeister series. The strongest effectiveness was observed for SO_4^{2-}. Moreover, anions appear to have a greater effect on protein solubility than cations. Zhang (2012) demonstrated as well that SO_4^{2-} is the most salting-out anion among those included in the series. This is in agreement with the low value of HCE obtained when the cleaning step was performed with Na_2SO_4 at a concentration of 100 mM. Zhang (2012) reported that at pH above the protein isoelectric point, when the protein is negatively charged, multivalent cations can neutralize the net protein charge, weakening the electrostatic intermolecular interactions more effectively than monovalent cations, and decreasing protein solubility.

On the other hand, Cl^- and NO_3^- are able to specifically bind to the proteins surface more strongly than monovalent cations. Therefore, the repulsive intermolecular interactions increase, thus reducing protein-protein interactions, and raising protein solubility. This can explain the higher value of HCE observed for chlorides and nitrates.

Among the salts with a high value of HCE, NaCl was chosen to continue this work, due to the lower pollutant character and cost compared to the other salts tested.

Effect of salt concentration

Fig. 31 shows the values of HCE obtained when NaCl solutions at different concentrations were used to clean the 5, 15 and 30 kDa MWCO membranes at two different temperatures: 25 and 50 ºC. At 50 ºC, it can be observed that HCE increased as NaCl concentration increased up to 2.5 mM for the 15 kDa membrane and up to 5 mM for the 5 and 30 kDa membranes. At these experimental conditions, HCE values of 100 % were achieved for all the membranes. At 25 ºC the HCE observed was lower and it increased with concentration up to 2.5 mM, however, a further increase of concentration resulted in a decrease of the HCE.

As other authors explained (Manciu *et al.*, 2003; Karraker and Radke, 2002; Petersen and Saykally, 2005), at low salt concentrations the surface tension decreases when salt concentration increases. However, at high salt concentrations the surface tension increases linearly with concentration.

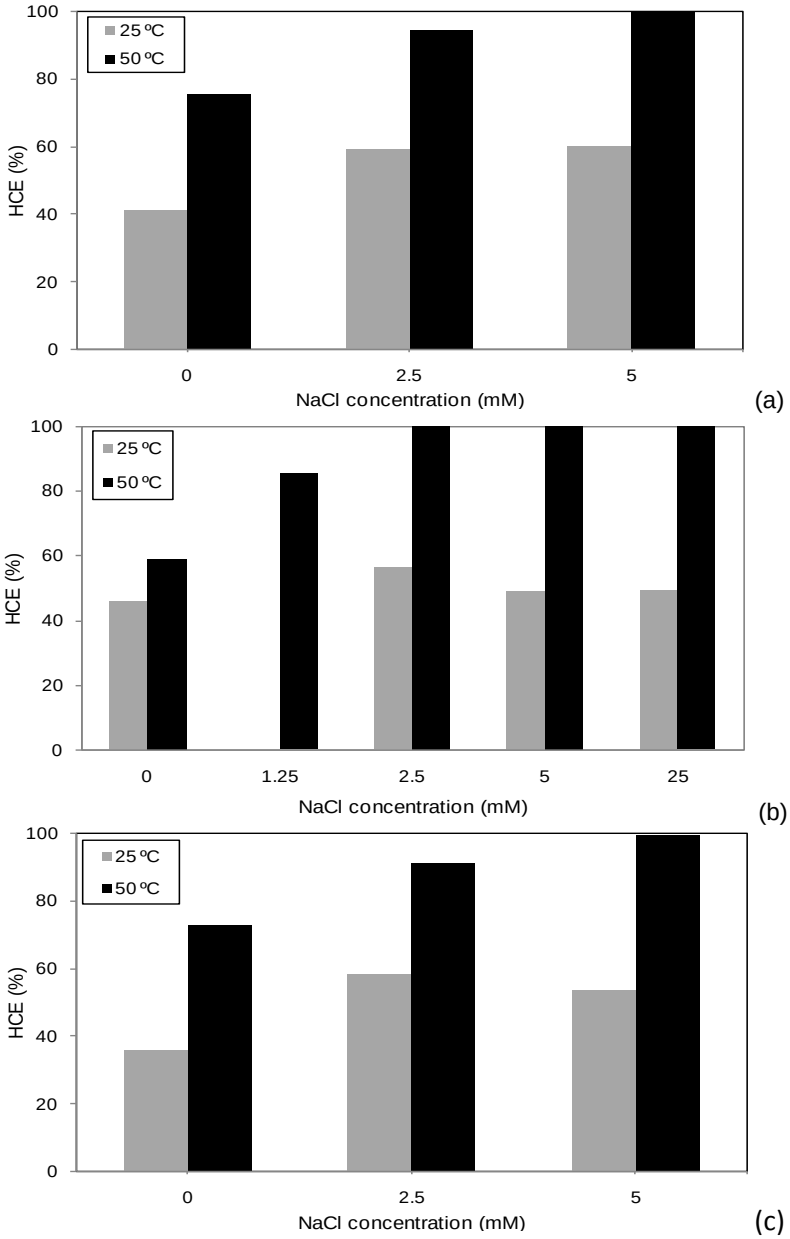

Fig. 31. *Influence of NaCl concentration on the values of HCE for the membranes of 5 kDa (a), 15 kDa (b) and 30 kDa (c), when the cleaning solution temperature is 25 ºC (grey bars) and 50 ºC (black bars) and the crossflow velocity is 2.18 $m \cdot s^{-1}$ for the 5 and 30 kDa membranes and 4.2 $m \cdot s^{-1}$ for the 15 kDa membrane*

According to Tsumoto *et al.* (2007), a decrease in the surface tension results in an enhancement of the salting-in effects of the saline solutions. Therefore, the salting-in effects are better observed at low salt concentrations. On the other hand, HCE cannot increase with salt concentration if the physical conditions for the mass transport of the protein deposits removed from the gel layer to the bulk solution are not the optimal. There is an optimal salt concentration to carry out the cleaning process. Up to this concentration, when salt concentration increases, HCE increases. But above this concentration HCE does not increase with salt concentration or it can even decrease. This may be due to the fact that membrane fouling due to the accumulation of salt molecules on the membrane surface or inside its pores may also occur. In this case, fouling and cleaning mechanisms become competitive. This is in agreement with the results reported by Lee and Elimelech (2007) and Cabero Cabero (1997). The increase in HCE with an increase of salt concentration is greater at high temperatures. This is due to the effect of temperature on protein deposits. This effect is commented in section "Effect of cleaning solution temperature".

Fig. 32 shows the values of the HCE when the 50 kDa membrane was cleaned with NaCl solutions at different concentrations at 50 ºC. As it can be observed, HCE increased as NaCl concentration increased up to a certain value (7.5 mM) and afterwards it decreased. However, the maximum value of HCE for the 50 kDa membrane was 79.19 %, while in the case of the 15, 5 and 30 kDa membranes (Fig. 31), a 100 % HCE was achieved at low salt concentrations (2.5 and 5 mM, respectively). Therefore, the 50 kDa membrane was not

completely cleaned with NaCl solutions at the experimental conditions tested. This can be due to the more severe fouling that was observed for this membrane as it was commented in section 5.1.4.1. In this case, the temperature of 25 ºC was not considered as even lower HCE could be expected.

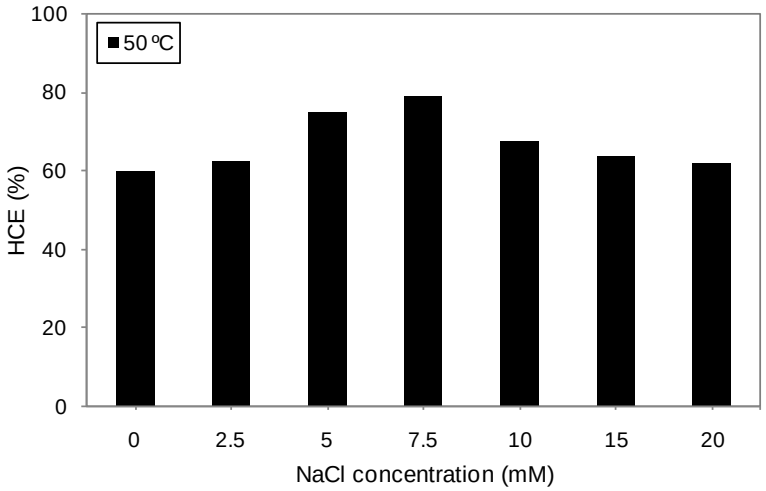

Fig. 32. *Influence of NaCl concentration on the values of HCE for the membrane of 50 kDa, when the cleaning solution temperature is 50 ºC and the crossflow velocity is 4.2 m·s^{-1}*

Effect of cleaning solution temperature

Fig. 33 shows the values of HCE for the 5, 15 and 30 kDa membranes when the cleaning step was performed at different temperatures and a NaCl concentration of 5 mM. According to Fig. 31, 100 % of HCE was achieved for all the membranes at 50 ºC, but not in the case of 25 ºC. Thus, an intermediate temperature (37.5 ºC) was considered as well to investigate the effect of the cleaning solution temperature on the HCE. As it can be observed, the higher

the temperature of the cleaning solution is, the higher the HCE is, achieving an efficiency of 100 % when the cleaning was carried out at 50 ºC for the 5, 15 and 30 kDa membranes.

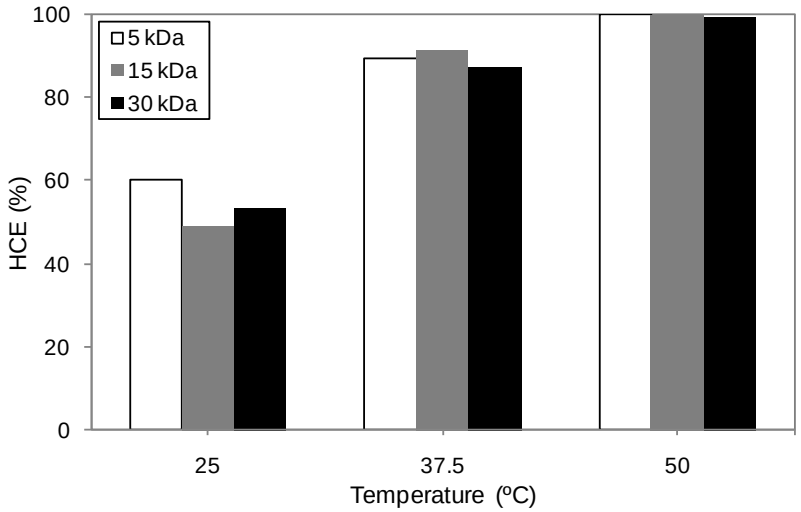

***Fig. 33**. Influence of temperature on the values of HCE for the membranes of 5 kDa (white bars), 15 kDa (dark grey bars) and 30 kDa (black bars), when NaCl concentration is 5 mM and the crossflow velocity is 2.18 $m \cdot s^{-1}$ for the 5 and 30 kDa membranes and 4.2 $m \cdot s^{-1}$ for the 15 kDa membrane*

The increase of HCE when temperature varies from 25 to 37.5 ºC is higher than the increase of HCE when temperature increases from 37.5 to 50 ºC (about 85 % in the first case and 9 % in the second case). This effect can also be observed in Fig. 31. In this case, HCE was plotted as a function of concentration for two different temperatures (25 and 50 ºC, respectively). As it can be observed, for each concentration HCE increases with temperature.

When the temperature of the saline solution increases, the surface tension decreases (Ali *et al.*, 2008; Shah *et al.*, 2013). The decrease in the surface tension is caused by the adsorption of hydrophilic ions from the air/water surface (Matubayasi and Yoshikawa, 2007). According to several authors, surface tension decreases linearly with temperature. As it was reported by Tsumoto *et al.* (2007), the higher the surface tension, the stronger the salting-out effects of the salt.

Temperature has also an effect on protein solubility. In general, protein solubility increases with temperature up to 50 ºC. However, when the temperature of the solution is high enough during a certain time, the protein is denatured. Proteins are denatured due to the effect of temperature on the non-covalent bonds involved in the stabilization of secondary and tertiary structure. Denaturation decreases protein solubility compared to the native protein (Pelegrine and Gasparetto, 2005). In addition, in mass transfer processes, the diffusivity coefficient increases as temperature rises. Therefore, the rate of transfer of solute molecules from the membrane surface towards the bulk solution is greater. Moreover, high temperatures can weaken the structural stability of the fouling layer, swelling it and facilitating its removal from the membrane surface. An increase in temperature may also increase the rate of the interaction between the salt and the deposited proteins (Lee and Elimelech, 2007).

For all these reasons, the most convenient temperature to carry out the cleaning of the 5, 15 and 30 kDa membranes fouled with BSA solutions is about 50 ºC (the highest temperature tested).

Fig. 34 shows the values of HCE obtained for the 50 kDa membrane when the cleaning step was performed at different temperatures (50, 60, 70 and 80 ºC) and a NaCl concentration of 7.5 mM. According to Fig. 32, at 50 ºC the highest HCE was obtained at a NaCl concentration of 7.5 mM for this membrane. Due to the effect of temperature on the HCE that was observed for the other membranes (5, 15 and 30 kDa), it was expected that an increase in temperature resulted in an increase in HCE for the 50 kDa membrane as well. From Fig. 34 it can be observed that HCE increases with temperature. However, the maximum value of HCE was 90.5 % at the highest temperature tested (80 ºC). Thus, the 50 kDa membrane was not completely cleaned despite the high temperatures considered. The reason for that is the more severe fouling due to the penetration of BSA molecules in the porous structure of this membrane in comparison with the membranes of lower MWCO (5, 15 and 50 kDa).

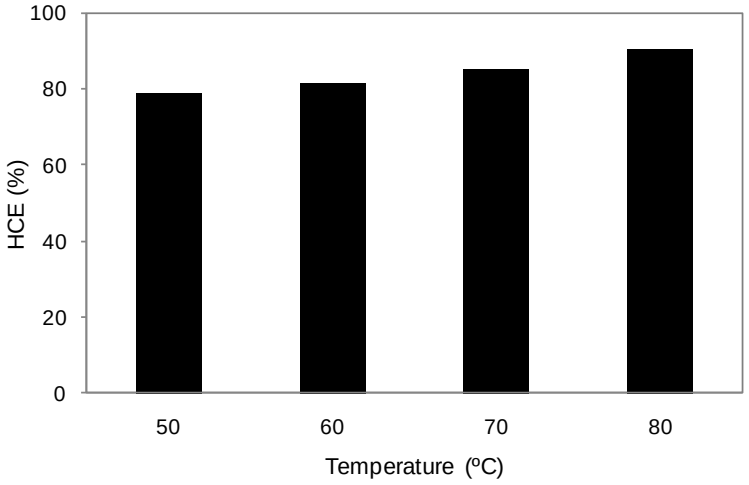

Fig. 34. *Influence of temperature on the values of HCE, when NaCl concentration is 7.5 mM and crossflow velocity is 4.2 m·s^{-1} for the 50 kDa membrane*

Effect of crossflow velocity

Fig. 35 shows the results of HCE for the 5, 15 and 30 kDa membranes when different crossflow velocities were tested at the optimal conditions of NaCl concentration (2.5 mM for the 15 kDa membrane and 5 mM for the 5 and 30 kDa membranes) and temperature (50 ºC). In the case of the ceramic membrane (15 kDa), higher crossflow velocities were tested due to the higher roughness of this membrane in comparison with the polymeric ones.

As it can be observed, when crossflow velocity increases HCE increases for all the membranes tested, achieving a HCE of 100 % at the highest crossflow velocity tested (4.2 $m \cdot s^{-1}$ for the 15 kDa membrane and 2.18 $m \cdot s^{-1}$ for the 5 and 30 kDa membranes). When crossflow velocity increases, the shear stress generated also increases and it can cause the erosion and removal of the protein deposit from the membrane surface (Daniş and Keskinler, 2009; Smith *et al.*, 2006).

The effect of the crossflow velocity on the HCE was not tested for the 50 kDa membrane. The reason is that 4.2 $m \cdot s^{-1}$ is the highest crossflow velocity that can be reached in the UF plant. As it was previously shown, the HCE for this membrane was lower than 100 % at this crossflow velocity. Taking into account the results shown in this section, even lower values of HCE were expected if the crossflow velocity is decreased.

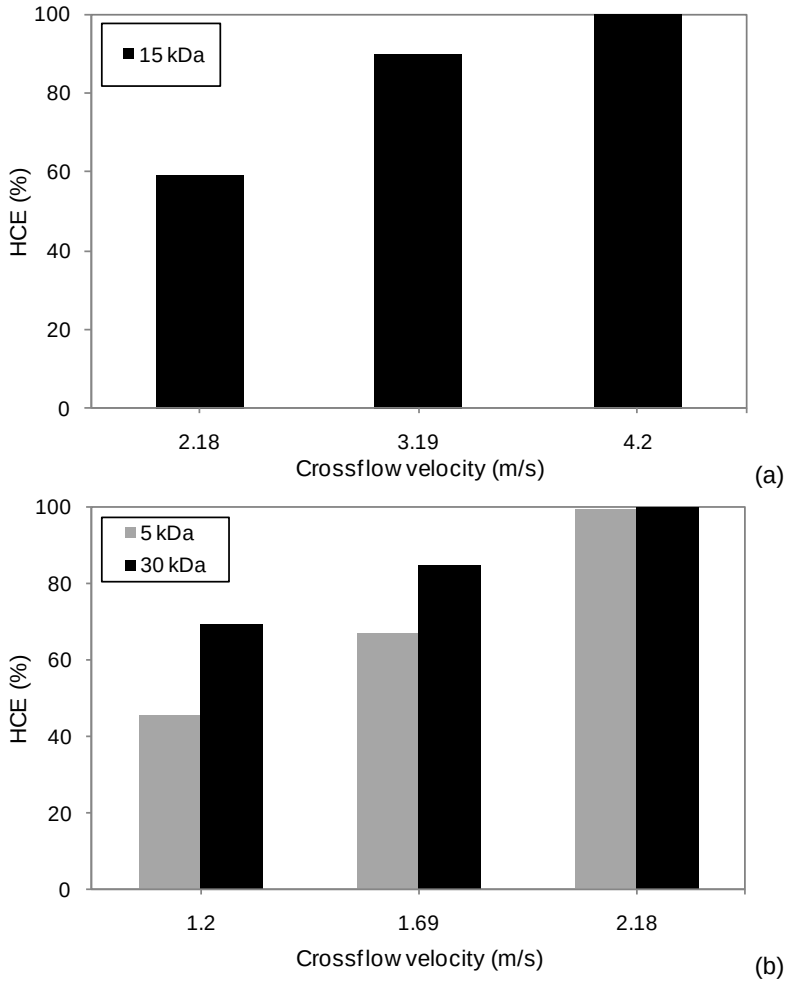

Fig. 35. *Influence of crossflow velocity on the values of HCE for the membranes of 15 kDa (a) and 5 and 30 kDa (b), when temperature is 50 ºC and NaCl concentration is 2.5 mM for the 15 kDa membrane and 5 mM for the 5 and 30 kDa membranes*

Statistical and optimization analysis

The efficiency of the cleaning process is influenced by operating conditions such as temperature, transmembrane pressure, crossflow

velocity, the nature of the cleaning agent and its concentration, pH and ionic strength (Blanpain-Avet *et al.*, 2009). In this work, three of these operating conditions (temperature, NaCl solution and crossflow velocity) were varied.

Fig. 36 shows the surface contours for the response variable (HCE) as a function of the operating conditions of temperature and NaCl concentration for the membranes of 5, 15 and 30 kDa studied. Crossflow velocity was set at 2.18 $m \cdot s^{-1}$ for the 5 and 30 kDa membranes and at 4.2 $m \cdot s^{-1}$ for the 15 kDa membrane. The grey colour in the lower left corner shows the most unfavourable conditions, because lower values of HCE were obtained (about 40 %). On the other hand, the black colour in the upper right corner represents the highest values of HCE achieved (greater than 95 %). At temperatures higher than 42-45 ºC and NaCl concentrations higher than 2.6-3 mM, the HCE was observed to be higher than 95 % for the three membranes considered. It is important to note that the higher the temperature of the cleaning solution was, the higher the HCE was for all the membranes tested. However, there was an optimal value of NaCl concentration to maximize the value of HCE, because further increases in salt concentration did not result in higher values of HCE.

In addition, mathematical relationships between the values of HCE and the operating conditions were obtained for the 5, 15 and 30 kDa membranes (Eqs. 23, 24 and 25, respectively). The statistically significant factors were the same for the 5 and 30 kDa membranes. The regression coefficients for each equation were 0.979, 0.893 and 0.962, respectively. Table 19 shows the results of the ANOVA.

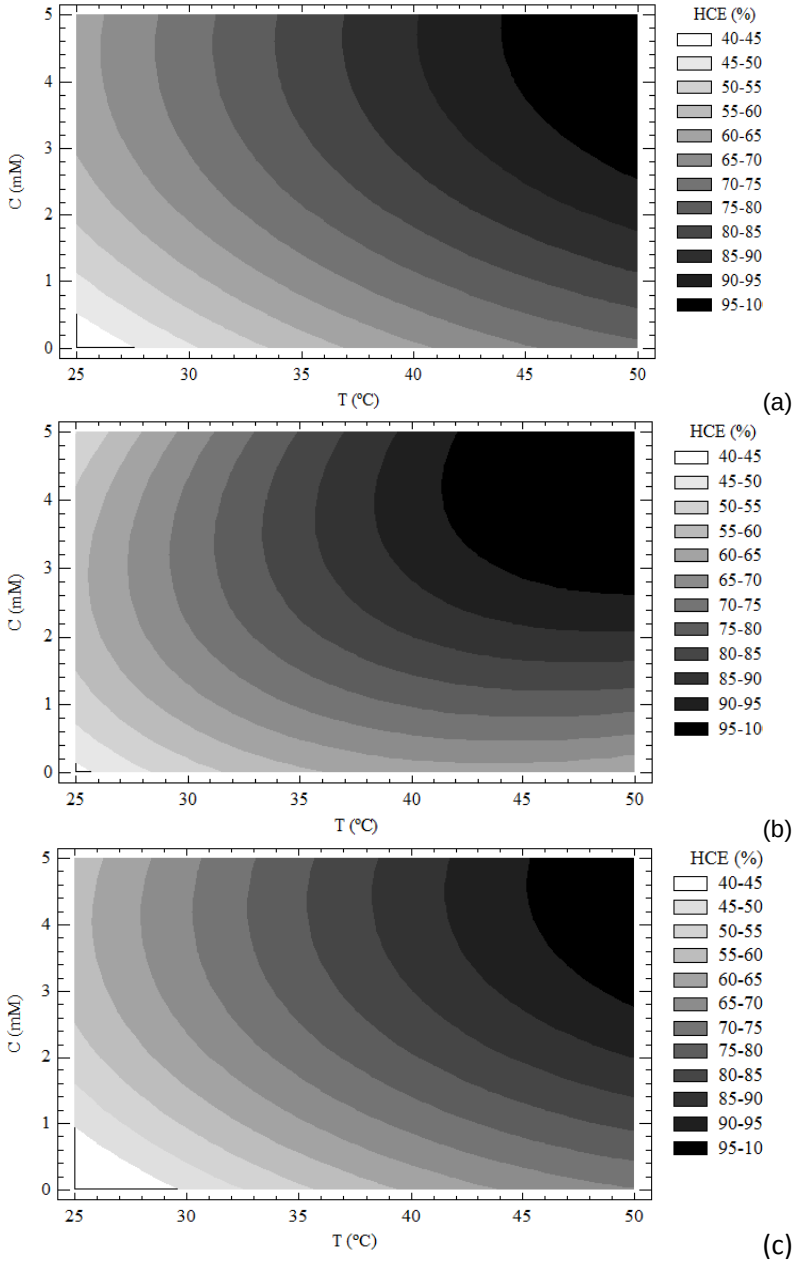

Fig. 36. *Contour plot for HCE as a function of temperature and NaCl concentration for the membranes of 5 kDa (a), 15 kDa (b) and 30 kDa (c) at a crossflow velocity of 2.18 m·s^{-1} for the 5 and 30 kDa membranes and 4.2 m·s^{-1} for the 15 kDa membrane*

$$HCE_5\ (\%) = a + b \cdot T_c + c \cdot C - d \cdot C^2 + e \cdot v^2 \qquad \text{Eq. 23}$$

$$HCE_{15}\ (\%) = a + f \cdot T_c \cdot C - d \cdot C^2 + g \cdot v \qquad \text{Eq. 24}$$

$$HCE_{30}\ (\%) = a + b \cdot T_c + c \cdot C - d \cdot C^2 + e \cdot v^2 \qquad \text{Eq. 25}$$

where HCE_5, HCE_{15} and HCE_{30} are the hydraulic cleaning efficiencies for the membranes of 5, 15 and 30 kDa, respectively, T_c is the temperature of the cleaning solution (ºC), C is the NaCl concentration (mM), v is the crossflow velocity ($m \cdot s^{-1}$) and a, b, c, d, e, f and g are the estimated coefficients for each statistically significant parameter.

Table 19. ANOVA results for the model equations that relate the hydraulic cleaning efficiency with the design variables

MWCO (kDa)	Parameter	Coefficient	Estimated value	p-value
5	Constant	a (%)	-77.179	0.0002
	T_c	b ($ºC^{-1}$)	1.448	0.0000
	C	c (mM^{-1})	10.922	0.0024
	C^2	d (mM^{-2})	-1.186	0.0292
	v^2	e ($m^{-2} \cdot s^2$)	17.024	0.0000
15	Constant	a (%)	-40.939	0.1015
	$T_c \cdot C$	f ($ºC^{-1} \cdot mM^{-1}$)	0.590	0.0001
	C^2	d (mM^{-2})	-3.207	0.0006
	v	g ($m^{-1} \cdot s$)	22.468	0.0026
30	Constant	a (%)	-46.222	0.0090
	T_c	b ($ºC^{-1}$)	1.556	0.0001
	C	c (mM^{-1})	11.948	0.0058
	C^2	d (mM^{-2})	-1.345	0.0493
	v^2	e ($m^{-2} \cdot s^2$)	8.873	0.0022

The results of the pattern-search optimization method are shown in Table 20. According to them, the optimal values of the design variables were: a cleaning solution temperature of 50 ºC for all the

membranes tested, a crossflow velocity of 2.18 $m \cdot s^{-1}$ for the polymeric membranes (5 and 30 kDa), a crossflow velocity of 4.2 $m \cdot s^{-1}$ for the ceramic membrane (15 kDa) and NaCl concentrations of 4.61, 4.56 and 4.44 for the 5, 15 and 30 kDa membranes, respectively.

Table 20. Optimal values of the design variables obtained with a pattern-search optimization method

MWCO (kDa)	T_c (ºC)	C (mM)	v ($m \cdot s^{-1}$)
5	50	4.61	2.18
15	50	4.56	4.20
30	50	4.44	2.18

5.1.5. Conclusions

Different saline solutions were tested to clean the 15 kDa membrane fouled with a 1 % (w/w) BSA aqueous solution. The highest values of HCE were achieved when the cleaning was performed with NaCl, KCl, $NaNO_3$ and NH_4Cl solutions. The lowest value of HCE was obtained when Na_2SO_4 solutions were used. NaCl was selected to be used as cleaning agent because of its lower cost and environmental impact.

The cleaning solution concentration, temperature and crossflow velocity had a great effect on HCE. The results obtained demonstrated that the higher the temperature of the cleaning solution was, the higher the HCE was. In addition, as crossflow velocity increased, HCE also increased. However, when salt concentration increased up to a certain value (2.5 mM for the 5, 15 and 30 kDa

membranes) HCE increased as well, but a further increase in NaCl concentration did not result in higher values of HCE or could even cause their decrease. Saline solutions were able to clean the 5, 15 and 30 kDa membranes. However, they were not effective to completely clean the 50 kDa membrane. This can be attributed to the more intense fouling observed for this membrane.

According to the results of the RSM analysis and the results of the pattern-search optimization method, the best operating conditions to clean the 5, 15 and 30 kDa membranes were a cleaning solution temperature of 50 ºC, crossflow velocities of 2.18 $m \cdot s^{-1}$ for the 5 and 30 kDa membranes and 4.2 $m \cdot s^{-1}$ for the 15 kDa membrane and NaCl concentrations of 4.61, 4.56 and 4.44 for the 5, 15 and 30 kDa membranes, respectively. The selected experimental conditions resulted in the maximum values of HCE_5, HCE_{15} and HCE_{30} (about 100 %).

An equation to relate HCE with the operating conditions was obtained by means of a Multiple Regression Analysis for the low MWCO membranes. For the polymeric membranes, the statistically significant factors were the same for both membranes.

Acknowledgements

The authors of this work wish to gratefully acknowledge the financial support from the Spanish Ministry of Science and Innovation through the project CTM2010-20186 and the Generalitat Valenciana through

the program “Ayudas para la realización de proyectos I+D para grupos de investigación emergentes GV/2013”.

Nomenclature

List of symbols

a	Model equation coefficient (%)
b	Model equation coefficient ($^oC^{-1}$)
c	Model equation coefficient (mM^{-1})
C	NaCl concentration (mM)
C_b	BSA concentration in the feed solution ($g \cdot L^{-1}$)
C_p	Permeate BSA concentration ($g \cdot L^{-1}$)
d	Model equation coefficient (mM^{-2})
e	Model equation coefficient ($m^{-2} \cdot s^2$)
f	Model equation coefficient ($^oC^{-1} \cdot mM^{-1}$)
g	Model equation coefficient ($m^{-1} \cdot s$)
J	Permeate flux ($m^3 \cdot m^{-2} \cdot s^{-1}$)
N_p	Number of points within the given area (dimensionless)
ΔP	Transmembrane pressure (bar)
R	Total hydraulic resistance (m^{-1})
R_m	Resistance of the new membrane (m^{-1})
R_f	Resistance after the fouling step (m^{-1})
R_{r1}	Resistance after the first rinsing step (m^{-1})
R_c	Resistance after the cleaning step (m^{-1})
R_{r2}	Resistance after the second rinsing step (m^{-1})
R_q	Root mean square roughness (nm)

t	Filtration time (s)
T_c	Temperature of the cleaning solution (ºC)
v	Crossflow velocity ($m \cdot s^{-1}$)
Z	Height values of the surface sample (nm)
Z_i	Z value currently measured (nm)
Z_{avg}	Average of the Z values of the sample (nm)

Greek letters

μ	Feed solution viscosity ($kg \cdot m^{-1} \cdot s^{-1}$)

Abbreviations

AFM	Atomic force microscopy
BSA	Bovine serum albumin
EOM	Extracellular organic matter
HCE	Hydraulic cleaning efficiency
HRE	Hydraulic rinsing efficiency
MWCO	Molecular weight cut off
PES	Polyethersulfone
pI	Isoelectric point
RSM	Response surface methodology
UF	Ultrafiltration

5.2. COMPROBACIÓN DE LA EFICACIA DEL PROCESO DE LIMPIEZA MEDIANTE MÉTODOS QUÍMICOS

Tal y como se ha explicado en el Capítulo II, además de los métodos hidráulicos utilizados para evaluar la eficacia del proceso de limpieza, existen métodos químicos basados en técnicas espectrofotométricas (SEM, EDX, AFM y ATR-FTIR). Por tanto, en este apartado se compara el valor de eficacia de limpieza obtenido mediante el método hidráulico (comparación de las resistencias hidráulicas en diferentes etapas del proceso) con el valor de eficacia obtenido mediante las técnicas anteriormente mencionadas. Para ello, se comparan entre sí los resultados obtenidos por medio de cada una de estas técnicas para las membranas nueva, sucia y limpia. Es importante destacar que, dada la naturaleza destructiva de los métodos químicos de determinación de la eficacia del proceso de limpieza y el elevado coste de las membranas cerámicas, esta comprobación sólo se ha llevado a cabo con las membranas poliméricas ensuciadas con disoluciones de BSA y tras el protocolo de limpieza con NaCl en las condiciones de operación que resultaron óptimas (concentración de NaCl de 5 mM, 50 ºC y 2.18 $m \cdot s^{-1}$).

En primer lugar, se muestran las imágenes obtenidas mediante el microscopio SEM de las membranas de 5 (Fig. 37) y 30 kDa (Fig. 38). Como puede observarse en ambas figuras, las imágenes correspondientes a las membranas nueva y limpia son muy similares,

confirmando el valor de EHL cercano al 100 % obtenido mediante el método hidráulico.

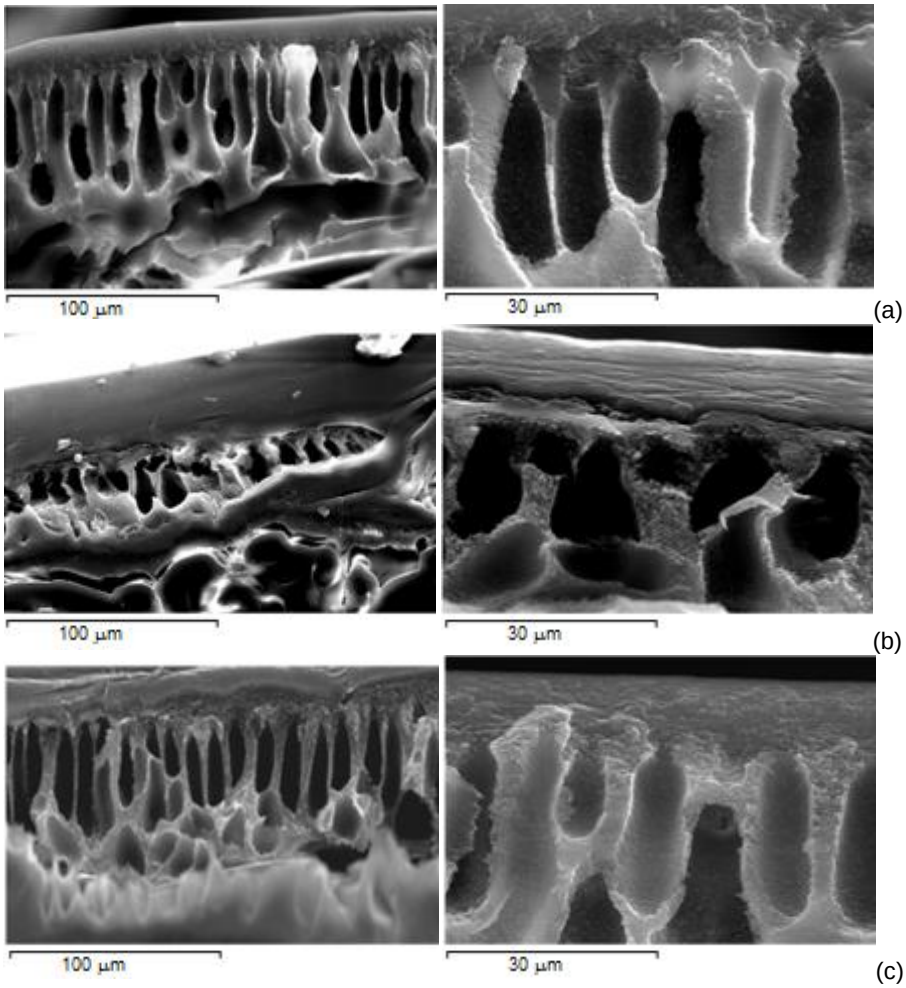

Fig. 37. *Imágenes de SEM de la membrana de 5 kDa (a) nueva, (b) tras el ensuciamiento con BSA y (c) tras la limpieza con NaCl en las condiciones óptimas*

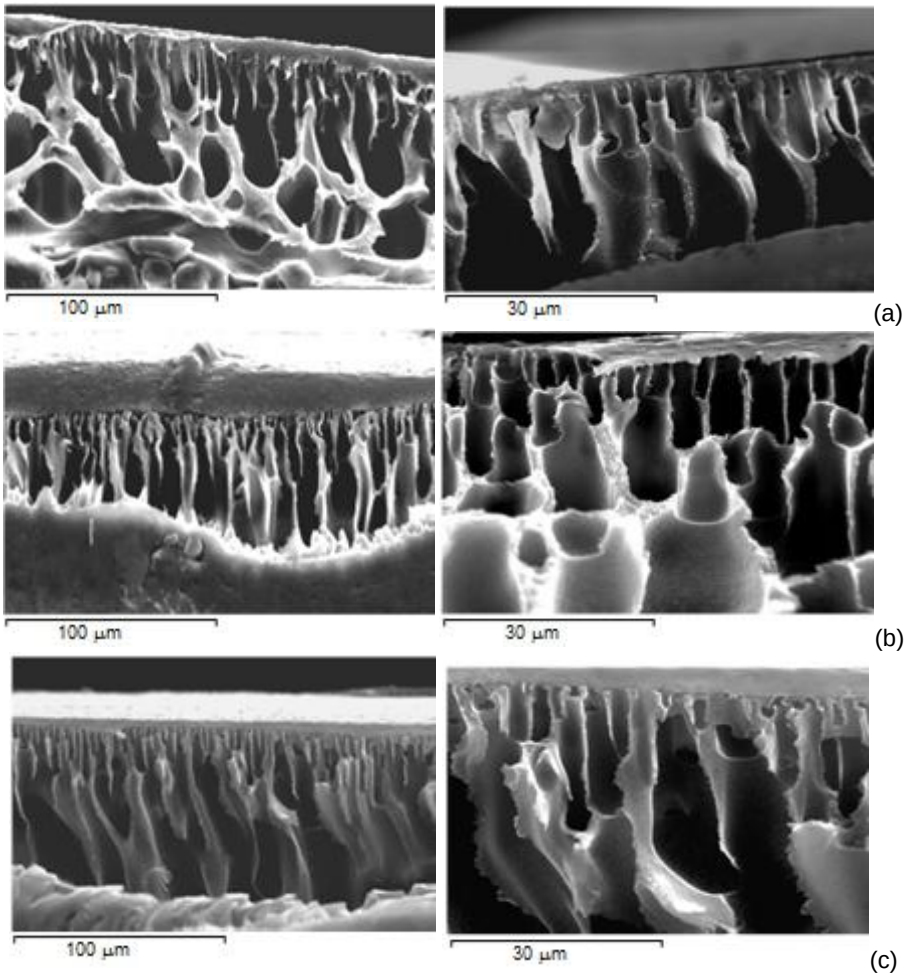

Fig. 38. *Imágenes de SEM de la membrana de 30 kDa (a) nueva, (b) tras el ensuciamiento con BSA y (c) tras la limpieza con NaCl en las condiciones óptimas*

Sin embargo, en el caso de las membranas sucias, se observan varios agregados sobre la superficie de las mismas, indicando la presencia de proteínas procedentes de la etapa de ensuciamiento. La densidad de agregados de proteínas por área de membrana es más elevada en el caso de la membrana de 5 kDa. Esto puede

deberse a la diferencia de material del que están fabricadas ambas membranas. Mientras que la membrana de 5 kDa es de PES, la membrana de 30 kDa es de PESH. Este hecho implica que la membrana de mayor MWCO es más hidrofílica y presenta mejores propiedades antiensuciamiento que la membrana de 5 kDa, por lo que la acumulación de agregados de proteínas sobre su superficie es menor. Además, puede distinguirse en ambas membranas una capa más densa formada sobre la superficie de la misma tras su ensuciamiento, especialmente en el caso de la membrana de 5 kDa. Este hecho es también un indicador de la formación de una capa de ensuciamiento debido a la acumulación de proteínas sobre la superficie de ambas membranas. Otros autores también demostraron la aparición de una capa de mayor grosor sobre la capa activa de la membrana (Rabiller-Baudry *et al.*, 2012). Estos autores ensuciaron membranas de PES con leche desnatada e indicaron la presencia de una capa de ensuciamiento sobre la superficie de las membranas utilizadas, debida a la acumulación de proteínas presentes en la disolución alimento.

A partir de estas imágenes se obtuvieron diferentes espectros de EDX, que permiten cuantificar la concentración de cada elemento químico presente en la estructura de cada una de las membranas. La Tabla 21 muestra el contenido en cada elemento químico para las membranas de 5 y 30 kDa nueva, tras el ensuciamiento (sucia) y tras el protocolo de limpieza (limpia). En el caso de las membranas sucias se detectó una pequeña concentración de nitrógeno, elemento característico de las proteínas. Esta concentración fue mayor en el caso de la membrana de 5 kDa, puesto que la mayor hidrofobicidad

de esta membrana favorece la mayor acumulación de proteínas en la superficie de la membrana. Además, la concentración de azufre disminuyó en las membranas sucias, comparadas con las membranas nuevas. Dado que la cantidad de azufre en la proteína BSA es muy reducida, la disminución de la concentración de este elemento químico se debe a la presencia de una capa de ensuciamiento sobre la superficie de la membrana. Comparando ambas membranas entre sí, puede observarse que la reducción en la concentración de azufre fue mayor en el caso de la membrana de 5 kDa, hecho que confirma la mayor tendencia al ensuciamiento de esta membrana.

Tabla 21. Resultados de EDX para las membranas poliméricas nuevas, ensuciadas con BSA y tras la limpieza con NaCl (concentración de sal: 5 mM, temperatura: 50 ºC)

Elemento (%p/p)	Membrana					
	5 kDa nueva	5 kDa sucia	5 kDa limpia	30 kDa nueva	30 kDa sucia	30 kDa limpia
C	65.47	73.99	71.29	72.55	86.18	77.27
O	7.94	18.04	15.63	16.29	5.53	10.50
S	26.59	5.58	12.67	11.08	7.55	11.27
N	-	2.40	-	-	0.70	-
Al	-	-	-	0.03	0.01	0.01
Si	-	-	-	0.05	0.01	0.01
Ti	-	-	-	0.01	0.01	0.01
Na	-	-	0.18	-	-	0.13
Cl	-	-	0.24	-	-	0.81

Por otra parte, los resultados del análisis de EDX demostraron que, una vez las membranas fueron sometidas al proceso de limpieza y tras el segundo aclarado, una pequeña cantidad de iones sodio y cloruro permanecen en la estructura de ambas membranas, en

cantidades muy similares independientemente del MWCO. Por el contrario, no se detectó nitrógeno en la composición de las membranas limpias, lo cual demuestra la efectividad del protocolo de limpieza ensayado. Finalmente, puesto que la membrana de 30 kDa es de poliétersulfona permanentemente hidrofílica, de acuerdo con el fabricante, se detectaron en la estructura de la misma trazas de diversos compuestos metálicos, como aluminio, titanio y silicio. Según distintos autores (García-Ivars *et al.*, 2014), este tipo de óxidos metálicos suelen utilizarse para modificar membranas de base polimérica con el fin de conferirles mejores propiedades antiensuciamiento.

La Fig. 39 muestra los espectros de ATR-FTIR de las membranas de 5 y 30 kDa nuevas, tras la etapa de ensuciamiento con BSA y tras la etapa de limpieza con NaCl. En ambos espectros se observa como la absorbancia medida en el caso de las membranas sucias es considerablemente superior a la correspondiente a la membrana nueva en las regiones entre 1500-1580 y 1600-1700 cm^{-1}. Estas regiones son características de las proteínas, debido a la presencia de grupos amida I, identificado a través de la vibración del enlace $C=O_{amida}$ (1650 cm^{-1}), y amida II, debido a los enlaces C-N y N-H (1545 cm^{-1}) (Pihlajamäki *et al.*, 1998; Rabiller-Baudry *et al.*, 2002). Todo ello confirma la acumulación de proteínas sobre la superficie de la membrana.

Otros autores (Rabiller-Baudry *et al.*, 2008) han utilizado la información proporcionada por las bandas de absorbancia a 1539 y 1240 cm^{-1} para cuantificar la cantidad de proteínas remanentes en la

superficie de las membranas antes y después del proceso de limpieza.

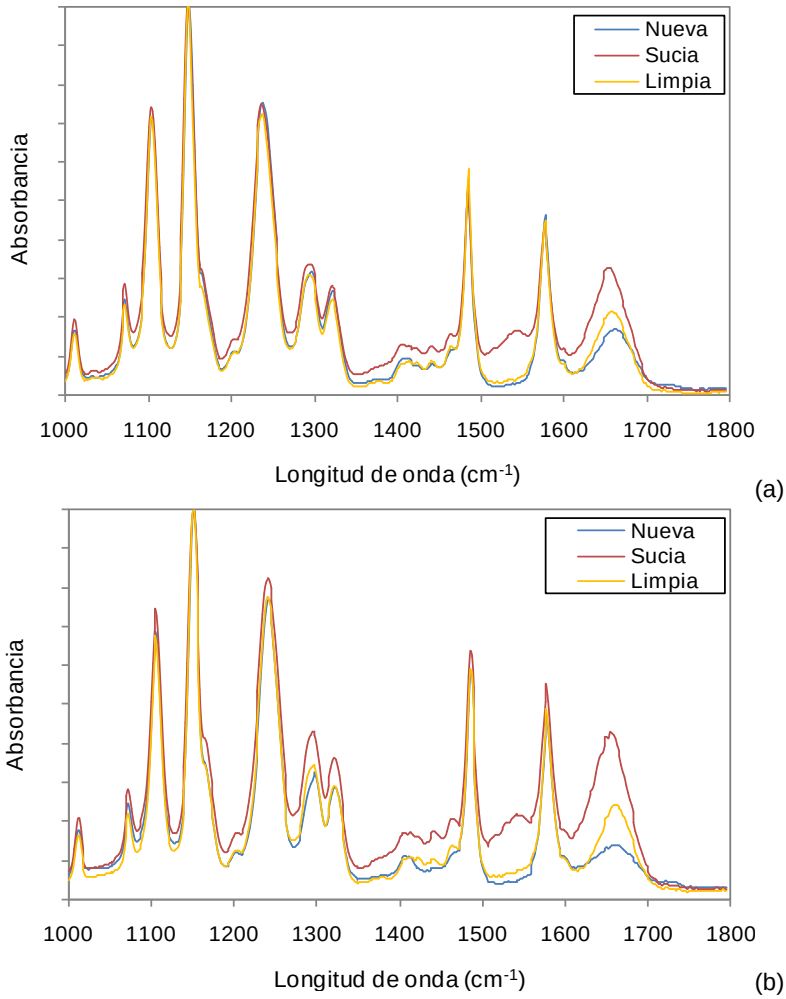

Fig. 39. *Espectros de ATR-FTIR de las membranas nuevas, tras el ensuciamiento con BSA y tras la limpieza con NaCl de (a) 5 kDa y (b) 30 kDa*

Estas bandas son características del grupo amida II de las proteínas (1539 cm^{-1}) y de la estructura base de la poliétersulfona, identificada a través del enlace C-O-C (1240 cm^{-1}). A partir del cociente de la absorbancia de estas dos bandas y mediante la ecuación que se mostrará en el Capítulo VIII, se puede determinar la concentración de proteínas por área de membrana en un rango entre 0.5 y 350 $\mu g \cdot cm^{-2}$ con una desviación máxima de 1 $\mu g \cdot cm^{-2}$ (Rabiller-Baudry *et al.*, 2012).

Los resultados de concentración residual de proteínas obtenidos se muestran en la Tabla 22. Como puede observarse, la concentración de proteínas disminuye significativamente tras el protocolo de limpieza con NaCl, obteniéndose valores inferiores a 10 $\mu g \cdot cm^{-2}$, los cuales, de acuerdo con Rabiller-Baudry *et al.* (2008) corresponden con los protocolos y agentes de limpieza más eficaces utilizados en la limpieza de membranas de poliétersulfona. Valores similares se obtuvieron en el caso de la membrana de 30 kDa ensuciada con disoluciones enzimáticas y tras llevar a cabo el mismo protocolo de limpieza con NaCl (Corbatón-Báguena *et al.,* 2015).

Tabla 22. Concentración residual de proteínas en las membranas poliméricas tras el ensuciamiento con BSA y la limpieza con NaCl en las condiciones óptimas

Membrana	Concentración residual de proteínas ($\mu g \cdot cm^{-2}$)	EHL (%)
5 kDa sucia	54.39±6.90	-
5 kDa limpia	5.24±0.72	100±2.01
30 kDa sucia	59.74±0.69	-
30 kDa limpia	8.47±0.51	99.46±1.99

Además, esta pequeña concentración de proteínas que permanece en la superficie de las membranas tras su limpieza no afecta a las propiedades permselectivas de las mismas, puesto que los valores de eficacia hidráulica obtenidos son aproximadamente del 100 %. Por tanto, queda demostrada la validez de los métodos hidráulicos utilizados para evaluar la eficacia del proceso de limpieza en este tipo de membranas.

La Fig. 40 muestra las imágenes obtenidas mediante el microscopio AFM de las membranas de 5 y 30 kDa nuevas, tras la etapa de ensuciamiento con BSA y tras la etapa de limpieza con NaCl en las condiciones óptimas. Además, la Tabla 23 recoge los valores de rugosidad promedio (R_a) y rugosidad cuadrática media (R_q) de todas las imágenes analizadas. De acuerdo con las imágenes proporcionadas por el microscopio SEM (Fig. 37 y Fig. 38), en el caso de la membrana de menor tamaño de poro se formaron más agregados sobre la superficie de la misma, hecho que queda confirmado por la Fig. 40a2. En el caso de la membrana de 30 kDa sucia, el número de agregados no fue tan elevado, aunque presentaban un tamaño mayor (Fig. 40b2). En esta última figura también se aprecia claramente la formación de una capa de ensuciamiento sobre la superficie de la membrana, que cubre completamente la rugosidad inicial de la membrana (Fig. 40b1).

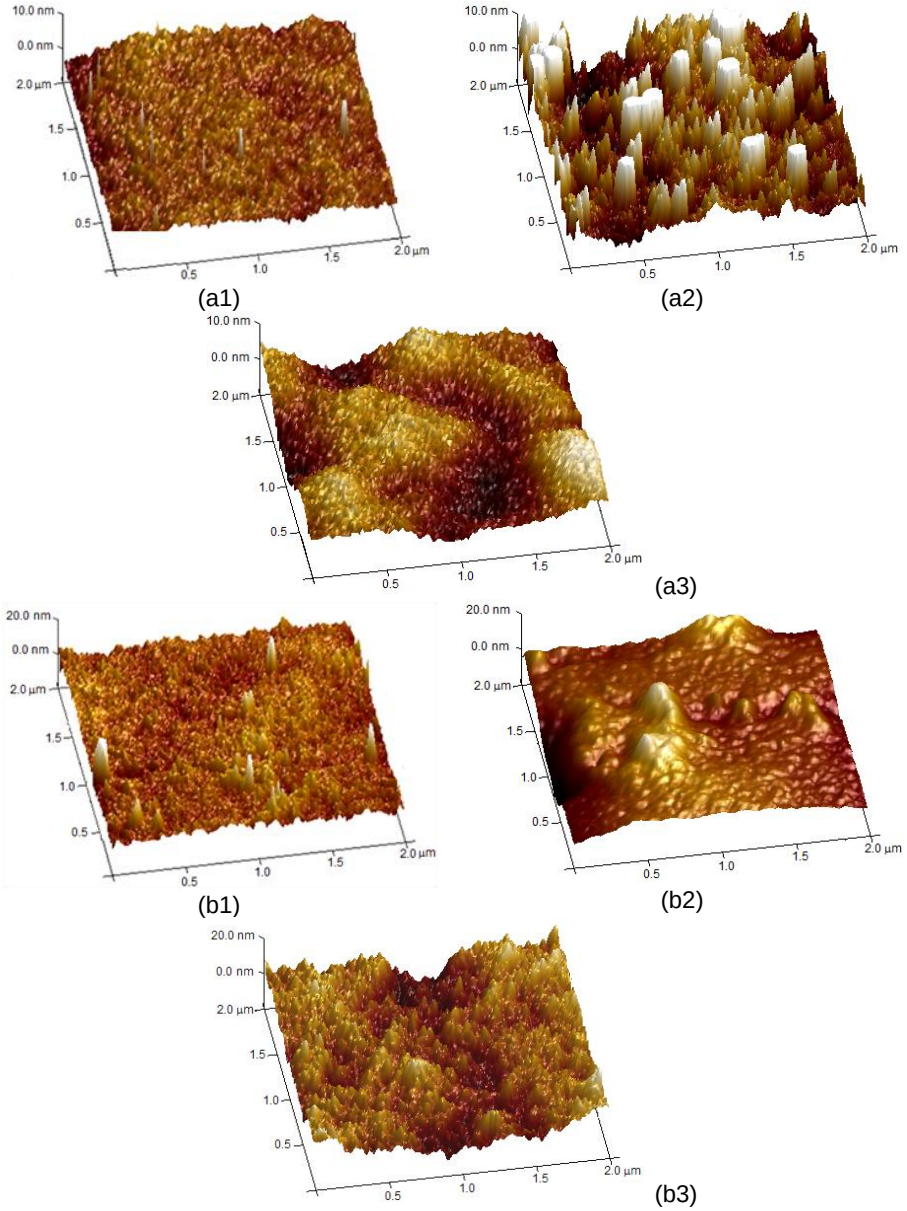

Fig. 40. *Imágenes de AFM de las membranas nueva (1), tras el ensuciamiento con BSA (2) y tras la limpieza con NaCl en las condiciones óptimas (3) de las membranas de (a) 5 kDa y (b) 30 kDa*

En el caso de las membranas tras el protocolo de limpieza, las imágenes muestran una recuperación casi total de superficie de la membrana (Fig. 40a3 y b3). Esta observación se corrobora con los valores de rugosidad de la Tabla 23, que aumentan en la membrana sucia con respecto a la membrana nueva y disminuyen tras la limpieza hasta valores cercanos a la rugosidad que presentaban inicialmente las membranas.

Tabla 23. Rugosidad de las membranas poliméricas utilizadas en la UF de disoluciones de BSA

Membrana	Rugosidad de la superficie (nm)	
	R_a	R_q
5 kDa nueva	0.616	0.767
5 kDa sucia	3.970	5.390
5 kDa limpia	0.829	1.053
30 kDa nueva	1.304	1.686
30 kDa sucia	4.487	5.684
30 kDa limpia	1.790	2.230

En estudios previos realizados con membranas similares, la elevada concentración de proteínas utilizada durante el ensuciamiento provocaba la formación de una capa sobre la superficie de la membrana que impidía visualizar la rugosidad original de la misma (Corbatón-Báguena *et al.*, 2015). Otros autores (Ohnishi *et al.*, 1998), demostraron que a medida que la concentración de proteínas adsorbidas sobre mica aumentó, la capa de proteínas formada fue más densa y aparecieron agregados dispersados por la superficie.

5.3. BIBLIOGRAFÍA

ADIKANE H.V., THAKAR D.M. y NENE S.N. (2004). "Optimisation of colour and sugar rejection of black liquor using membranes" en *Separation and Purification Technology*, vol. 36, p. 229-234.

AFONSO A., MIRANDA J.M. y CAMPOS J.B.L.M. (2009). "Numerical study of BSA ultrafiltration in the limiting flux regime – effect of variable physical properties" en *Desalination*, vol. 249, p. 1139-1150.

ALI K., SHAH A-u-H.A. y BILAL S. (2008). "Thermodynamic parameters of surface formation of some aqueous salt solutions" en *Colloids and Surfaces A: Physicochemical Engineering Aspects*, vol. 330, p. 28-34.

ALMÉCIJA M.C. *et al.* (2009a). "Influence of the cleaning temperature on the permeability of ceramic membranes" en *Desalination*, vol. 245, p. 708-713.

ALMÉCIJA M.C. *et al.* (2009b). "Analysis of cleaning protocols in ceramic membranes by liquid-liquid displacement porosimetry" en *Desalination*, vol. 245, p. 541-545.

BLANPAIN-AVET P., MIGDAL J.F. y BÉNÉZECH T. (2009). "Chemical cleaning of a tubular ceramic microfiltration membrane fouled with a whey protein concentrate suspension – characterization of hydraulic and chemical cleanliness" en *Journal of Membrane Science*, vol. 337, p. 153-174.

CABERO CABERO M.L. (1997). *Limpieza química de membranas inorgánicas: Aplicación al tratamiento de lactosuero.* Tesis Doctoral. Oviedo: Universidad de Oviedo, <http://hdl.handle.net/10651/13566>.

CABERO M.L. *et al.* (1999). "Rinsing of ultrafiltration ceramic membranes fouled with whey proteins: effects on cleaning procedures" en *Journal of Membrane Science*, vol. 154, p. 239-250.

CHUNG T.-S. *et al.* (2002). "Visualization of the effect of die shear rate on the outer surface morphology of ultrafiltration membranes by AFM" en *Journal of Membrane Science*, vol. 196, p. 251-266.

COJOCARU C. y ZAKRZEWSKA-TRZNADEL G. (2007). "Response surface modeling and optimization of copper removal from aqua solutions using polymer assisted ultrafiltration" en *Journal of Membrane Science*, vol. 298, p. 56-70.

CORBATÓN-BÁGUENA M.J. *et al.* (2015). "Destabilization and removal of immobilized enzymes adsorbed onto polyethersulfone ultrafiltration membranes by salt solutions" en *Journal of Membrane Science*, vol. 486, p. 207-214.

CURTIS R.A. y LUE L. "A molecular approach to bioseparations: protein-protein and protein-salt interactions" en *Chemical Engineering Science*, vol. 61, p. 907-923.

DANIŞ Ü. y KESKINLER B. (2009). "Chromate removal from wastewater using micellar enhanced crossflow filtration: Effect of transmembrane pressure and crossflow velocity" en *Desalination*, vol. 249, p. 1356-1364.

DAUFIN G. *et al.* (2001). "Recent and emerging applications of membrane processes in the food and dairy industry" en *Food and Bioproducts Processing*, vol. 79, p. 89-102.

GARCÍA-IVARS J. *et al.* (2014). "Development of fouling-resistant polyethersulfone ultrafiltration membranes via surface UV photografting with polyethylene glicol/aluminum oxide nanoparticles" en *Separation and Purification Technology*, vol. 135, p. 88-99.

GARG U.K. *et al.* (2008). "Removal of nickel (II) from aqueous solution by adsorption on agricultural waste biomass using a response surface methodological approach" en *Bioresource Technology*, vol. 99, p. 1325-1331.

HOFMEISTER F. (1888). "Zur lehre von der wirkung der salze" en *Archiv for Experimentelle Pathologie und Pharmakologie*, vol. 24, p. 247.

KARRAKER K.A. y RADKE R.J. (2002). "Disjoining pressures, zeta potentials and surface tensions of aqueous non-ionic surfactant/electrolyte solutions: theory and comparison to experiment" en *Advances in Colloid Interface Sciences*, vol. 96, p. 231-264.

KAZEMIMOGHADAM M. y MOHAMMADI T. (2007). "Chemical cleaning of ultrafiltration membranes in the milk industry" en *Desalination*, vol. 204, p. 213-218.

LEE S. y ELIMELECH M. (2007). "Salt cleaning of organic-fouled reverse osmosis membranes" en *Water Research*, vol. 41, p. 1134-1142.

LLANOS J. *et al.* (2010). "Characterization of a ceramic ultrafiltration membranes in different operational states after its used in a heavy-metal ion removal process" en *Water Research*, vol. 44, p. 3522-3530.

MANCIU M. y RUCKENSTEIN E. (2003). "Specific ion effects via ion hydration: I. Surface tension" en *Advances in Colloid and Interface Science*, vol. 105, p. 63-101.

MATUBAYASI N. y YOSHIKAWA R. (2007). "Thermodynamic quantities of surface formation of aqueous electrolyte solutions VII. Aqueous solution of alkali metal nitrates $LiNO_3$, $NaNO_3$ and KNO_3" en *Journal of Colloid Interface Science*, vol. 315, p. 597-600.

MATZINOS P. y ÁLVAREZ R. (2002). "Effect of ionic strength on rinsing and alkaline cleaning of ultrafiltration inorganic membranes fouled with whey proteins" en *Journal of Membrane Science*, vol. 208, p. 23-20.

MUTHUKUMARAN S. *et al.* (2004). "The use of ultrasonic cleaning for ultrafiltration membranes in the dairy industry" en *Separation and Purification Technology*, vol. 39, p. 99-107.

MUTHUKUMARAN S. *et al.* (2007). "The application of ultrasound to dairy ultrafiltration: the influence of operating conditions" en *Journal of Food Engineering*, vol. 81, p. 364-373.

OGUNBIYI O.O., MILES N.J. y HILAL N. (2008). "The effects of performance and cleaning cycles of new tubular ceramic microfiltration membrane fouled with a model yeast suspension" en *Desalination*, vol. 220, p. 273-289.

OHNISHI S., MURATA M. y HATO M. (1998). "Correlation between surface morphology and surface forces of protein A adsorbed on mica" en *Biophysical Journal*, vol. 74, p. 455-465.

PELEGRINE D.H.G. y GASPARETTO C.A. (2005). "Whey proteins solubility as function of temperature and pH" en *Lebensmittel-Wissenschaft und-Technologie*, vol. 38, p. 77-80.

PETERSEN P.B. y SAYKALLY R.J. (2005). "Adsorption of ions to the surface of dilute electrolyte solutions: the Jones-Ray effect revisited" en *Journal of the American Chemical Society*, vol. 127, p. 15446-15452.

PIHLAJAMÄKI A., VÄISÄNEN P. y NYSTRÖM M. (1998). "Characterization of clean and fouled polymeric ultrafiltration membranes by Fourier transform IR spectroscopy-attenuated total

reflection" en *Colloids Surfaces A: Physicochemical Engineering Aspects*, vol. 138, p. 323-333.

QU F. *et al.* (2014). "Ultrafiltration membrane fouling caused by extracellular organic matter (EOM) from Microcystis aeruginosa: Effects of membrane pore size and surface hydrophobicity" en *Journal of Membrane Science*, vol. 449, p. 58-66.

RABILLER-BAUDRY M. *et al.* (2002). "Characterisation of cleaned and fouled membrane by ATR-FTIR and EDX analysis coupled with SEM: application to UF of skimmed milk with a PES membrane" en *Desalination*, vol. 146, p. 123-128.

RABILLER-BAUDRY M. *et al.* (2008). "A dual approach of membrane cleaning based on physic-chemistry and hydrodynamics. Application to PES membrane of dairy industry" en *Chemical Engineering and Processing*, vol. 47, p. 267-275.

RABILLER-BAUDRY M. *et al.* (2012). "Coupling of SEM-EDX and FTIR-ATR to (quantitatively) investigate organic fouling on porous organic and composite membranes" en Méndez-Vilas A. *Current Microscopy Contributions to Advances in Science and Technology.* Badajoz: Formatex.

RUBY FIGUEROA R.A., CASSANO A. y DRIOLI E. (2011). "Ultrafiltration of orange press liquor: Optimization for permeate flux and fouling index by response surface methodology" en *Separation and Purification Technology*, vol. 80, p. 1-10.

SCHÄFER A.I., FANE A.G. y WAITE T.D. (2000). "Fouling effects on rejection in the membrane filtration of natural waters" en *Desalination*, vol. 131, p. 215-224.

SHAH A-u-H.A., ALI K. y BILAL S. (2013). "Surface tension, surface excess concentration, enthalpy and entropy of surface formation of

aqueous salt solutions" en *Colloids and Surfaces A: Physicochemical Engineering Aspects*, vol. 417, p. 183-190.

SMITH P.J. *et al.* (2006). "Productivity enhancement in a cross-flow ultrafiltration membrane system through automated de-clogging operations" en *Journal of Membrane Science*, vol. 280, p. 82-88.

SUTTIPRASIT P., KRISDHASIMA V. y MCGUIRE J. (1992). "The surface activity of α-lactabumin, β-lactoglobulin and bovine serum albumin" en *Journal of Colloid and Interface Science*, vol. 154, p. 316-326.

TARAZAGA C.C., CAMPDERRÓS M.E. y PÉREZ-PADILLA A. (2006). "Physical cleaning by means of electric field in the ultrafiltration of a biological solution" en *Journal of Membrane Science*, vol. 278-p. 219-224.

TSUMOTO K. *et al.* (2007). "Effects of salts on protein-surface interactions: Applications for column chromatography" en *Journal of Pharmaceutical Science*, vol. 96, p. 1677-1690.

WANG Y-N. y TANG C.Y. (2011). "Protein fouling of nanofiltration, reverse osmosis, and ultrafiltration membranes-The role of hydrodynamic conditions, solution chemistry and membrane properties" en *Journal of Membrane Science,* vol. 376, p. 275-282.

ZHANG J. (2012). "Protein-protein interactions in salt solutions" en Cai W. y Hong H. *Protein-protein interactions – Computational and experimental tools*. Intech.

CAPÍTULO VI

Limpieza mediante disoluciones salinas de membranas ensuciadas con proteínas y sales

6.1. LIMPIEZA DE MEMBRANAS DE ULTRAFILTRACIÓN ENSUCIADAS CON SEROALBÚMINA BOVINA Y $CaCl_2$

En este Capítulo se presenta una adaptación al formato de la Tesis Doctoral del artículo titulado "Salt cleaning of ultrafiltration membranes fouled by whey model solutions", publicado en la revista Separation and Purification Technology. En él se evaluó la eficacia del proceso de limpieza mediante NaCl en membranas de 5, 15 y 30 kDa ensuciadas con disoluciones modelo de lactosuero consistentes en proteínas (BSA) y sales ($CaCl_2$) y se obtuvieron las condiciones experimentales óptimas (concentración de NaCl, temperatura y velocidad tangencial de la disolución de limpieza) que maximizan la eficacia de limpieza. Los datos bibliográficos del artículo se destacan a continuación:

Autores: *M.-J. Corbatón-Báguena, S. Álvarez-Blanco, M.-C. Vincent-Vela*

Título: *Salt cleaning of ultrafiltration membranes fouled by whey model solutions*

Editorial: *Elsevier*

Revista: *Separation and Purification Technology*
año: 2014 vol. 132 p. 226-233

Doi: *http://dx.doi.org/10.1016/j.seppur.2014.05.029*

Salt cleaning of ultrafiltration membranes fouled by whey model solutions

María-José Corbatón-Báguena, Silvia Álvarez-Blanco*, María-Cinta Vincent-Vela

Department of Chemical and Nuclear Engineering, Universitat Politècnica de València, C/Camino de Vera s/n 46022 Valencia, Spain

*Corresponding author: sialvare@iqn.upv.es
Tel: +34963879630 (Ext.: 796383)
Fax: +34963877639 (Ext.: 77639)

Abstract

In this work, three ultrafiltration (UF) membranes were fouled with whey model solutions that contained BSA (1 % w/w) and $CaCl_2$ (0.06 % w/w). These membranes were cleaned with NaCl solutions. Temperature, crossflow velocity and concentration were varied. The membranes considered were a polyethersulfone (PES) membrane, a ceramic ZrO_2-TiO_2 membrane and a permanently hydrophilic polyethersulfone (PESH) membrane. Their molecular weight cut-offs (MWCOs) are 5, 15 and 30 kDa, respectively. The cleaning efficiency was related to the MWCO, membrane material and operating conditions. The results obtained demonstrated that NaCl solutions were able to clean the membranes tested. In addition, the higher the

temperature and the crossflow velocity of the cleaning solution, the higher the cleaning efficiency was. However, there was an optimum value of NaCl concentration to clean the membranes effectively. When concentration was higher than the optimum, the cleaning efficiency decreased. The relationship between the cleaning efficiency and the operating conditions was obtained with statistical and optimization analysis.

Keywords: Ultrafiltration; whey model solutions; NaCl solutions; membrane cleaning

6.1.1. Introduction

In dairy industries, ultrafiltration (UF) is one of the most widely used membrane separation processes. Its most important applications are milk dehydration, whey concentration and protein fractionation or purification (Ogunbiyi *et al.*, 2008; Kazemimoghadam and Mohammadi, 2007). However, the major drawback in the application of UF processes is the progressive flux decline due to the fouling phenomena. In the dairy industry, membrane fouling is mainly caused by protein deposition on the membrane surface and adsorption inside its porous structure (Almécija *et al*, 2009a). To minimize membrane fouling, several authors have investigated protein-protein, protein-membrane and also, protein-inorganic compounds interactions (Almécija *et al.,* 2009a; Ang and Elimelech, 2007; Mo *et al*, 2008). Almécija *et al.* (2009a) studied the influence of calcium salts on the UF of whey using a 50 kDa ceramic membrane. They demonstrated

that these salts can act as binding agents between proteins. When the concentration of calcium salts increased, the percentage of membrane blocked pores during UF increased while the permeate flux through the membrane decreased. Ang and Elimelech (2007) studied the effect of calcium concentration on the bovine serum albumin (BSA) fouling of reverse osmosis membranes. They reported that permeate flux decline was greater when calcium concentration increased, due to the reduction of the electrostatic repulsion among BSA molecules. Mo *et al.* (2008) studied the effect of several cations and ionic strength on BSA fouling on reverse osmosis membranes. Calcium cations acted as crosslinking agents with BSA molecules. Fouling experiments demonstrated that BSA fouling rate increased when calcium was present in the feed solution. Fouling rate also increased as ionic strength of the feed solution increased.

To overcome membrane fouling, membranes have to be cleaned to remove the deposits. In dairy industries, chemical cleaning procedures are carried out even twice a day (Blanpain-Avet *et al.*, 2009). The conventional procedure to clean membranes fouled with whey solutions consists of several steps of alkali, acid and disinfectant washings (Ogunbiyi *et al.*, 2008; Kazemimoghadam and Mohammadi, 2007; Almécija *et al*, 2009a; Almécija *et al*, 2009b). However, membranes may be damaged by these cleaning agents, reducing the membrane lifetime and causing a negative impact on the environment when they are discharged as wastewaters. Therefore, alternative cleaning techniques have been developed in the last years such as electromagnetic fields (Tarazaga *et al*, 2006), ultrasounds (Muthukumaran *et al*, 2004) and saline solutions. Several authors

(Tsumoto *et al.,* 2007; Zhang, 2012; Hofmeister, 1888) have investigated the effect of salts on protein-protein interactions. Tsumoto *et al.* (2007) studied the effect of several salts on protein-protein interactions. They observed that, at the same concentration, some salts (such as Na_2SO_4) caused a decline in protein solubility while other salts (such as NaCl) increased the solubility of proteins. The effect of salts that decreased protein solubility is known as salting-out effect. On the other hand, the effect of increasing protein solubility is known as salting-in effect. Zhang (2012) reported that Cl^- was able to specifically bind to the proteins surface more strongly than other cations and anions. Thus, the repulsive intermolecular interactions increase and protein solubility also increases. Hofmeister (1888) proposed a ranking of the capability of several cations and anions to salt-out or salt-in proteins. Based on the Hofmeister series, Nucci and Vanderkooi (2008) reported a series of divalent and monovalent cations and classified them in order of their ability to precipitate proteins. According to these series, calcium cation is one of the most salting-out ions, which is in agreement with other works about the effect of calcium on protein fouling (Almécija *et al*, 2009a; Ang and Elimelech, 2007).

However, only a few papers investigated membrane cleaning by means of saline solutions (Lee and Elimelech, 2007; Corbatón-Báguena *et al*., 2014). Lee and Elimelech (2007) cleaned reverse osmosis membranes fouled with alginate and calcium solutions with NaCl aqueous solutions at different concentrations. Their results showed that cleaning efficiencies of about 90 % were achieved with NaCl solutions of 50 mM. However, increasing NaCl concentration

from 50 to 300 mM did not cause an increase in the cleaning efficiency. In a previous work, Corbatón-Báguena *et al.* (2014) cleaned a 15 kDa MWCO UF membrane fouled with BSA solutions with different saline solutions (Na_2SO_4, NaCl, $NaNO_3$, NH_4Cl and KCl). The highest values of hydraulic cleaning efficiency (HCE) were obtained with NaCl, $NaNO_3$, NH_4Cl and KCl solutions.

The aim of this work is to evaluate the ability of NaCl solutions to clean a monotubular ceramic UF membrane of 15 kDa and two flat-sheet polymeric UF membranes of 5 and 30 kDa fouled by whey model solutions. The solutions consisted of BSA 1 % (w/w) and $CaCl_2$ (0.06 % (w/w) in calcium). The influence of the operating conditions (temperature, crossflow velocity and NaCl concentration of the cleaning solution), membrane material and molecular weight cut-off (MWCO) on the membrane cleaning efficiency was investigated. In order to determine the optimal values of the cleaning operating conditions to achieve the highest cleaning efficiency, statistical and optimization analyses were performed.

6.1.2. Materials and methods

6.1.2.1. Materials

Fouling experiments were performed using aqueous solutions that contained BSA (1 % (w/w)) and $CaCl_2$ (0.06 % (w/w) in calcium) as feed solutions. BSA (prepared by heat shock fractionation, lyophilized powder, 98 % purity, A3733, Sigma-Aldrich, Germany) and $CaCl_2$

(95 % purity, Panreac, Spain) were dissolved in deionized water until the above mentioned concentration was achieved. Isoelectric point of BSA is 4.9, according to the manufacturer. Feed solutions had a pH of about 7, thus BSA has mainly negative net charge on its surface. Its configuration is elliptic (11.6x2.7x2.7 nm) and it is one of the most widely used whey proteins to prepare model solutions for UF experiments (Corbatón-Báguena *et al.*, 2014; Suttiprasit *et al*., 1992; Wang and Tang, 2011; Afonso *et al*., 2009). $CaCl_2$ is one of the most often used salts to study the interactions between whey proteins and salts (Almécija *et al.*, 2009a; Ang and Elimelech, 2007; Mo *et al*., 2008).

Membranes were cleaned with NaCl aqueous solutions (121659, Panreac, Spain) at a pH ranging from 6.8 to 7. NaOH aqueous solutions (211687, Panreac, Spain) and NaClO aqueous solutions (211921, Panreac, Spain) at a pH 11 were used as alkaline cleaning agents.

6.1.2.2. Membranes

The membranes used in the experiments were: a flat sheet polyethersulfone (PES) membrane of 5 kDa (reference UP005), a flat sheet permanentely hydrophilic polyethersulfone (PESH) membrane of 30 kDa (reference UH030) and a monotubular ceramic membrane of 15 kDa. The polymeric membranes were supplied by Microdyn-Nadir, Germany. They had an effective area of 100 cm^2. The ceramic membrane was supplied by TAMI Industries, France. It consisted of a

TiO_2 support layer and a ZrO_2-TiO_2 active layer and its effective area was 35.5 cm^2. It was 20 cm long with an internal diameter of 0.6 cm and an external diameter of 1 cm. The properties of these membranes are shown in Table 24. These membranes were selected for this study because their MWCO was lower than the molecular weight of BSA (67 kDa). This fact ensured high BSA rejection values. Moreover, they have MWCOs within the typical range for the production of whey protein concentrates. In addition, high thermal stability was desirable because high temperatures favour membrane cleaning. According to Table 24, this characteristic was common to all the membranes tested. Three different MWCOs (5, 15 and 30 kDa) and different membrane materials (PES, ZrO_2-TiO_2 and PESH) were selected to investigate their influence on the cleaning efficiency.

Table 24. Main properties of the membranes used

Item	UP005	INSIDE-CERAM™	UH030
Manufacturer	Microdyn Nadir	TAMI Industries	Microdyn Nadir
Type	Flat-sheet	Tubular	Flat-sheet
MWCO (kDa)	5	15	30
Active layer	PES	ZrO_2-TiO_2	PESH
Effective area (cm^2)	100.00	35.51	100.00
Water permeability 25ºC ($L \cdot m^{-2} h^{-1} \cdot bar^{-1}$)	42.61	60.37	106.17
Maximum operating temperature (ºC)	95	95	95
pH range	0-14	0-14	0-14

6.1.2.3. Experimental set-up

A VF-S11 UF plant (supplied by Orelis, France) was used to perform the fouling and cleaning experiments. It consisted of a 10 L stainless steel feed tank, a variable speed volumetric pump to control de crossflow velocity of each step, two manometers to measure the pressure drop across the membrane module, a temperature regulating system and a scale (0.001 g accuracy) to gravimetrically determine the permeate flux. This experimental set-up was described elsewhere (Corbatón-Báguena *et al.*, 2014).

All the experiments were performed in total recirculation mode, except in the case of the rinsing step. Operating conditions during the fouling experiments were a transmembrane pressure of 2 bar, a crossflow velocity of 2 $m \cdot s^{-1}$ and a temperature of 25 ºC. The duration of the tests was 3 h. These experimental conditions were selected according to previous studies on whey and protein ultrafiltration (Corbatón-Báguena *et al.*, 2014; Matzinos and Álvarez, 2002).

6.1.2.4. Experimental procedure

Fouling experiments

Permeate flux, hydraulic resistance and rejection were measured during the fouling process to ensure that the values obtained were reproducible in all runs. Each fouling experiment was repeated a minimum of 10 times.

BSA rejection coefficient (Eq. 26) was calculated by measuring the permeate BSA concentration during the fouling tests. Measurements were performed by an UV-visible spectrophotometer (Hewlett-Packard 8453) at the wavelength corresponding with the maximum of BSA absorbance (278 mn).

$$Rejection(\%) = \left(1 - \frac{C_p}{C_b}\right) \cdot 100 \qquad \text{Eq. 26}$$

In Eq. 1 C_b is the BSA concentration in the feed solution (1 % (w/w)) and C_p is the permeate BSA concentration.

The hydraulic resistance (R) was determined by means of Darcy's law (Eq. 27) at the end of each fouling run.

$$J = \frac{\Delta P}{\mu \cdot R} \qquad \text{Eq. 27}$$

where J is the permeate flux, ΔP is the transmembrane pressure, R is the total hydraulic resistance and μ is the feed solution viscosity.

Rinsing and cleaning experiments

After the fouling experiments, a washing step with deionized water prior to membrane cleaning (first rinsing) was performed to remove the reversible fouling from the membrane. Then, a cleaning step with NaCl solutions that allows the removal of the irreversible fouling was

carried out. After the cleaning procedure, another rinsing step (second rinsing) with deionized water can be performed in order to remove the remaining loose foulant matter from the membrane surface and the cleaning agent molecules.

Cleaning experiments were performed at a transmembrane pressure of 1 bar, different crossflow velocities (1.2, 1.69, 2.18, 2.68, 3.19 and 4.2 $m \cdot s^{-1}$), five NaCl concentrations (0, 2.5, 5, 7.5 and 10 mM) and three temperatures (25, 37.5 and 50 º C). The pH of all the NaCl solutions ranged from 6.8 to 7. Each cleaning procedure was performed in duplicate. Before and after the cleaning step the membranes were rinsed at 25 ºC and the same transmembrane pressure and crossflow velocity as the cleaning step. During the rinsing and cleaning steps, low transmembrane pressure (1 bar) favours the relaxation of the compressible fouling layer formed in the fouling step and its removal (Blanpain-Avet *et al.*, 2009).

The steps of cleaning and rinsing ended when the permeate flux and the hydraulic resistance of each step remained constant with time. The duration of the rinsing steps was 45 minutes, while the duration of the cleaning step ranged from 70 to 80 minutes.

After the last rinsing step, if the initial permeability conditions of the membranes were not recovered, membranes were cleaned with alkaline solutions. Polymeric membranes (5 and 30 kDa) were cleaned with NaOH aqueous solutions at 45 ºC and a pH of 11. The 15 kDa membrane was cleaned with 250 ppm NaClO aqueous solutions at a pH of 11. These cleaning procedures were

recommended by the manufacturers to restore the membrane permselectivity properties.

6.1.2.5. Evaluation of membrane cleanliness

Daufin *et al.* (2001) and Matzinos and Álvarez (2002) developed a method to calculate the efficiency of rinsing and cleaning protocols. In these works, membranes were cleaned with NaOH solutions and the hydraulic resistance of the membrane after each step (fouling, first rinsing, cleaning and second rinsing) was determined by means of Darcy's law. These authors proposed an equation to evaluate the efficiency of the first rinsing to restore the membrane permeability. To evaluate the cleaning efficiency of the entire cleaning protocol to restore the initial membrane permeability, a similar equation (Eq. 28) was used (Daufin *et al.*, 2001; Matzinos and Álvarez, 2002; Muthukumaran *et al.*, 2007):

$$HCE = \frac{R_f - R_{r2}}{R_f - R_m} \cdot 100 \qquad \text{Eq. 28}$$

where *HCE* is the hydraulic cleaning efficiency, R_f is the fouling resistance, R_m is the resistance of the new membrane and R_{r2} is the hydraulic resistance after the second rinsing.

6.1.2.6. Statistical and optimization analysis

Results of the cleaning experiments were used to determine the relationship between the values of the cleaning operating conditions (temperature, T_c, NaCl concentration, C, and crossflow velocity, v) and the HCE by means of a Response Surface Methodology (RSM) analysis. This analysis was performed with the Statgraphics® software using a factorial design. After that, a Multiple Linear Regression analysis was carried out to obtain a model equation for HCE as a function of the operating conditions studied. In a first step, T_c, C, v and their interactions were considered. If a regression model coefficient had a p-value higher than 0.05, it was neglected because it was not statistically significant. Thus, a new regression analysis was performed until all the coefficients were statistically significant.

To determine the values of temperature, NaCl concentration and crossflow velocity that maximize the value of HCE for each membrane tested, an optimization method was performed with the model equations obtained in the RSM analysis. The optimization algorithm was based on the "patternsearch" function of Matlab® software, which finds the minimum of an objective function by means of a pattern search. Therefore, in this work the objective functions are the opposite functions of the model equations of HCE for each membrane. Additional parameters were included in the "patternsearch" function as the maximum value of temperature (50 ºC) and the maximum value of crossflow velocity (3.19 $m \cdot s^{-1}$ for the 5 and 30 kDa membranes and 4.2 $m \cdot s^{-1}$ for the 15 kDa

membrane), as these were the higher values tested of these operating conditions.

6.1.2.7. AFM measurements

A Multimode Atomic Force Microscope (supplied by Veeco, Santa Barbara, CA, USA) with a NanoScope V controller was used to measure membranes roughness. Samples of 5 μm × 5 μm samples were used. Roughness was obtained by means of the tapping mode of imaging and the results were presented in terms of the Root Mean Square roughness (R_q). This parameter considers the standard deviation of the surface height values in a specific area (Eq. 29) (Chung *et al.*, 2002):

$$R_q = \sqrt{\frac{\sum \left(Z_i - Z_{avg}\right)^2}{N_p}} \qquad \text{Eq. 29}$$

In this equation, N_p is the number of points in the selected area, Z_i is the height value currently measured and Z_{avg} is the average of the height values.

6.1.3. Results and discussion

The values of R_m for the membranes used in the experiments were: $9.453 \cdot 10^{12}$, $5.001 \cdot 10^{12}$ and $3.794 \cdot 10^{12}$ m^{-1}, for the membranes of 5, 15 and 30 kDa, respectively. These values were taken as a reference to calculate HCE.

6.1.3.1. Fouling experiments

Evolution of permeate flux with time during the fouling step for the 5, 15 and 30 kDa membranes is shown in Fig. 41. Among all the membranes tested, the PESH 30 kDa membrane showed the lowest flux decline (19.96 %) during the fouling step in comparison with the PES 5 kDa membrane (34.62 %) and the ceramic 15 kDa membrane (39.82 %). The reason for that is the hydrophilic nature of the 30 kDa membrane. According to Rahimpour and Madaeni (2010), the higher the hydrophilicity of the membrane surface is, the better the antifouling properties (high rejection coefficient, low permeate flux decline and low total filtration resistance) are. These authors tested the behavior of several PES membranes during the crossflow filtration of non-skim milk. Their results demonstrated that the hydrophilic PES membranes had a lower permeate flux decline (about 16 %) than the unmodified hydrophobic PES membrane (about 40 %). In addition, protein rejection was higher for the hydrophilic membranes than for the hydrophobic one. On the other hand, membrane fouling is also related to the surface roughness. When membrane roughness increases, fouling becomes more severe, because rougher surfaces favour the entrapment of foulant molecules (Evans *et al.*, 2008). This phenomenon can be observed for the membranes tested comparing permeate flux decline with the values of roughness (R_q) for each membrane tested. The highest flux decline was achieved for the 15 kDa membrane (R_q = 17.900 nm), followed by the 5 kDa membrane (R_q = 0.487 nm and hydrophobic) and the 30 kDa membrane (R_q = 1.657 nm and hydrophilic).

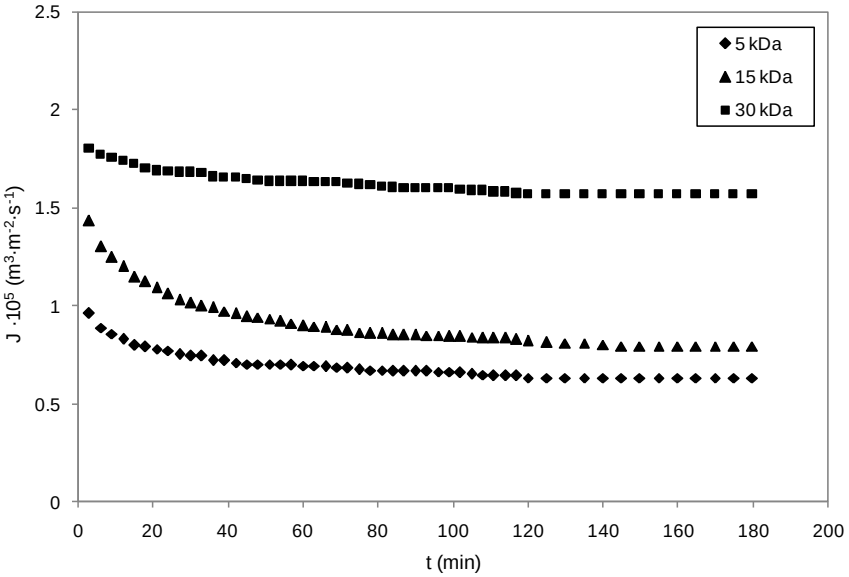

Fig. 41. *Variation of permeate flux with time during fouling experiments at 2 bar, 2 m·s^{-1} and 25 ºC*

The variation of the rejection coefficient with time for the 5, 15 and 30 kDa membranes during the fouling step can be observed in Fig. 42. After 120 min of UF, BSA rejection was very similar for all the membranes tested (99.55 %, 99.64 % and 99.61% for the 5, 15 and 30 kDa membrane, respectively). These high rejection coefficients may be due to the great difference between the size of BSA molecules and the membrane pore size. When the foulant molecule size is much higher than the membrane pore size, these molecules can be retained on the membrane surface (Schäfer *et al.*, 2000; Adikane *et al.*, 2004).

Fig. 43 shows the evolution of the hydraulic resistance during the fouling, first rinsing, cleaning and second rinsing steps. The

experimental conditions of transmembrane pressure, temperature and crossflow velocity were the same for all the membranes tested in the rinsing and cleaning steps: 1 bar, 2.18 $m \cdot s^{-1}$ and 25 ºC during the rinsing steps and 1 bar, 2.18 $m \cdot s^{-1}$ and 50 ºC in the cleaning step. However, NaCl concentration was higher for the polymeric membranes (7.5 mM) than in the case of the ceramic one (5 mM), because these were the values of NaCl concentration to obtain the highest HCE for each membrane at the experimental conditions above mentioned.

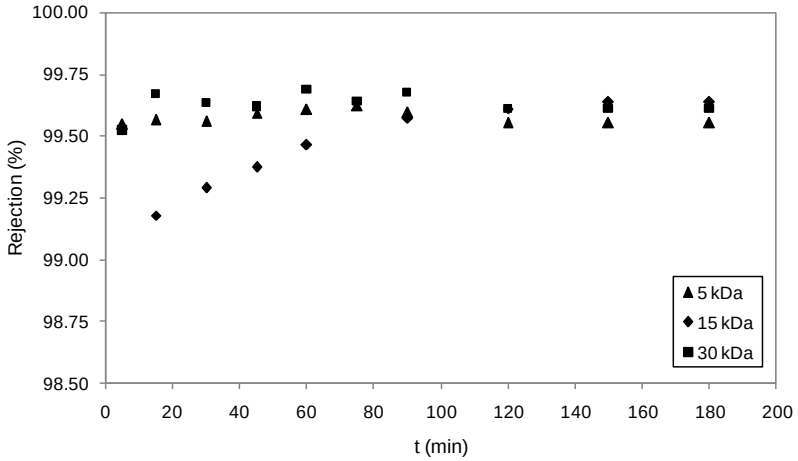

Fig. 42. *Variation of BSA rejection with time during the fouling step for each membrane*

According to Fig. 43, the HCE obtained for the 15 kDa membrane was the lowest (56.27 %), while the HCE for the 5 and 30 kDa membranes were higher than 90 % (90.98 % and 98.43 %, respectively). The reason for that is the higher roughness of the 15 kDa membrane compared with the 5 and 30 kDa membranes (R_q values of 0.487 and 1.657 nm, respectively). Therefore, higher values

of crossflow velocity were tested for the 15 kDa membrane in order to achieve greater values of HCE.

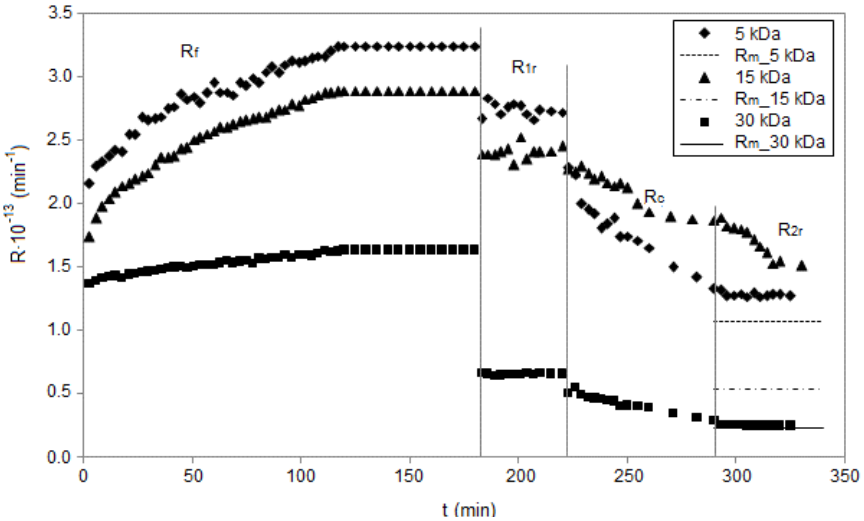

Fig. 43. *Variation of total hydraulic resistance with time for each membrane when the experimental conditions were: 25 ºC, 2 bar and 2 m·s^{-1} in the fouling step; 25 ºC, 1 bar and 2.18 m·s^{-1} in the rinsing steps; 50 ºC, 1 bar and 2.18 m·s^{-1} in the cleaning step. NaCl concentration in the cleaning solution was 7.5 mM for the 5 and 30 kDa membranes and 5 mM for the 15 kDa membrane*

6.1.3.2. Cleaning experiments

Influence of NaCl concentration

The effect of NaCl concentration on the values of HCE for each membrane was investigated. Several NaCl concentrations (0, 2.5, 5, 7.5, 10 and 12.5 mM) at two different temperatures (25 and 50 ºC) were considered. Crossflow velocity was set at 2.18 m·s^{-1} for the polymeric membranes (5 and 30 kDa) and at 4.2 m·s^{-1} for the 15 kDa

membrane. Fig. 44 shows the results of the influence of NaCl concentration on the HCE. In the case of the polymeric membranes, HCE increased as NaCl concentration increased up to 7.5 mM for the two temperatures tested. However, above this salt concentration, HCE decreased (Fig. 44a and Fig. 44c). The same effect can be observed in Fig. 44b for the ceramic membrane: HCE increased as NaCl concentration increased up to 5 mM, but a higher increase in salt concentration caused a decrease in HCE for both temperatures studied. It can also be observed that, at the same experimental conditions (50 ºC and 7.5 mM of NaCl), the highest value of HCE was obtained for the 30 kDa membrane (98.42 %). The reason for this is the hydrophilic nature of the 30 kDa membrane as well as the small roughness that this membrane presents. Thus, this membrane showed less severe fouling than that of the 5 and 15 kDa membranes as it was already commented and it can be cleaned more easily (Rahimpour and Madaeni, 2010).

Other authors (Tsumoto *et al.*, 2007; Lee and Elimelech, 2007; Cabero Cabero, 1997) observed as well that there is an optimal value of the cleaning agents to clean different membranes. They reported that the cleaning efficiency increased as their concentration increased up to this optimal concentration. However, the cleaning efficiency did not increase or it could even decrease if the cleaning agent concentration increased above the optimal value.

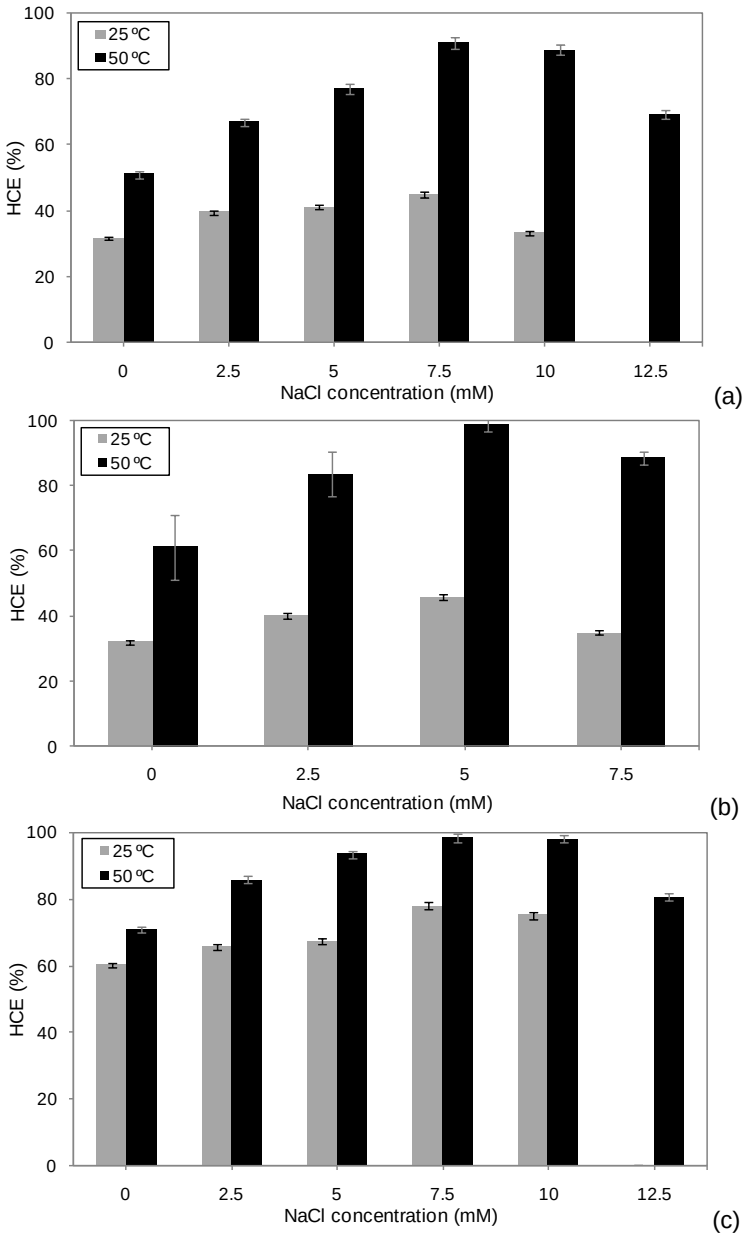

Fig. 44. *Influence of NaCl concentration on the values of HCE for the membranes of 5 kDa (a), 15 kDa (b) and 30 kDa (c), when the cleaning solution temperature is 25 ºC (grey bars) and 50 ºC (black bars) and the crossflow velocity is 2.18 m·s^{-1} for the polymeric membranes and 4.2 m·s^{-1} for the ceramic membrane*

Lee and Elimelech (2007) used NaCl solutions at different concentrations (0, 10, 25, 50, 100 and 300 mM) to clean reverse osmosis membranes fouled with alginate and calcium solutions. They achieved HCE values of about 90 % at a NaCl concentration of 50 mM. However, when NaCl concentration increased, the values of HCE remained constant. This may be due to the fact that the physical conditions for effective mass transfer were below the optimal ones (Lee and Elimelech, 2007). Cabero Cabero (1997) used conventional cleaning agents (alkaline and detergent aqueous solutions) to clean a ceramic UF membrane fouled with whey protein concentrate solutions. This author reported that fouling and cleaning mechanisms may become competitive and that the cleaning agent molecules can be accumulated on the membrane surface or inside its pores.

In addition, Tsumoto *et al.* (2007) studied the effect of several salt concentrations on the surface tension. At low salt concentrations, the surface tension decreases as salt concentration increases, but the surface tension increases linearly with concentration at high salt concentrations. They also demonstrated that the salting-in effects of saline solutions are enhanced with a decrease in the surface tension. Thus, the salting-in effects of NaCl solutions are better observed at low salt concentrations.

Influence of cleaning solution temperature

Cleaning experiments were performed at three temperatures (25, 37.5 and 50 ºC) and two different NaCl concentrations and crossflow

velocities (7.5 mM and 2.18 $m \cdot s^{-1}$ for the polymeric membranes and 5 mM and 4.2 $m \cdot s^{-1}$ for the ceramic membrane) to investigate the effect of the cleaning solution temperature on HCE for each membrane tested. The results obtained are shown in Fig. 45.

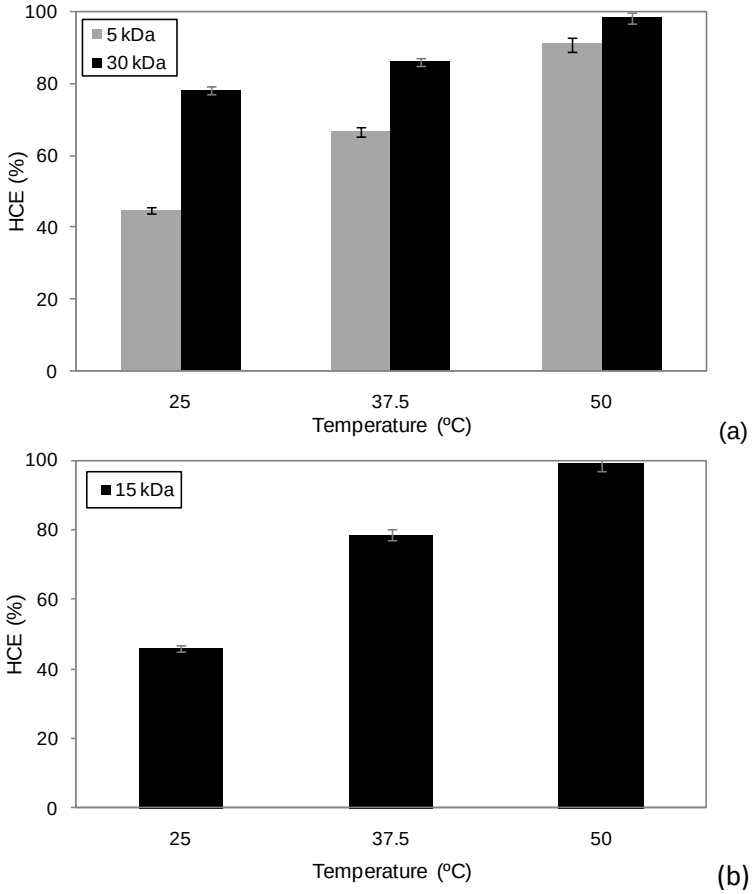

Fig. 45. *Influence of temperature on the values of HCE for the membranes of: (a) 5 kDa (grey bars) and 30 kDa (black bars) at 2.18 $m \cdot s^{-1}$ and a NaCl concentration of 7.5 mM, and (b) 15 kDa at 4.2 $m \cdot s^{-1}$ and a NaCl concentration of 5 mM*

As it can be observed, HCE increases as cleaning solution temperature increases for all the membranes tested. The highest HCE values (90.98 %, 99.05 % and 98.43 %) were achieved at the highest temperature tested (50 ºC) for the membranes of 5, 15 and 30 kDa respectively. Some authors related the surface tension of a saline solution to the temperature (Ali *et al.*, 2008; Shah *et al.*, 2013). As temperature increases, the hydrophilic ions are adsorbed from the air/water surface and thus, the surface tension of the saline solution decreases (Matubayasi and Yoshikawa, 2007).

As it was explained in section “Influence of NaCl concentration”, the lower the surface tension is, the more enhanced the salting-in effects are (Tsumoto *et al.*, 2007). On the other hand, temperatures up to 50 ºC increase protein solubility and can weaken the structural stability of the fouling layer, swelling it and favouring its removal from the membrane surface (Pelegrine and Gasparetto, 2005). The rate of foulant molecules transferred from the membrane surface to the feed solution also increases when the cleaning solution temperature increases, due to the increase in the diffusivity coefficient as temperature rises. Moreover, the rate of the interaction between the salt and the deposited proteins may be increased by an increase in temperature (Lee and Elimelech, 2007). For all these reasons, the highest temperature tested (50 ºC) is the most convenient temperature to perform the cleaning process when the membranes are fouled with BSA and $CaCl_2$ solutions.

Influence of crossflow velocity

Fig. 46 shows the variation of HCE with crossflow velocity for all the membranes tested.

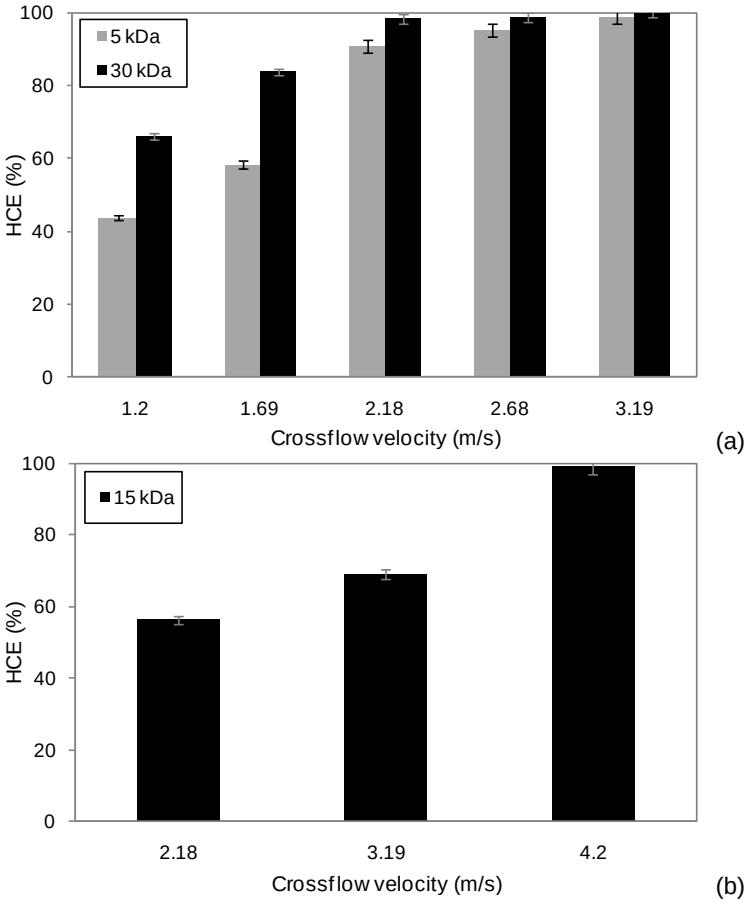

Fig. 46. *Influence of crossflow velocity on the values of HCE for the membranes of: (a) 5 kDa (grey bars) and 30 kDa (black bars) at 50 ºC and a NaCl concentration of 7.5 mM, and (b) 15 kDa at 50 ºC and a NaCl concentration of 5 mM*

The values of NaCl concentration and temperature that were selected to study the influence of the crossflow velocity on HCE were the ones

at which the highest values of HCE were obtained. These conditions were a NaCl concentration of 7.5 mM and 50 ºC for the polymeric membranes and a NaCl concentration of 5 mM and 50 ºC for the ceramic membrane. In the case of the 5 and 30 kDa membranes (Fig. 46a), lower values of crossflow velocity were tested (1.2 and 1.69 $m \cdot s^{-1}$), due to the lower roughness of these membranes compared with the ceramic one.

Fig. 46 shows that when crossflow velocity increases, HCE increases. For all the membranes tested, values of HCE near 100 % were achieved at the highest crossflow velocity tested (3.19 $m \cdot s^{-1}$ for the 5 and 30 kDa membranes and 4.2 $m \cdot s^{-1}$ for the 15 kDa membrane). As the crossflow velocity increases, the shear force increases as well favouring the removal of foulant molecules from the membrane surface (Daniş and Keskinler, 2009; Smith *et al.*, 2006; Choi *et al.*, 2005).

6.1.3.3. Statistical and optimization analysis

The influence of the operating conditions (temperature, NaCl concentration and crossflow velocity) on the values of HCE was evaluated by means of statistical (RSM and Multiple Linear Regression) and optimization (pattern search algorithm) analysis.

The effect of temperature and NaCl concentration on HCE for the 5, 15 and 30 kDa membranes is shown in Fig. 47. Light grey and white colours in the lower left corner of the surface contours represented

the most unfavourable conditions to perform the cleaning procedure. These conditions corresponded to the lowest temperature (25 ºC) and NaCl concentration (0 mM) tested. On the other hand, the highest values of HCE (higher than 90 %) were achieved at temperatures higher than 46-50 ºC and NaCl concentrations ranging from 7.5 to 10 mM for the 5 and 30 kDa membranes and from 4.5 to 5 mM in the case of the 15 kDa membrane. These experimental conditions are coloured in black in Fig. 47.

After the RSM analysis, a Multiple Linear Regression was performed to relate HCE with temperature, NaCl concentration and crossflow velocity. Eqs. 30, 31 and 32 show these mathematical relationships for the 5, 15 and 30 kDa membranes, respectively. The regression coefficients for each equation were 0.976, 0.970 and 0.962, respectively. Table 25 shows the results of the ANOVA.

$$HCE_5\ (\%) = a + b \cdot v + c \cdot T_c \cdot C + d \cdot T_c^2 + e \cdot C^2 + f \cdot v^2 \qquad \text{Eq. 30}$$

$$HCE_{15}\ (\%) = a + g \cdot T_c + c \cdot T_c \cdot C + e \cdot C^2 + f \cdot v^2 \qquad \text{Eq. 31}$$

$$HCE_{30}\ (\%) = a + h \cdot C + b \cdot v + d \cdot T_c^2 + e \cdot C^2 + f \cdot v^2 \qquad \text{Eq. 32}$$

In these equations, HCE_5, HCE_{15} and HCE_{30} are the hydraulic cleaning efficiencies for the membranes of 5, 15 and 30 kDa, respectively, T_c is the temperature of the cleaning solution (ºC), C is the NaCl concentration (mM), v is the crossflow velocity ($m \cdot s^{-1}$) and a, b, c, d, e, f, g and h are the estimated coefficients for each statistically significant parameter. Their estimated values are shown in Table 25.

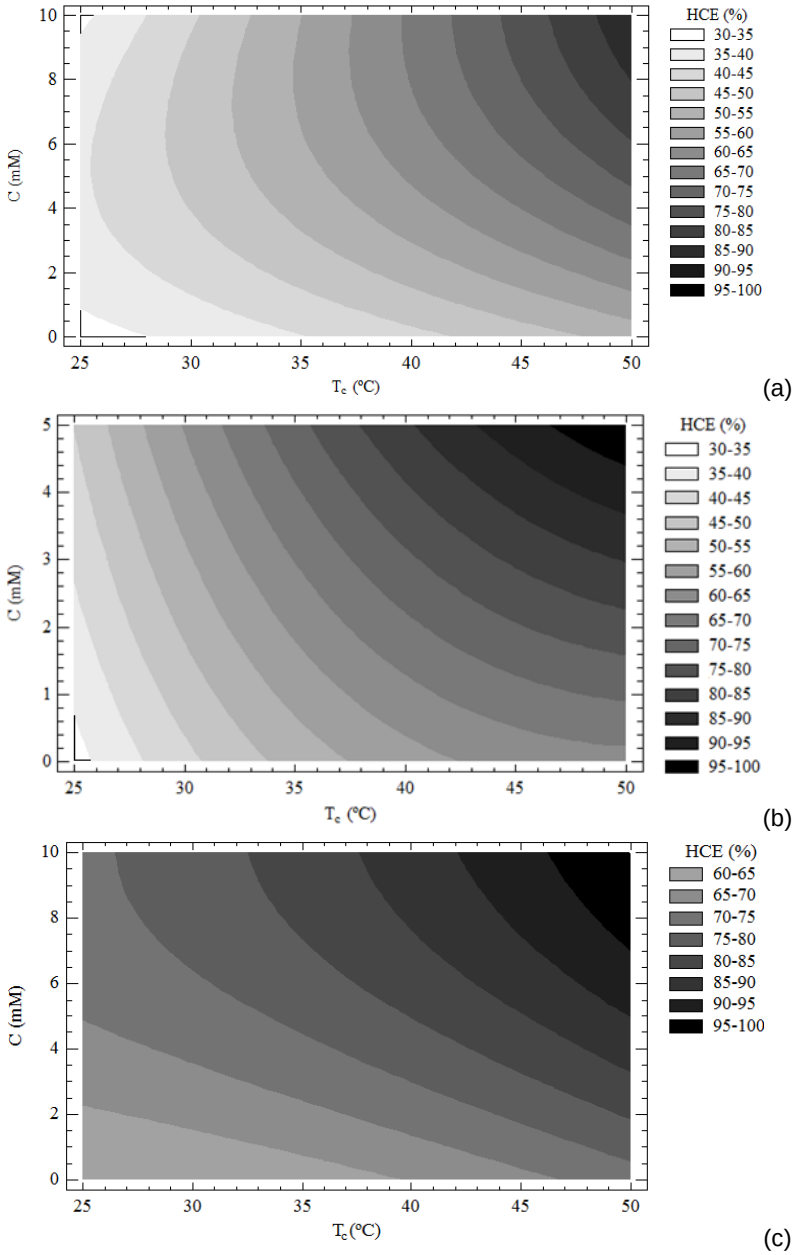

Fig. 47. *Contour plot for HCE as a function of temperature and NaCl concentration for the membranes of 5 kDa (a), 15 kDa (b) and 30 kDa (c) at a crossflow velocity of 2.18 m·s^{-1} for the polymeric membranes and 4.2 m·s^{-1} for the ceramic membrane*

Table 25. ANOVA results for the model equations that relate HCE with the operating parameters

MWCO (kDa)	Parameter	Coefficient	Estimated value	p-value
5	Constant	a (%)	-112.043	0.0000
	v	b ($m^{-1}\cdot s$)	97.093	0.0000
	$T_c \cdot C$	c ($ºC^{-1}\cdot mM^{-1}$)	0.134	0.0000
	T_c^2	d ($ºC^{-2}$)	0.010	0.0001
	C^2	e (mM^{-2})	-0.299	0.0010
	v^2	f ($m^{-2}\cdot s^2$)	-15.391	0.0007
15	Constant	a (%)	-43.946	0.0024
	T_c	g ($ºC^{-1}$)	1.088	0.0006
	$T_c \cdot C$	c ($ºC^{-1}\cdot mM^{-1}$)	0.187	0.0010
	C^2	e (mM^{-2})	-0.653	0.0054
	v^2	f ($m^{-2}\cdot s^2$)	2.968	0.0001
30	Constant	a (%)	-50.809	0.0029
	C	h (mM^{-1})	4.322	0.0001
	v	b ($m^{-1}\cdot s$)	75.194	0.0000
	T_c^2	d ($ºC^{-2}$)	0.011	0.0000
	C^2	e (mM^{-2})	-0.221	0.0095
	v^2	f ($m^{-2}\cdot s^2$)	-13.333	0.0002

The values of the coefficients of the significant parameters are in agreement with the experimental observations. Within the range of values of the operating parameters considered in this work, the equations for the polymeric membranes predicted that HCE increases with v and decreases with v^2. The values of the coefficients indicate that the increase in HCE with this variable was much more significant at low values of v, while at the largest values of v the increase in HCE was much lower. However, in the case of the ceramic membrane HCE was highly affected by v and linearly increased with this variable for all the operating conditions tested, probably due to the greater roughness of this membrane. The model equations predicted as well that HCE was highly affected by T_c and it significantly increased with

this variable for all the membranes. Regarding the effect of NaCl concentration on HCE, the model equations predicted that HCE increased with *C* and decreased with C^2. This indicates that at low values of NaCl concentration HCE increases with this variable up to an optimum concentration and a further increase in NaCl concentration caused a decrease in HCE. For some of the membranes there was an interaction between concentration and temperature, which indicates that the effect of concentration on HCE is greater at higher NaCl concentrations and vice versa.

Results of the optimization analysis based on the "patternsearch" function of Matlab® are shown in Table 26. According to them, the optimal cleaning solution temperature was 50 ºC for all the membranes tested. Optimal values of crossflow velocity and NaCl concentration were: 3.15 $m \cdot s^{-1}$ and 10 mM for the 5 kDa membrane, 4.2 $m \cdot s^{-1}$ and 7.17 mM for the 15 kDa membrane and 2.82 $m \cdot s^{-1}$ and 9.76 mM for the 30 kDa membrane.

Table 26. Optimal values of the operating parameters obtained by means of a pattern-search algorithm

MWCO (kDa)	T_c (ºC)	C (mM)	v ($m \cdot s^{-1}$)
5	50	10.00	3.15
15	50	7.17	4.20
30	50	9.76	2.82

6.1.4. Conclusions

- Three different ultrafiltration membranes of 5, 15 and 30 kDa that had been previously fouled with whey model solutions

consisting of BSA (1 % w/w) and $CaCl_2$ (0.06 % w/w in calcium) were effectively cleaned with NaCl solutions. NaCl was effective as a cleaning agent at the experimental conditions tested due to the salting-in effect of this salt.

- An increase in temperature and crossflow velocity resulted in an increase in HCE.
- There was an optimal value of NaCl concentration to clean the membranes. If NaCl concentration increased up to this optimal value, HCE increased; but a further increase in NaCl concentration caused a decrease in the values of HCE.
- The optimal operating conditions that resulted in the maximum values of HCE (about 100 %) were: a temperature of 50 ºC for all the membranes, a crossflow velocity of 3.15 $m \cdot s^{-1}$ and a NaCl concentration of 10 mM for the 5 kDa membrane, a crossflow velocity of 4.2 $m \cdot s^{-1}$ and NaCl concentration of 7.17 mM for the 15 kDa membrane and a crossflow velocity of 2.82 $m \cdot s^{-1}$ and a NaCl concentration of 9.76 mM for the 30 kDa membrane.
- Mathematical relationships between HCE and the operating conditions were determined for all the membranes considered using a multiple linear regression analysis.

Acknowledgements

The authors of this work wish to gratefully acknowledge the financial support from the Spanish Ministry of Science and Innovation through the project CTM2010-20186 and the Generalitat Valenciana through

the program “Ayudas para la realización de proyectos I+D para grupos de investigación emergentes GV/2013”.

Nomenclature

List of symbols

a	Model equation coefficient (%)
b	Model equation coefficient ($m^{-1}\cdot s$)
c	Model equation coefficient ($ºC^{-1}\cdot mM^{-1}$)
C	NaCl concentration (mM)
C_b	BSA concentration in the feed solution ($g\cdot L^{-1}$)
C_p	BSA concentration in the permeate ($g\cdot L^{-1}$)
d	Model equation coefficient ($ºC^{-2}$)
e	Model equation coefficient (mM^{-2})
f	Model equation coefficient ($m^{-2}\cdot s^2$)
g	Model equation coefficient ($ºC^{-1}$)
h	Model equation coefficient (mM^{-1})
J	Permeate flux ($m^3\cdot m^{-2}\cdot s^{-1}$)
N_p	Number of points within the given area (dimensionless)
ΔP	Transmembrane pressure (bar)
R	Total hydraulic resistance (m^{-1})
R_m	Resistance of the new membrane (m^{-1})
R_f	Resistance after the fouling step (m^{-1})
R_{r1}	Resistance after the first rinsing step (m^{-1})
R_c	Resistance after the cleaning step (m^{-1})
R_{r2}	Resistance after the second rinsing step (m^{-1})

t	Filtration time (s)
T_c	Temperature of the cleaning solution (ºC)
v	Crossflow velocity ($m \cdot s^{-1}$)
Z_i	Value of height currently measured (nm)
Z_{avg}	Average of the height values of the sample (nm)

Greek letters

μ	Feed solution viscosity ($kg \cdot m^{-1} \cdot s^{-1}$)

Abbreviations

AFM	Atomic force microscopy
BSA	Bovine serum albumin
HCE	Hydraulic cleaning efficiency
HRE	Hydraulic rinsing efficiency
MWCO	Molecular weight cut off
PES	Polyethersulfone
pI	Isoelectric point
RSM	Response surface methodology
UF	Ultrafiltration

6.2. BIBLIOGRAFÍA

ADAMS M.C., ZULEWSKA J. y BARBANO D.M. (2013). "Effect of annatto addition and bleaching treatments on ultrafiltration flux during production of 80 % whey protein concentrate and 80 % serum protein concentrate" en *Journal of Dairy Science*, vol. 96, p. 2035-2047.

ADIKANE H.V., THAKAR D.M. y NENE S.N. (2004). "Optimisation of colour and sugar rejection of black liquor using membranes" en *Separation and Purification Technology*, vol. 36, p. 229-234.

AFONSO A., MIRANDA J.M. y CAMPOS J.B.L.M. (2009). "Numerical study of BSA ultrafiltration in the limiting flux regime – effect of variable physical properties" en *Desalination*, vol. 249, p. 1139-1150.

ALI K., SHAH A-u-H.A. y BILAL S. (2008). "Thermodynamic parameters of surface formation of some aqueous salt solutions" en *Colloids and Surfaces A: Physicochemical Engineering Aspects*, vol. 330, p. 28-34.

ALMÉCIJA M.C. *et al.* (2009a). "Influence of the cleaning temperature on the permeability of ceramic membranes" en *Desalination*, vol. 245, p. 708-713.

ALMÉCIJA M.C. *et al.* (2009b). "Analysis of cleaning protocols in ceramic membranes by liquid-liquid displacement porosimetry" en *Desalination*, vol. 245, p. 541-545.

ANG W.S. y ELIMELECH M. (2007). "Protein (BSA) fouling of reverse osmosis membranes: Implications for wastewater reclamation" en *Journal of Membrane Science*, vol. 296, p. 83-92.

BLANPAIN-AVET P., MIGDAL J.F. y BÉNÉZECH T. (2009). "Chemical cleaning of a tubular ceramic microfiltration membrane

fouled with a whey protein concentrate suspension – characterization of hydraulic and chemical cleanliness" en *Journal of Membrane Science*, vol. 337, p. 153-174.

CABERO CABERO M.L. (1997). *Limpieza química de membranas inorgánicas: Aplicación al tratamiento de lactosuero.* Tesis Doctoral. Oviedo: Universidad de Oviedo, <http://hdl.handle.net/10651/13566>.

CHOI H. *et al.* (2005). "Influence of cross-flow velocity on membrane performance during filtration of biological suspension" en *Journal of Membrane Science*, vol. 248, p. 189-199.

CHUNG T.-S. *et al.* (2002). "Visualization of the effect of die shear rate on the outer surface morphology of ultrafiltration membranes by AFM" en *Journal of Membrane Science*, vol. 196, p. 251-266.

CORBATÓN-BÁGUENA M.J., ÁLVAREZ-BLANCO S. y VINCENT-VELA M.C. (2014). "Cleaning of ultrafiltration membranes fouled with BSA by means of saline solutions" en *Separation and Purification Technology*, vol. 125, p. 1-10.

DANIŞ Ü. y KESKINLER B. (2009). "Chromate removal from wastewater using micellar enhanced crossflow filtration: Effect of transmembrane pressure and crossflow velocity" en *Desalination*, vol. 249, p. 1356-1364.

DAUFIN G. *et al.* (2001). "Recent and emerging applications of membrane processes in the food and dairy industry" en *Food and Bioproducts Processing*, vol. 79, p. 89-102.

EVANS P.J. *et al.* (2008). "The influence of hydrophobicity, roughness and charge upon ultrafiltration membranes for black tea liquor clarification" en *Journal of Membrane Science*, vol. 313, p. 250-262.

HOFMEISTER F. (1888). “Zur lehre von der wirkung der salze” en *Archiv for Experimentelle Pathologie und Pharmakologie*, vol. 24, p. 247.

KAZEMIMOGHADAM M. y MOHAMMADI T. (2007). “Chemical cleaning of ultrafiltration membranes in the milk industry” en *Desalination*, vol. 204, p. 213-218.

LEE S. y ELIMELECH M. (2007). “Salt cleaning of organic-fouled reverse osmosis membranes” en *Water Research*, vol. 41, p. 1134-1142.

MATUBAYASI N. y YOSHIKAWA R. (2007). “Thermodynamic quantities of surface formation of aqueous electrolyte solutions VII. Aqueous solution of alkali metal nitrates $LiNO_3$, $NaNO_3$ and KNO_3” en *Journal of Colloid Interface Science*, vol. 315, p. 597-600.

MATZINOS P. y ÁLVAREZ R. (2002). “Effect of ionic strength on rinsing and alkaline cleaning of ultrafiltration inorganic membranes fouled with whey proteins” en *Journal of Membrane Science*, vol. 208, p. 23-20.

MO H., TAY K.G. y NG H.Y. (2008). “Fouling of reverse osmosis membrane by protein (BSA): Effects of pH, calcium, magnesium, ionic strength and temperature” en *Journal of Membrane Science*, vol. 315, p. 28-35.

MUTHUKUMARAN S. *et al.* (2004). “The use of ultrasonic cleaning for ultrafiltration membranes in the dairy industry” en *Separation and Purification Technology*, vol. 39, p. 99-107.

MUTHUKUMARAN S. *et al.* (2007). “The application of ultrasound to dairy ultrafiltration: the influence of operating conditions” en *Journal of Food Engineering*, vol. 81, p. 364-373.

NUCCI N.V. y VANDERKOOI J.M. (2008). "Effects of salts of the Hofmeister series on the hydrogen bond network of water" en *Journal of Molecular Liquids*, vol. 143, p. 160-170.

OGUNBIYI O.O., MILES N.J. y HILAL N. (2008). "The effects of performance and cleaning cycles of new tubular ceramic microfiltration membrane fouled with a model yeast suspension" en *Desalination*, vol. 220, p. 273-289.

PELEGRINE D.H.G. y GASPARETTO C.A. (2005). "Whey proteins solubility as function of temperature and pH" en *Lebensmittel-Wissenschaft und-Technologie*, vol. 38, p. 77-80.

RAHIMPOUR A. y MADAENI S.S. (2010). "Improvement of performance and surface properties of nano-porous polyethersulfone (PES) membrane using hydrophilic monomers as additives in the casting solution" en *Journal of Membrane Science*, vol. 360, p. 371-379.

SCHÄFER A.I., FANE A.G. y WAITE T.D. (2000). "Fouling effects on rejection in the membrane filtration of natural waters" en *Desalination*, vol. 131, p. 215-224.

SHAH A-u-H.A., ALI K. y BILAL S. (2013). "Surface tension, surface excess concentration, enthalpy and entropy of surface formation of aqueous salt solutions" en *Colloids and Surfaces A: Physicochemical Engineering Aspects*, vol. 417, p. 183-190.

SMITH P.J. *et al.* (2006). "Productivity enhancement in a cross-flow ultrafiltration membrane system through automated de-clogging operations" en *Journal of Membrane Science*, vol. 280, p. 82-88.

SUTTIPRASIT P., KRISDHASIMA V. y MCGUIRE J. (1992). "The surface activity of α-lactabumin, β-lactoglobulin and bovine serum

albumin" en *Journal of Colloid and Interface Science*, vol. 154, p. 316-326.

TARAZAGA C.C., CAMPDERRÓS M.E. y PÉREZ-PADILLA A. (2006). "Physical cleaning by means of electric field in the ultrafiltration of a biological solution" en *Journal of Membrane Science*, vol. 278-p. 219-224.

TSUMOTO K. *et al.* (2007). "Effects of salts on protein-surface interactions: Applications for column chromatography" en *Journal of Pharmaceutical Science*, vol. 96, p. 1677-1690.

WANG Y-N. y TANG C.Y. (2011). "Protein fouling of nanofiltration, reverse osmosis, and ultrafiltration membranes-The role of hydrodynamic conditions, solution chemistry and membrane properties" en *Journal of Membrane Science,* vol. 376, p. 275-282.

ZHANG J. (2012). "Protein-protein interactions in salt solutions" en Cai W. y Hong H. *Protein-protein interactions – Computational and experimental tools*. Intech.

CAPÍTULO VII

Limpieza mediante disoluciones salinas de membranas ensuciadas con disoluciones de lactosuero

7.1. LIMPIEZA DE MEMBRANAS DE ULTRAFILTRACIÓN ENSUCIADAS CON CONCENTRADOS DE PROTEÍNAS DE LACTOSUERO

A continuación se presenta una adaptación al formato de la Tesis Doctoral del artículo titulado "Utilization of NaCl solutions to clean ultrafiltration membranes fouled by whey protein concentrates", publicado en la revista Separation and Purification Technology. En él se ensuciaron tres membranas de UF de diferentes materiales y MWCO (5, 15 y 30 kDa) con disoluciones de WPC a diferentes concentraciones (22.2, 33.3 y 150.0 $g \cdot L^{-1}$). Además, se investigó la influencia de las condiciones de operación durante la etapa de limpieza sobre la eficacia de dicho proceso. Estas condiciones fueron la concentración de NaCl, la temperatura y la velocidad tangencial de la disolución de limpieza. Los datos bibliográficos del artículo se destacan a continuación:

Autores: *M.-J. Corbatón-Báguena, S. Álvarez-Blanco, M.-C. Vincent-Vela, J. Lora-García*

Título: *Utilization of NaCl solutions to clean ultrafiltration membranes fouled by whey protein concentrates*

Editorial: *Elsevier*

Revista: *Separation and Purification Technology*

año: 2015 vol. 150 p. 95-101

Doi: *http://dx.doi.org/10.1016/j.seppur.2015.06.039*

Utilization of NaCl solutions to clean ultrafiltration membranes fouled by whey protein concentrates

María-José Corbatón-Báguena, Silvia Álvarez-Blanco*, María-Cinta Vincent-Vela, Jaime Lora-García

Department of Chemical and Nuclear Engineering, Universitat Politècnica de València, C/Camino de Vera s/n 46022 Valencia, Spain

*Corresponding author: sialvare@iqn.upv.es
Tel: +34963879630 (Ext.: 796383)
Fax: +34963877639 (Ext.: 77639)

Abstract

In this work, whey protein concentrate (WPC) solutions at different concentrations (22.2, 33.3 and 150 $g \cdot L^{-1}$) were used to foul three ultrafiltration (UF) membranes of different materials and molecular weight cut-offs (MWCOs): a polyethersulfone (PES) membrane of 5 kDa, a ceramic ZrO_2-TiO_2 membrane of 15 kDa and a permanently hydrophilic polyethersulfone (PESH) membrane of 30 kDa. NaCl solutions at different salt concentrations, temperatures and crossflow velocities were used to clean the UF membranes tested. The cleaning efficiency was related to the MWCO, membrane material and operating conditions during fouling and cleaning steps. NaCl solutions were able to completely clean the membranes fouled with the WPC

solutions at the lowest concentration tested. As WPC concentration increased, the hydraulic cleaning efficiency (HCE) decreased. The results demonstrated that an increase in temperature and crossflow velocity of the cleaning solution caused an increase in the HCE. Regarding NaCl concentration, the HCE increased up to an optimal value. As the concentration was greater than this value, the cleaning efficiency decreased. In addition, an equation that correlates the cleaning efficiency to the operating parameters studied in this work (temperature, NaCl concentration, crossflow velocity in the cleaning procedure and WPC concentration during the fouling step) was developed and then, an optimization analysis was performed to determine the values of the parameters that lead to a 100 % cleaning efficiency.

Keywords: Ultrafiltration; membrane cleaning; whey protein concentrate; NaCl solutions

7.1.1. Introduction

Nowadays, whey is one of the most important by-products in dairy industries during cheese and casein production: 8-9 kg of whey are produced per each 1-2 kg of cheese (Baldasso *et al.*, 2011). Whey is rich in proteins, lactose, minerals and water-soluble vitamins. Thus, it is considered a valuable product for applications in food and pharmaceutical industries rather than a wastewater (Sanmartín *et al.*, 2012). Among whey components, proteins have a high nutritional and functional value due to their high content of essential amino acids and

their gelatinization and emulsifying properties (Wit, 1998). Because of the interest of its protein fraction, whey is usually transformed to obtain whey protein concentrates (WPC) with a protein content of 35-80 % w/w in dry basis (31.23 – 234.3 $g \cdot L^{-1}$) and whey protein isolates (WPI) with more than 85 % w/w in dry basis (237.1 $g \cdot L^{-1}$) of protein content (Sanmartín *et al.*, 2012). The manufacture of these products involves different processes: ultrafiltration (UF), diafiltration, concentration by evaporation under reduced pressure and spray drying (Hussain *et al*, 2012). However, during the UF process, the production efficiency is limited because of membrane fouling, which results in a decline in permeate flux. As proteins and minerals are the main foulants in whey and WPC solutions, several pretreatments can be performed in order to increase protein solubility and limit calcium phosphate precipitation and calcium bridging during the UF process (Adams *et al*., 2013).

As pretreatments are not enough to avoid membrane fouling, membranes have to be cleaned with conventional and non conventional techniques. In dairy industries, conventional cleaning agents as alkalis, acids and disinfectants are used in several washing steps (Ogunbiyi *et al.*, 2008; Kazemimoghadam and Mohammadi, 2007; Almécija *et al*., 2009a; Almécija *et al*., 2009b). However, in some cases, membrane lifetime may be reduced and a negative impact on the environment may be caused when these aggressive agents are used. To overcome these problems, some non conventional cleaning techniques have been developed in the last years (Tarazaga *et al.*, 2006; Muthukumaran *et al.*, 2004; Argüello *et al.*, 2003). For instance, the use of enzymes as cleaning agents has

been reported by other authors as an effective alternative technique on membranes used for whey treatment (Argüello *et al.*, 2003; Argüello *et al.*, 2005). The main advantage of this technique is the utilization of mild pH values, so that the membranes may not be affected by acids and/or alkalis. Another innovative cleaning protocol is based on the utilization of saline solutions. Some authors (Hofmeister, 1888; Tsumoto *et al.*, 2007; Nucci and Vanderkooi, 2008) have reported the effect of cations and anions on the interactions among proteins. According to their capability to increase or decrease protein solubility, Hofmeister (1888) proposed a ranking of salts. Based on the Hofmeister series, Tsumoto *et al.* (2007) reported that some salts (such as NaCl) caused an increase in protein solubility (salting-in effect) while other salts (such as Na_2SO_4) decreased it (salting-out effect). Nucci and Vanderkooi (2008) studied the ability of divalent and monovalent cations to precipitate proteins. They demonstrated that calcium is one of the most salting-out cations. This is in a good agreement with other works about the influence of calcium on protein bridging and membrane fouling (Almécija *et al.*, 2009; Ang and Elimelech, 2007).

However, only a few papers are focused on the utilization of salts as membrane cleaning agents. Lee and Elimelech (2007) tested NaCl solutions at different concentrations to clean reverse osmosis membranes fouled with alginate and calcium solutions. They achieved values of cleaning efficiency of about 90 % when a salt concentration of 50 mM was used. In a previous work, Corbatón-Báguena *et al.* (2014a) studied the influence of several salts (Na_2SO_4, NaCl, $NaNO_3$, NH_4Cl and KCl) on the cleaning efficiency of a 15 kDa

ceramic UF membrane fouled with protein solutions. They demonstrated that chloride and nitrate salts were the most effective.

The aim of this work was to investigate the effectiveness of NaCl solutions to clean three different UF membranes fouled with WPC solutions at different concentrations. The effect of membrane material and MWCO on the effectiveness of the cleaning protocol was studied by testing a 15 kDa monotubular ceramic membrane, a 5 kDa flat- sheet polyethersulfone (PES) membrane and a 30 kDa flat-sheet permanently hydrophilic polyethersulfone (PESH) membrane. The influence of the operating conditions during the cleaning procedure (temperature, NaCl concentration and crossflow velocity) was also investigated. The best experimental cleaning conditions to achieve the highest cleaning efficiency were estimated by a statistical analysis.

7.1.2. Materials and methods

7.1.2.1. Materials

Renylat WPC solutions (Industrias Lácteas Asturianas S.A., Spain) at different concentrations (22.2, 33.3 and 150 $g \cdot L^{-1}$) were used as feed solutions during the fouling steps. WPC was supplied in powder form and it was dissolved in deionized water until the final concentration was achieved. Table 27 shows the composition of the WPC. Determination of each component in the WPC was performed as follows: total protein concentration was determined by means of the

Bradford method (Sigma Aldrich, Germany) (Bradford, 1976), lactose amount was estimated by reaction with 3,5-dinitrosalicylic acid (DNS, Sigma Aldrich, Germany) (Miller, 1959), ash content was calculated by using a muffle furnace at 540 ºC (AOAC method 930.30) (AOAC, 1930), cations concentration was determined using a "790 Personal IC" chromatograph with a Metrosep C 2 150 column (both from Metrohm, Switzerland), anions concentration was obtained by using Spectroquant chloride and phosphate testing kits (Merck Millipore, Spain) (Mak *et al.*, 2003) and fat content was measured by a MilkoScan FT120 (Gerber Instruments, Switzerland) (Chessa *et al.*, 2014). Absorbance at 595 nm was measured by means of an UV-visible spectrophotometer (Hewlett-Packard 8453).

Table 27. Composition of the commercial Renylat WPC used

Component	Weight percentage in dry basis (% w/w)
Dry matter	93.66 ± 0.95
Proteins	40.74 ± 0.79
Lactose	38.27 ± 0.49
Fat	8.14 ± 0.20
Ash	7.85 ± 0.07
Ca	0.79 ± 0.06
Na	1.21 ± 0.09
K	1.42 ± 0.02
Cl	4.07 ± 0.24
PO_4-*P*	0.37 ± 0.03

If initial membrane permeability was not completely recovered after the salt cleaning procedure, NaClO aqueous solutions (10 % w/v, Panreac, Spain) at pH 11 and 45 ºC and NaOH aqueous solutions (98 % purity, Panreac, Spain) at pH 11 and 45 ºC were used to clean

the ceramic and polymeric membranes, respectively. These conventional cleaning protocols are in accordance with those suggested by the manufacturers.

7.1.2.2. Membranes

Three different UF membranes were used to perform the experiments: a monotubular ZrO_2-TiO_2 membrane of 15 kDa (TAMI Industries, France), a flat-sheet PES membrane of 5 kDa (UP005, Microdyn Nadir, Germany) and a flat-sheet PESH membrane of 30 kDa (UH030, Microdyn Nadir, Germany). The effective area of these membranes was 35.5 cm^2 for the ceramic membrane and 100 cm^2 for the polymeric membranes. These materials and MWCOs were selected in order to study their influence on the membrane cleaning efficiency. In addition, the MWCOs selected in this work are in the range of the typical MWCOs used in the manufacture and treatment of whey and WPC (Hobman, 1992; Marella *et al.*, 2011).

7.1.2.3. Experimental set-up

Fouling and cleaning experiments were carried out in a VF-S11 UF plant (Orelis, France) with a stainless steel feed tank of 10 L. Crossflow velocity and pressure drop across the module were controlled by a variable speed volumetric pump and two manometers placed at the inlet and outlet sides of the module. Permeate flux was measured gravimetrically using a scale (0.001 g accuracy). All the experiments were performed in total recirculation mode, except the

rinsing steps. The experimental set-up was described elsewhere (Corbatón-Báguena *et al.*, 2014a).

7.1.2.4. Experimental procedure

Fouling experiments

Fouling experiments were performed in total recirculation mode at a transmembrane pressure of 2 bar, a crossflow velocity of 2 $m \cdot s^{-1}$ and a temperature of 25 ºC. In addition, different WPC concentrations were used to simulate the effect of the increase in protein concentration during the UF process. These operating conditions were selected according to the literature about whey protein UF (Corbatón-Báguena *et al.*, 2014a; Matzinos and Álvarez, 2002). Permeate flux and rejection values were measured during the fouling step to ensure the reproducibility of all the runs with each feed solution. Each fouling test was repeated a minimum of 10 times.

Protein rejection was determined by Eq. 33 for all the membranes tested.

$$Rejection(\%) = \left(1 - \frac{C_p}{C_b}\right) \cdot 100 \qquad \text{Eq. 33}$$

Where C_b is protein concentration in the WPC feed solution and C_p is protein concentration in the permeate.

Rinsing and cleaning experiments

Reversible fouling was removed from the membrane surface by rinsing the membranes with deionized water after the fouling step at a transmembrane pressure of 1 bar, different crossflow velocities (1.2-4.2 $m \cdot s^{-1}$) and 25 ºC with the permeate valve opened. Then, NaCl cleaning step was carried out to allow the removal of the irreversible fouling. Operating conditions during the cleaning step were the following: four different NaCl concentrations (0-7.5 mM), four temperatures (50-80 ºC) and the same transmembrane pressure and crossflow velocity as those considered for the rinsing step. The pH values of all the saline solutions ranged from 6.8 to 7. After the saline cleaning procedure, another washing step with deionized water was performed to completely remove the loose foulant molecules as well as the cleaning agent molecules from the membrane surface. When permeate flux achieved the steady-state value, cleaning and rinsing steps ended. Duration of these steps was 45 min for the rinsing steps and 70-80 min for the cleaning step. After the last rinsing step, a conventional chemical cleaning with alkaline solutions was performed if the initial permeability conditions were not achieved, as it was mentioned and described in the “Materials” section.

7.1.2.5. Evaluation of membrane cleanliness

The hydraulic efficiencies of the first rinsing step (HRE) and of the complete cleaning procedure (HCE), i.e. after the second rinsing step, were calculated by Eq. 34 and 35. Other authors (Daufin *et al.,* 2001;

Matzinos and Álvarez, 2002) reported equations to determine the efficiency of rinsing and cleaning steps when alkaline solutions were used to restore the initial permeability of the membranes. Their equations were based on a relation among the membrane hydraulic resistance obtained after each step (fouling, first rinsing, cleaning and second rinsing) by means of the Darcy's law. In this work, similar equations (Eqs. 34 and 35) were proposed to calculate the hydraulic rinsing and cleaning efficiencies (HRE and HCE, respectively).

$$HRE\ (\%) = \left(\frac{R_f - R_{r1}}{R_f - R_m} \right) \cdot 100 \qquad \text{Eq. 34}$$

$$HCE\ (\%) = \left(\frac{R_f - R_{r2}}{R_f - R_m} \right) \cdot 100 \qquad \text{Eq. 35}$$

Where R_f is the fouling resistance, R_{r1} is the hydraulic resistance after the first rinsing step, R_{r2} is the hydraulic resistance after the second rinsing step and R_m is the resistance of the new membrane, which were calculated by means of the Darcy's law (Corbatón-Báguena *et al.*, 2014a).

When HCE values obtained at the end of the cleaning procedure were of 100 %, the saline cleaning can substitute the conventional alkaline/acid cleaning, as the membrane permselective properties were completely restored.

7.1.3. Results and discussion

In order to calculate HCE for each membrane tested, the values of R_m were necessary. These values were: $9.453 \cdot 10^{12}$, $5.001 \cdot 10^{12}$ and $3.794 \cdot 10^{12}$ m^{-1}, for the membranes of 5, 15 and 30 kDa, respectively.

7.1.3.1. Fouling experiments

Fig. 48 shows the evolution of permeate flux with time for each membrane and feed solution tested. As it was expected, the higher the WPC concentration in the feed solution was, the lower the steady-state permeate flux was. This is due to the fact that an increase in protein concentration results in a more severe membrane fouling due to an increase in concentration polarization and adsorption phenomena as protein concentration increases. Regarding the permeate flux decline, the PESH 30 kDa membrane showed the lowest one for all the feed solutions tested compared with the other membranes. For instance, for the most severe fouling conditions (WPC concentration of 150 $g \cdot L^{-1}$), the percentage of permeate flux decline was 44.73, 56.64 and 26.84 % for the 5, 15 and 30 kDa membranes, respectively. The reason for that is the combination of low membrane surface roughness and high hydrophilicity of the PESH membrane in comparison with the PES and the ceramic membrane (Corbatón-Báguena *et al.*, 2015). According to other authors (Rahimpour and Madaeni, 2010; Evans *et al.*, 2008; García-Ivars *et al.*, 2014), both high hydrophilicity and low surface roughness result in membranes with better antifouling properties.

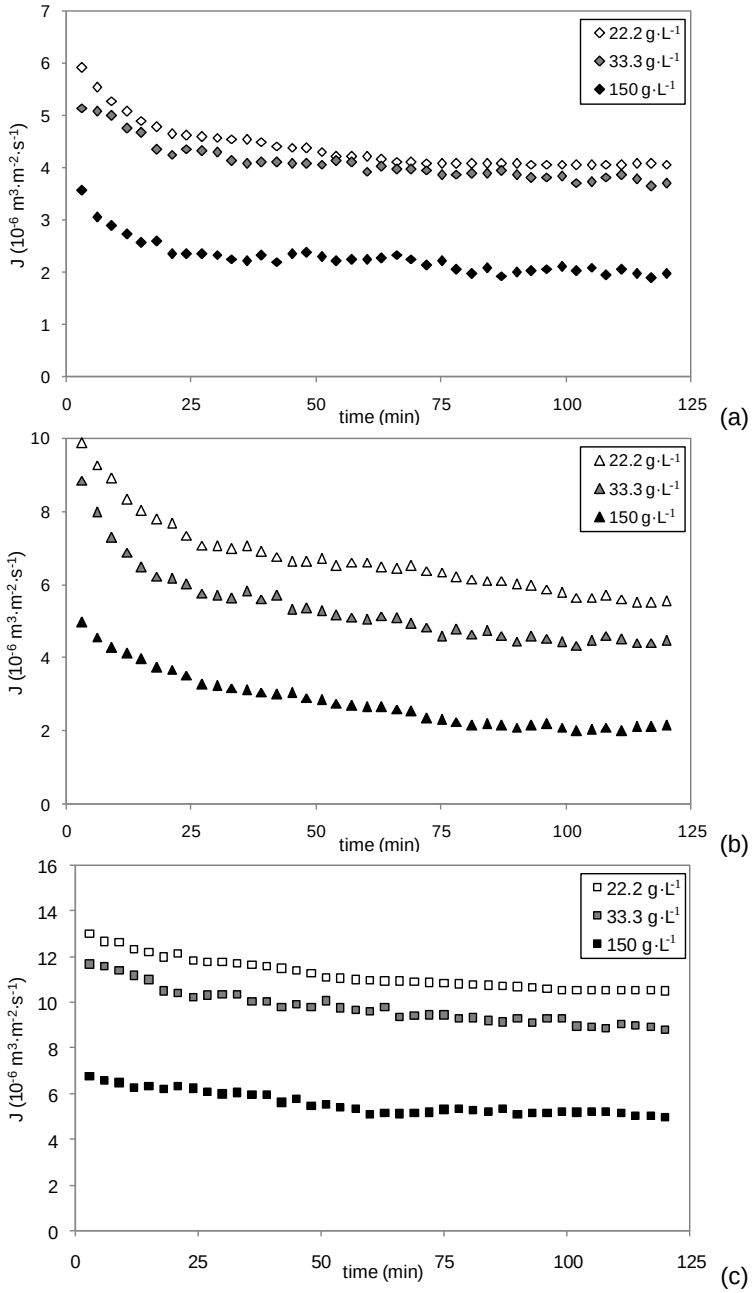

Fig. 48. *Evolution of permeate flux with time for the 5 kDa (a), 15 kDa (b) and 30 kDa (c) membranes with WPC solutions at different concentrations*

Evans *et al.* (2008) studied the influence of surface roughness and membrane hydrophobicity on the UF of black tea using membranes made of different materials. They found that fouling was more severe in the case of the rougher and more hydrophobic membranes. Rahimpour and Madaeni (2010) investigated the effect of the modification of the membrane with different hydrophilic monomers on the performance of several PES membranes during the filtration of non-skim milk. They demonstrated that, among all the modified and unmodified membranes tested, the highest protein rejection and lowest fouling resistances were obtained with the membranes that showed the most hydrophilic and smooth surfaces. García-Ivars *et al.* (2014) also tested modified and unmodified PES membranes with different hydrophilicity and surface roughness in several fouling/rinsing cycles. They obtained better performances for the more hydrophilic and less rougher membranes. All these results are in good agreement with the results obtained in this work. According to the AFM measurements for the new membranes described by the authors elsewhere (Corbatón-Báguena *et al.*, 2014a), the values of Root Mean Square roughness (R_q) were 0.487, 17.900 and 1.657 nm for the 5, 15 and 30 kDa membranes, respectively. On the other hand, while the 5 kDa membrane was hydrophobic, the 15 and 30 kDa membranes were hydrophilic. Therefore, the lowest permeate flux decline was obtained for the 30 kDa membrane, followed by the 5 and 15 kDa membranes for all the feed solutions tested.

Fig. 49 shows the changes on protein rejection values with time for all the membranes and feed solutions considered.

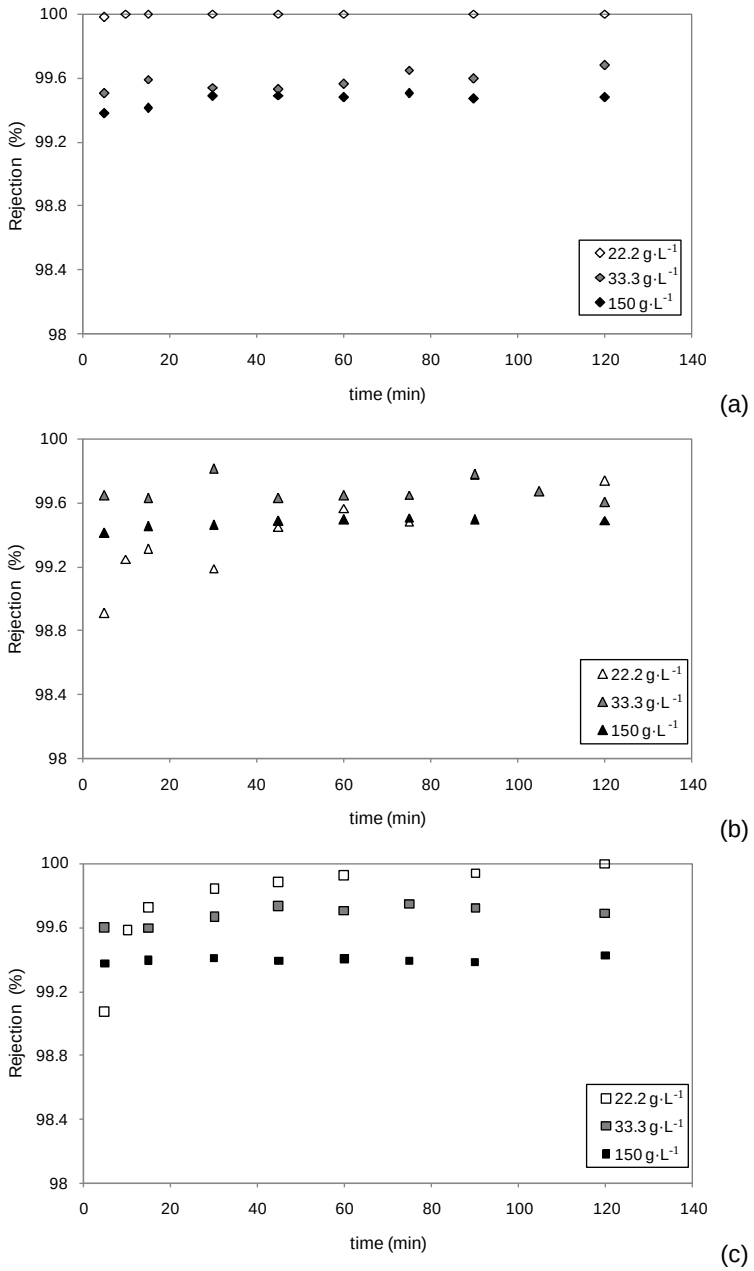

Fig. 49. *Evolution of rejection values with time for the 5 kDa (a), 15 kDa (b) and 30 kDa (c) membranes with WPC solutions at different concentrations*

As WPC concentration increased, the steady-state rejection values slightly decreased for all the membranes tested. Mathew *et al.* (2008) also studied the influence of protein concentration on the percentage of rejection. They demonstrated that an increase in protein concentration resulted in a decrease in the rejection values using multilayer membranes with the same number of bilayers.

7.1.3.2. Cleaning experiments

Effect of NaCl concentration on HCE

The influence of NaCl concentration on the effectiveness of the cleaning protocol is shown in Fig. 50. The rest of experimental conditions were set at 50 ºC and 2.18 $m \cdot s^{-1}$ (for the 5 and 30 kDa membranes) and 4.2 $m \cdot s^{-1}$ (for the 15 kDa membrane). These different crossflow velocities were selected due to the higher surface roughness of the ceramic membrane in comparison with the polymeric ones. The rougher the membrane surface was, the more severe the fouling was and thus, the highest crossflow velocity that can be achieved in the experimental set-up was selected in order to remove the foulant deposits.

As it can be observed in Fig. 50, an increase in salt concentration resulted in an increase in the values of HCE for each membrane tested when a WPC concentration of 22.2 $g \cdot L^{-1}$ was used. NaCl concentration ranged from 0 (deionized water) to 7.5 mM, according to previous studies about salt cleaning of protein fouled membranes

(Corbatón-Báguena *et al.*, 2014b), and the highest values of HCE were obtained at a NaCl concentration of 5 mM in all the cases. The efficiency of NaCl to clean membranes fouled with protein solutions was also reported in the literature. Lee and Elimelech (2007) investigated the effect of NaCl concentration on the cleaning efficiency of reverse osmosis membranes that were fouled with feed solutions containing alginate and calcium. They reported that values of cleaning efficiency of 90 % were achieved at NaCl concentrations of 50 mM due to a decrease in foulant-foulant adhesion forces caused by the salt solutions, while using higher salt concentrations (100-300 mM) did not result in higher efficiency values.

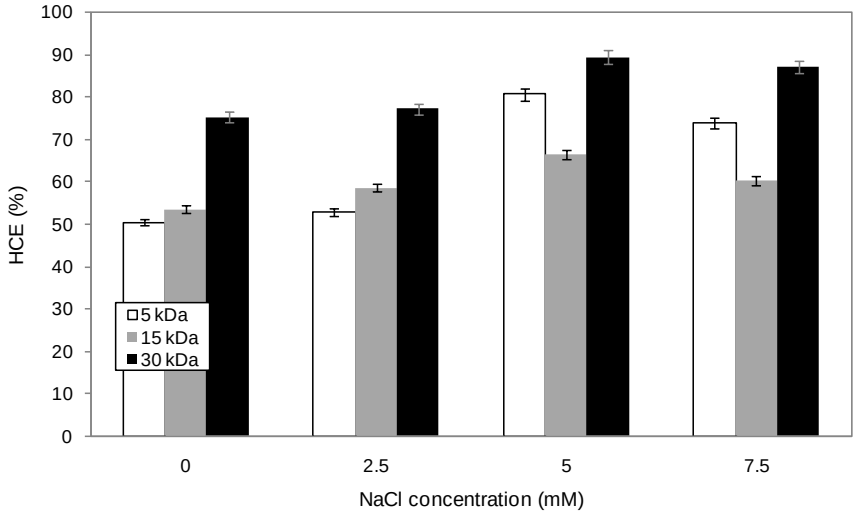

Fig. 50. *Effect of NaCl concentration on HCE (WPC concentration: 22.2 g·L^{-1}; temperature: 50 ºC; crossflow velocity: 2.18 m·s^{-1} for the 5 and 30 kDa membranes and 4.2 m·s^{-1} for the 15 kDa membrane)*

It can also be observed in Fig. 50 that a greater increase in the concentration of NaCl above 5 mM caused a decrease in HCE. This

may be due to the fact that fouling and cleaning mechanisms became competitive and the experimental conditions used did not favour the effective mass transfer of foulant molecules from the membrane surface back to the bulk solution (Cabero Cabero, 1997). In addition, other authors demonstrated the effect of salt solutions and their concentration on protein solubility. Hofmeister (1888) ranked different cations and anions depending of their ability to act as protein stabilizers. As a consequence, ions were divided into salting-in or salting-out depending on the increase or decrease in protein solubility that they caused, respectively. Based on the Hofmeister series, Tsumoto *et al.* (2007) observed that low surface tension favours the salting-in effects of salt solutions. Since surface tension decreases when salt concentration increases at low salt concentrations, the effectiveness of NaCl as a cleaning agent is enhanced at low NaCl concentrations. On the other hand, Zhang (2012) demonstrated that Cl^- can specifically bind to the protein surface and proposed a mechanism to explain why this phenomenon takes place. The law of matching water affinities states that ions with similar water affinity tend to bond each others. According to this law, Cl^- is a weakly hydrated monovalent anion and thus, it preferably binds to the positive-charged side chains of the proteins as well as the non-polar groups. As a result, Cl^- may act as a binding agent to the protein surface and facilitates their removal from the membrane surface.

In addition, the highest HCE values were achieved with the 30 kDa membrane for all the NaCl concentrations tested. As it was above mentioned, high hydrophilicity and low surface roughness favour the membrane antifouling properties and thus, milder experimental

conditions have to be used in order to clean such membrane. For this reason, at the same salt concentration, temperature and crossflow velocity, the 30 kDa membrane showed the highest values of HCE.

Effect of temperature on HCE

In order to increase the HCE values obtained for the best NaCl concentration (see Fig. 50), several cleaning experiments at different temperatures were performed. In this way, temperatures ranging from 50 to 80 ºC were tested to study the influence of this parameter on HCE, while the other experimental conditions were maintained constant for all the experiments at a NaCl concentration of 5 mM and crossflow velocities of 2.18 $m \cdot s^{-1}$ (for the 5 and 30 kDa membranes) and 4.2 $m \cdot s^{-1}$ (for the 15 kDa membrane).

Fig. 51 shows the values of HCE for the different temperatures and membranes tested. Increasing the temperature of the cleaning solution from 50 to 80 ºC resulted in an increase in HCE, achieving efficiency values of 100 % at the highest temperature for all the membranes used when the fouling experiments were performed with a WPC concentration of 22.2 $g \cdot L^{-1}$. As it was above mentioned, the lower the surface tension is, the greater the salting-in effect is (Tsumoto *et al.*, 2007). High temperatures lead to a decrease in the surface tension, which enhances the effectiveness of NaCl as cleaning agent. The interactions salt-proteins also increased as the temperature of the cleaning solution increased, due to the effect of temperature on the diffusivity coefficient. In this way, an increase in temperature causes an increase in that coefficient, which results in an

enhancement of the mass transfer process of protein molecules from the membrane surface to the bulk solution (Lee and Elimelech, 2007).

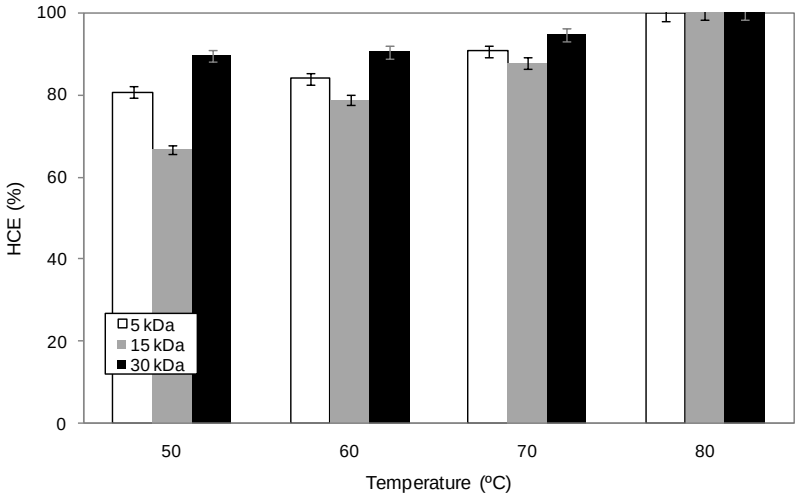

Fig. 51. *Effect of temperature on HCE (WPC concentration: 22.2 g·L^{-1}; NaCl concentration: 5 mM; crossflow velocity: 2.18 m·s^{-1} for the 5 and 30 kDa membranes and 4.2 m·s^{-1} for the 15 kDa membrane)*

Effect of crossflow velocity on HCE

Membranes fouled with WPC solutions of 22.2 g·L^{-1} were cleaned at a NaCl concentration of 5 mM, a temperature of 80 ºC and different crossflow velocities to study the influence of this operating parameter on the HCE values. As it is shown in Fig. 52, an increase in crossflow velocity from 1.2 to 2.18 m·s^{-1} caused an increase in the HCE values obtained for all the membranes tested. The greatest HCE (about 100 %) was achieved at a crossflow velocity of 2.18 m·s^{-1}. As Lee *et al.* (2001) demonstrated, the higher the crossflow velocity during the cleaning procedure of a PES UF membrane was, the higher the flux

recovery was. These authors achieved approximately the same permeate flux as that at the beginning of the UF process, removing the gel layer formed by natural organic matter on the membrane surface. This is in accordance with the fact that a crossflow velocity value about 2.18 $m \cdot s^{-1}$ was the optimal to effectively clean the membranes tested in this work.

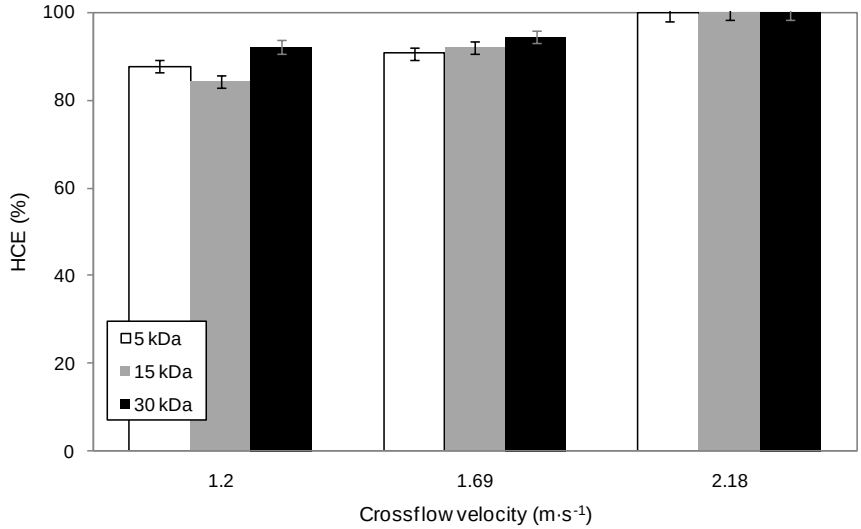

Fig. 52. *Effect of crossflow velocity on HCE (WPC concentration: 22.2 $g \cdot L^{-1}$; NaCl concentration: 5 mM; temperature: 80 ºC)*

Effect of WPC concentration on HCE

Fig. 53 shows the effect of WPC concentration during the fouling step on the HCE values obtained at the end of the cleaning procedure. Firstly, membranes fouled with WPC solutions at 22.2 and 33.3 $g \cdot L^{-1}$ were cleaned with NaCl solutions at the best cleaning conditions

above mentioned (NaCl concentration of 5 mM, temperature of 80 ºC and a crossflow velocity of 2.18 $m \cdot s^{-1}$).

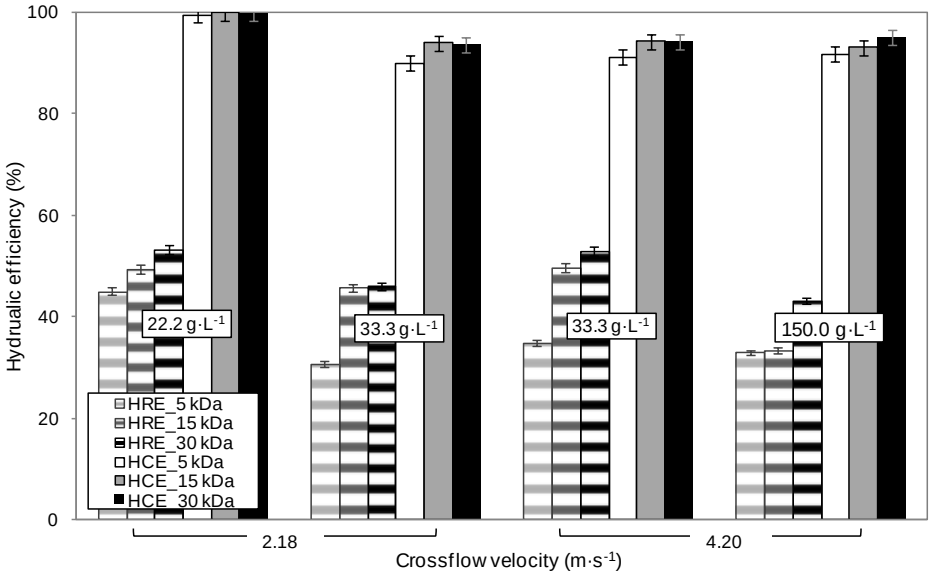

Fig. 53. *Effect of WPC concentration during fouling step on HRE and HCE at different crossflow velocities (NaCl concentration: 5 mM; temperature: 80 ºC)*

As it can be observed in Fig. 53, the HRE and HCE values decreased for all the membranes tested as the WPC concentration in the feed solution increased, due to the more severe fouling caused on the membranes. In a previous work, Corbatón-Báguena *et al.* (2015) investigated the fouling mechanisms dominating the UF of WPC solutions on ceramic and polymeric membranes by fitting several mathematical models. They confirmed that both complete blocking and cake formation were the main fouling mechanisms responsible for membrane fouling and that an increase in WPC concentration in the feed solution during the fouling step caused a more severe fouling

on the membrane surface because the values of the model parameters increased as the WPC concentration increased. They observed that the resistance due to concentration polarization and adsorption as well as the resistance due to cake formation increased for all the membranes tested when WPC concentration increased from 22.2 to 33.3 $g \cdot L^{-1}$.

In order to obtain higher HCE results, the crossflow velocity during the cleaning step was increased at 4.2 $m \cdot s^{-1}$. At this new value, two different WPC concentrations were tested (33.3 and 150.0 $g \cdot L^{-1}$). Comparing the HRE and HCE values achieved at 2.18 and 4.2 $m \cdot s^{-1}$ when a WPC concentration of 33.3 $g \cdot L^{-1}$ was used in the fouling step, it can be observed that, although slightly higher HRE was obtained when crossflow velocity increased, almost identical results were obtained for all the membranes tested. This indicated that this increase in crossflow velocity could not completely remove the protein deposits on the membrane surface and thus, did not result in an increase in the HCE values. This pattern also occurred when the WPC concentration increased up to 150.0 $g \cdot L^{-1}$. In this case, the HCE achieved was the same as that obtained for all the membranes fouled with a WPC concentration of 33.3 $g \cdot L^{-1}$. Therefore, there is a maximum quantity of proteins that can be removed from the membrane surface when NaCl solutions were used as cleaning agents and as a consequence, a maximum HCE of about 90-95 % can be achieved with this cleaning method at the highest WPC concentration tested.

Statistical and optimization analysis

An equation that relates HCE to the operating conditions and their interactions was developed by means of the Statgraphics software (Eq. 36). These conditions were: temperature during cleaning step, T; NaCl concentration, C_{NaCl}; crossflow velocity, v; membrane surface roughness, R_q and WPC concentration during the fouling step, C_{WPC}. The regression coefficient R^2 for Eq. 36 was 0.980 at a confidence level of 95 % (p-values lower than 0.05).

$$HCE\,(\%) = 303.028 - 3.392 \cdot T + 10.236 \cdot C_{NaCl} - 123.544 \cdot v + 17.930 \cdot R_q - \\ - 0.719 \cdot C_{NaCl}{}^2 - 2.197 \cdot v^2 - 0.183 \cdot R_q{}^2 + 0.006 \cdot C_{WPC}{}^2 + \\ + 1.864 \cdot T \cdot v - 0.181 T \cdot R_q - 0.636 \cdot C_{NaCl} \cdot v - 0.267 \cdot v \cdot C_{WPC}$$

Eq. 36

To obtain the optimal conditions resulting in a HCE value of 100 %, the Microsoft Excel Solver tool was used. Those optimal conditions were a temperature of 80.00 ºC, a NaCl concentration of 5.01 mM, a crossflow velocity of 2.23 $m \cdot s^{-1}$, a membrane surface roughness of 2.02 nm and a WPC concentration of 22.19 $g \cdot L^{-1}$. These values are in a good agreement with those related to the best conditions to obtain the highest HCE observed in Figs. 50-52 for the PESH 30 kDa membrane used (R_q = 1.657 nm). Therefore, low membrane roughness favours the cleaning process at milder conditions of crossflow velocity and cleaning agent concentration, while high temperatures result in greater cleaning efficiency values when low protein concentration in the fouling feed solution was used.

7.1.4. Conclusions

NaCl solutions were able to effectively clean three UF membranes of different materials and MWCOs (a PES membrane of 5 kDa, a ceramic ZrO_2-TiO_2 membrane of 15 kDa and a PESH membrane of 30 kDa) fouled with WPC solutions, resulting in high values of HCE for all the membranes and WPC solutions tested.

Cleaning results demonstrated that an increase in temperature and crossflow velocity of the cleaning solution caused an increase in the HCE. Regarding NaCl concentration, there was an optimal value up to which the HCE increased (about 5 mM for all the membranes tested). When the concentration was greater than this value, the cleaning efficiency decreased possibly due to the competition between cleaning and fouling mechanisms and the reduction in surface tension. On the other hand, the higher the WPC concentration in the feed solution during the fouling step was, the lower the HCE was, due to the more severe fouling caused when protein concentration in the feed solution increased. The highest values of the cleaning efficiency (100 %) were achieved for the lowest WPC concentration tested (22.2 $g \cdot L^{-1}$).

An equation that correlates the HCE to the operating parameters (temperature, NaCl concentration, crossflow velocity in the cleaning procedure and WPC concentration during the fouling step) was obtained with high accuracy (R^2 = 0.980) at a confidence level of 95%. The optimization analysis performed showed that a temperature

of 80.00 ºC, a NaCl concentration of 5.01 mM, a crossflow velocity of 2.23 $m \cdot s^{-1}$, a membrane surface roughness of 2.02 nm and a WPC concentration of 22.19 $g \cdot L^{-1}$ resulted in a 100 % of HCE, which corresponded to the best conditions experimentally obtained for the 30 kDa membrane.

Acknowledgements

The authors of this work wish to gratefully acknowledge the financial support from the Spanish Ministry of Science and Innovation through the project CTM2010-20186.

Nomenclature

List of symbols

C_b	Protein concentration in the feed solution ($g \cdot L^{-1}$)
C_{NaCl}	NaCl concentration (mM)
C_p	Protein concentration in the permeate ($g \cdot L^{-1}$)
C_{WPC}	WPC concentration in the feed solutions ($g \cdot L^{-1}$)
J	Permeate flux ($m^3 \cdot m^{-2} \cdot s^{-1}$)
ΔP	Transmembrane pressure (bar)
R	Total hydraulic resistance (m^{-1})
R_m	Resistance of the new membrane (m^{-1})
R_f	Resistance after the fouling step (m^{-1})
R_{r1}	Resistance after the first rinsing step (m^{-1})
R_{r2}	Resistance after the second rinsing step (m^{-1})

R_q	Root Mean Square Roughness (nm)
t	Filtration time (s)
T	Temperature of the cleaning solution (ºC)
v	Crossflow velocity ($m \cdot s^{-1}$)

Greek letters

μ	Feed solution viscosity ($kg \cdot m^{-1} \cdot s^{-1}$)

Abbreviations

AFM	Atomic force microscopy
BSA	Bovine serum albumin
HCE	Hydraulic cleaning efficiency
HRE	Hydraulic rinsing efficiency
MWCO	Molecular weight cut off
PES	Polyethersulfone
UF	Ultrafiltration
WPC	Whey protein concentrate

7.2. BIBLIOGRAFÍA

ADAMS M.C., ZULEWSKA J. y BARBANO D.M. (2013). "Effect of annatto addition and bleaching treatments on ultrafiltration flux during production of 80 % whey protein concentrate and 80 % serum protein concentrate" en *Journal of Dairy Science*, vol. 96, p. 2035-2047.

ALMÉCIJA M.C. *et al.* (2009a). "Influence of the cleaning temperature on the permeability of ceramic membranes" en *Desalination*, vol. 245, p. 708-713.

ALMÉCIJA M.C. *et al.* (2009b). "Analysis of cleaning protocols in ceramic membranes by liquid-liquid displacement porosimetry" en *Desalination*, vol. 245, p. 541-545.

ANG W.S. y ELIMELECH M. (2007). "Protein (BSA) fouling of reverse osmosis membranes: Implications for wastewater reclamation" en *Journal of Membrane Science*, vol. 296, p. 83-92.

AOAC Official Method 930.30. (1930). "Ash of Dried Milk". First action 1930.

BALDASSO C., BARROS T.C. y TESSARO I.C. (2011). "Concentration and purification of whey proteins by ultrafiltration" en *Desalination*, vol. 278, p. 381-386.

BRADFORD M.M. (1976). "A rapid and sensitive method for the quantitation of microgram quantities of protein utilizing the principle of protein-dye binding" en *Analytical Biochemistry*, vol. 72, p. 248-254.

CABERO CABERO M.L. (1997). *Limpieza química de membranas inorgánicas: Aplicación al tratamiento de lactosuero.* Tesis Doctoral. Oviedo: Universidad de Oviedo, <http://hdl.handle.net/10651/13566>.

CHESSA S. *et al.* (2014). "Selection for milk coagulation properties predicted by Fourier transform infrared spectroscopy in the Italian Holstein-Friesian breed" en *Journal of Dairy Science,* vol. 97, p. 4512-4521.

CORBATÓN-BÁGUENA M.J., ÁLVAREZ-BLANCO S. y VINCENT-VELA M.C. (2014a). "Cleaning of ultrafiltration membranes fouled with BSA by means of saline solutions" en *Separation and Purification Technology*, vol. 125, p. 1-10.

CORBATÓN-BÁGUENA M.J., ÁLVAREZ-BLANCO S. y VINCENT-VELA M.C. (2014b). "Salt cleaning of ultrafiltration membranes fouled by whey model solutions" en *Separation and Purification Technology*, vol. 132, p. 226-233.

CORBATÓN-BÁGUENA M.J., ÁLVAREZ-BLANCO S. y VINCENT-VELA M.C. (2015). "Fouling mechanisms of ultrafiltration membranes fouled with whey model solutions" en *Desalination*, vol. 360, p. 87-96.

DAUFIN G. *et al.* (2001). "Recent and emerging applications of membrane processes in the food and dairy industry" en *Food and Bioproducts Processing*, vol. 79, p. 89-102.

EVANS P.J. *et al.* (2008). "The influence of hydrophobicity, roughness and charge upon ultrafiltration membranes for black tea liquor clarification" en *Journal of Membrane Science*, vol. 313, p. 250-262.

GARCÍA-IVARS J. *et al.* (2014). "Development of fouling-resistant polyethersulfone ultrafiltration membranes via surface UV photografting with polyethylene glicol/aluminum oxide nanoparticles" en *Separation and Purification Technology*, vol. 135, p. 88-99.

HOFMEISTER F. (1888). “Zur lehre von der wirkung der salze” en *Archiv for Experimentelle Pathologie und Pharmakologie*, vol. 24, p. 247.

HUSSAIN R., GAIANI C. y SCHER J. (2012). “From high milk protein powders to the rehydrated dispersions in variable ionic environments: A review” en *Journal of Food Engineering*, vol. 113, p. 486-503.

KAZEMIMOGHADAM M. y MOHAMMADI T. (2007). “Chemical cleaning of ultrafiltration membranes in the milk industry” en *Desalination*, vol. 204, p. 213-218.

LEE H. *et al.* (2001). “Cleaning strategies for flux recovery of an ultrafiltration membrane fouled by natural organic matter” en *Water Research*, vol. 35, p. 3301-3308.

LEE S. y ELIMELECH M. (2007). “Salt cleaning of organic-fouled reverse osmosis membranes” en *Water Research*, vol. 41, p. 1134-1142.

MAK W.C. *et al.* (2003). “Biosensor for rapid phosphate monitoring in a sequencing batch reactor (SBR) system” en *Biosensors and bioelectronics*, vol. 19, p. 233-237.

MATHEW J., ARAVINDAKUMAR C.T. y ARAVIND U.K. (2008). “Effect of ionic strength and protein concentration on the transport of proteins through chitosan/polystyrene sulfonate multilayer membrane” en *Journal of Membrane Science*, vol. 325, p. 625-632.

MATZINOS P. y ÁLVAREZ R. (2002). “Effect of ionic strength on rinsing and alkaline cleaning of ultrafiltration inorganic membranes fouled with whey proteins” en *Journal of Membrane Science*, vol. 208, p. 23-20.

MILLER G.L. (1959). "Use of dinitrosalicylic acid reagent for determination of reducing sugar" en *Analytical Chemistry*, vol. 31, p. 426-428.

MUTHUKUMARAN S. *et al.* (2004). "The use of ultrasonic cleaning for ultrafiltration membranes in the dairy industry" en *Separation and Purification Technology*, vol. 39, p. 99-107.

NUCCI N.V. y VANDERKOOI J.M. (2008). "Effects of salts of the Hofmeister series on the hydrogen bond network of water" en *Journal of Molecular Liquids*, vol. 143, p. 160-170.

OGUNBIYI O.O., MILES N.J. y HILAL N. (2008). "The effects of performance and cleaning cycles of new tubular ceramic microfiltration membrane fouled with a model yeast suspension" en *Desalination*, vol. 220, p. 273-289.

RAHIMPOUR A. y MADAENI S.S. (2010). "Improvement of performance and surface properties of nano-porous polyethersulfone (PES) membrane using hydrophilic monomers as additives in the casting solution" en *Journal of Membrane Science*, vol. 360, p. 371-379.

SANMARTÍN B. *et al.* (2012). "Composition of caprine whey protein concentrates produced by membrane technology after clarification of cheese whey" en *Small Ruminant Research*, vol. 105, p. 186-192.

TARAZAGA C.C., CAMPDERRÓS M.E. y PÉREZ-PADILLA A. (2006). "Physical cleaning by means of electric field in the ultrafiltration of a biological solution" en *Journal of Membrane Science*, vol. 278-p. 219-224.

TSUMOTO K. *et al.* (2007). "Effects of salts on protein-surface interactions: Applications for column chromatography" en *Journal of Pharmaceutical Science*, vol. 96, p. 1677-1690.

ZHANG J. (2012). “Protein-protein interactions in salt solutions” en Cai W. y Hong H. *Protein-protein interactions – Computational and experimental tools*. Intech.

CAPÍTULO VIII

Limpieza mediante disoluciones salinas de membranas ensuciadas con enzimas

8.1. LIMPIEZA DE MEMBRANAS DE ULTRAFILTRACIÓN ENSUCIADAS CON DISOLUCIONES ENZIMÁTICAS

Este Capítulo constituye una adaptación al formato de la Tesis Doctoral del artículo titulado "Destabilization and removal of immobilized enzymes adsorbed onto polyethersulfone ultrafiltration membranes by salt solutions", publicado en la revista Journal of Membrane Science. En él se evaluó la efectividad de dos disoluciones salinas (NaCl y Na_2SO_4) para limpiar membranas de 30 kDa que habían sido ensuciadas con disoluciones enzimáticas. La eficacia del proceso de limpieza se determinó mediante técnicas de AFM y ATR-FTIR. Además, los modelos matemáticos descritos en el Capítulo IV se utilizaron para determinar los mecanismos responsables del ensuciamiento de las membranas. Los datos bibliográficos del artículo se destacan a continuación:

***Autores**: M.-J. Corbatón-Báguena, A. Gugliuzza, A. Cassano, R. Mazzei, L. Giorno*

***Título**: Destabilization and removal of immobilized enzymes adsorbed onto polyethersulfone ultrafiltration membranes by salt solutions*

***Editorial**: Elsevier*

***Revista**: Journal of Membrane Science*

año: 2015 vol. 486 p. 207-214

***Doi**: http://dx.doi.org/10.1016/j.memsci.2015.03.061*

Destabilization and removal of immobilized enzymes adsorbed onto polyethersulfone ultrafiltration membranes by salt solutions

María-José Corbatón-Báguena[1*], Annarosa Gugliuzza[2*], Alfredo Cassano[2], Rosalinda Mazzei[2], Lidietta Giorno[2]

[1]*Department of Chemical and Nuclear Engineering, Universitat Politècnica de València, C/Camino de Vera s/n 46022 Valencia, Spain*

[2]*Institute on Membrane Technology, ITM-CNR, c/o University of Calabria, via P. Bucci, 17/C, I-87030 Rende (Cosenza), Italy*

*Corresponding author 1:
María-José Corbatón-Báguena
Ph : +34963879633
Fax : +34963877639
e-mail: macorba@upvnet.upv.es

*Corresponding author 2:
Dr Annarosa Gugliuzza Ph.D.
Ph : +39 0984 49 2026 / 2004 / 2005
Fax : +39 0984 40 2103
e-mail: a.gugliuzza@itm.cnr.it

Abstract

In this work the effectiveness of two saline solutions (NaCl and Na_2SO_4) to clean a permanently hydrophilic polyethersulfone (PESH) ultrafiltration (UF) membrane with a molecular weight cut-off (MWCO) of 30 kDa previously fouled with enzymatic solutions was investigated. The influence of protein concentration in the enzymatic solution during the fouling step and the effect of salt type during the cleaning procedure were studied.

The protein aggregation was analysed in solution and onto the membrane surface by using several techniques including Dynamic Light Scattering (DLS), Atomic Force Microscopy (AFM) and Infrared Spectroscopy with Attenuated Total Reflectance (ATR-FTIR). In addition, mechanisms that dominate membrane fouling were studied by fitting some mathematical models (Hermia's models adapted to crossflow filtration, a combined model based on the complete blocking and cake formation equations and a resistance-in-series model) to the experimental data.

Fouling results showed that the complete blocking/adsorption on membrane surface was the predominant fouling mechanism. Regarding the cleaning results, higher cleaning efficiency and low residual protein concentration was obtained with NaCl solutions for all the feed solutions tested due to the favourable interaction between Cl^- and proteins.

Keywords: membrane cleaning; protein fouling; salt solutions; ultrafiltration; mathematical models

8.1.1. Introduction

Fouling due to protein-membrane interactions can influence and strongly limit the performance of membranes in several processes such as: proteins separation/fractionation, removal of denatured enzymes in biocatalytic membrane reactors and clarification of food streams.

It is well known that pectinases are enzymes largely used in fruit juice microfiltration (MF) or ultrafiltration (UF) in order to hydrolize pectic substances, i.e. complex glycosidic macromolecules with high molecular weight and negative charge (Jayani *et al.*, 2005) which are responsible for membrane fouling. In addition, pectinases can be also immobilized on different supports depending on the industrial application including fruit juice and olive mill wastewater processing (Ramírez *et al.*, 2013; Gebreyohannes *et al.*, 2013).

Enzyme immobilization techniques and membrane fouling mechanisms have similar characteristics, physical and/or interfacial donor/acceptor interactions being surface controlling factors (Mazzei *et al.*, 2010; De Bartolo *et al.*, 2004; Yua *et al.*, 2013; De Luca *et al.*, 2009). In this way, Luo *et al.* (2013) stated that enzymatic entrapment on membranes may be considered as a pore blocking mechanism

and the adsorption fouling can be related to the enzymatic adsorption on the membrane surface due to hydrophobic and electrostatic interactions. In their work, fouling mechanisms that dominate the enzyme filtration were analyzed by two different mathematical models: a resistance-in-series model considering the intrinsic membrane resistance, the reversible fouling resulting from concentration polarization layer or particle deposit and the irreversible fouling including pore blocking or cake deposit and the classical Hermia's models applied to dead-end filtration. Other authors also used these models to investigate membrane fouling. Vincent-Vela *et al.* (2009) fitted the Hermia's models adapted to crossflow filtration to the experimental data obtained during the UF of polyethylenglycol. They concluded that the intermediate and complete blocking mechanisms were the models with the highest fitting accuracy for most of the operating conditions tested. De Barros *et al.* (2003) identified the fouling mechanism as a function of the membrane material used during the crossflow UF of pineapple juice previously treated with enzymes.

Results after fitting the Hermia's models adapted to crossflow showed that complete pore blocking and cake formation were the predominant mechanisms when using the ceramic and polymeric membranes, respectively. Similarly, Cassano *et al.* (2007) established that the fouling mechanism involved in the crossflow UF of blood orange juice with a tubular polyvinylidenefluoride (PVDF) membrane evolved from a partial to a complete pore blocking in dependence of the axial feed velocity. Choi *et al.* (2000) applied a resistance-in-series model to the MF of bovine serum albumin (BSA) taking into

account the membrane resistance, the gel layer resistance and the fouling resistance due to the foulant deposits inside the membrane pores. They obtained good agreement with the experimental data recorded. Machado *et al.* (2012) investigated the effect of an enzymatic treatment with pectin lyase of açaí pulp on its crossflow MF. They also studied the predominant fouling mechanisms by a resistance-in-series and the Hermia's models adapted to crossflow ones. They observed that fouling resistance decreased after the enzymatic treatment as well as the cake formation followed by intermediate and complete pore blocking mechanisms dominated the MF process.

However, as Luo *et al.* described (2013), during the immobilization of enzymes the convective transport of enzymes to the membrane surface makes these particles to be retained on it and thus, enzymes cause an increase in the local concentration. As a result, concentration polarization increases and a fouling layer can be formed on the membrane surface or inside its pores. In order to remove such a fouling layer, membranes have to be cleaned. Conventional cleaning protocols involve chemical cleaning agents such as alkalis, acids, disinfectants, surfactants or combinations of them (Ogunbiyi *et al.*, 2008). However, these conventional cleaning methods may be aggressive for the membranes and their lifetime and selectivity may be reduced. In addition, these conventional cleaning agents cause a negative environmental impact when they are discharged as wastewaters after the cleaning step. For all these reasons, new alternative cleaning techniques, including ultrasounds (Muthukumaran *et al.*, 2004), electromagnetic fields (Tarazaga *et al.*,

2006) and saline solutions (Lee and Elimelech, 2007) have been developed in the recent years to overcome these problems. Regarding the use of saline solutions, previous studies reported the salting-in and salting-out effect of different cations and anions to increase or decrease, respectively, protein solubility at pH values above and below the isoelectric point of the protein (Curtis and Lue, 2006; Zhang, 2012). Lee and Elimelech (2007) also investigated the cleaning mechanism of saline solutions: in a first stage, the difference between the bulk solution concentration and the gel layer concentration on the membrane surface causes changes on the cross-linked fouling layer. Then, an ion-exchange reaction takes place between the ions forming the gel layer on the membrane surface and the salt ions of the cleaning solution that diffuse in the gel layer. This ion exchange results in a swelling and removal of the gel layer by freeing the protein molecules and favouring their transport to the bulk solution.

The aim of this work is to investigate the effectiveness of NaCl and Na_2SO_4 solutions for cleaning a PESH UF membrane with a molecular weight cut-off (MWCO) of 30 kDa that was previously fouled with enzymatic solutions of pectinases at different protein concentration (2, 7.5 and 15 g/L). The influence of protein concentration on membrane fouling was studied by AFM and ATR-FTIR techniques and the fouling mechanism that dominates the UF of each feed solution tested was also determined by fitting three mathematical models to the experimental data: Hermia's models adapted to crossflow filtration, a combined model based on the complete blocking and cake formation mechanisms and a resistance-

in-series model. The membrane cleanliness was evaluated by ATR-FTIR measurements and the residual protein concentration adsorbed on the membrane surface was also quantified.

8.1.2. Materials and methods

8.1.2.1. Chemicals

Enzymatic solutions of pectinases (Pectinex Smash XXL, Novozymes) at different protein concentrations (2, 7.5 and 15 g/L) were used as feed solutions during the fouling step. According to the manufacturer information, the enzymatic solution is mainly composed of pectin lyases from *Aspergillus niger*. NaCl and Na_2SO_4 solutions were the cleaning agents tested. Protein concentration in the enzymatic solutions was determined by the Bicinchoninic Acid (BCA) assay (Sigma Aldrich).

8.1.2.2. Experimental set-up

A permanently hydrophilic polyethersulfone (PESH) ultrafiltration membrane (Microdyn Nadir, Germany) with a MWCO of 30 kDa was tested in the experiments. The main characteristics of the virgin membrane are shown in Table 28.

All the fouling and cleaning experiments were performed in a conventional crossflow UF system. It consisted of a feed tank of 1 L, a variable speed pump, a stainless-steel cell able to accommodate a

flat-sheet membrane and a permeate tank. Transmembrane pressure was measured by two manometers allocated before and after the membrane module and regulated by a pressure control valve located on the retentate line. Crossflow velocity was controlled by a digital flowmeter. Temperature was set at 25 ± 1 ºC during the fouling and rinsing steps using a cooling system fed with tap water, while during the cleaning step temperature was set at 50 ± 3ºC using a heater.

Table 28. Main properties of the membrane used

Commercial code	UH030
Manufacturer	Microdyn Nadir
Type	Flat-sheet
Nominal MWCO (kDa)	30
Active layer	PESH
Effective area (cm^2)	35.25
Water permeability at 25ºC ($L/m^2 \cdot h \cdot bar$)	106.00
Maximum operating temperature (ºC)	95
pH range	0-14

8.1.2.3. Experimental procedure

Fouling tests were carried out with an enzymatic solution at three different protein concentrations (2, 7.5 and 15 g/L) without pH adjustment (pH value of about 4.3). Experimental conditions of transmembrane pressure, crossflow velocity and temperature were set at 2 bar, 2 m/s and 25 ºC, respectively. The duration of the fouling tests was 2 h. These conditions were selected according to previous studies on protein solutions ultrafiltration (Corbatón-Báguena *et al.*, 2014a; Corbatón-Báguena *et al.*, 2014b; Matzinos and Álvarez, 2002).

After the fouling step, a first rinsing with distilled water was performed during 30 min at a transmembrane pressure of 1 bar and a crossflow velocity of 2.18 m/s. According to the literature (Blanpain-Avet *et al.*, 2009), low transmembrane pressures and high crossflow velocities favour the removal of solute molecules deposited on the membrane surface. Then, a cleaning step with saline solutions during 60 min and a second rinsing step with distilled water during 30 min were carried out at the same experimental conditions of transmembrane pressure as the first rinsing step. NaCl and Na_2SO_4 solutions were tested during the cleaning protocol at a concentration of 5 mM and a temperature of 50 ºC. These conditions were the optimal ones in previous studies about saline cleaning of membranes fouled with protein solutions (Corbatón-Báguena *et al.*, 2014a; Corbatón-Báguena *et al.*, 2014b).

Permeate flux and hydraulic resistance were monitored during all the steps of the experimental procedure. Once the cleaning procedure was finished, water permeability was measured again in order to evaluate the cleaning efficiency, expressed as:

$$CE = \frac{WP_1}{WP_0} \cdot 100 \qquad \text{Eq. 37}$$

where WP_1 and WP_0 are the water permeability of the cleaned and virgin membrane, respectively.

8.1.2.4. Characterization of the enzymatic solutions

The BCA assay was used to determine the protein concentration in the enzymatic solutions (Morton and Evans, 1992; Krieg *et al.*, 2005). This assay is a colorimetric method based on the formation of a Cu^{+2}-protein complex under alkaline conditions. Then, reduction of Cu^{+2} to Cu^{+1} takes place and the amount of reduction is directly proportional to the amount of protein in the sample. According to the standard assay protocol, 0.1 mL of sample were mixed with 2 mL of the BCA working reagent and incubated at 37 ºC during 30 min. Then, samples were cooled at room temperature and absorbance was measured at a wavelength of 562 nm by a UV-visible spectrophotometer. By using a calibration test performed with the bovine serum albumin (BSA) standard solution, protein concentration in the enzymatic solutions was estimated. Each sample was duplicated for the measurement.

Size measurements of protein particles were carried out by Zetasizer nano (Malvern Instruments). The Zetasizer system determines the particles size by measuring the Brownian motion of the particles in a sample using Dynamic Light Scattering (DLS). Previous studies demonstrated that these techniques were suitable for protein characterization (Mattison and Kaszuba, 2004; Schultz *et al.*, 2008). In order to analyse the particle size in pectinase solution in the conditions in which membrane was fouled with pectinase (at 25 °C) and during cleaning treatment (at 50 °C in presence of NaCl), different analysis were carried out by DLS varying protein

concentration (2, 7, 15 g/L). In addition protein size measurements at 15 g/L were also carried out in presence of NaCl (5mM). Hypothesis testing considering a confidence interval of 95 % and using the Statgraphics® Centurion XVI software were performed in order to determine if statistically significant differences exist among the particle size distributions at 25 ºC, 50 ºC and the combination of 50 ºC and NaCl (Alcheikhhamdon *et al.*, 2015).

8.1.2.5. Membrane characterization

Prior to the fouling experiments, the membrane was compacted with ultrapure water by increasing and decreasing the transmembrane pressure from 1 bar to 4 bar until a constant hydraulic permeability was obtained. Accordingly, the intrinsic membrane resistance (R_m) was calculated. Ultrapure water was used in order to prevent additional dirty on the membrane surface.

Infrared spectra in ATR mode were collected onto the membrane surface before and after each fouling and cleaning experiments by using an ATR-FTIR spectrometer (Spectrum One, Perkin Elmer). The adsorption and deposition of proteins on the membrane surface and related changes in the surface roughness were detected by using Atomic Force Microscopy (AFM), Nanoscope III (Digital Instruments, VEECO Metrology Group). Tapping Mode AFM operated by scanning a tip attached to the end of an oscillating cantilever across 2.5x2.5 μm of sample surface.

The amount of residual material adsorbed onto the membrane surface was quantified according to the following equation (Rabiller-Baudry *et al.*, 2008):

$$\frac{H_{1539}}{H_{1240}} = 0.0034 \cdot C_{protein} + 0.0165 \qquad \text{Eq. 38}$$

where H_{1539} is the height of the absorption band at 1539 cm^{-1} (amide 2), H_{1240} is the height of the absorption band at 1240 cm^{-1} (PES membrane) and $C_{protein}$ is the residual protein concentration deposited on membrane surface. This equation is valid in the protein concentration range of 0.5-350 $\mu g/cm^2$ with a maximum deviation of 1 $\mu g/cm^2$, according to Rabiller-Baudry *et al.* (2012).

8.1.2.6. Mathematical modelling

Different mathematical models were fitted to the experimental data obtained during the UF of pectinase solutions using the MathCad® Genfit algorithm, which minimizes the overall difference between experimental and predicted results by the Levenberg-Marquadt method. The success of fitting was evaluated in terms of regression coefficient R^2 and standard deviation SD.

Hermia's models

Hermia (1982) developed four models based on classical constant pressure dead-end filtration equations in order to describe four main

types of membrane fouling: complete blocking, intermediate blocking, standard blocking and cake layer formation. Several authors (Field *et al.*, 1995; de Barros *et al.*, 2003; Cassano *et al.*, 2007; Vincent-Vela *et al.*, 2009) adapted these models to crossflow configuration by incorporating the flux associated with the back-transport mass transfer, which is evaluated at the steady-state (Jarusutthirak *et al.*, 2007). Eq. 39 shows the general equation for Hermia's models adapted to crossflow UF:

$$-\frac{dJ}{dt} = K\left(J - J_{SS}\right)J^{2-n} \qquad \text{Eq. 39}$$

where J is the permeate flux, K is a model constant, n is the model parameter and J_{ss} is the permeate flux when the steady-state is achieved.

Four different models corresponding to the four fouling mechanisms above mentioned are considered depending on the value of the parameter n: complete blocking (n = 2), intermediate blocking (n = 1), standard blocking (n = 1.5) and gel layer formation (n = 0).

Complete blocking model takes into account that a solute molecule that reaches to membrane surface blocks a pore entrance completely without penetrating inside the pores. This model assumes that a monomolecular layer is formed on the membrane surface.

The intermediate blocking model considers that a solute molecule can deposit on previously settled ones. However, as in the complete blocking model, fouling takes place only on the membrane surface.

When solute molecules are smaller than membrane pore size, these molecules can penetrate inside the pores. This is the main hypothesis of the standard blocking model.

Cake formation model is based on the assumption that solute molecules accumulate on membrane surface because they have a larger size than membrane pores. Therefore, a permeable layer is formed on the membrane surface.

Combined model

Previous studies (Field *et al.*, 1995; Ho and Zydney, 2000; Jarusutthirak *et al.*, 2007; de la Casa *et al.*, 2008) reported that the typical variation of permeate flux with time includes two fouling mechanisms: a rapid flux decline during the first minutes of operation due to pore blocking and an accumulation of foulants on the membrane surface that causes a long term flux decline due to a cake formation. In this work, a combined model considering the Hermia's equations for crossflow UF corresponding to complete blocking and cake formation was used to predict the permeate flux decline. Therefore, the general equation of the combined model is Eq. 40, where α is the fraction of membrane pores that are completely blocked:

$$J_{combined\ \ model} = \alpha J_{complete\ \ blocking\ model} + (1-\alpha) J_{cake\ formation\ \ model} \qquad \text{Eq. 40}$$

Eq. 40 involves two different constants depending on the fouling mechanism: K_c for the complete blocking model and K_{cf} for the cake formation model. The parameter K_c corresponds to the blocked membrane surface per unit of total permeate volume and unit of membrane surface porosity. On the other hand, K_{cf} represents the ratio between the cake characteristics (specific cake resistance and cake mass per unit of total permeate volume) and the original membrane ones (Vincent-Vela *et al.*, 2009).

Resistance-in-series model

According to the Darcy's law (Eq. 41), permeate flux is related to the transmembrane pressure and the total hydraulic resistance:

$$J = \frac{\Delta P}{\mu \cdot R} \qquad \text{Eq. 41}$$

where ΔP is the transmembrane pressure, μ is the feed solution viscosity and R is the total hydraulic resistance.

In the resistance-in-series model, the total hydraulic resistance is the sum of different resistances that contribute to the permeate flux decline during the UF process. In this work, the membrane resistance, the cake resistance and the adsorption and concentration polarization resistances were considered (Eq. 42):

$$J = \frac{\Delta P}{\mu \cdot (R_m + R_{ad} + R_c)} \qquad \text{Eq. 42}$$

where R_m is the virgin membrane resistance, R_c is the cake resistance and R_{ad} is the resistance due to adsorption on/in membrane surface and pores and concentration polarization. In addition, R_{ad} can be expressed as an exponential function of the steady-state adsorption and concentration polarization resistance and the rate at which foulant molecules are deposited on the membrane (Choi *et al.*, 2000; Carrère *et al.*, 2001). Therefore, Eq. 43 shows the general equation for the resistance-in-series model:

$$J = \frac{\Delta P}{\mu \cdot (R_m + R'_{ad}\,(1 - exp(-bt)) + R_c)} \qquad \text{Eq. 43}$$

where R'_{ad} is the steady-state adsorption and concentration polarization resistance and b is the fouling rate due to adsorption.

8.1.3. Results and discussion

8.1.3.1. Fouling results

Determination of protein fouling

DLS measurements on protein solutions (Table 29) showed a bimodal distribution for all the protein concentrations tested at 25 °C. As it is possible to observe, the particle size belonging to distribution

2 increased as a function of concentration, reaching a value of 410 ± 221 nm at 15 g/L. The increase in size, as well as the high PDI, suggested a severe protein aggregation which is expected to lead to a higher fouling during the UF process when the protein concentration is increased.

Table 29. Particle size measurements of pectinase solutions by DLS at various concentration and temperature

Temperature (°C)	Protein concentration (g/l)	Particle distribution 1 (nm)	PDI_1 (%)	Particle distribution 2 (nm)	PDI_2 (%)
25 °C	15	15±4	27	410±221	54
	7	6±1	17	91±38	42
	2	6±0.6	10	61±18	29
50 °C	15	12±3	25	288±105	36
	7	6±1	17	17±4	23
	2	6±0.8	13	19±4	21

PDI: polidispersity index percentage = standard deviation/ intensity weighted Z average

AFM and ATR-FTIR measurements also demonstrated that protein fouling increased with the protein concentration in the enzymatic solution, causing a general increase in the surface roughness as well. Fig. 54 shows the 2D AFM images of the virgin and fouled membranes at different protein concentration (2, 7.5 and 15 g/L). When protein concentration was 2 g/L big protein aggregates can be well distinguished from membrane surface while the membrane surface continues to exhibit the same surface morphology of the initial one, causing a dramatic increase in the surface roughness with value of R_a of 28±8 nm (Fig. 54b). At 7.5 g/L the layer is partially formed on the membrane surface, revealing heterogeneous regions where initial membrane structure and isolated protein aggregates are well

distinguished (Fig. 54c). In comparison with previous situation (2 g/L) the protein clusters decrease in size but increase in number. At the highest concentration tested, a gel layer that completely covers the original membrane surface can be observed, producing an increase in surface roughness (Fig. 54d) as compared with the virgin membrane. On this basis it can be assumed that protein-membrane interaction, as well as protein cluster disassembling, is favoured when protein concentration is raised.

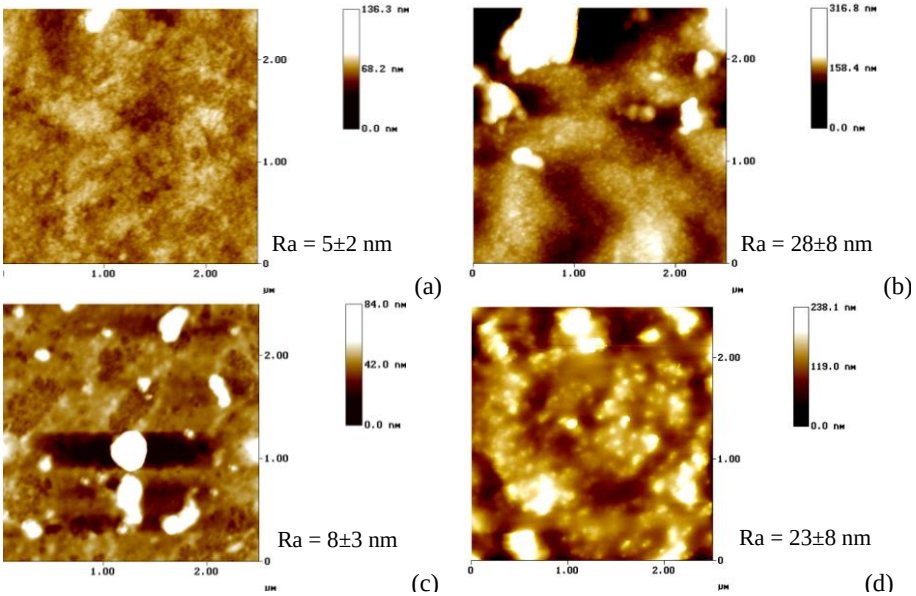

Fig. 54. *AFM images of new membrane (a) and membranes fouled with enzymatic solutions at 2 g/L (b), 7.5 g/L (c) and 15 g/L (d)*

On the other hand, it is relevant to underline that the convective transport to the membrane enhances protein overlapping with gel formation. These results are in agreement with those obtained by

Ohnishi *et al.* (1998), who demonstrated protein layer was denser at the highest concentration tested, as it occurs in our work.

ATR-FTIR spectra were collected onto virgin and fouled membranes. An intense absorption band can be detected at about 1650 cm^{-1} due to the stretching vibration of $C=O_{amide}$ typical of the amide I group (Fig. 55a). This band becomes more intense for membranes fouled with solutions at 2 g/L. The broadness of this band along with the appearance of a strong IR mode at 1504 cm^{-1}, which is typical of a $C-H_{arom}$ bond, suggests a strong contribution of the aromatic component to the spectrum due to different rearrangement of the protein aggregates when binding the membrane surface. Also, at 1168 cm^{-1} an IR mode associated to C-O-C stretching vibrations appears to be more intense confirming a different local chemical environment due to a varied rearrangement of the protein assembling. It is noteworthy that stretching located at 1620 towards higher frequency suggests intermolecular β-sheets bonds confirming a protein aggregation state (Blume *et al.*, 2015; Matheus *et al.*, 2006).

Another diagnostic weak band is observed at around 1730 cm^{-1}, which corresponds to $C=O_{ester}$ bond. This infrared mode was detected in the spectra for all the fouled membranes with the same band intensity, whereas it was never observed in the new membrane spectrum. It is relevant to underline that the strong IR absorption bands, which characterize the spectrum of fouled membranes with 2.0 g/L, are due to local adsorption of protein aggregates completely spanned at higher concentration as confirmed by AFM images (Fig. 54b,d).

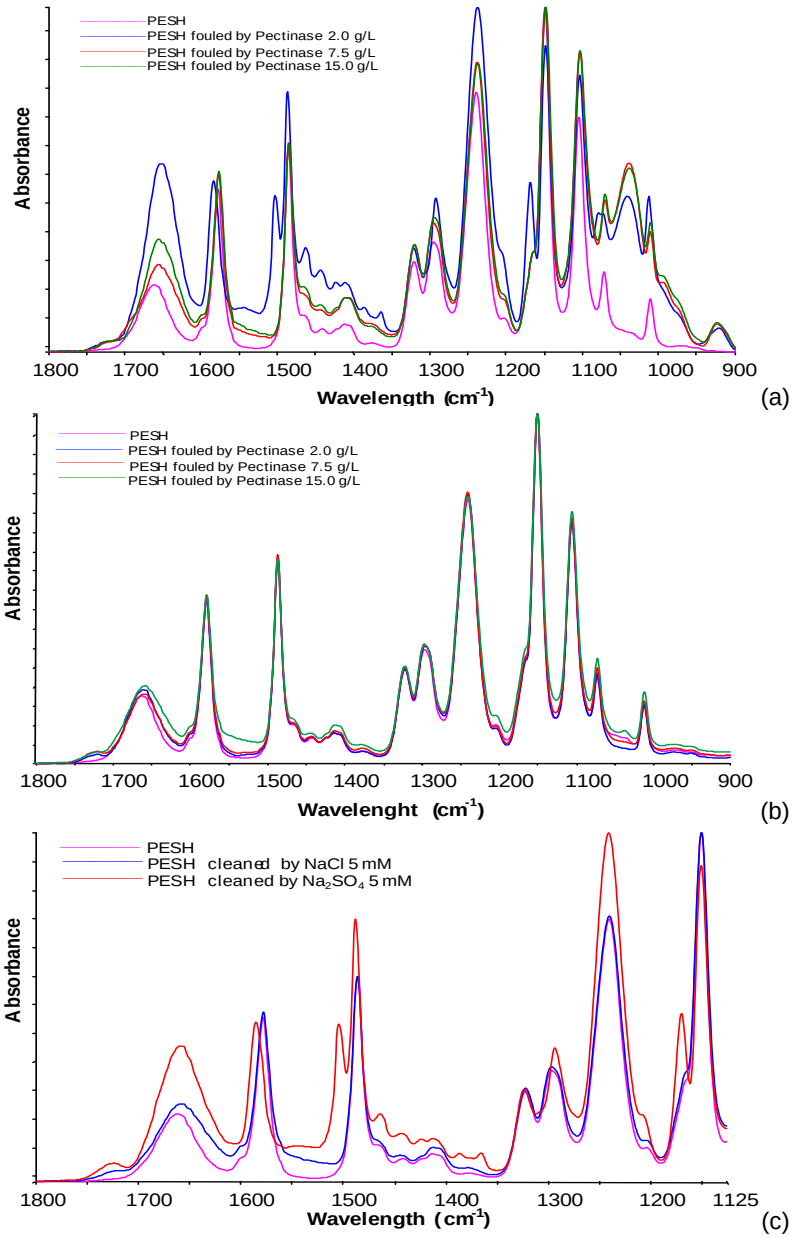

Fig. 55. *ATR-FTIR spectra of new membrane and (a) membranes fouled with enzymatic solutions at 2, 7.5 and 15 g/L; (b) membranes cleaned with NaCl (enzymatic solution concentration during fouling: 2, 7.5 and 15 g/L); (c) membranes cleaned with NaCl and Na_2SO_4 (enzymatic solution concentration during fouling: 15 g/L)*

Mathematical modelling

The mean value of the intrinsic membrane resistance (R_m) was $3.8 \cdot 10^{12}$ m^{-1}. This value was taken as a constant in the resistance-in-series model.

Fig. 56 shows the time evolution of the experimental permeate flux obtained for all the feed solutions tested. As expected, a lower permeate flux was measured by increasing the protein concentration due to a more severe membrane fouling.

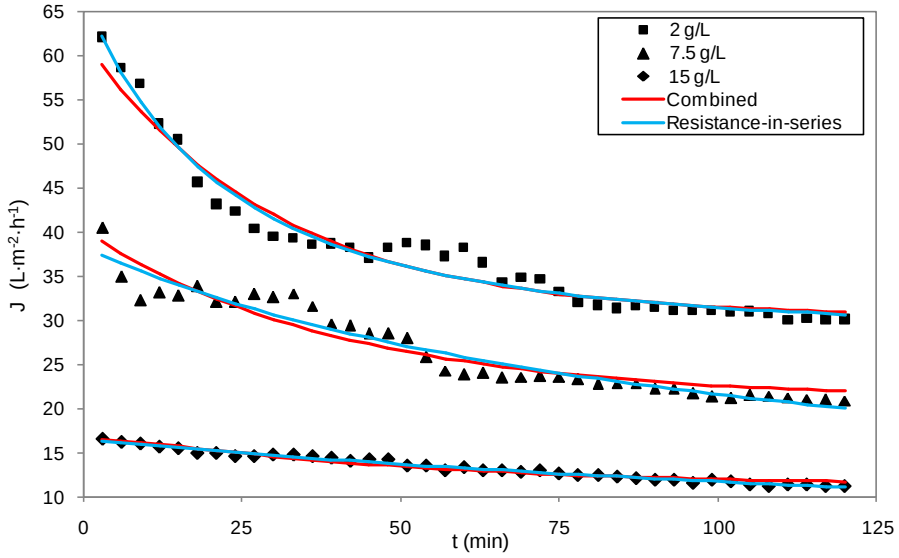

Fig. 56. *Permeate flux predictions for the best fitting models using enzymatic solutions (lines: estimated results; symbols: experimental data)*

This is in accordance with the AFM image (Fig. 54d) where all the membrane pores appear to be fully covered by a protein layer. Fig. 56

also shows the permeate flux predictions by the two models with the highest fitting accuracy (highest regression coefficient, R^2, and lowest standard deviation, SD). In all cases, resistance-in-series and the combined model were the models with the best fitting accuracy for all the feed solutions tested, with values of R^2 ranging from 0.91 to 0.99 and SD values from 0.01 to 0.04, while the accuracy of Hermia's models varied from 0.85 to 0.96 for R^2 values and from 0.03 to 0.06 for SD. Both resistance-in-series and combined models considered that complete blocking/adsorption and cake formation were the main mechanisms contributing to membrane fouling. Therefore, both mechanisms should be considered to explain the membrane fouling with enzymatic solutions at the experimental conditions tested (2 bar, 2 m/s and 25 ºC).

Table 30 shows the values of model parameters for the best fitting models. The values of the parameters R'_{ad}, R_c, K_c, K_{cf} and α increased when protein concentration increased. This is due to the fact that more severe membrane fouling occurs with increasing protein concentration in the feed solutions. A similar behaviour was observed in the MF process of BSA solutions (de la Casa *et al.*, 2008).

Table 30. Values of model parameters for the best fitting models

Protein concentration (g/L)	Resistance-in-series model			Combined model		
	R'_{ad} (m^{-1})	b (s^{-1})	R_c (m^{-1})	K_c (s^{-1})	K_{cf} (s/m^2)	α
2	$1.54 \cdot 10^{13}$	$3.63 \cdot 10^{-4}$	$8.18 \cdot 10^{12}$	32.55	$2.51 \cdot 10^{6}$	0.937
7.5	$8.86 \cdot 10^{13}$	$3.38 \cdot 10^{-5}$	$1.72 \cdot 10^{13}$	36.10	$1.87 \cdot 10^{7}$	0.967
15	$3.71 \cdot 10^{17}$	$8.99 \cdot 10^{-9}$	$4.51 \cdot 10^{13}$	60.85	$5.07 \cdot 10^{9}$	1.000

Regarding the value of the parameter α, which indicates the fraction of completely blocked pores (Eq. 40), the predominant fouling mechanism was complete blocking for all the feed solutions tested. This is in agreement with the particle size measured: the largest size of pectinase molecules (50 kDa) compared to the membrane MWCO (30 kDa) allows these particles to be deposited on the membrane surface blocking the pore entrance. On the other hand, concentration polarization increased when protein concentration increased (Jarusutthirak *et al.*, 2007) and thus, the value of the resistance R'_{ad} that considers both adsorption and concentration polarization phenomena at steady-state, was the highest at 15 g/L. In addition, as displayed in AFM images (Fig. 54d), at the highest concentration tested, the cake formed on the membrane surface was denser. This resulted in the increased parameters related to the cake formation, R_c and K_{cf}. Regarding the intermediate pectinase concentration (7.5 g/L), the values of all these parameters also increased from those obtained at 2 g/L, due to the partial formation of the protein layer on the membrane surface (Fig. 54c). However, the values of the model parameters were much lower than those obtained at 15 g/L, as there were initial membrane regions uncovered at the intermediate protein concentration. However, the same pattern was not observed for the parameter *b*, which represents the rate at which foulant molecules are adsorbed on membrane surface. In this case, when protein concentration increased, the value of *b* decreased. As the ATR-FTIR spectra of the fouled membranes indicated, at the lowest concentration used (2 g/L), the protein-membrane interaction became greater due to the low amount of proteins compared to that when working at 15 g/L. As a consequence, proteins were deposited on

membrane surface at a higher rate than in the case of high protein concentration.

8.1.3.2. Membrane cleaning

Fig. 55b shows the spectra of the virgin and the cleaned membranes that were fouled with enzymatic solutions at protein concentrations of 2, 7.5 and 15 g/L. As it can be observed, an almost total overlapping among all the spectra was obtained, which is an indicator of the removal of protein deposits on the membrane surface using NaCl as cleaning agent at a concentration of 5 mM and 50 ºC. The only exceptions are the appearance of a band at a frequency of 1750 cm^{-1}, which can be attributed to ester carbonyl and a band at a frequency of 1040 cm^{-1}, which can be related to the C-N stretching vibrations typical of proteins (Pihlajamäki *et al.*, 1998). The band intensity is somewhat significant on fouled membranes (Fig. 55a) whereas it remained becomes negligible after the cleaning procedure (Fig. 55b). This provides indications about the efficiency of the cleaning procedures, the presence of some residual contaminants being onto the membrane surface.

Table 31 shows the results of residual protein concentration adsorbed on membranes and of the cleaning efficiency. Regarding the values of protein concentration after NaCl cleaning, it can be observed that all membranes showed a low amount of proteins on their surface, even if a gradual increase in the residual adsorption was detected for membranes fouled at higher protein concentration. Indeed the

deposition of larger amount of protein at higher concentration was also revealed by AFM analyses. These results are in good agreement with those obtained by Rabiller-Baudry *et al.* (2012) which studied the efficiency of several cleaning agents for PES UF membranes fouled with skim milk. In this case the best cleaning agents led to a residual protein concentration from 3 to 11 μg/cm^2 at a transmembrane pressure of 1 bar. On the other hand, according to the cleaning efficiency evaluation (Table 31), it can be concluded that the low protein amount deposited on the membrane surface for the different protein concentrations tested did not greatly affect the membrane permeation properties.

Table 31. Residual protein concentration after cleaning procedure and water permeability recovery

Membrane	Protein concentration during fouling (g/L)	Residual protein concentration (μg/cm^2)	Cleaning efficiency (%)
Cleaned with NaCl	2	4±1	100±3
	7.5	9±1	100±3
	15	14±2	100±1
Cleaned with Na_2SO_4	15	25±1	97±1

The effect of salt type on the cleaning efficiency was also studied by means of ATR-FTIR measurements. Fig. 55c shows the spectra of the virgin and cleaned membranes, previously fouled with a 15 g/L protein concentration, by using NaCl and Na_2SO_4 solutions. It is relevant to observe the appearance of two bands at 1504 cm^{-1} and 1168 cm^{-1} in the spectrum associated to membranes cleaned with Na_2SO_4 (Fig. 55c). This suggests the presence of residual proteins not completely removed by the cleaning procedure. As previously

described, these two bands indicate a different protein rearrangement on the membrane surface at lower protein concentration. Indeed, the spectrum is comparable to that recorded onto membranes fouled with 2 g/L pectinase (Fig. 55a). In addition, the shift of the infrared mode located around 1620 cm^{-1} towards higher frequency suggests a contribution of the band usually assigned to intermolecular β-sheets bonds, well known as "aggregation band" (Blume *et al.*, 2015; Matheus *et al.*, 2006). This shift is also observable for membranes coming in contact with 2 g/L pectinase solution (Fig. 55a).

The residual protein concentration quantified from the ATR-FTIR spectrum was calculated for the Na_2SO_4 cleaning protocol (Table 31). In this table, the greatest amount of protein deposited on the membrane surface after cleaning procedure was obtained with Na_2SO_4 (24.68 µg/cm^2) and the cleaning efficiency was slightly lower than those obtained when NaCl was used as cleaning agent.

The different cleaning efficiency obtained with the two salt solutions can be ascribed to salting-in and salting-out mechanisms. Na_2SO_4 showed a strong salting-out effect and enhanced protein aggregation and adsorption according to Tsumoto *et al.* (2007). In addition, SO_4^{2-} exhibits a salting-out effect higher than Cl^-, causing a protein precipitation. This is due to the different ability of anions to interact with water molecules (Curtis and Lue, 2008). According to the law of matching water affinities, monovalents anions (as Cl^-) are weakly hydrated because they have a larger size than monovalent cations and they preferably interact with the positive-charged side chains of proteins and with the non-polar functional groups that are weakly

hydrated as well (Zhang, 2012). This behaviour was also observed in a previous study about salt cleaning of membranes fouled with whey model solutions (Corbatón-Báguena *et al.*, 2014b), in which similar efficiencies to those reported in Table 31 after the cleaning procedure were achieved.

On the basis of these experimental findings, DLS analyses were also performed in order to evaluate the combined effect of NaCl and temperature on protein aggregates destabilization/solubilisation. As it can be observed in Table 29 membrane cleaning with NaCl at 50 °C led to an additional protein aggregates destabilization that enhances salting-in effects. In particular, when the temperature was increased from 25 °C to 50 °C, with and without NaCl, the changes in size observed for the particles belonging to both the first and second distribution were statistically significant (p-values lower than 0.05), while a big effect of particle decrease is observed for the distribution 2. This effect demonstrated that the distribution 2 is characterized by big aggregates that, thanks to a temperature effect, are destabilized. In addition, for what concerns particles belonging to distribution 1, any substantial change is observed both increasing temperature and in presence of NaCl (5mM), but a greater change in size is observed for particles belonging to distribution 2. In this last case, the combination of NaCl and temperature (50 ºC) resulted in a decrease in particle size from 288 to 240 nm. At higher temperature protein hydration is favoured. This means that protein-water bonds are predominant, causing solubilisation of protein aggregates. In the presence of NaCl, protein-protein interactions are further broken due to salting-in effects,

thus promoting higher hydration shell (Tsumoto *et al.*, 2007; Zhang *et al.*, 2012).

8.1.4. Conclusions

Fouling experiments performed with enzymatic solutions of pectinases at different protein concentrations (2, 7.5 and 15 g/L) demonstrated that a higher protein concentration caused a more severe UF membrane fouling. AFM images as well as ATR measurements carried out on the virgin and fouled membranes confirmed that a continuous protein layer was formed on the membrane surface when a concentration of 15 g/L was used.

The mathematical models studied in this work predicted with high accuracy the experimental permeate flux decline corresponding to the UF of enzymatic solutions of pectinases at different protein concentration (2, 7.5 and 15 g/L), 2 bar and 2 m/s. The Hermia's standard blocking model did not fit well the experimental data since the solute molecules size was larger than the membrane pore size and thus, these molecules cannot penetrate inside the membrane pores. Adversely, the models that showed the best fitting accuracy were the combined model and the resistance-in-series, one of which suggested a predominant pore blocking/adsorption mechanism, followed by a cake formation.

Among the salts tested, NaCl showed better results than Na_2SO_4 due to a better ability to dissolve proteins from membrane surface for

salting-in effect. The cleaning efficiency of NaCl in combination with temperature was also investigated by DLS experiments, thus confirming a cooperation of the two parameters in the protein aggregates destabilization. The cleaning efficiency was investigated through water permeability measurements. Although some residual contaminants were still present after cleaning with NaCl solution, the initial permeability value was completely restored. The suitability and reliability of the cleaning procedure with NaCl was confirmed with other protein solutions (whey model solutions), achieving similar cleaning efficiencies.

Acknowledgements

María-José Corbatón-Báguena wishes to gratefully acknowledge the financial support from the Spanish Ministry of Economy and Competitiveness through the grant EEBB-I-14-09011 (project CTM2010-20186). The authors acknowledge the European Union, Fondo Europeo di Sviluppo Regionale, The Ministero dell'Istruzione, dell'Università e della Ricerca - MIUR, The Ministero dello Svilupppo Economico - MSE - for the financial support to the project “Sistemi tecnologici avanzati e processi integrati della filiera olivicola per la valorizzazione dei prodotti e dei sottoprodotti, lo sviluppo di nuovi settori e la creazione di sistemi produttivi Eco-compatibili” (PON Olio Più, PON01_01545), within the framework PON Ricerca e Competitività 2007-2013.

8.2. BIBLIOGRAFÍA

ALCHEIKHHAMDON A.A., DARWISH N.A. y HILAL N. (2015). "Statistical analysis of air-gap membrane desalination experimental data: Hypothesis testing" en *Desalination,* vol. 362, p. 117-125.

BLANPAIN-AVET P., MIGDAL J.F. y BÉNÉZECH T. (2009). "Chemical cleaning of a tubular ceramic microfiltration membrane fouled with a whey protein concentrate suspension – characterization of hydraulic and chemical cleanliness" en *Journal of Membrane Science*, vol. 337, p. 153-174.

BLUME K. *et al.* (2015). "Exploring the relationship between protein secondary structures, temperature-dependent viscosities, and technological treatments in egg yolk and LDL by FTIR and rheology" en *Food Chemistry*, vol. 173, p. 584-593.

CARRÈRE H., BLASZKOW F. y ROUX DE BALMANN H. (2001). "Modelling the clarification of lactic acid fermentation broths by cross-flow microfiltration" en *Journal of Membrane Science*, vol. 186, p. 219-230.

CASSANO A., MARCHIO M. y DRIOLI E. (2007). "Clarification of blood orange juice by ultrafiltration: analyses of operating parameters, membrane fouling and juice quality" en *Desalination*, vol. 212, p. 15-27.

CHOI S-W. *et al.* (2000). "Modeling of the permeate flux during microfiltration of BSA-adsorbed microspheres in a stirred cell" en *Journal of Colloid and Interface Science*, vol. 228, p. 270-278.

CORBATÓN-BÁGUENA M.J., ÁLVAREZ-BLANCO S. y VINCENT-VELA M.C. (2014a). "Cleaning of ultrafiltration membranes fouled

with BSA by means of saline solutions" en *Separation and Purification Technology*, vol. 125, p. 1-10.

CORBATÓN-BÁGUENA M.J., ÁLVAREZ-BLANCO S. y VINCENT-VELA M.C. (2014b). "Salt cleaning of ultrafiltration membranes fouled by whey model solutions" en *Separation and Purification Technology*, vol. 132, p. 226-233.

CURTIS R.A. y LUE L. "A molecular approach to bioseparations: protein-protein and protein-salt interactions" en *Chemical Engineering Science*, vol. 61, p. 907-923.

DE BARROS S.T.D. *et al.* (2003). "Study of fouling mechanism in pineapple juice clarification by ultrafiltration" en *Journal of Membrane Science*, vol. 215, p. 213-224.

DE BARTOLO L. *et al.* (2004). "Novel PEEK-WC membranes with low plasma protein affinity related to surface free energy parameters" en *Journal of Materials Science: Materials in Medicine*, vol. 15, p. 877-883.

DE LA CASA E.J. *et al.* (2008). "A combined fouling model to describe the influence of the electrostatic environment on the cross-flow microfiltration of BSA" en *Journal of Membrane Science*, vol. 318, p. 247-254.

DE LUCA G., GUGLIUZZA A. y DRIOLI E. (2009). "Competitive hydrogen-bonding interactions in modified polymer membranes: A density functional theory investigation" en *Journal of Physical Chemistry B,* vol. 113, p. 5473-5477.

FIELD R.W. *et al.* (1995). "Critical flux concept for microfiltration fouling" en *Journal of Membrane Science*, vol. 100, p. 259–272.

GEBREYOHANNES A.Y. *et al.* (2013). "Study on the *in situ* enzymatic self-cleansing of microfiltration membrane for valorization

of olive mill wastewater" en *Industrial & Engineering Chemistry Research*, vol. 52, p. 10396-10405.

HERMIA J. (1982). "Constant pressure blocking filtration laws – application to powerlaw non-newtonian fluids" en *Trans IChemE*, vol. 60, p. 183-187.

HO C-C. y ZYDNEY A.L. (2000). "A combined pore blockage and cake filtration model for protein fouling during microfiltration" en *Journal of Colloid and Interface Science*, vol. 232, p. 389-399.

JARUSUTTHIRAK C., MATTARAJ S. y JIRARATANANON R. (2007). "Influence of inorganic scalants and natural organic matter on nanofiltration membrane fouling" en *Journal of Membrane Science*, vol. 287, p. 138-145.

JAYANI R.S., SAXENA S. y GUPTA R. (2005). "Microbial pectinolytic enzymes: A review" en *Process Biochemistry*, vol.40, p. 2931-2944.

KRIEG R.C. *et al.* (2005). "Protein quantification and its tolerance for different interfering reagents using the BCA-method with regard to 2D SDS PAGE" en *Journal of Biochemical and Biophysical Methods*, vol. 65, p. 13-19.

LEE S. y ELIMELECH M. (2007). "Salt cleaning of organic-fouled reverse osmosis membranes" en *Water Research*, vol. 41, p. 1134-1142.

LUO J. *et al.* (2013). "Fouling-induced enzyme immobilization for membrane reactors" en *Bioresource Technology,* vol. 147, p. 260-268.

MACHADO R.M.D. *et al.* (2012). "Effect of enzymatic treatment on the cross-flow microfiltration of açaí pulp: Analysis of the fouling and recovery of phytochemicals" en *Journal of Food Engineering*, vol. 113, p. 442-452.

MATHEUS S., MAHLER H.C. y FRIESS W. (2006). "A critical evaluation of T-m (FTIR) measurements of high-concentration IgG(1) antibody formulation development tool" en *Pharmaceutical Research*, vol. 23, p. 1617-1627.

MATTISON K.W. y KASZUBA M. (2004). "Automated protein characterization" en *American Biothecnology Laboratory*, vol. 22, p. 8-11.

MATZINOS P. y ÁLVAREZ R. (2002). "Effect of ionic strength on rinsing and alkaline cleaning of ultrafiltration inorganic membranes fouled with whey proteins" en *Journal of Membrane Science*, vol. 208, p. 23-20.

MAZZEI R., DRIOLI E. Y GIORNO L. (2010). "Membranes and Membrane Bioreactors" en Drioli E., Giorno L. *Comprehensive Membrane Science and Engineering*. Reino Unido: Academic Press.

MORTON R.E. y EVANS T.A. (1992). "Modification of the bicinchoninic acid protein assay to eliminate lipid interference in determining lipoprotein protein content" en *Analytic Biochemistry*, vol. 204, p. 332-334.

MUTHUKUMARAN S. *et al.* (2004). "The use of ultrasonic cleaning for ultrafiltration membranes in the dairy industry" en *Separation and Purification Technology*, vol. 39, p. 99-107.

OGUNBIYI O.O., MILES N.J. y HILAL N. (2008). "The effects of performance and cleaning cycles of new tubular ceramic microfiltration membrane fouled with a model yeast suspension" en *Desalination*, vol. 220, p. 273-289.

OHNISHI S., MURATA M. y HATO M. (1998). "Correlation between surface morphology and surface forces of protein A adsorbed on mica" en *Biophysical Journal*, vol. 74, p. 455-465.

PIHLAJAMÄKI A., VÄISÄNEN P. y NYSTRÖM M. (1998). "Characterization of clean and fouled polymeric ultrafiltration membranes by Fourier transform IR spectroscopy-attenuated total reflection" en *Colloids Surfaces A: Physicochemical Engineering Aspects*, vol. 138, p. 323-333.

RABILLER-BAUDRY M. *et al.* (2008). "A dual approach of membrane cleaning based on physic-chemistry and hydrodynamics. Application to PES membrane of dairy industry" en *Chemical Engineering and Processing*, vol. 47, p. 267-275.

RABILLER-BAUDRY M. *et al.* (2012). "Coupling of SEM-EDX and FTIR-ATR to (quantitatively) investigate organic fouling on porous organic and composite membranes" en Méndez-Vilas A. *Current Microscopy Contributions to Advances in Science and Technology.* Badajoz: Formatex.

RAMÍREZ H.L. *et al.* (2013). "Immobilization of pectinase by adsorption on an alginate-coated chitin support" en *Biotecnología Aplicada*, vol. 30, p. 101-104.

SCHULTZ N. *et al.* (2008). "Zeta potential measurement as a diagnostic tool in enzyme immobilization" en *Colloids Surface B: Biointerfaces*, vol. 66, p. 39-44.

TARAZAGA C.C., CAMPDERRÓS M.E. y PÉREZ-PADILLA A. (2006). "Physical cleaning by means of electric field in the ultrafiltration of a biological solution" en *Journal of Membrane Science*, vol. 278-p. 219-224.

TSUMOTO K. *et al.* (2007). "Effects of salts on protein-surface interactions: Applications for column chromatography" en *Journal of Pharmaceutical Science*, vol. 96, p. 1677-1690.

VINCENT VELA M.C. *et al.* (2009). "Analysis of membrane pore blocking models adapted to crossflow ultrafiltration in the ultrafiltration of PEG" en *Chemical Engineering Journal*, vol. 149, p. 232-241.

YUA L. *et al.* (2013). "Adaptive hydrophobic and hydrophilic interactions of mussel foot proteins with organic thin films" en *Proceedings of the National Academy of Sciences*, vol. 110, p. 15680-15685.

ZHANG F. *et al.* (2012). "Hydration and interactions in protein solutions containing concentrated electrolytes studied by small-angle scattering" en *Physical Chemistry Chemical Physics,* vol. 14, p. 2483-2493.

ZHANG J. (2012). "Protein-protein interactions in salt solutions" en Cai W. y Hong H. *Protein-protein interactions – Computational and experimental tools*. Intech.

CAPÍTULO IX

Limpieza de membranas mediante campos eléctricos

9.1. LIMPIEZA DE MEMBRANAS DE ULTRAFILTRACIÓN ENSUCIADAS CON DISOLUCIONES MODELO DE LACTOSUERO

El presente Capítulo constituye una adaptación al formato de la Tesis Doctoral del artículo titulado "Application of electric fields to clean ultrafiltration membranes fouled with whey model solutions", en revisión en la revista Separation and Purification Technology. En él se investiga la eficacia del proceso de limpieza de membranas de UF ensuciadas con disoluciones modelo de lactosuero y limpiadas mediante la aplicación de un método físico (campos eléctricos). Para ello, se utilizaron membranas cerámicas de 15 y 50 kDa ensuciadas con BSA, BSA con $CaCl_2$ y WPC. Además, se estudió la influencia de las condiciones de operación durante la etapa de limpieza (concentración de NaCl, temperatura y potencial de campo eléctrico aplicado), sobre la eficacia hidráulica del proceso de limpieza. Los datos bibliográficos del artículo se destacan a continuación:

***Autores**: M.-J. Corbatón-Báguena, S. Álvarez-Blanco, M.-C. Vincent-Vela, E. Ortega-Navarro, V. Pérez-Herranz*

***Título**: Application of electric fields to clean ultrafiltration membranes fouled with whey model solutions*

***Editorial**: Elsevier*

***Revista**: en revisión en Separation and Purification Technology*

***Doi**:*

Application of electric fields to clean ultrafiltration membranes fouled with whey model solutions

María-José Corbatón-Báguena[1], Silvia Álvarez-Blanco[1], María-Cinta Vincent-Vela[1], Emma Ortega-Navarro[2], Valentín Pérez-Herranz[2]

[1]*Institute for Industrial, Radiophysical and Environmental Safety, Department of Chemical and Nuclear Engineering, Universitat Politècnica de València, C/Camino de Vera s/n 46022 Valencia, Spain*

[2]*IEC Group, Departament d'Enginyeria Química i Nuclear, Universitat Politècnica de València, C/Camino de Vera s/n 46022 Valencia, Spain*

*Corresponding author: sialvare@iqn.upv.es
Tel: +34963879630 (Ext.: 796383)
Fax: +34963877639 (Ext.: 77639)

Abstract

In this work, the effectiveness of electric fields to clean two ZrO_2-TiO_2 ultrafiltration (UF) membranes fouled with three types of whey model solutions was investigated. Membranes tested had different molecular weight cut-offs (MWCOs) (15 and 50 kDa). Whey model solutions consisted of aqueous solutions of bovine serum albumin (BSA) at 10 $g \cdot L^{-1}$, a mixture of BSA (10 $g \cdot L^{-1}$) and $CaCl_2$ (1.65 $g \cdot L^{-1}$) and whey protein concentrate (WPC) (total protein content 45 %) solutions at

different concentrations (22.2, 33.3 and 150.0 $g \cdot L^{-1}$). The hydraulic cleaning efficiency (HCE) achieved by means of the application of the electric fields was evaluated as a function of the membrane MWCO and the operating conditions of the cleaning technique (applied potential, temperature of the cleaning solution and concentration of NaCl). The results demonstrated that the presence of NaCl favoured the removal of protein deposits on the membrane layer. On the other hand, the higher the temperature of the cleaning solution and the applied potential were, the higher HCE was achieved. Regarding the membrane MWCO, the permselective properties of the 15 kDa membrane were completely recovered after the cleaning procedure by electric field for all the feed fouling solutions tested, whereas this technique could not completely remove the protein deposits on the 50 kDa membrane when BSA solutions were used as feed.

Keywords: Ultrafiltration; membrane cleaning; electric fields; whey model solutions.

9.1.1. Introduction

Ultrafiltration (UF) is one of the most widely used techniques in dairy industries to dehydrate milk, concentrate whey and fractionate and purify proteins (Ogunbiyi *et al.*, 2008; Kazemimoghadam and Mohammadi, 2007). However, the implementation of membrane separation processes at industrial scale has a major limitation: membrane fouling. This drawback is due to the combination of several phenomena, such as concentration polarization, pore blocking or cake formation, among others (Zumbusch *et al.*, 1998).

In dairy industries, proteins are one of the compounds mainly responsible for membrane fouling, because they can be deposited on membrane surface and also, be adsorbed inside the membrane porous structure (Almécija *et al.*, 2009). In addition, when whey and WPC solutions are ultrafiltered, the salts presented in these solutions (especially calcium salts) can act as binding agents between proteins, favouring their aggregation and accumulation onto the membrane surface (Ang and Elimelech, 2007). In order to minimize membrane fouling, several researchers have investigated the interaction among proteins, between proteins and membranes and also, protein-inorganic compounds interactions (Almécija *et al.*, 2009; Ang and Elimelech, 2007; Mo *et al.*, 2008). Other authors studied different pretreatments focused on increasing protein solubility and limiting salt-protein bridging during the UF process (Adams *et al.*, 2013).

Since pretreating the feed solutions used during the UF may not be enough to completely avoid membrane fouling, membranes have to be cleaned to remove the foulant deposits and restore their initial permeation properties. The conventional cleaning protocol employed when treating dairy solutions includes an alkali cleaning step followed by an acid cleaning stage. If this cleaning procedure cannot completely remove the protein deposits, a subsequent cleaning step using sodium hypochlorite or sodium dodecyl sulphate can be carried out (Ogunbiyi *et al.*, 2008; Kazemimoghadam and Mohammadi, 2007; Almécija *et al.*, 2009). However, as these procedures may be performed even once per day in dairy industries (Blanpain-Avet *et al.*, 2009), the abovementioned conventional cleaning agents may damage the membranes, reducing their lifetime and causing

morphological modifications. In addition, the discharge of these chemicals as wastewaters results in a negative environmental impact. For all these reasons, during the last years several researchers have focused their studies on the development and implementation of non conventional cleaning techniques, for instance, ultrasounds (Muthukumaran *et al.*, 2007), saline solutions (Lee and Elimelech, 2007; Corbatón-Báguena 2014b) or electric fields.

This last technique, the application of electric fields, has been used by other authors to improve permeate flux during the UF of different feed solutions. They demonstrated that the total hydraulic resistance achieved at the end of this process is reduced and concentration polarization is minimized (Zumbusch *et al.*, 1998; Tarazaga *et al.*, 2006; Song *et al.*, 2010; Holder *et al.*, 2013). This technique is based on two electrokinetic phenomena: on one hand, the charged particles move towards the electrode with opposite sign when the electric field is applied (electrophoresis) and, on the other hand, a liquid (usually water, as most of the times aqueous solutions are ultrafiltered) is forced to move to a charged surface (for example, the membrane pores), which is known as electro-osmosis. Both effects, electrophoresis and electro-osmosis, are achieved by placing two electrodes at both sides of the membrane or using only one electrode, being the membrane the other one. This last case is very often used in the case of ceramic membranes, as they are made of electrically conductive materials (Shi *et al.*, 2014).

Zumbusch *et al.* (1998) investigated the utilization of alternating electrical fields to reduce membrane fouling during the UF of biological suspensions and studied the effect of several operating conditions (field strength, protein concentration and conductivity) on fouling decrease. Although both direct and alternating current can be used, the former is suitable only when the particles in the feed fouling solution have a uniform charge. They reported that high field strength and an increase in conductivity up to the limiting electrolytic current led to a more effective cleaning procedure. However, the increase in protein concentration reduced the effect of the electric field applied. Tarazaga *et al.* (2006) used electric field pulses of 2-3 min to restore the initial membrane permeate flux during the filtration of bovine plasma at a concentration of 0.5 %w/w at a pH of 7.8. They applied three different potentials (10, 15 and 30 V) and demonstrated that the higher the electric potential was, the greater the permeate flux was after the electric pulses. Holder *et al.* (2013) investigated the effect of electric fields on the fractionation of bio-functional peptides from micellar casein hydrolysate. After the UF experiments, these authors reversed the polarity of the electrodes in order to study the effectiveness of electric fields to clean the membranes. They indicated that this technique was able to completely remove some peptides deposited on membrane surfaces because Van der Waals forces also influenced the fouling process.

Although there are several works available in the literature focused on the application of electric fields, they applied electric pulses during the feed solution filtration to recover the permeate flux once it decreased up to a certain value or to minimize the concentration polarization

phenomenon. However, only a few papers deal with the application of this technique during the cleaning step, i.e. after the membrane was fouled by the feed solution treatment (Holder *et al.*, 2013). The main goal of this work is to evaluate the effectiveness of a physical cleaning procedure based on the application of electric fields to clean membranes previously fouled with whey model solutions. In addition, the effect of different cleaning operating conditions, such as applied potential, temperature of the cleaning solution and concentration of NaCl used as electrolyte, on the efficiency of the cleaning procedure was determined. The novelty of this work lies in the application of the electric fields during the cleaning step in order to remove the irreversible fouling caused on the membranes and not during the fouling stage as other authors reported to minimize fouling and the concentration polarization phenomena (Tarazaga *et al.*, 2006; Sarkar *et al.*, 2009).

9.1.2. Materials and methods

9.1.2.1. Chemicals

Whey model solutions used during the fouling step consisted of BSA (10 $g \cdot L^{-1}$), BSA (10 $g \cdot L^{-1}$) with $CaCl_2$ (1.65 $g \cdot L^{-1}$) and WPC (22.2, 33.3 and 150.0 $g \cdot L^{-1}$) aqueous solutions. As these products were supplied in powder form, a certain amount was weighted and dissolved in deionized water until the desired concentration was achieved. Renylat WPC solutions were supplied by Industrias Lácteas Asturianas S.A. (Spain), BSA (lyophilized powder after heat shock fractionation, 98 % purity, A3733) was provided by Sigma-Aldrich (Germany) and $CaCl_2$

(95 % purity) was purchased from Panreac (Spain). The main components of the WPC used are shown in Table 32. The methods employed for determining the concentration of each component are described elsewhere (Corbatón-Báguena *et al.*, 2015). Due to the neutral pH of the feed solutions, BSA and the main proteins of WPC were negatively charged.

Table 32. Main components of the Renylat WPC used as feed solution

Component	Dry basis concentration (% w/w)
Dry matter	93.66 ± 0.95
Proteins	40.74 ± 0.79
Lactose	38.27 ± 0.49
Fat	8.14 ± 0.20
Ash	7.85 ± 0.07
Ca	0.79 ± 0.06
Na	1.21 ± 0.09
K	1.42 ± 0.02
Cl	4.07 ± 0.24
PO_4-*P*	0.37 ± 0.03

Previous authors (Wang and Tang, 2011; Afonso *et al.*, 2009) reported the utilization of BSA and WPC solutions as whey model solutions for UF tests. In order to study the influence of salt presence on protein behaviour, $CaCl_2$ was one of the salts most often used as calcium ion favours protein-protein interactions and Cl^- is the main anion in whey and WPC [Corbatón-Báguena *et al.*, 2014b; Ang and Elimelech, 2007; Mo *et al.*, 2008).

Finally, NaCl (Panreac, Spain) aqueous solutions were used to clean the membranes in combination with the application of electric fields. In addition, NaOH (98 % purity, Panreac, Spain) aqueous solutions were used to clean the UF membranes if the permselective properties

of the original membranes were not recovered at the end of the cleaning protocol.

9.1.2.2. Membranes

Two monotubular ZrO_2-TiO_2 INSIDE CéRAM^{TM} membranes of 15 and 50 kDa (TAMI Industries, France) were used to perform the experiments. The dimensions of these membranes were a length of 20 cm, an internal diameter of 0.6 cm and an external diameter of 1 cm. Their effective area was 35.5 cm^2. It is important to highlight that these membranes acted as a cathode during the cleaning step.

9.1.2.3. Experimental set-up

All fouling and cleaning tests were carried out in a VF-S11 UF plant (Orelis, France). This plant was equipped with a 10 L feed tank, a variable speed volumetric pump that allowed the crossflow velocity to be maintained constant, two manometers placed at the inlet and outlet streams of the membrane module to measure the transmembrane pressure, a temperature regulating system to control the temperature during the fouling and cleaning stages and a scale (±0.001 g accuracy) to gravimetrically determine the permeate flux.

The abovementioned membranes were placed in a Plexiglas GS® tubular membrane module (Metaval Abella S.L., Spain) and rolled on their external surface by a copper wire to ensure a constant potential distribution on this membrane side. Then, the external membrane surface was connected to the cathode. The second electrode (anode)

consisted of a titanium electrode with an iridium coating (MAGNETO Special Anodes B.V., The Netherlands). The anode was placed inside the membrane, crossing it along the tubular channel. Both cathode and anode were connected to a direct current supplier (Konstanter SSP, Gossen, Germany). It is important to highlight that both electrodes were situated in the position aforementioned in order to promote protein migration from the membrane active layer to the bulk solution, due to the negative charge of most of the whey proteins in the feed fouling solutions. Experiments with the electric fields were performed in potentiostatic mode. The experimental set-up is shown in Fig. 57.

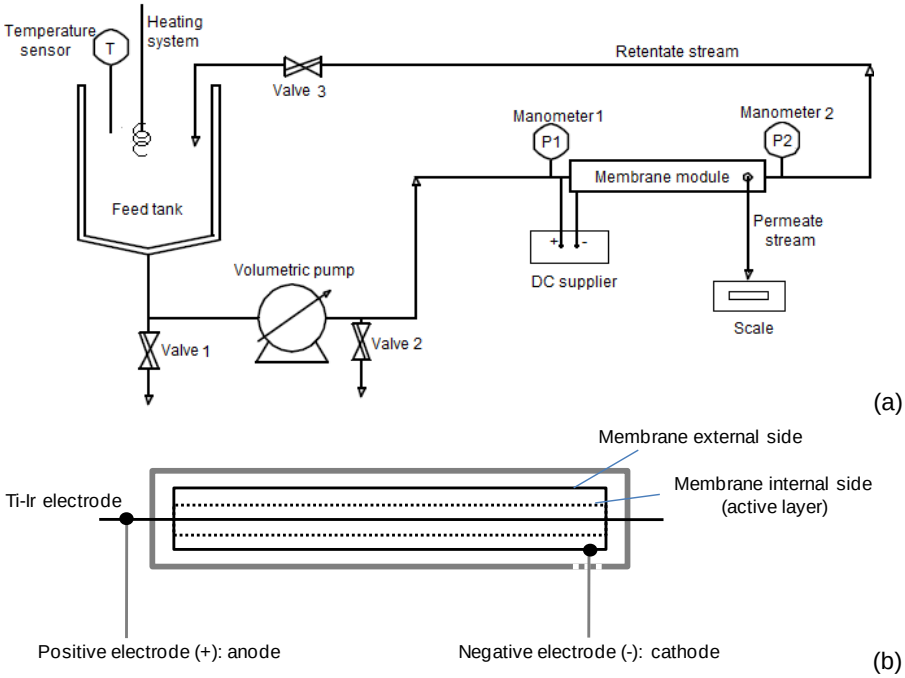

Fig. 57. *Schematic representation of the VF-S11 UF plant connected to a direct current (DC) supplier (a) and electrodes connection in the membrane module (b)*

9.1.2.4. Experimental procedure

Firstly, membranes were fouled with the different feed solutions at a transmembrane pressure of 2 bar, a crossflow velocity of 2 $m \cdot s^{-1}$ and a temperature of 25 ºC, according to previous studies about protein UF (Matzinos and Álvarez, 2002; Corbatón-Báguena *et al.*, 2015).

After the fouling step, membranes were rinsed with deionized water during 30 min at a transmembrane pressure of 1 bar and 4.2 $m \cdot s^{-1}$. Several studies reported that low transmembrane pressures and high crossflow velocities favour the removal of proteins deposited on membrane surfaces (Blanpain-Avet *et al.*, 2009; Lee *et al.*, 2001). Then, a cleaning procedure was carried out at the same transmembrane pressure and crossflow velocities as the rinsing step and varying the applied potential (0, 15 and 30 V), the NaCl concentration (0 and 5 mM) and the temperature of the cleaning solution (25-50 ºC). These conditions were selected according to other works about membrane cleaning by means of electric fields and saline solutions (Tarazaga *et al.*, 2006; Corbatón-Báguena *et al.*, 2014a). Finally, membranes were rinsed again with deionized water to remove the loose protein deposits from the membrane surface as well as the cleaning agents. During all these steps, both the permeate flux and the hydraulic resistance were determined.

An additional conventional cleaning step was performed when needed if the initial membrane hydraulic resistance was not completely recovered after the cleaning procedure. This step was performed with NaOH at a temperature of 50 ºC and pH values about

8.5-9. These conditions were selected to avoid damage of the electrodes or the membrane module.

9.1.2.5. Evaluation of the cleaning efficiency

Due to the destructive nature of the chemical methods to evaluate the efficiency of the cleaning procedure, which consist of the determination of chemical species on the membrane structure by spectroscopic techniques, a hydraulic method was used to calculate the efficiency of the cleaning protocol (HCE). Several authors reported different equations to determine the HCE from the resistance of the membrane after the rinsing and cleaning steps and to the original membrane resistance (Daufin *et al.*, 2001; Matzinos and Álvarez, 2002; Muthukumaran *et al.*, 2007). The values of the membrane resistances after the abovementioned steps were calculated by the Darcy's law (Eq. 44).

$$J = \frac{\Delta P}{\mu \cdot R_m} \qquad \text{Eq. 44}$$

The efficiency after the end of the cleaning protocol was estimated using Eq. 45.

$$HCE\,(\%) = \left(\frac{R_f - R_{r2}}{R_f - R_m} \right) \cdot 100 \qquad \text{Eq. 45}$$

Where HCE is the hydraulic cleaning efficiency, R_f is the resistance at the end of the fouling step, R_{r2} is the resistance at the end of the second rinsing and R_m is the resistance of the original membrane.

9.1.3. Results and discussion

9.1.3.1. Cleaning of membranes fouled with BSA solutions

Results for the 15 kDa membrane

Fig. 58 shows the values of HCE obtained for the 15 kDa membrane using two different cleaning solutions: deionized water at different temperatures (25 and 50 ºC) and NaCl solutions at a concentration of 5 mM and three different temperatures (25, 37.5 and 50 ºC). NaCl concentration was selected according to a previous work by the authors dealing with membrane cleaning by means of saline solutions. These experiments were performed at three different electric field potentials (0, 15 and 30 V) in order to check the influence of both temperature and applied potential on the HCE.

As it can be observed from Fig. 58, an increase in temperature and applied potential during the cleaning step resulted in an increase in the values of HCE achieved. This pattern was previously confirmed by other authors (Tarazaga *et al.*, 2006; Chen *et al.,* 2007; Shi *et al.*, 2014; Corbatón-Báguena *et al.*, 2014a).

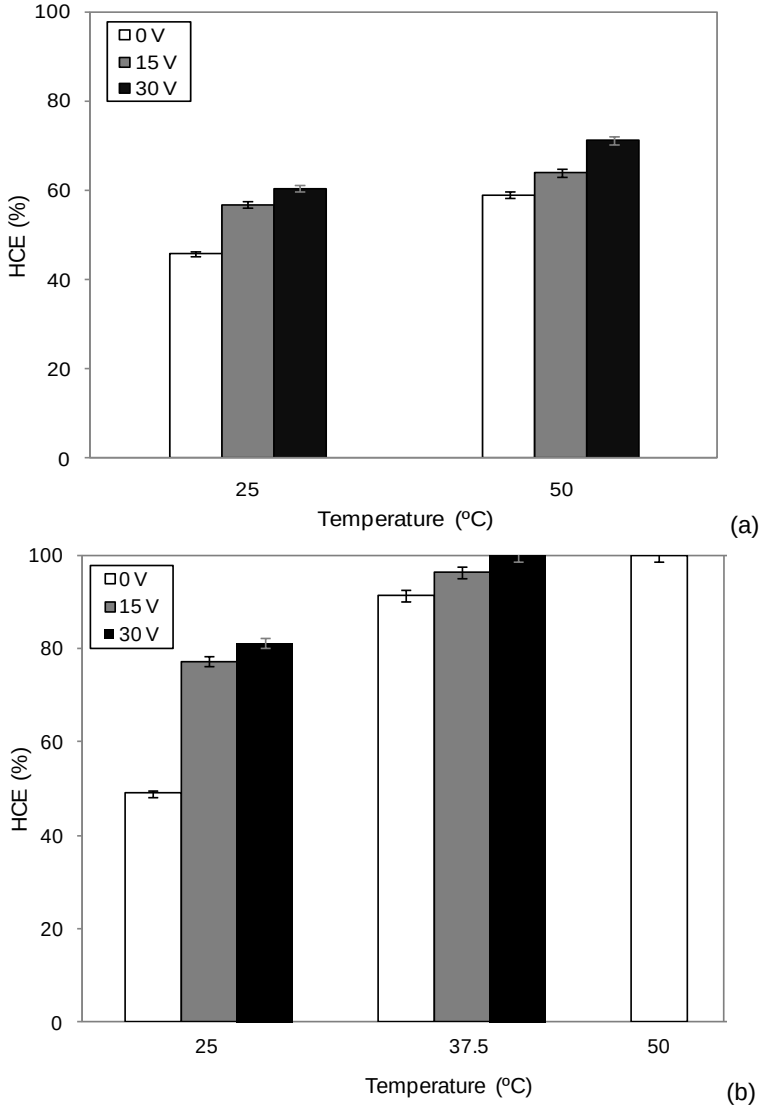

Fig. 58. *Influence of temperature of the cleaning solution and electric field potential on HCE for the 15 kDa membrane using (a) deionized water and (b) NaCl at a concentration of 5 mM as cleaning solution (fouling solution: BSA; operating conditions during cleaning: 1 bar and 4.2 m·s^{-1})*

Tarazaga *et al.* (2006) demonstrated that an increase in the electric field potential caused an increase in the permeate flux obtained

during the membrane fouling with bovine plasma solutions. *Chen et al.* (2007) reported that electric field strengths greater than 15 V resulted in a dramatic decrease of the hydraulic resistance when membranes were fouled with sewage water. This should be due to the greater amount of charged particles migrating from one electrode to another when high electric field potential was applied. This effect was also demonstrated by Shi *et al.* (2014) and Huotari *et al.* (1999) using oily wastewaters during the membrane fouling. According to these authors, the electrophoretic forces increase as the electric field potential increases. These forces are ascribed to the movement of charged particles towards the electrode of opposite sign. In their works, this electrode is placed on the bulk solution channel. For all these reasons, HCE increased as the electric potential increased.

On the other hand, Corbatón-Báguena *et al.* (2014a) tested different temperatures during the cleaning of several UF membranes with deionzed water as well as NaCl solutions. In all cases, an increase in temperature resulted in an increase in the values of HCE achieved. This trend was corroborated by Lee and Elimelech (2007), who demonstrated that the mass transfer process as well as the chemical reactions velocity increased when temperature increased, favouring the weakness of the fouling layer on the membrane surface and easing its removal. Regarding the effect of the saline solutions, results shown in Fig. 58 indicated that higher HCE values were obtained when cleaning was carried out in presence of NaCl at low concentrations (5 mM). When an electric field is applied on NaCl aqueous solutions, different cathodic and anodic reactions occurred on the electrode surfaces (Mook *et al.*, 2012):

Cathode: $2H_2O + 2e^- \rightarrow H_2 + 2OH^-$

Anode: $4OH^- \rightarrow O_2 + 2H_2O + 4e^-$

$2Cl^- \rightarrow Cl_2 + 2e^-$

In addition, when chlorine is in contact with water molecules, hypochlorite is formed due to the following reaction (Mook *et al.*, 2012):

$$Cl_2 + H_2O \rightarrow HOCl + H^+ + Cl^-$$

Hypochlorite formed in this last reaction oxidizes the organic pollutant species (proteins in this work), breaking their bonds to partially decompose them and favouring their removal from the system (Yasri *et al.*, 2015). This technique is known as indirect electrochemical oxidation and has been successfully implemented in the treatment of different organic effluents (Naumczyk *et al.*, 1996; Donaldson *et al.*, 2002). Therefore, as it was expected, the HCE values obtained in presence of NaCl 5 mM were greater than those obtained with deionized water, due to the oxidation of proteins deposited on the membrane surface.

Therefore, the best operating conditions to clean the 15 kDa membrane fouled with BSA solutions were a temperature of 37.5 ºC, an electric field potential of 30 V and a NaCl concentration of 5 mM. When cleaning with NaCl solutions was performed without applying electric fields, a greater temperature (50 ºC) was required to achieve the same HCE, showing that the combination of electric fields and the addition of NaCl is a more efficient membrane cleaning procedure.

Results for the 50 kDa membrane

Fig. 59 shows the effect of temperature of the cleaning solution on the HCE values obtained when the 50 kDa membrane was fouled with BSA solutions and cleaned with different cleaning agents and different electric potentials: NaCl at a concentration of 7.5 mM at 0 and 30 V and NaOH at a concentration of 5 $g \cdot L^{-1}$. These cleaning agent concentrations were selected according to the range of pH recommended by the manufacturer to clean this membrane and previous works about salt cleaning of UF membranes (Corbatón-Báguena *et al.*, 2014a).

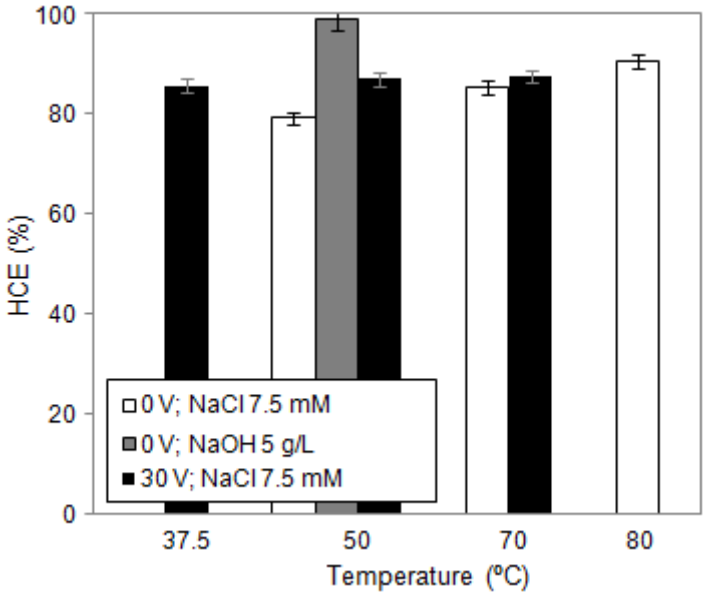

Fig. 59. *Influence of temperature of the cleaning solution and electric field potential on HCE for the 50 kDa membrane using different cleaning agents (fouling solution: BSA; operating conditions during cleaning: 1 bar and 4.2 $m \cdot s^{-1}$)*

As it can be observed, the highest cleaning efficiency was achieved when the conventional cleaning with NaOH solutions was performed. Regarding the cleaning with NaCl solutions, negligible differences in HCE were observed between the cleaning protocol carried out at 37.5 ºC and 30 V and that performed at 80 ºC and 0 V. This fact demonstrated the greater efficiency reached when electric fields were applied, as it was reported for the 15 kDa membrane (Fig. 58). Higher temperatures are required if no electric fields are used to reach the same HCE. Despite the good results obtained when the electrochemical oxidation took place, this technique was not as efficient as the conventional cleaning protocol, even when higher temperatures were used to facilitate protein removal. This may be due to the fact that the amount of hypochlorite formed when an electric field was applied was too low to completely clean this membrane. In a previous work by the authors where this membrane was used to ultrafilter BSA solutions, it was observed that, this membrane shows a very sharp permeate flux decrease at the beginning of the UF process, which indicates severe membrane fouling (Corbatón-Báguena *et al.,* 2014a). The reason for this fact is the similar size between membrane pores (50 kDa) and BSA molecules (67 kDa), which favours that these molecules completely block the membrane pores and/or penetrate inside its porous structure, as it was reported by other authors (Qu *et al.*, 2014). However, permeate flux decline was much lower for the 15 kDa membrane (Corbatón-Báguena *et al.*, 2014a). Therefore, fouling was less severe for this membrane and easier to remove.

9.1.3.2. Cleaning of the 15 kDa membrane fouled with whey model solutions

As electric fields were not able to completely restore the initial membrane permeselective properties in the case of the 50 kDa membrane, only the 15 kDa membrane was used to test the effectiveness of the electrochemical process when whey model solutions (BSA with $CaCl_2$ and WPC solutions at different concentrations) were employed as feed during the fouling step.

The same cleaning operating conditions that resulted in the best HCE values when the membrane was fouled by BSA (1 bar, 4.2 $m \cdot s^{-1}$, 37.5 ºC, 30 V and a NaCl concentration of 5 mM) were tested with the 15 kDa membrane once it was fouled with BSA and $CaCl_2$ and WPC (22.2 $g \cdot L^{-1}$) solutions. The results shown in Fig. 60 demonstrated that the maximum HCE achieved was about 90 % in both cases at the experimental conditions tested. This is due to the more severe membrane fouling caused when salts are introduced in the protein solution. These salts can act as bridging agents between proteins, aggregating them and favouring its deposition on the membrane surface. This behaviour was previously reported by other authors (Nucci and Vanderkooi, 2008; Ang and Elimelech, 2007).

In order to improve the efficiency of the cleaning process, the 15 kDa membrane was cleaned at three different temperatures within the range 37.5-50 ºC. Fig. 61 shows the evolution of HCE with temperature for the BSA with $CaCl_2$ and WPC (22.2, 33.3 and 150.0 $g \cdot L^{-1}$) solutions.

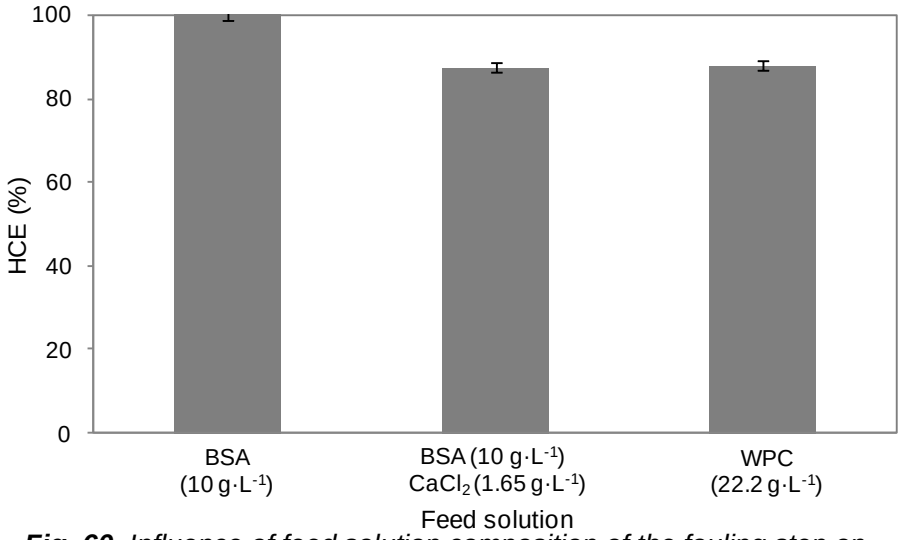

Fig. 60. *Influence of feed solution composition of the fouling step on HCE for the 15 kDa membrane (operating conditions during cleaning: 1 bar, 4.2 m·s^{-1}, 37.5 ºC, 30 V and 5 mM NaCl).*

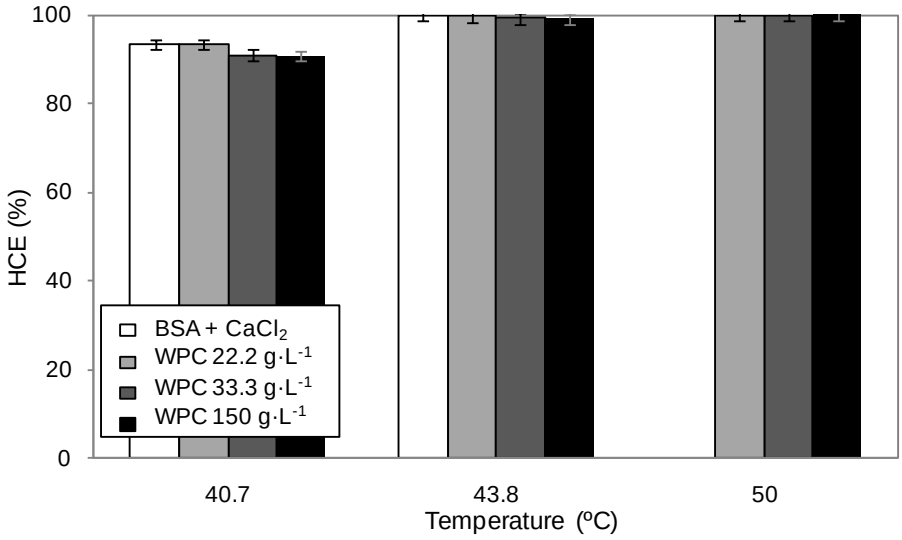

Fig. 61. *Influence of temperature of the cleaning solution on HCE for the 15 kDa membrane (operating conditions during cleaning: 1 bar, 4.2 m·s^{-1}, 30 V and 5 mM NaCl)*

As it can be observed, HCE values about 100 % were obtained at temperatures of 43.8 and 50 ºC. Therefore, an increase in the cleaning solution temperature caused an increase in the HCE as it had been previously observed when this membrane was fouled with BSA solutions (Fig. 58). Therefore, the best operating conditions to carry out the cleaning protocol of the 15 kDa membrane fouled with whey model solutions were 1 bar, 4.2 $m \cdot s^{-1}$, 30 V, 43.8 ºC and a NaCl concentration of 5 mM. As it was expected, the higher the protein concentration in the feed solution was, the more severe the membrane fouling was due to the greater protein aggregation and accumulation on the membrane surface. This fact was previously reported by the authors in works about membrane fouling characterization and modelling in the case of UF membranes fouled with whey model solutions (Corbatón-Báguena *et al.*, 2015). Therefore, the more severe fouling caused by an increase in protein concentration decreased the HCE achieved with the cleaning procedure, requiring harsher operating conditions (higher temperature) to achieve similar HCE values (Zumbusch *et al.*, 1998).

9.1.4. Conclusions

- Cleaning by means of the application of electric fields combined with the addition of NaCl solutions was effective to completely restore the 15 kDa membrane initial permeation properties when it was used to treat different whey model solutions. However, the 50 kDa membrane could not be completely cleaned by this cleaning procedure, probably due

to the more severe fouling that proteins caused in this membrane.

- Results demonstrated that the higher the temperature of the cleaning solution as well as the electric potential were, the higher HCE values were achieved.
- The presence of NaCl at low concentrations (5 mM) favoured membrane cleaning, obtaining HCE values about 100 % at mild temperatures (37.5-50 ºC) for the 15 kDa membrane. This fact is due to the electrochemical oxidation process that occurs when NaCl is used as electrolyte and transformed to hypochlorite by the application of electric fields.
- The best operating conditions to clean the 15 kDa membrane fouled by whey model solutions were a NaCl concentration of 5 mM, a transmembrane pressure of 1 bar, a crossflow velocity of 4.2 $m \cdot s^{-1}$, a electric field potential of 30 V and a temperature around 43.8 ºC.

Acknowledgements

The authors of this work wish to gratefully acknowledge the financial support from the Spanish Ministry of Science and Innovation through the project CTM2010-20186 and the company MAGNETO Special Anodes B.V. for supplying the Ti-Ir electrode.

9.2. BIBLIOGRAFÍA

ADAMS M.C., ZULEWSKA J. y BARBANO D.M. (2013). "Effect of annatto addition and bleaching treatments on ultrafiltration flux during production of 80 % whey protein concentrate and 80 % serum protein concentrate" en *Journal of Dairy Science*, vol. 96, p. 2035-2047.

AFONSO A., MIRANDA J.M. y CAMPOS J.B.L.M. (2009). "Numerical study of BSA ultrafiltration in the limiting flux regime – effect of variable physical properties" en *Desalination*, vol. 249, p. 1139-1150.

ALMÉCIJA M.C. *et al.* (2009). "Influence of the cleaning temperature on the permeability of ceramic membranes" en *Desalination*, vol. 245, p. 708-713.

ANG W.S. y ELIMELECH M. (2007). "Protein (BSA) fouling of reverse osmosis membranes: Implications for wastewater reclamation" en *Journal of Membrane Science*, vol. 296, p. 83-92.

BLANPAIN-AVET P. MIGDAL J.F. y BÉNÉZECH T. (2009). "Chemical cleaning of a tubular ceramic microfiltration membrane fouled with a whey protein concentrate suspension – characterization of hydraulic and chemical cleanliness" en *Journal of Membrane Science*, vol. 337, p. 153-174.

CHEN J.-P. *et al.* (2007). "Study of the influence of the electric field on membrane flux of a new type of membrane bioreactor" en *Chemical Engineering Journal,* vol. 128, p. 177-180.

CORBATÓN-BÁGUENA M.J., ÁLVAREZ-BLANCO S. y VINCENT-VELA M.C. (2014a). "Cleaning of ultrafiltration membranes fouled with BSA by means of saline solutions" en *Separation and Purification Technology*, vol. 125, p. 1-10.

CORBATÓN-BÁGUENA M.J., ÁLVAREZ-BLANCO S. y VINCENT-VELA M.C. (2014b). "Salt cleaning of ultrafiltration membranes fouled by whey model solutions" en *Separation and Purification Technology*, vol. 132, p. 226-233.

CORBATÓN-BÁGUENA M.J., ÁLVAREZ-BLANCO S. y VINCENT-VELA M.C. (2015). "Fouling mechanisms of ultrafiltration membranes fouled with whey model solutions" en *Desalination*, vol. 360, p. 87-96.

DAUFIN G. *et al.* (2001). "Recent and emerging applications of membrane processes in the food and dairy industry" en *Food and Bioproducts Processing*, vol. 79, p. 89-102.

DONALDSON J.D. *et al.* (2002). "Anodic oxidation of the dye materials methylene blue, acid blue 25, reactive blue 2 and reactive blue 15 and the characterization of novel intermediate compounds in the anodic oxidation of methylene blue" en *Journal of Chemical Technology and Biotechnology*, vol. 77, p. 756-760.

HOLDER A., WEIK J. y HINRICHS J. (2013). "A study of fouling during long-term fractionation of functional peptides by means of cross-flow ultrafiltration and cross-flow electro membrane filtration" en *Journal of Membrane Science*, vol. 446, p. 440-448.

HUOTARI H.M., HUISMAN I.H. y TRÄGÅRDH G. (1999). "Electrically enhanced crossflow membrane filtration of oily wastewater using the membrane as a cathode" en *Journal of Membrane Science*, vol. 156, p. 49-60.

KAZEMIMOGHADAM M. y MOHAMMADI T. (2007). "Chemical cleaning of ultrafiltration membranes in the milk industry" en *Desalination*, vol. 204, p. 213-218.

LEE H. *et al.* (2001). "Cleaning strategies for flux recovery of an ultrafiltration membrane fouled by natural organic matter" en *Water Research*, vol. 35, p. 3301-3308.

LEE S. y ELIMELECH M. (2007). "Salt cleaning of organic-fouled reverse osmosis membranes" en *Water Research*, vol. 41, p. 1134-1142.

MATZINOS P. y ÁLVAREZ R. (2002). "Effect of ionic strength on rinsing and alkaline cleaning of ultrafiltration inorganic membranes fouled with whey proteins" en *Journal of Membrane Science*, vol. 208, p. 23-20.

MO H., TAY K.G. y NG H.Y. (2008). "Fouling of reverse osmosis membrane by protein (BSA): Effects of pH, calcium, magnesium, ionic strength and temperature" en *Journal of Membrane Science*, vol. 315, p. 28-35.

MOOK W.T. *et al.* (2012). "Removal of total ammonia nitrogen (TAN), nitrate and total organic carbon (TOC) from aquaculture wastewater using electrochemical technology: A review" en *Desalination*, vol. 285, p. 1-13.

MUTHUKUMARAN S. *et al.* (2007). "The application of ultrasound to dairy ultrafiltration: the influence of operating conditions" en *Journal of Food Engineering*, vol. 81, p. 364-373.

NAUMCZYK J., SZPYRKOWICZ L. y ZILIOGRANDI F. (1996). "Electrochemical treatment of textile wastewater" en *Water Science and Technology*, vol. 34, p. 17-24.

NUCCI N.V. y VANDERKOOI J.M. (2008). "Effects of salts of the Hofmeister series on the hydrogen bond network of water" en *Journal of Molecular Liquids*, vol. 143, p. 160-170.

OGUNBIYI O.O., MILES N.J. y HILAL N. (2008). "The effects of performance and cleaning cycles of new tubular ceramic microfiltration membrane fouled with a model yeast suspension" en *Desalination*, vol. 220, p. 273-289.

QU F. *et al.* (2014). "Ultrafiltration membrane fouling caused by extracellular organic matter (EOM) from Microcystis aeruginosa: Effects of membrane pore size and surface hydrophobicity" en *Journal of Membrane Science,* vol. 449, p. 58-66.

SARKAR B., DASGUPTA S. y DE S. (2009). "Application of external electric field to enhance the permeate flux during micellar enhanced ultrafiltration" en *Separation and Purification Technology,* vol. 66, p. 263-272.

SHI X. *et al.* (2014). "Fouling and cleaning of ultrafiltration membranes: A review" en *Journal of Water Process Engineering*, vol. 1, p. 121-138.

SONG W. *et al.* (2010). "Rapid concentration of protein solution by a crossflow electro-ultrafiltration process" en *Separation and Purification Technology,* vol. 73, p. 310-318.

TARAZAGA C.C., CAMPDERRÓS M.E. y PÉREZ-PADILLA A. (2006). "Physical cleaning by means of electric field in the ultrafiltration of a biological solution" en *Journal of Membrane Science*, vol. 278-p. 219-224.

WANG Y-N. y TANG C.Y. (2011). "Protein fouling of nanofiltration, reverse osmosis, and ultrafiltration membranes - The role of hydrodynamic conditions, solution chemistry and membrane properties" en *Journal of Membrane Science,* vol. 376, p. 275-282.

YASRI N.G., YAGHMOUR A. y GUNASEKARAN S. (2015). "Effective removal of organics from corn wet milling steepwater effluent by

electrochemical oxidation and adsorption on 3-D granulated graphite electrode" en *Journal of Environmental Chemical Engineering*, vol. 3, p. 930-937.

ZUMBUSCH P.v., KULCKE W. y BRUNNER G. (1998). "Use of alternating electrical fields as anti-fouling strategy in ultrafiltration of biological suspensions – Introduction of a new experimental procedure for crossflow filtration" en *Journal of Membrane Science*, vol. 142, p. 75-86.

CAPÍTULO X

Conclusiones finales

10.1. CONCLUSIONES FINALES

10.1.1. Modelización del ensuciamiento de las membranas

- Los diferentes modelos matemáticos de UF considerados en esta Tesis Doctoral (los modelos de Hermia adaptados a flujo tangencial, un modelo combinado que considera los mecanismos de bloqueo completo de poros y formación de torta y un modelo de resistencias en serie) fueron capaces de predecir con gran precisión (valores de R^2 mayores de 0.904 y valores de desviación estándar menores de 0.040) el descenso de la densidad de flujo de permeado con el tiempo para todas las membranas seleccionadas (5, 15, 30 y 50 kDa) durante la UF a 2 bar y 2 $m \cdot s^{-1}$ de diversas disoluciones propias de la industria alimentaria: disoluciones modelo de lactosuero que contenían BSA (10 $g \cdot L^{-1}$), BSA (10 $g \cdot L^{-1}$) con $CaCl_2$ (1.65 $g \cdot L^{-1}$) y WPC (22.2, 33.3 y 44.4 $g \cdot L^{-1}$), y disoluciones enzimáticas de pectinasas con distintas concentraciones de proteínas (2, 7.5 y 15 $g \cdot L^{-1}$).
- El modelo de Hermia de bloqueo estándar de poros fue el único con el que no se obtuvo una buena precisión en el ajuste a los datos experimentales (con valores de R^2 negativos y valores de desviación estándar superiores a 1), debido a que las moléculas de soluto eran de un tamaño mayor que el tamaño de poro de las membranas, por lo que

no podían penetrar dentro de la estructura porosa de dichas membranas.

- Entre los modelos matemáticos considerados, aquellos con los que se obtuvieron ajustes más precisos (con mayor valor de R^2 y menor valor de desviación estándar) fueron el modelo combinado y el modelo de resistencias en serie para todas las membranas y disoluciones alimento ensayadas. Este hecho indicó que tanto la formación de torta como el bloqueo de poros contribuyeron al ensuciamiento de las membranas.
- De entre todas las membranas utilizadas, la que mostró un menor descenso de la densidad de flujo de permeado con el tiempo y menores valores de los parámetros de los modelos para todas las disoluciones alimento consideradas fue la membrana de 30 kDa, puesto que la combinación de alta hidrofilicidad y baja rugosidad superficial que presenta da como resultado una membrana con mejor comportamiento antiensuciamiento.
- La mayor concentración de proteínas en la disolución alimento, así como la presencia de iones en dichas disoluciones (como en el caso de las disoluciones de BSA y $CaCl_2$ y WPC) conllevó un ensuciamiento de las membranas más severo. Esto es debido a varias razones: por un lado, un aumento de la concentración de proteínas favorece la interacción entre ellas y, por tanto, la mayor acumulación de las mismas sobre la superficie de las membranas. Por otra parte, los iones divalentes (como el calcio) actúan como enlace entre las cadenas de proteínas, facilitando también la agregación de las mismas.

10.1.2. Limpieza de membranas mediante disoluciones salinas

- En cuanto al tipo de sal utilizado como agente de limpieza para la membrana de 15 kDa ensuciada con disoluciones de BSA a una concentración de 10 $g \cdot L^{-1}$, los mayores valores de EHL fueron obtenidos cuando la etapa de limpieza se realizó con disoluciones de NaCl, KCl, $NaNO_3$ y NH_4Cl. El menor valor de EHL se obtuvo al utilizar disoluciones de Na_2SO_4. Esta diferencia se debe a la mejor habilidad de los iones Na^+, K^+, NH_4^+, Cl^- y NO_3^- para disolver las proteínas de la superficie de la membrana debido a su carácter "salting-in".
- La sal NaCl fue seleccionada para utilizarse como agente de limpieza para las membranas de 5, 15, 30 y 50 kDa ensuciadas con disoluciones modelo de lactosuero (BSA, BSA con $CaCl_2$ y WPC) y disoluciones enzimáticas debido a su bajo coste e impacto ambiental.
- Las disoluciones de NaCl fueron capaces de limpiar, de manera efectiva, las membranas de 5, 15 y 30 kDa ensuciadas con disoluciones modelo de lactosuero (BSA, BSA con $CaCl_2$ y WPC) así como con disoluciones enzimáticas en las condiciones experimentales ensayadas en cada caso, alcanzando valores de EHL cercanos a 100 % en todos ellos. Sin embargo, estas disoluciones no fueron efectivas para limpiar completamente la membrana de 50 kDa ensuciada con disoluciones modelo de lactosuero. Esto puede atribuirse al ensuciamiento más severo observado en esta membrana.

- Los resultados obtenidos demostraron que a mayor temperatura de la disolución de limpieza y a mayor velocidad tangencial, mayor valor de EHL. Esta tendencia se confirmó con todas las disoluciones alimento y membranas ensayadas.
- Al aumentar la concentración de sal hasta un cierto valor (entre 2.5 y 10 mM), el valor de EHL aumentó también. Sin embargo, un mayor incremento en la concentración de NaCl no resultó en valores más elevados de EHL e, incluso, causó su descenso. Este descenso en la eficacia de limpieza pudo deberse a la competición entre los mecanismos de ensuciamiento y limpieza y a la reducción de la tensión superficial.
- En cuanto a la concentración de proteínas en la disolución alimento durante la etapa de ensuciamiento, cuanto mayor fue dicha concentración, menor fue la EHL obtenida, debido al ensuciamiento más severo causado sobre las membranas conforme la concentración de proteínas aumentó. Esta tendencia se confirmó con disoluciones de WPC (22.2, 33.3 y 150 $g \cdot L^{-1}$), así como con disoluciones enzimáticas (2, 7.5 y 15 $g \cdot L^{-1}$).
- De acuerdo con los resultados de los análisis de superficie respuesta (RSM) y los resultados de los métodos de optimización utilizados, las mejores condiciones de operación para limpiar las membranas de 5, 15 y 30 kDa ensuciadas con disoluciones modelo de lactosuero fueron: temperaturas de 50 ºC (para las disoluciones de BSA y BSA con $CaCl_2$) y 80 ºC (para las disoluciones de WPC), concentraciones de NaCl entre 5 y 10 mM y velocidades tangenciales de

2.18 $m \cdot s^{-1}$ (para las membranas poliméricas) y 4.2 $m \cdot s^{-1}$ (para la membrana de 15 kDa).

- Diversas ecuaciones que correlacionan los valores de EHL con los parámetros de operación (temperatura, concentración de NaCl, velocidad tangencial durante el protocolo de limpieza y concentración de WPC durante la etapa de ensuciamiento) se obtuvieron mediante análisis de regresión múltiple para las membranas de 5, 15 y 30 kDa con elevado grado de ajuste (valores de R^2 mayores de 0.893).
- Las imágenes de SEM y AFM, así como las medidas de ATR-FTIR llevadas a cabo sobre las membranas poliméricas nuevas, sucias y limpias, confirmaron la formación de una capa de proteínas en la superficie de la membrana de 30 kDa sucia, mientras que la densidad de agregados de proteínas fue mayor sobre la membrana de 5 kDa. La razón para estas diferencias radica en la naturaleza hidrofílica de la membrana de 30 kDa, que le confiere mejores propiedades antiensuciamiento y, por tanto, menor acumulación de agentes de suciedad en su superficie.
- La elevada eficacia de limpieza estimada mediante los métodos hidráulicos (basados en la comparación de la resistencia total al final del protocolo de limpieza con la resistencia de la membrana original) se corroboró al determinar mediante ATR-FTIR valores muy pequeños de concentración residual de proteínas (menores de 14 $\mu g \cdot cm^{-2}$) sobre la superficie de las membranas limpias. Aunque reducidas cantidades de contaminantes residuales permanecieron presentes después de la limpieza con

disoluciones de NaCl, los valores de permeabilidad inicial fueron completamente recuperados.

10.1.3. Limpieza de membranas mediante campos eléctricos

- La aplicación de campos eléctricos combinados con disoluciones de NaCl fue una técnica de limpieza efectiva para recuperar las propiedades permselectivas de la membrana cerámica tubular de 15 kDa ensuciada con distintas disoluciones modelo de lactosuero que consistían en BSA (10 $g \cdot L^{-1}$), BSA (10 $g \cdot L^{-1}$) con $CaCl_2$ (1.65 $g \cdot L^{-1}$) y WPC (22.2, 33.3 y 150.0 $g \cdot L^{-1}$). Sin embargo, la membrana cerámica de 50 kDa no pudo ser completamente limpiada después de este protocolo de limpieza, probablemente debido al ensuciamiento más severo que las proteínas causan sobre dicha membrana.
- En cuanto a las condiciones de operación, un aumento en la temperatura de la disolución de limpieza y en el potencial de campo eléctrico aplicado resultaron en un aumento de los valores de EHL obtenidos, para todas las disoluciones alimento ensayadas con la membrana de 15 kDa.
- La utilización de bajas concentraciones de NaCl en combinación con los campos eléctricos favoreció la limpieza de la membrana de 15 kDa en comparación con la utilización de agua desionizada, alcanzando valores de EHL cercanos al 100 % a temperaturas moderadas (alrededor de 43.8 ºC para disoluciones de WPC). La razón de este comportamiento es

la producción de hipoclorito cuando los campos eléctricos se aplicaron utilizando NaCl como electrolito, que oxida las proteínas presentes en la superficie de la membrana y favorece la disgregación de dichos depósitos.

- Las mejores condiciones de operación para limpiar la membrana de 15 kDa fueron una concentración de NaCl de 5 mM, una presión transmembranal de 1 bar, una velocidad tangencial de 4.2 $m \cdot s^{-1}$, un potencial de campo eléctrico de 30 V y temperaturas entre 37.5 y 43.8 ºC.

10.2. FINAL CONCLUSIONS

10.2.1. Membrane fouling modelling

- The different mathematical UF models selected in this PhD Thesis (Hermia's models adapted to crossflow, a combined model that considers both complete blocking and cake formation mechanisms and a resistance-in-series model) were able to predict with high accuracy (values of R^2 higher than 0.904 and values of SD lower than 0.040) the permeate flux decline obtained with time for all the membranes tested (5, 15, 30 and 50 kDa) during the UF at 2 bar and 2 $m \cdot s^{-1}$ of several food solutions: whey model solutions that contained BSA (10 $g \cdot L^{-1}$), BSA (10 $g \cdot L^{-1}$) with $CaCl_2$ (1.65 $g \cdot L^{-1}$) and WPC (22.2, 33.3 and 44.4 $g \cdot L^{-1}$) and enzymatic solutions of pectinases at different protein concentrations (2, 7.5 and 15 g/L).
- Only the Hermia's standard blocking model did not show a very accurate fitting (with negative values of R^2 and SD values higher than 1) to the experimental data, because solute molecules were higher than membrane pore size, thus they cannot penetrate inside the membrane porous structure.
- Among the mathematical models tested, those that showed the best fitting accuracy (the highest R^2 and lowest SD) were the combined model and the resistance-in-series model for all the membranes and feed solutions considered. This fact indicated that both cake layer formation and pore blocking contributed to membrane fouling.

- Among the different membranes used, the one that showed the lowest permeate flux decline with time and the lowest values of model parameters for all the feed solutions considered was the 30 kDa membrane, because the combination of high hydrophilicity and low surface roughness resulted in a membrane with better antifouling properties.
- An increase in protein concentration in the feed solutions and the presence of calcium ions in these solutions (as in the case of BSA with $CaCl_2$ and WPC solutions) resulted in a more severe membrane fouling. This is due to several reasons: on one hand, an increase in protein concentration favours the interaction among them and thus, the greater protein accumulation on the membrane surface. On the other hand, salts such as calcium acts as binding agent between protein chains, easing their aggregation.

10.2.2. Membrane cleaning by means of saline solutions

- Regarding the type of salt used as cleaning agent for the 15 kDa membrane fouled with BSA solutions at a concentration of 10 $g \cdot L^{-1}$, the highest values of HCE were achieved when the cleaning stage was performed with NaCl, KCl, $NaNO_3$ and NH_4Cl solutions. The lowest value of HCE was obtained when Na_2SO_4 solutions were used. This difference is due to the better ability of Na^+, K^+, NH_4^+, Cl^- y NO_3^- ions to dissolve proteins from membrane surface due to the salting-in effect.

- NaCl was selected to be used as cleaning agent for the membranes of 5, 15, 30 and 50 kDa fouled with whey model solutions (BSA, BSA with $CaCl_2$ and WPC solutions) and enzymatic solutions because of its lower cost and environmental impact.
- NaCl solutions were able to effectively clean the 5, 15 and 30 kDa membranes fouled with whey model solutions (BSA, BSA with $CaCl_2$ and WPC solutions) as well as with enzymatic solutions at the experimental conditions tested, achieving values of HCE about 100 % in all cases. However, they were not effective to completely clean the 50 kDa membrane fouled with whey model solutions. This can be attributed to the more intense fouling observed for this membrane.
- The cleaning results obtained demonstrated that the higher the temperature of the cleaning solution and the crossflow velocity were, the higher HCE was achieved. This trend was confirmed with all the feed solutions and membranes tested.
- When salt concentration increased up to a certain value (ranging from 2.5 to 10 mM), HCE increased as well. However, a further increase in NaCl concentration did not result in higher values of HCE or could even cause their decrease. The cleaning efficiency decrease may be due to the competition between cleaning and fouling mechanisms and the reduction in surface tension.
- Regarding the protein concentration in the feed solution during the fouling step, the higher this concentration was, the lower the HCE was, due to the more severe fouling caused when

protein concentration in the feed solution increased. This pattern was confirmed with the WPC solutions (22.2, 33.3 and 150 $g \cdot L^{-1}$) as well as the enzymatic solutions (2, 7.5 and 15 $g \cdot L^{-1}$).

- According to the results of the RSM analyses and the results of the optimization methods, the best operating conditions to clean the 5, 15 and 30 kDa membranes fouled with whey model solutions were: temperatures of 50 ºC (for BSA and BSA with $CaCl_2$ solutions) and 80 ºC (for WPC solutions), NaCl concentrations ranging from 5 to 10 mM and crossflow velocities of 2.18 $m \cdot s^{-1}$ (for the polymeric membranes) and 4.2 $m \cdot s^{-1}$ (for 15 kDa membrane).
- Several equations that correlated HCE to the operating parameters (temperature, NaCl concentration, crossflow velocity in the cleaning procedure and WPC concentration during the fouling step) were obtained by means of a Multiple Regression Analysis for the 5, 15 and 30 kDa membranes. The accuracy of these equations was very high (values of R^2 higher than 0.893).
- SEM and AFM images as well as ATR-FTIR measurements carried out on the virgin, fouled and cleaned polymeric membranes, confirmed that a continuous protein layer was formed on the fouled 30 kDa membrane surface, while the density of protein aggregates was greater on the fouled 5 kDa membrane surface. The reason for this difference is the hydrophilic nature of the 30 kDa membrane, which results in better antifouling properties and thus, lower accumulation of foulants on its surface.

- The high cleaning efficiency estimated by means of the hydraulic methods (by comparing the total resistance at the end of the cleaning protocol to the original membrane resistance) was corroborated as very low values of residual protein concentration on the surface of the clean membranes was measured by ATR-FTIR. Although small quantities of residual contaminants were still present after cleaning with NaCl solutions, the initial permeability value was completely restored.

10.2.3. Membrane cleaning by means of electric fields

- Electric fields combined with NaCl solutions were an effective cleaning technique to restore the permselective properties of a ceramic monotubular 15 kDa membrane fouled with different whey model solutions consisting of BSA (10 $g \cdot L^{-1}$), BSA (10 $g \cdot L^{-1}$) with $CaCl_2$ (1.65 $g \cdot L^{-1}$) and WPC (22.2, 33.3 and 150.0 $g \cdot L^{-1}$). However, the 50 kDa ceramic membrane could not be completely cleaned after this cleaning procedure, probably due to the more severe fouling that proteins caused in this membrane.
- Regarding the cleaning operating conditions, an increase in temperature of the cleaning solution and in the potential of the electric field applied resulted in an increase in the HCE values achieved for all the feed solutions tested for the 15 kDa membrane.

- The utilization of low concentrations of NaCl combined with the application of electric fields favoured the membrane cleaning of the 15 kDa membrane in comparison with the utilization of deionized water. HCE values about 100 % were achieved at mild temperatures (about 43.8 ºC for the WPC solutions). The reason for this observation is the production of hypochlorite when electric fields are applied using NaCl as electrolyte, which oxidises the protein deposits on the membrane surface and favours the disaggregation of these deposits.
- The best operating conditions to clean the 15 kDa membrane were a NaCl concentration of 5 mM, a transmembrane pressure of 1 bar, a crossflow velocity of 4.2 $m \cdot s^{-1}$, an electric field potential of 30 V and temperatures ranging from 37.5 to 43.8 ºC.